THE INFLUENCE OF PRIMARY AND SECONDARY NITROGEN DONOR ATOMS ON THE THERMODYNAMICS OF COMPLEX FORMATION IN AQUEOUS SOLUTION

by

Bice Susan Martincigh

Submitted in partial fulfilment of the
requirements for the degree of
Doctor of Philosophy
in the
Department of Chemistry and Applied Chemistry,
University of Natal

Durban
1987

ai mie genitors

ABSTRACT

The experimental work described in this thesis is aimed at testing the assertion that, in the absence of ring strain effects, the formation of metal ion-secondary nitrogen bonds is enthalpy-stabilized in comparison with metal ion-primary nitrogen bonds. To this end the stability constants of the ligand 2-(2-aminoethyl)aminoethanol (etolen) with the ions H^+, Ni^{2+}, Co^{2+} and Zn^{2+}, and those of the ligand 2,2'-oxybisethanamine (oden) with the ions H^+, Ni^{2+} and Co^{2+}, have been determined by glass electrode potentiometry at 25°C in 0.5 mol dm^{-3} KNO_3. In addition, the enthalpies of reaction have been determined by titration calorimetry under the same conditions. The results obtained for these various systems, together with some available from the literature, are compared and discussed.

The differences between the thermodynamic parameters of the etolen complexes and those of oden give a measure of the relative bonding capacities of secondary and primary nitrogen donors. From these differences the following general observations are made:

1. The six metal ions considered turn out to split into two distinct groups: one in which CFSE is expected and the etolen complexes are more stable, and one in which CFSE is not expected and the oden complexes are more stable.

2. The $\Delta(\log K_{011})$ values for each group show at least approximately a linear relationship with the hardness parameter of the metal ion, and with the radius of the metal ion.

3. For all metal ions considered, the addition of a second ligand molecule to the ML complex leads to enhancement of secondary over primary nitrogen bonding.

4. The $\Delta(\Delta H^{\ominus}_{011})$ values for those metal ions where CFSE is expected show at least approximately a linear relationship with both the hardness and the radius of the metal ion.

It is therefore tentatively concluded that metal ion - secondary nitrogen bonds are not in general stronger than those involving primary nitrogen. They are stronger only in those cases where crystal field stabilization energy is present and the metal ion is small. This enhanced stability appears to decrease as the size or the hardness of the metal ion increases.

PREFACE

The experimental work described in this thesis was carried out in the Department of Chemistry and Applied Chemistry, University of Natal, Durban, under the supervision of Professor F. Marsicano.

These studies represent original work by the author and have not been submitted in any form to another University. Where use was made of the work of others it has been duly acknowledged in the text.

ACKNOWLEDGEMENTS

I am indebted to many people and organizations for their assistance during the course of this work.

Firstly, I must thank my supervisor, Prof. F. Marsicano, for his advice and encouragement, and his painstaking comments on all parts of the thesis.

I must also thank Prof. J.W. Bayles for his interest and support, and for occasionally waving the big stick.

I am grateful to Siva Moodley, for recording the infrared spectra, and Dan Pienaar, for recording the n.m.r. and mass spectra. The technical staff of the Department, especially Dave Balson, helped me in many respects, and were always cheerful and cooperative. Bernice Liguori did a marvellous job of accurate and speedy typing. My laboratory colleagues Faizel Mulla and Chris Monberg provided a convivial working environment, and stimulating (and at times robust) discussion of technical matters. Various friends, including Leo Salter and Rodney Hansen, provided encouragement and assistance.

I owe much to my parents and my sister, for all their support and sacrifices over many years. Their encouragement has meant much to me.

I also owe much to Iain MacDonald for his indefatigable help and extreme patience. His encouragement and support made the task much easier and for this I am extremely grateful.

Finally, I wish to acknowledge, with gratitude, the financial support of several bodies: AECI and the CSIR, both of whom generously supported my work for several years; the University of Natal, who awarded me a graduate assistantship for one year; and the Natal Technikon, who granted me two months' leave from my lecturing duties to work on my thesis.

CONTENTS

GLOSSARY OF ABBREVIATIONS

Abbreviation	Formula and Ligand Name
aea$^-$	$H_2N(CH_2)_2OCH_2COO^-$ 2-aminoethoxyacetate
bdta	$(CH_2CO_2H)_2N(CH_2)_4N(CH_2CO_2H)_2$ 1,4-diamino-N,N,N',N'-tetraacetic acid butane
bimp	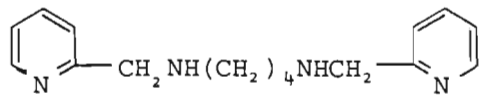 butylenebis(iminomethylene-2-pyridine)
bipy	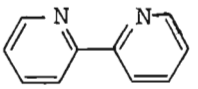 2,2'-bipyridine
cyclam	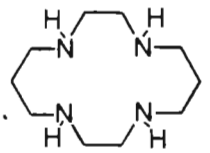 1,4,8,11-tetraazacyclotetradecane
dien	$NH_2(CH_2)_2NH(CH_2)_2NH_2$ diethylenetriamine
dpt	$NH_2(CH_2)_3NH(CH_2)_3NH_2$ dipropylenetriamine
edta	$(CH_2CO_2H)_2N(CH_2)_2N(CH_2CO_2H)_2$ 1,2-diamino-N,N,N',N'-tetraacetic acid ethane
eimp	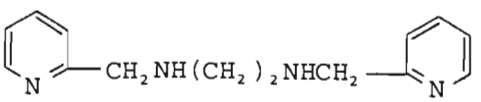 ethylenebis(iminomethylene-2-pyridine)
en	$NH_2CH_2CH_2NH_2$ ethylenediamine
eten	$CH_3CH_2NHCH_2CH_2NH_2$ N-ethylethylenediamine
etolen	$HO(CH_2)_2NH(CH_2)_2NH_2$ 2-(2-aminoethyl)aminoethanol
etolen$^-$	$^-O(CH_2)_2NH(CH_2)_2NH_2$ 2-(2-aminoethyl)aminoethoxide
heg$^-$	$HO(CH_2)_2NHCH_2COO^-$ N-(2-hydroxyethyl)glycinate

2-hn	$HO(CH_2)_2NH(CH_2)_2NH(CH_2)_2OH$
	N,N'-di(2-hydroxyethyl)ethylenediamine
oden	$(H_2NCH_2CH_2)_2O$
	2,2'-oxybisethanamine
pdta	$(CH_2CO_2H)_2N(CH_2)_3N(CH_2CO_2H)_2$
	1,3-diamino-N,N,N',N'-tetraacetic acid propane
penten	$(H_2NCH_2CH_2)_2N(CH_2)_2N(CH_2CH_2NH_2)_2$
	N,N,N',N'-tetra-(2-aminoethyl)ethylenediamine
pimp	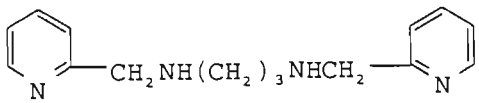
	propylenebis(iminomethylene-2-pyridine)
py	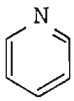
	pyridine
2,3,2-tet	$NH_2(CH_2)_2NH(CH_2)_3NH(CH_2)_2NH_2$
	3,7-diazanonane-1,9-diamine
3,2,3-tet	$NH_2(CH_2)_3NH(CH_2)_2NH(CH_2)_3NH_2$
	4,7-diazadecane-1,10-diamine
3,3,3-tet	$NH_2(CH_2)_3NH(CH_2)_3NH(CH_2)_3NH_2$
	1,5,9,13-tetra-azatridecane
tetren	$NH_2(CH_2)_2NH(CH_2)_2NH(CH_2)_2NH(CH_2)_2NH_2$
	tetraethylenepentamine
tn	$NH_2(CH_2)_3NH_2$
	1,3-diaminopropane
tren	$N(CH_2CH_2NH_2)_3$
	2,2',2''-triaminotriethylamine
2,3-tri	$NH_2(CH_2)_2NH(CH_2)_3NH_2$
	3-azahexane-1,6-diamine
trien	$NH_2(CH_2)_2NH(CH_2)_2NH(CH_2)_2NH_2$
	triethylenetetramine

CHAPTER ONE

INTRODUCTION

The thermodynamics of metàl-ligand complex formation reactions has been the subject of fairly intensive research effort over the past 20 - 25 years. Much data has been gathered concerning free-energy changes (1,2) and for a number of years discussion of metal complex formation in solution was limited to a rationalisation of free energy changes. However with the advent of improved temperature-sensing devices, viz. thermistors, calorimeters have been developed which enable values of $\Delta H^{\ominus}$ to be determined directly, and hence a number of precise measurements on the enthalpy changes of complex formation have been made (3,4). This has led to the belief that the stability of a complex is best explained in terms of the corresponding enthalpy and entropy contributions, i.e. in terms of the equation

$$\Delta G^{\ominus} = \Delta H^{\ominus} - T\Delta S^{\ominus}.$$

It has been found though that a study of the $\Delta H^{\ominus}$ values for a wide variety of reactions presents a more complex picture than does a study of the corresponding free energy changes (5,6). However for more closely related systems the irregularity in the $\Delta H^{\ominus}$ values is not so marked.

This chapter will describe:

(i) the debate over the existence and origin of the 'chelate' effect;
(ii) the various interpretations presented of the rôle enthalpy and entropy changes play in complex formation;
(iii) attempts to explain and predict values of $\Delta H^{\ominus}$;
(iv) the aim of this project; and
(v) (in outline) the experimental techniques employed in this work to measure stability constants and enthalpy changes.

1.1. The chelate effect

It is experimentally observed that complexes formed with polydentate ligands are more stable than the corresponding complexes formed with monodentate ligands. This enhanced stability was termed the 'chelate effect' by Schwarzenbach in 1952 (7). Since then, this effect has been the subject of much debate. Most of the controversy has arisen not through the experimentally observed phenomenon but through trying to describe the effect quantitatively. This confusion has even led to the question of whether or not there is a real chelate effect.

1.1.1. The great debate: Arguments about definition and existence

To illustrate the chelate effect Schwarzenbach considered the replacement reaction

$$MA_2 + L \rightleftharpoons ML + 2A, \qquad (1.1)$$

where M is the metal ion, A is a monodentate ligand and L is a bidentate ligand. He hypothesized that the donor groups of both ligands had the same affinity for the metal ion, and hence that the heat of reaction was zero. This implied that the stabilizing chelate effect was due to a favourable entropy change. This prediction is consistent with the experimental values of the thermodynamic functions for the reaction

$$M(NH_3)_n^{2+} + L \rightleftharpoons ML^{2+} + n(NH_3),$$

where L is a polyamine ligand. Typical values for this reaction are given in Table 1.1.

As can be seen the entropy contribution increases with increasing denticity of the chelating ligand. The metal-polyamine complexes are more stable than the corresponding ammonia complexes, largely because of the large positive entropy changes accompanying the release of increasing numbers of ammonia molecules. This view was also proposed by Calvin and Bailes (13) in their study of the stability of various copper chelates.

TABLE 1.1

Thermodynamic data for the reaction $M(NH_3)_n^{2+} + L \rightleftharpoons ML^{2+} + n(NH_3)$.

M^{2+}	n	L*	$\Delta G^{\ominus}$/kJmol^{-1}	$\Delta H^{\ominus}$/kJmol^{-1}	$T\Delta S^{\ominus}$/kJmol^{-1}	Reference	
Ni^{2+}	3	dien	-22.22	- 5.65	16.34	8	Thermodynamic data
	4	trien	-33.72	0	33.68	9	for the metal-
	5	tetren	-50.50	- 5.86	44.78	10	ammonia reactions
	6	penten	-59.87	5.65	65.62	11	have been taken
							from reference 4.
Cu^{2+}	3	dien	-30.17	-12.55	17.84	8	
	4	trien	-42.55	- 6.49	36.05	9	
	5	tetren	-61.17	- 7.32	53.89	10	

This table is substantially the same as Table 5 in reference 12.

*dien = diethylenetriamine
trien = triethylenetetramine
tetren = tetraethylenepentamine
penten = N,N,N',N'-tetra-(2-aminoethyl)ethylenediamine

Schwarzenbach (7,14) tried to describe the chelate effect in terms of a model where in the first step one of the donor atoms of the bidentate ligand attaches itself to the metal ion. He assumed this intermediate to have the same stability as the complex MA with the corresponding monodentate ligand. Hence the second donor atom may move only in a reduced volume dictated by the length of the chain joining the two donor atoms. In the second step the second donor atom of the chelating ligand attaches itself to the metal ion and the ring is formed, whereas for the formation of MA_2 a second freely mobile ligand must be obtained from the solution. Thus the second donor atom of the chelating ligand has a higher activity with respect to attachment to the metal ion and this activity can be calculated from the reduced volume. Thus this model provides an explanation for the decrease in stability of the chelate complex with increasing distance between the two donor groups of the ligand. Cotton and Harris (15) calculated the entropy changes accompanying ring closures on the basis of this model. However these applications failed to give agreement with experiment.

Schwarzenbach (7) defined the chelate effect quantitatively by

$$\text{Chelate Effect} = \log K(ML) - \log \beta_2(MA_2), \qquad (1.2)$$

where the constants K and β_2 refer to the equilibria:

$$M + L \rightleftharpoons ML \qquad K = \frac{[ML]}{[M][L]} \qquad (1.3)$$

$$M + 2A \rightleftharpoons MA_2 \qquad \beta_2 = \frac{[MA_2]}{[M][A]^2} \qquad (1.4)$$

Thus this quantity is in fact the logarithm of the stability constant of the replacement reaction (1.1). Since (in this case) the 'chelate effect' is the logarithm of a concentration, it will depend on the units chosen to express concentration.

Equilibrium constants are however actually defined in terms of activities rather than concentrations (as done here), and the standard states usually chosen for the components in solution are different. For solvents the standard state is taken to be the pure liquid, whereas for solutes the

standard state is defined in terms of a hypothetical ideally dilute 1 mol kg^{-1} solution. This led Adamson (16) to point out that the magnitude of the chelate effect depends on the standard state chosen for the solutes. He interpreted the chelate effect as being an increase in the translational entropy for the replacement reaction (1.1) resulting from an increase in the number of species present in solution, as did Schwarzenbach. Adamson showed that if the unit mole fraction standard state is used for the solutes instead of the commonly used one molal standard state the extra stability of the chelate complex more or less disappears. He chose the hypothetical unit mole fraction standard state because this state 'is one of minimum translational entropy for a solute retaining the properties it possesses in dilute solution' (16). This choice removes the influence of cratic effects.

Adamson is therefore often quoted for his statement that 'the chelate effect is largely a consequence of the arbitrary asymmetry in the usual choice of standard states'. Jones and Harrop (17) explain how this asymmetry arises. In the expressions for K and β_2 we have neglected the loss of coordinated water molecules from the hydration sphere of the metal ion upon complex formation, since it is generally assumed that the activity of water is one. In dilute aqueous solution the concentration of water is unit mole fraction. Thus the standard state for water is unit mole fraction whereas the standard states for the solutes are unit molal (molar) concentrations. This asymmetry is thus inherent in the expression for the chelate effect. In using the unit mole fraction standard state throughout Adamson removed this asymmetry.

Calculations of the type performed by Adamson led to the conclusions that 'the chelate effect ceases to be of any special importance' (18) and 'the apparent extra stability of chelate complexes disappears' (16), and to claims of 'the non-existence of the chelate effect' (18).

Alternatively if a standard state of 0.001 molal (mol kg^{-1}) is used for the solutes the chelate effect becomes much larger. Notwithstanding the asymmetry of the standard state, one must not lose sight of the fact that the chelate effect is still experimentally observed, as has been pointed out by Martell (19) and Munro (20).

Jones and Harrop (17) have shown that the removal of the asymmetry of the standard states need not necessarily lead to the conclusion that the chelate effect does not exist. They showed that, if the asymmetry of standard states is removed by using unit molar standard states throughout, the chelate effect is important. They concluded that for dilute standard states a real chelate effect is obtained (as reflected by a significant and negative value for the free energy change), whereas for concentrated standard states the effect is diminished. This conclusion is in keeping with Adamson's findings.

In practice stability constants are often given in terms of concentrations instead of activities. This has led to another source of confusion which arises from the definition of the chelate effect as given by equation (1.2). Agterdenbos (21) stated that it was incorrect to compare the stability constants of complexes involving polydentate ligands with those of complexes involving monodentate ligands. The error lies in the fact that the two stability constants have different units and this can lead to erroneous conclusions about the relative stabilities of the complexes.

Jones and Harrop (17) emphasize that a change of concentration units represents a corresponding change in standard states and hence that the choice of concentration units fixes the standard states of the solutes. They remind the reader that provided identical standard states are chosen the comparison of stability constants of complexes involving polydentate and monodentate ligands is valid for concentration conditions in the vicinity of those chosen for the standard state.

It is generally agreed that since the choice of concentration units implies a choice of standard state the latter should be close to the concentrations used in practice. Hence the use of the molar scale is generally accepted (17,20,22), whereas use of a mole fraction of one is not, since the latter is physically impossible during a reaction (20,22).

1.1.2. Further attempts to quantify the chelate effect

Since the quantitative definition of the chelate effect given by equation (1.2) various authors have tried to define this quantity in different ways. At times this was done in an attempt to obtain a definition which avoids the problems that arose from Schwarzenbach's definition.

Prue (23) tried to show the relationship between various non-identical equations in the literature relating the stability constants of complexes to the sizes of the ions and the dielectric constant of the solvent. From his model he illustrated the rôle enthalpy and entropy play in complex formation and the chelate effect.

In his model he showed that if two molecules are closer to one another than a distance a + da where a is the mean collision diameter, and have an interaction energy ω, then an expression for their association constant is given by

$$K = 4 \pi a^2 \, (da) \, N \, e^{-\omega/kT} \, . \qquad (1.5)$$

In this equation $4 \pi a^2 \, (da)$ is (approximately) the volume of a spherical shell of thickness da, $e^{-\omega/kT}$ is the Boltzmann factor and N is Avogadro's constant. In this treatment the solvent is a structureless dielectric continuum of dielectric constant ε. From this expression for K the equations for ion association derived by various authors can be simply deduced.

If the two molecules are oppositely charged non-polarizable ions ω is given by Coulomb's Law and on integration through the abovementioned shell from r = a to r = a + da one obtains the Bjerrum (24) expression for ionic association:

$$K = \int_a^{a+da} 4 \pi N r^2 \, dr \, \exp \, (z_+ z_- e^2 / \varepsilon r k t) . \qquad (1.6)$$

(The cation and anion carry charges z_+e and z_-e respectively.)

If da in (1.5) is set to $\frac{1}{3}a$ and ω is again determined by Coulomb's Law, we obtain Fuoss's equation (25) for the association constant

$$K = \frac{4}{3} \pi a^3 \, N \, \exp \, (z_+ z_- e^2 / \varepsilon a k T) . \qquad (1.7)$$

Also the expression of Eigen (26), which he derived from a kinetic argument, can be obtained:

$$K = V \exp \, (z_+ z_- e^2 / \varepsilon a k T) , \qquad (1.8)$$

where V is the shell volume.

For this model ion pair formation occurs essentially because of the coulombic forces between oppositely charged ions. Prue showed that if one treats $\Delta G^{\ominus}$ as a consequence of changes in $\Delta H^{\ominus}$ and $T\Delta S^{\ominus}$ the latter terms depend on the temperature coefficient of the dielectric constant. If the solvent is water this model gives an endothermic $\Delta H^{\ominus}$ value and hence an unfavourable contribution to association. However, if one assumes covalent bonding instead of coulombic attraction between the molecules, exothermic values of $\Delta H^{\ominus}$ are obtained. Charge-solvent interactions exert the major influence on $\Delta S^{\ominus}$ for ion association reactions, irrespective of the nature of the bonding.

From his model Prue showed that if one assumes the chelate effect is an entropy effect then the association constant for the replacement reaction (1.1) is given by:

$$\frac{K}{\beta_2} = V^{-1} = (\frac{4}{3} \pi Na^3)^{-1}. \qquad (1.9)$$

In obtaining this expression he assumed the interaction energy of the central ion with a bidentate ligand was twice the interaction energy between the central ion and the analogous monodentate ligand. (Of course, this assumption is an idealisation.) Taking a = 2.75 Å he obtained $\frac{K}{\beta_2}$ = 19 mol dm^{-3}, which is roughly of the correct order of magnitude.

Rosseinsky (27) established, using a continuum treatment of chelation, that the contrasting models of Prue (23) and Schwarzenbach (7,14) refer to short and long chelates respectively, depending on whether the ligand is shorter or longer than about 8 Å.

In Prue's model it is assumed that both ends of the bidentate ligand enter the shell volume about the central ion, occupancy of which denotes bonding. Rosseinsky assumed that this was the case for a short ligand, that is, a ligand whose length is comparable to the contact distance a, e.g. ethylenediamine. He calculated the value of $\frac{K}{\beta_2}$ for various complexes of ethylenediamine and methylamine and found that they bracketed Prue's value of 19 mol dm^{-3}. Hence he concluded that ethylenediamine is the ideal short chelate. In this case he assumed that the interaction energy of the central ion with two molecules of methylamine (the monodentate ligand) is equal to that of the central ion with one molecule of ethylenediamine

(the bidentate ligand). Hence

$$\frac{K}{\beta_2} \text{ (ideal)} = V^{-1} = (\frac{4}{3} \pi Na^3)^{-1}. \qquad (1.10)$$

When he compared the complexes of bipyridyl (also a short chelate) with those of pyridine he found that the value of $\frac{K}{\beta_2}$ greatly exceeded the calculated value of V^{-1}. He called this enhancement of chelation 'non-ideality' and ascribed it to differences in the interaction energies. Hence

$$\frac{K}{\beta_2} \text{ (non-ideal)} = (\frac{4}{3} \pi Na^3)^{-1} \, e^{[(2u_m - 2u_{chel})/kT]}, \qquad (1.11)$$

where $2u_m$ is the sum of the interaction energies for the attachment of two monodentate ligands and $2u_{chel}$ is the interaction energy for the coordination of the bidentate ligand.

For long chelates, that is, ligands whose length ℓ greatly exceeds the contact distance a, Rosseinsky made use of the Schwarzenbach model of chelation. If one end of the ligand is bonded and the other end is free, the unattached end can occupy any position in a volume equal to $\frac{4}{3} \pi \ell^3$ centred on the point of attachment. Hence for ideal long chelates

$$\frac{K}{\beta_2} \text{ (ideal)} = V_s^{-1} = (\frac{4}{3} \pi N \ell^3)^{-1}, \qquad (1.12)$$

which is analogous to the expression for ideal short chelates. Butane 1,4-diamine was deemed the ideal long chelate. Again Rosseinsky ascribed non-ideality to differences in the interaction energies. Hence the relevant expression is

$$\frac{K}{\beta_2} \text{ (non-ideal)} = (\frac{4}{3} \pi N \ell^3)^{-1} \, e^{[(2u_m - 2u_{chel})/kT]}. \qquad (1.13)$$

(In his model Schwarzenbach termed V_s an activity.)

The same arguments as stated before apply in the work of Rosseinsky if different concentration units are used (i.e. different values for the chelate effect are obtained). He claimed that the ideal long chelate model can be used to infer chelation and hence the chelate effect.

If the chelate-length is known from independent sources such as spatial models or diffraction data on the solid, then chelation is unambiguous if

$$\frac{K}{\beta_2} \geqslant \left(\frac{4}{3}\ \pi\ N\ \ell^3_{expt}\right)^{-1}. \qquad (1.14)$$

Both sides of this inequality have dimensions of concentration and hence it is immaterial what units are used. This thus removes previous contentions regarding the choice of concentration scale. The equality sign indicates ideality whereas the reverse inequality < indicates the absence of chelation.

Simmons (22) expanded the idea of Prue (23) of expressing the chelate effect in terms of molecular volumes. In his treatment he assumed, as did Schwarzenbach, that the chelate effect is an entropy effect and that the enthalpy change for the replacement reaction (1.1) is zero. He obtained essentially the same expression for the chelate effect as did Rosseinsky (27) in his model for ideal long chelates, namely:

$$\text{Chelate Effect} = \log \frac{K}{\beta_2}$$

$$\cong - \log V_a N\ , \qquad (1.15)$$

where V_a is the volume accessible to the unattached donor atom of the bidentate ligand in the complex with one donor atom of the ligand already attached. In obtaining this expression Simmons obtained equations for the equilibrium constants of reactions (1.3) and (1.4) on the basis of probability. For example, for reaction (1.4) the probability of one molecule of A being attached to M is proportional to the relative volume available for it to be attached. He also assumed that the energy involved in attaching two monodentate ligands is the same as that for attaching one bidentate ligand.

Simmons thought that his equation for the chelate effect, based on the concept of accessible volume, was difficult to use quantitatively but should rather be used qualitatively to predict such things as crowding effects and the structure of the intermediate. For example, the observation that the chelate effect decreases with increase in chelate ring size can be predicted from this equation since the volume accessible to the chelating atom

is larger the longer the ligand, hence the chelate effect is smaller.

Hancock and Marsicano (28) proposed an equation to predict the stability constants of metal-polyamine complexes (with five-membered chelate rings) from the stability constants of the analogous ammonia complexes. The equation has the form:

$$\log K_1(\text{polyamine}) = 1.152 \log \beta_n(NH_3) + (n-1) \log 55.5, \qquad (1.16)$$

where n is the denticity of the polyamine. (The form of this equation is easily obtained if one considers the removal of the asymmetry of standard states in the expression for the equilibrium constant of the appropriate replacement reaction - see Appendix I.)

In this equation $\log \beta_n(NH_3)$ refers to the cumulative stability constant for the formation of the analogous ammonia complex. The factor of 1.152 is obtained from $pK_a(\text{alkylamine})/pK_a(NH_3)$ in order to account for the inductive effect of the ethylene bridges. This factor when multiplied by $\log \beta_n(NH_3)$ generates $\log \beta_n$ for a hypothetical non-sterically hindered alkylamine which was thought to be a more appropriate monodentate analogue for comparison with the polyamines than ammonia would have been. The term (n-1) log 55.5 accounts for the asymmetry of the standard state.

Hancock and Marsicano found that the following modification of equation (1.16) had improved predictive powers:

$$\log K_1(\text{polyamine}) = 1.152 \left[n \log K_1(NH_3) - \frac{n}{2}(n-1)\lambda\right] + (n-1) \log 55.5. \qquad (1.17)$$

The term in λ was originally introduced to represent $\log K_n(NH_3) - \log K_{n+1}(NH_3)$, and λ was set equal to an empirical value of 0.5 for nickel(II)-polyamine complexes. The term in λ was thought to account for the steady decrease in $\log K_n(NH_3)$ as n increases (i.e. as more ligands are added), an effect that was believed to be due to the electrostatic repulsion between dipoles. Subsequently (29) the term in λ has been re-interpreted as being of largely steric origin and relating to steric strain developed in the polyamine ring system.

This equation was extended (30) to accommodate ligands containing other donor groups such as the carboxylate group:

$$\log K_1(\text{polyaminocarboxylate}) = 1.152\ n \log K_1(NH_3) - \frac{n}{2}(n-1)\ \lambda_N + m \log K_1(CH_3COO^-) - \frac{m}{2}(m+1)\ \lambda_o + (m + n - 1) \log 55.5 \ . \qquad (1.18)$$

Thus equation (1.18) relates the equilibrium constant of a polyaminocarboxylate complex having n nitrogen donors and m carboxylate groups, to the equilibrium constants of the corresponding ammonia and acetate complexes.

The quantity λ_o is the λ appropriate to carboxylate groups and is empirically set equal to $0.26 \log K_1(CH_3COO^-) - 0.19$.

These equations successfully predicted stability constants for complexes having five-membered chelate rings but not for those containing six-membered chelate rings. However, by empirically altering the terms due to steric hindrance, i.e. the terms involving λ, good agreement was obtained between calculated and observed stability constants for complexes of six-membered and larger rings.

These equations were found especially useful in estimating the stability constants of complexes containing monodentate ligands which are unstable in aqueous solution, e.g. the ammonia complexes of Pb(II), which are hydrolysed in water.

Recently a new definition for the chelate effect was introduced by Fraústo da Silva (31). He based his definition on the experimental observation that the chelate complex ML forms preferentially in a solution which contains M, L and A and in which L and A can both offer the same total number of donor atoms to the metal ion.

He redefined the chelate effect to be

$$\text{Chelate Effect} = \log \frac{[ML]}{[MA_2]} \ . \qquad (1.19)$$

With this definition a positive chelate effect means that $[ML] > [MA_2]$.

Equation (1.19) can be rewritten to give

$$\text{Chelate Effect} = \log \frac{K}{\beta_2} + 2 \log \alpha_H^A - \log \alpha_H^L$$

$$- 2 \log 2 + (1 - 2) \log [L]_T \ , \qquad (1.20)$$

or more generally

$$\text{Chelate Effect} = \log\left(\frac{\beta_{ML_m}}{\beta_{MA_n}}\right) + n \log \alpha_H^A - m \log \alpha_H^L$$

$$- n \log \left(\frac{n}{m}\right) + (m-n) \log [L]_T \ . \qquad (1.21)$$

In equation (1.21) β_{ML_m} and β_{MA_n} are the overall stability constants of ML_m and MA_n respectively, where L is the polydentate ligand and A is the analogous monodentate ligand. $[L]_T$ is the total concentration of the polydentate ligand and α_H^A and α_H^L are defined as follows:

$$\alpha_H^A = 1 + K_{HA}[H^+]$$

$$\alpha_H^L = 1 + \sum_{i=1}^{r} \beta_i^{H_iL} [H^+]^i \ .$$

In obtaining equation (1.20) or the more general equation (1.21) it was assumed that ML and MA_2 are equally hydrated, i.e. the same number of water molecules are released on formation of ML and MA_2; the total concentration of the ligands is very much higher than the total concentration of metal and the solution contains an equal concentration of donor atoms from A and L, i.e. $[A]_T = 2\,[L]_T$.

Thus equation (1.21) shows that the chelate effect (as defined by Fraústo da Silva) depends on the free energy change of the replacement reaction, on differences in basicity of the ligands, on the pH of the medium, on the types of chelates formed and on the concentration of the ligands in solution. This equation also has the advantage that it is dimensionless and hence does not suffer the limitations of concentration units and stan-

dard states which gave rise to so much debate about the chelate effect.

The equation is also in agreement with several experimental observations. Since (m-n) is always negative, the chelate effect decreases with an increase in concentration of the ligands, in keeping with the conclusion reached by Jones and Harrop (17) that for concentrated standard states the chelate effect diminishes and even disappears. Equation (1.21) also shows that the chelate effect decreases with increase in n and with increase in pH.

Its major limitation is that of being applicable only to conditions of large excess of ligands relative to the metal ion.

Fraústo da Silva regards the idea that the chelate effect is an entropy effect to be an oversimplification which arose as a result of the previous definition. He feels that both enthalpy and entropy contributions have to be considered when one examines the origin of the chelate effect. Among the enthalpy effects which he feels are important are:

1. differences in basicity of donor atoms;
2. distortion of bond angles in the chain of polydentate ligands;
3. group repulsions in polydentate ligands compared with those in monodentate ligands;
4. interligand repulsion;
5. differences in orbital overlap in chelates compared with the simple complexes; and
6. differences in ligand-field effects.

1.1.3. Is it an entropy or enthalpy effect?

The idea that the chelate effect is both an enthalpy and an entropy effect is in keeping with the findings of several other authors.

Myers (32) has shown that values of $\Delta H^{\ominus} \cong 0$ and $\Delta S^{\ominus}$ near the calculated values for the replacement reaction (1.1) can be the result of the confluence of several large and opposing enthalpy and entropy changes. He calculated the enthalpy and entropy changes in the gas phase for some typical chelation reactions in order to estimate the influence of various solvation effects on the chelate effect. Previously the process of

chelation had only been considered in solution.

He found that the enthalpy of solution of the bidentate ligand is not double that of the monodentate ligands, the requirement for the enthalpy change for the chelation reaction to be zero. He also compared the enthalpy change of the replacement reaction (1.1) in the gas phase with that in solution and found that the enthalpy change for a change in ligands (e.g. from methylamine to ethylenediamine), for the same metal ion, is not zero and can be as large as or even larger than the chelate effect. Also, there is no regularity, which makes it impossible to predict the relative strength of metal-ligand bonds.

He found that the entropy changes involved when two bidentate ligands are replaced in solution by four monodentate ligands, differed significantly from the ideal value of 67 J mol^{-1} K^{-1}.

Hence Myers concluded that there are many contributions to the chelate effect. These push the reaction in different directions and are of such different magnitudes that it is probably a coincidence if the standard enthalpy change for a chelation reaction turns out to be near zero and the entropy change is positive and near the theoretical value of 67 J $mol^{-1}K^{-1}$ (for two rings).

Although there undoubtedly is an increase in the translational entropy when molecules are released in solution in the chelation process, the solutions are far from ideal and the actual entropies of solution of all the species are needed. The entropies of solution of the monodentate and chelated cations can differ by as much as 142 J mol^{-1} K^{-1}. Hence Myers feels that it is coincidental if the entropy change for a chelation reaction is close to the ideal value. Similarly the enthalpies of solution of the ligands can differ by as much as 20 kJ mol^{-1} from the ideal value.

Atkinson and Bauman (33) studied the chelate effect with the pyridine and 2,2'-bipyridine complexes of Mn^{2+}, Ni^{2+}, Cu^{2+} and Zn^{2+}. From this study they also concluded that both enthalpy and entropy changes contribute to the chelate effect. They determined $\Delta G^{\ominus}$, $\Delta H^{\ominus}$ and $\Delta S^{\ominus}$ for the reactions:

$$M(py)_2 + bipy \rightleftharpoons M(bipy) + 2py \qquad (1.22)$$

$$M(py)_4 + 2bipy \rightleftharpoons M(bipy)_2 + 4py \cdot \qquad (1.23)$$

They found that for Cu^{2+} and Ni^{2+} the chelate effect was due to the contribution of a large enthalpy term whereas for Mn^{2+} and Zn^{2+} it was due to the entropy term. Crystal field effects were invoked to explain the enhanced stability of the bipyridine complexes of Ni^{2+} and Cu^{2+} since it is observed that the spectroscopic Dq is greater for bipyridine than for pyridine complexes. Mn^{2+}, having a half-filled d-shell, and Zn^{2+}, having a full d-shell, are not stabilized by such effects.

The authors further examined the chelate effect by separating both $\Delta G^{\ominus}$ and $\Delta S^{\ominus}$ into a unitary part dependent on the characteristics of the particles during a reaction, and a cratic term due to a change in the number of particles during a reaction. The values of the unitary portion of the entropy change for reaction (1.22) were found to be negative, thus indicating that considerably more ordering is required to form a chelate ring than to form the corresponding bis-coordinated complex. Further they found that elimination of the cratic term produced positive free energies for the Mn^{2+} and Zn^{2+} complexes in reaction (1.22), thus indicating that the chelated complex is no longer the more stable one. Hence it can be concluded that for these metal ions the enhanced stability observed is due to the increase in the number of particles upon chelate formation. Cu^{2+} and Ni^{2+} remain stabilized by an enthalpy term.

Similarly Spike and Parry (34) observed that for the complexes of Zn^{2+} and Cd^{2+} the increased stability due to chelation is an entropy effect (these two metal ions have no crystal field stabilization energy-CFSE) whereas for the complexes of Cu^{2+} the increased stabilization is accompanied by an increase in the bond strength which is reflected in a larger negative enthalpy term.

In 1977 Munro (20) published a paper which identified the three main misunderstandings over which the chelate effect debate had raged. These are:

(i) the experimentally observed phenomenon of ligand competition;
(ii) the problems associated with the parameters used to quantify the chelate effect; and
(iii) the explanations proposed for the origin of the chelate effect.

By now there is no doubt that metal ions in solution form complexes with polydentate ligands in preference to the analogous monodentate ligands.

Munro points out that although a change in concentration units will lead to a change in the numerical value of the chelate effect it does not necessarily mean that this comparison of stability constants is invalid. He regards these variations as reflecting the fact that 'dissociation of a complex and the extent of competition between ligands depend on the concentrations of solutions in which they are studied'. In agreement with several other authors he feels that concentrations of unit mole fraction are practically unrealisable and hence should not be used.

Although it may seem possible to evade the problem of comparison of equilibrium constants having different units by comparing the corresponding thermodynamic quantities $\Delta G^{\ominus}$, $\Delta H^{\ominus}$ and $\Delta S^{\ominus}$ (which have consistent units), Munro reminds us that the values of $\Delta G^{\ominus}$ and $\Delta S^{\ominus}$ do in fact depend on the choice of concentration for the reference state.

Munro upholds the idea of Schwarzenbach (7) that the chelate effect is an entropy effect arising from the increase in the number of molecules in solution on chelation. Munro used the approach developed by Rasmussen (35) to calculate the entropy change on chelation. However the calculated values were larger than the experimentally observed values. Munro explained this difference in terms of the change in internal entropy of the bidentate ligand on formation of a complex. Hence he concluded that the entropy differences alone are sufficient to give rise to a chelate effect.

Anderegg (36), in reply to Munro's article, points out that for a valid estimation of the entropy of a reaction the partial molar entropies of all the reaction partners must be considered. Munro, he claims, has failed to consider the entropies of the complexes MA_2 and ML.

Munro briefly mentions that 'differences must arise when ligands are con-

strained in a chelated complex and it is likely that there will also be some differences in the bond energy values (ΔE) of monodentate and half-bidentate ligands joined to the cation'. Sanger (37) (in keeping with the idea that the chelate effect is an entropy effect) points out that sometimes these enthalpy effects can be so large and so adverse that they override the favourable entropy change on complex formation and so the chelate effect does not dominate in every case.

Powell (38) points out that Munro has neglected the contribution of $\Delta H^{\ominus}$ to chelation. In his examples Munro unfortunately chose Cd^{2+} to illustrate his ideas. This is an unfortunate choice since for Cd^{2+} the CFSE is zero as Cd^{2+} is a d^{10} ion, and its reactions are largely entropy stabilized.

Atkinson and Bauman (33) have argued that the enthalpy contribution to chelation arises predominantly from the higher CFSE for chelate complexes. A coordinated bidentate ligand generates a larger crystal field splitting energy than does a pair of analogous monodentate ligands.

Powell (38) however feels that to attribute chelate enthalpy change to CFSE alone overlooks two opposing factors. For chelates the basicity will be smaller, thus a reduced σ-bonding strength per donor is predicted. In contrast, chelate stability may be enhanced when the polar donor groups in the chelating ligand are held close together - possibly at an appropriate separation for coordination.

Rode (39) has studied certain quantum chemical aspects of the chelate effect. He has shown, from ab initio calculations on the $Li(HCONH_2)_2^+$ complex in different geometrical arrangements, that for the chelate conformation shown in Figure 1.1 there is a remarkable increase in stability which is not due only to the formation of hydrogen bonds. He concludes that this increase of chelate stabilization energy should be even greater for metal ions of higher atomic number with more polarizable electrons. He also found that in the chelate arrangement a very symmetric distribution of electron density existed between the metal ion and the donor atoms, unlike the distribution in the other geometric arrangements. Hence he showed that the chelate effect was associated with a strikingly different electron density and electronic energy.

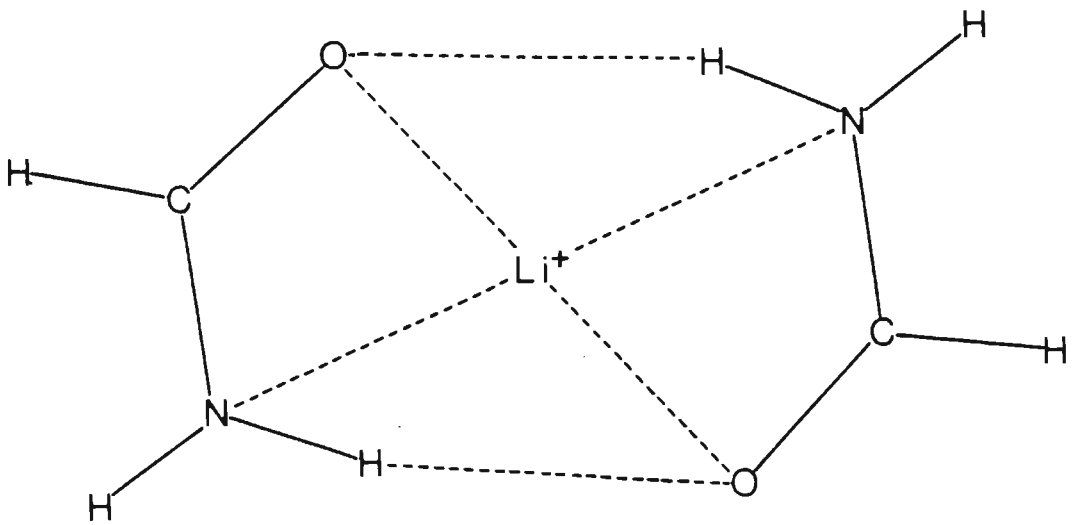

Figure 1.1 The chelate conformation for the $Li(HCONH_2)_2^+$ complex.

Hence the chelate effect is a more complicated process than originally supposed; it is not due merely to the entropy increase resulting from the fact that more molecules of monodentate ligand are liberated in solution than molecules of chelating ligand are used in the reaction. Some of the various enthalpy and entropy factors which contribute to chelate stabilities will now be examined.

1.1.4. Enthalpy and entropy factors contributing to chelate stabilities

Irving *et al.* (40) noted that as the size of the chelate ring increased the stability of the metal complex decreased but the tendency of the ligand to complex with protons increased. This decrease observed was in keeping with Schwarzenbach's (7,14) theory of chelation but his theory underestimated the magnitude of this decrease.

Schwarzenbach's theory assumed that the enthalpy change for the replacement reaction (1.1) was zero and that the chelate effect was determined by entropy considerations. From this it follows that the magnitude of the chelate effect and the magnitude of the stability decrease with ring enlargement should be independent of the metal ions involved. Irving *et al.* found that their experimental data did not support this conclusion. Hence they proposed that Schwarzenbach's theory was oversimplified and that the enthalpy change for the replacement reaction (1.1) need not necessarily be zero and does play a part in the chelate effect.

It was first pointed out by Williams (41) that the decrease in enthalpy associated with metal complex formation can account for the greater stability of chelate complexes. At the time this appeared to contradict the previous assertion by Schwarzenbach (7) that this enhanced effect is due to a more favourable translational entropy change. The fact that the value of $\Delta H^{\ominus}$ greatly influences the stability of a chelate complex is particularly marked for $3d^n$ ions where $n \neq 0$, 5 or 10. Thermodynamic data to illustrate this effect are shown in Table 1.2. Since the only quantity in the equation $\Delta G^{\ominus} = \Delta H^{\ominus} - T\Delta S^{\ominus}$ which is more or less independent of the choice of standard state is the change in enthalpy, it would be most desirable to explain the chelate effect in terms of enthalpy changes.

The study of the thermodynamics of metal-polyamine complex formation has made

TABLE 1.2

Thermodynamic data for the reaction $M(NH_3)_n^{2+} + x(en) \rightleftharpoons M(en)_x^{2+} + n(NH_3)$.

(All the data have been taken from reference 4.)

M^{2+}	n	x	$\Delta G^{\ominus}$/kJmol^{-1}	$\Delta H^{\ominus}$/kJmol^{-1}	$T\Delta S^{\ominus}$/kJmol^{-1}	Conditions
Ni^{2+}	2	1	-14.39	- 8.58	5.86	μ = 1 mol dm^{-3}, t = 25°C
	4	2	-34.14	-16.32	18.09	
	6	3	-55.02	-26.78	28.19	
Cu^{2+}	2	1	-17.61	-12.55	5.11	μ = 1 mol dm^{-3}, t = 25°C
	4	2	-42.26	-22.59	19.59	
Cd^{2+}	2	1	- 5.06	0.38	5.41	μ = 2 mol dm^{-3}, t = 25°C
	4	1	-18.16	- 3.35	14.72	

possible a clarification of the rôle of $\Delta H^{\ominus}$ and $\Delta S^{\ominus}$ in metal-complex formation reactions.

Paoletti *et al.* (42) have put forward a model for the formation of metal-polyamine complexes in aqueous solution in order to interpret the thermodynamic data for the formation of these complexes. The model can be represented by the following equation:

$$M(H_2O)_6.\ell H_2O + L.3H_2O \rightarrow ML(H_2O)_3.nH_2O + (\ell + 6 - n)H_2O.$$

In the above M is the metal ion surrounded by six coordinated water molecules forming the first hydration sphere, and ℓ water molecules are hydrogen bonded to the coordinated water molecules and constitute a secondary hydration sphere. L is a tridentate ligand with one molecule of water bound to each nitrogen atom. Thus water of hydration is liberated from the primary and secondary coordination spheres of the aquo ion and from the uncoordinated ligand.

This model of complex formation reactions between 3d metal ions and chelating amines can account for the exothermic heats of reaction observed, the increase in exothermicity with the successive additions of ligand molecules, and the decrease in $\Delta S^{\ominus}$ with successive steps of the reaction.

It may be noticed that the formation of some chelate complexes from the corresponding complex involving analogous monodentate ligands is favoured by the enthalpy term, whilst others are not.

The more favourable enthalpy change observed in the formation of the chelate complex than in the analogous monodentate complex can be, in part, the result of having overcome the mutually repulsive forces between the donor groups in synthesizing the polydentate chelating ligand (19). Hence the enthalpy effect should manifest itself even more with increasing polarity or charge on the donor groups of the polydentate ligand.

Ligand field effects have also been invoked as contributors to the heats of complex formation (33). Ciampolini *et al.* (43) found, from the values of $\Delta H^{\ominus}$ and $\Delta S^{\ominus}$ for the complexes of ethylenediamine and ammonia, that the chelate effect is in part an enthalpy effect. For the complexes of Ni^{2+} they found that the differences

$$\Delta H^{\ominus}_{Ni(en)_x} - \Delta H^{\ominus}_{Ni(NH_3)_{2x}} \qquad \text{(for } x = 1, 2 \text{ and } 3\text{)}$$

are of the same order of magnitude as the differences in crystal field stabilization energy (CFSE) for the two types of complex. The differences between the heats of formation of the complexes of ammonia and those of ethylenediamine cannot be attributed to the CFSE alone in the case of Cu^{2+} because of the Jahn-Teller effect. In the case of Zn^{2+} one would expect this difference to be zero if it were the result of CFSE only. However Ciampolini *et al.* found that this is not the case, possibly because of geometric and steric factors.

Enthalpy also plays a part in the variation of stability with chelate ring size. As the chain length between the donor groups increases greater coulombic repulsive forces (between charged donor groups) and mutual electrostatic repulsive forces (between dipoles) must be overcome to bring these groups together, and hence formation of the complexes becomes less exothermic. This effect is especially noticeable as one goes from five- to eight-membered rings. From the thermodynamic data given in Table 1.3 for the formation of metal chelates of edta homologues, one observes that the decrease in stability with increasing ring size is mainly an enthalpy effect, because the entropy increase remains about the same as the size of the chelate rings increases from five- to seven-membered (19). One notices a similar trend in the thermodynamic data given in Table 1.4 for the formation of metal chelates with homologues of the uncharged ligand ethylenebis(iminomethylene-2-pyridine) (eimp). For these latter data changes in $\Delta S^{\ominus}$ are small, which again indicates that the variation of stability with chelate ring size is an enthalpy effect. As pointed out by Anderegg (44) this is in contrast to the theory of Schwarzenbach (7) which predicts a decrease in $\Delta S^{\ominus}$ of about 25 J $mol^{-1}K^{-1}$ for an increase of one in the chelate ring size and a constant value of $\Delta H^{\ominus}$. For polyamine complexes this increasing endothermicity with increasing chelate ring size is caused by the greater ring strain in the higher homologues. An example of this can be observed in a comparison of the structural and thermodynamic parameters of the complexes $[Cu(en)_2]^{2+}$ and $[Cu(tn)_2]^{2+}$ shown in Figure 1.2. In the latter compound the bond angles are appreciably distorted so that the nitrogen atoms in the ligand are unfavourably orientated for the donation of a lone pair to the Cu^{2+} ion. This results in

TABLE 1.3

Thermodynamic data for the formation of metal chelates of edta homologues. (All data are at μ = 0.1 mol dm^{-3} and t = 20°C, and have been taken from reference 4.)

M^{2+}		edta [a]	pdta [b]	bdta [c]
Mn^{2+}	$\Delta G^{\ominus}$/kJmol^{-1}	- 77.45	- 56.07	- 53.48
	d $\Delta H^{\ominus}$/kJmol^{-1}	- 19.08	- 3.01(?)	14.27
	$\Delta S^{\ominus}$/J K^{-1} mol^{-1}	199.2	221.3 (?)	231.0
Co^{2+}		- 91.53	- 87.27	- 87.89
	d	- 17.57	- 10.88	- 6.69
		252.3	260.2	277.4
Ni^{2+}		-104.50	-101.86	- 97.43
	d	- 31.59	- 27.87	- 29.08
		248.5	252.3	232.2
Cu^{2+}		-105.51	-106.18	- 97.26
	d	- 34.10	- 32.38	- 27.28
		243.5	251.5	238.5
Zn^{2+}		- 92.60	- 85.64	- 84.24
	d	- 20.29	- 9.50	- 14.56
		246.9	258.6	237.7
Cd^{2+}		- 92.38	- 78.01	- 67.46
	d	- 37.87	- 22.76	- 12.05
		185.8	188.3	189.1

[a] edta = $(CH_2CO_2H)_2NCH_2CH_2N(CH_2CO_2H)_2$, 1,2-diamino-N,N,N',N'-tetraacetic acid ethane.

[b] pdta = $(CH_2CO_2H)_2N(CH_2)_3N(CH_2CO_2H)_2$, 1,3-diamino-N,N,N',N'-tetraacetic acid propane.

[c] bdta = $(CH_2CO_2H)_2N(CH_2)_4N(CH_2CO_2H)_2$, 1,4-diamino-N,N,N',N'-tetraacetic acid butane.

TABLE 1.4

Thermodynamic data for the formation of metal chelates of eimp homologues. (All data are at μ = 0.1 mol dm^{-3} and t = 25°C, and have been taken from reference 44.)

M^{2+}		eimp [a]	pimp [b]	bimp [c]
Mn^{2+}	$\Delta G^{\ominus}$/kJmol^{-1}	-31.8	-25.5	-15.1
	d $\Delta H^{\ominus}$/kJmol^{-1}	-18.8	-13.4	- 0.8
	$\Delta S^{\ominus}$/ J K^{-1} mol^{-1}	43.5	40.6	47.7
Co^{2+}		-68.2	-64.0	-45.6
	d	-59.4	-55.2	-35.1
		29.3	29.3	35.1
Ni^{2+}		-82.8	-81.2	-63.6
	d	-72.8	-68.2	-51.9
		33.5	43.5	39.3
Cu^{2+}		-97.1	-104.6	-88.7
	d	-76.1	-84.1	-70.3
		70.3	68.6	61.9
Zn^{2+}		-63.6	-59.0	-43.9
	d	-47.3	-40.6	-24.7
		54.8	61.9	64.4
Cd^{2+}		-55.2	-49.0	-40.2
	d	-40.6	-32.6	-28.0
		49.0	54.8	40.6

[a] eimp = ethylenebis(iminomethylene-2-pyridine)

[b] pimp = propylenebis(iminomethylene-2-pyridine)

[c] bimp = butylenebis(iminomethylene-2-pyridine)

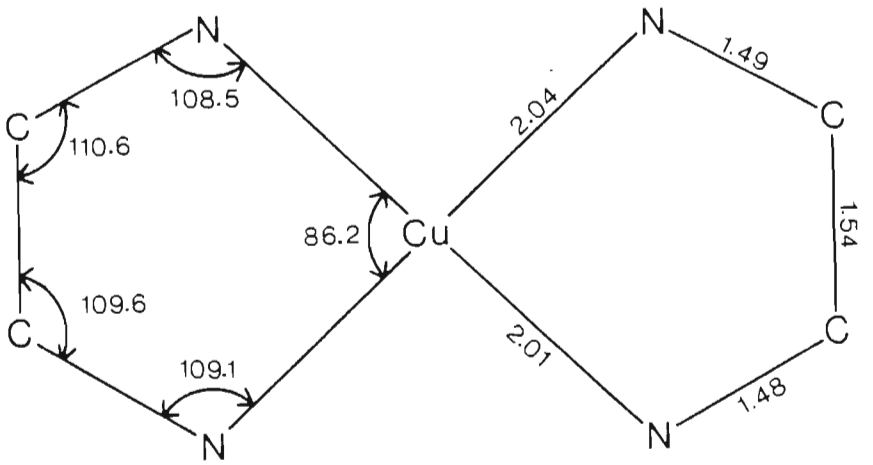

$$\log K = 19.7$$

$$-\Delta H^{\ominus} = 105 \text{ kJ mol}^{-1}$$

$$\Delta S^{\ominus} = 24 \text{ J K}^{-1} \text{ mol}^{-1}$$

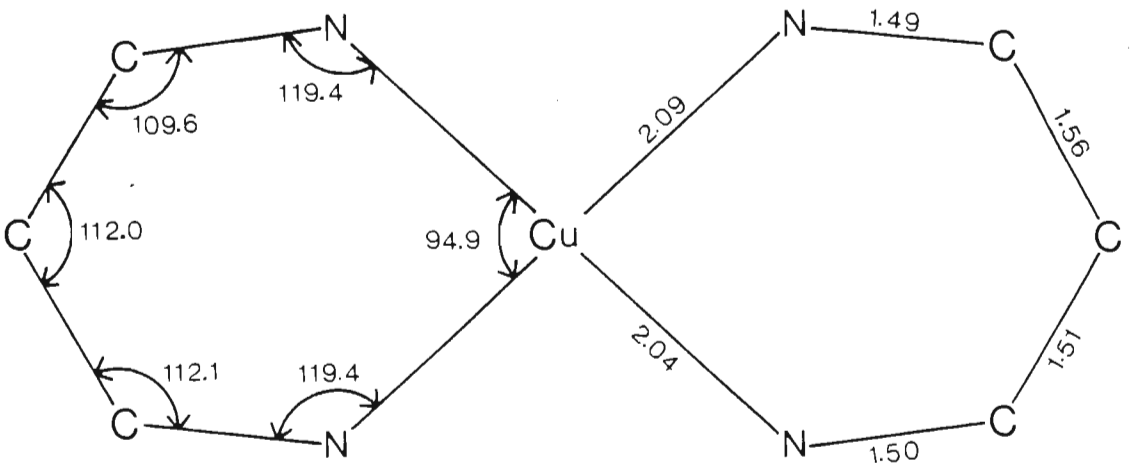

$$\log K = 17.3$$

$$-\Delta H^{\ominus} = 92.0 \text{ kJ mol}^{-1}$$

$$\Delta S^{\ominus} = 23 \text{ J K}^{-1} \text{ mol}^{-1}$$

Figure 1.2 Structural and thermodynamic parameters for the complexes of Cu^{2+} with ethylenediamine and 1,3-diaminopropane. (Taken from reference 42.)

the formation of a weaker bond and hence a less exothermic reaction. As can be seen the higher stability of the complex having five-membered rings is entirely due to a more favourable enthalpy term.

Paoletti *et al.* (46) determined the crystal structures of $Ni(dpt)_2(Cl O_4)_2$ and $Ni(dien)_2Cl_2.H_2O$ in order to confirm the enhanced stability of five-membered rings compared with six-membered rings, and to study the nature of the strain. It was found that in the former compound the Ni- secondary N bond lengths are approximately 0.2 Å longer than in $Ni(dien)_2^{2+}$, which possibly accounts for the lower enthalpy of formation of the compound. Also the six-membered rings were found to be strained due to ligand-ligand interactions.

McDougall *et al.* (47) have shown quantitatively, by means of empirical force-field calculations, that the difference in the enthalpy of formation between five- and six-membered chelate rings is due mainly to steric strain in polyamines. These authors calculated the differences between the total conformational energies of the complexes $Ni(en)_3^{2+}$ and $Ni(tn)_3^{2+}$, and between $Ni(dien)_2^{2+}$ and $Ni(dpt)_2^{2+}$. However these values had to be corrected for the difference in strain energy between the two free ligands. The difference in strain energy between en and tn was found to be 1.15 kJ mol^{-1}. Hence it was assumed that the increase in the total strain energy of a molecule on the introduction of an extra methylene group is 1.15 kJ mol^{-1}. The results obtained by these authors are summarized in Table 1.5.

From the table one can see that the values of ΔU obtained agree fairly well with the differences in $\Delta H^{\ominus}$ between the five- and six-membered chelate ring complexes. This supports the idea that six-membered polyamine chelate rings are less stable than five-membered polyamine chelate rings because of strain considerations, and the effect is exhibited in a smaller negative enthalpic contribution to $\Delta G^{\ominus}$.

It has also been noticed that when two or more rings are fused a further decrease in the exothermicity of the heat of reaction occurs (45). This appears to be so because the increased accumulation of strain in the molecule leads to a destabilization of the coordinate bonds formed relative to those formed in the analogous complexes having separate chelate

TABLE 1.5

Results obtained from empirical force-field calculations by McDougall *et al.* (47) for the Ni^{2+} complexes of polyamines.*

	en	tn	$Ni(en)_3^{2+}$	$Ni(tn)_3^{2+}$	$Ni(dien)_2^{2+}$	$Ni(dpt)_2^{2+}$
Total conformational potential energy, $U/kJmol^{-1}$	3.72	4.87	19.12	54.85	49.62	89.16
Difference in strain energy, $\Delta U/kJmol^{-1}$		1.15		35.73		39.54
Strain energy corrected for additional methylene groups				32.30		34.94
Difference in enthalpy change on complex formation, $\Delta(\Delta H^{\ominus})/kJmol^{-1}$				27.61		31.80

*All data are as given in reference 47.

rings. This effect is illustrated by the data presented in Table 1.6 for the formation of complexes with the tridentate ligands dien (two linked consecutive 5-membered rings) and dpt (two linked consecutive 6-membered rings), and the quadridentate ligands trien (three linked 5-membered rings) and 3,3,3-tet (three linked consecutive 6-membered rings) as compared with the formation of the analogous complexes of en and tn, which have unconnected 5- and 6-membered chelate rings respectively. (For the full names and formulae of the ligands mentioned see the Glossary of Abbreviations.) However it has been found that this lower heat of complexation occurs only when the fused chelate rings are of the same size (42).

The nickel complex with the ligand 2,3,2-tet, which has two five-membered rings with a central six-membered ring, is much more stable than the analogous complex $Ni(trien)^{2+}$ because of a very high (exothermic) heat of reaction. (See Table 1.6.) Thus the introduction of a methylene group in the central ring of three linked consecutive five-membered rings removes some of the increased strain of the external five-membered rings, and this is reflected in a greater (exothermic) heat of complex formation. Similarly the complex $Ni(3,2,3\text{-tet})^{2+}$, in which the ring sequence is 6, 5, 6, shows enhanced stability because of a more favourable enthalpic contribution on formation.

Boeyens *et al.* (48) extended the work of McDougall *et al.* (47) by including parameters for the coordinated water molecules in the strain energy calculations previously performed. They also calculated the difference in strain energy, ΔU, between the two complexes $Ni(2,3,2\text{-tet})^{2+}$ and $Ni(trien)^{2+}$. However they found that the difference in U, viz. 7.66 kJ mol^{-1}, is in poor agreement with the difference of 19.66 kJ mol^{-1} in $\Delta H^{\ominus}$ for the two complexes. Nevertheless the lower value of U for the $Ni(2,3,2\text{-tet})^{2+}$ complex is in accord with the suggestion that the inserted six-membered ring stabilizes the complex by release of cumulative ring strain. This, according to Boeyens *et al.* (48), is to be expected since the alternating sequence of chelate rings allows closer accommodation of the 90° angles required in octahedral coordination.

This alternating sequence of chelate rings is also found to favour the formation of stronger coordinate bonds (reflected in a greater negative enthalpy of formation) for triamines. It can be seen from the data in Table 1.6 that the complexes formed with the ligand 2,3-tri (ring sizes

TABLE 1.6

Thermodynamic data for the formation of various Ni^{2+} - polyamine complexes. ($Ni^{2+} + nL \rightleftharpoons NiL_n^{2+}$) (All data taken from reference 4 or reference 42.)

L	n	$\Delta H^{\ominus}$/kJmol^{-1}	$T\Delta S^{\ominus}$/kJmol^{-1}
dien	2	-105.86	0.0
en	3	-117.19	-17.5
dpt	2	- 73.81	- 1.1
tn	3	- 89.12	-20.7
trien	1	- 58.58	20.0
en	2	- 72.17	4.2
3,3,3-tet	1	- 55.23	4.6
tn	2	- 62.76	- 1.4
2,3,2-tet	1	- 74.89	18.8
3,2,3 -tet	1	- 80.29	3.6
dien	1	- 49.58	10.6
dpt	1	- 44.18	8.2
2,3-tri	1	- 56.48	7.4

5 and 6) are more stable than the analogous complexes formed with dien (ring sizes 5 and 5) and dpt (ring sizes 6 and 6).

Powell (38,49) disputes the conclusion that a combination of alternating five- and six-membered chelate rings in a ligand imparts extra stability to a complex because of the release of accumulated ring strain. He suggests that other authors have overlooked the fact that ligands with different combinations of ring sizes are of different basicity. Thus when comparing the relative stabilities of the complexes formed we are considering the combined effect of both ligand basicity and the stability associated with ring size. Powell suggests that, in order to study only the stability associated with ring size, we consider the thermodynamic functions for the following reaction:

$$ML^{2+} + nH^{+} \rightleftharpoons M^{2+} + H_nL^{n+} \quad . \qquad (1.24)$$

If this is done we see that (both for triamines and for tetra-amines) the greatest ring stability is for linked 5-membered chelate rings, in spite of ring strain. This conclusion is at variance with those of others, and Powell suggests that others have in fact neglected a certain destabilizing effect. They have (he claims) ignored the fact that, for a larger chelate ring to be formed, it is necessary that the mutually repelling forces of the dipoles (or charges) be overcome. This is an endothermic effect, and so destabilizes the complex.

Thus in the heats of complex formation obtained is reflected the ability of the ligand to position its donor atoms in such a way that stronger bonds are formed and the resulting complex is relatively free of steric strain. This ability on the part of the ligand depends on its structure, the length of the chain joining the donor atoms, and the electronic requirements of the metal ion (42).

In some cases complexation is favoured by an increase in the entropy of complex formation as was noticed with the thermodynamic data given in Table 1.1.

Williams (41) stated that favourable entropy increases occur whenever positive and negative ions combine in aqueous solution, i.e. when complexes

are formed by displacement of water molecules from the hydrated constituents. The reason is that solvated water molecules are released on charge neutralization. The entropy must increase in such cases because the product is always much less hydrated than the reactants, and hence the number of particles on the right hand side of the reaction equation is greater than that on the left.

An example of this is the formation of metal-carboxylate complexes (12). In most of these complexes the associated heats of formation are endothermic. Nevertheless the complexes are stabilized by the accompanying relatively large positive entropy changes because of the liberation of water molecules from the ions on complex formation. Data illustrating this are given in Table 1.7.

Similar stabilization through positive entropy changes is observed for the formation of metal complexes with aminopolycarboxylate ligands (12).

Thus complexes formed through predominantly electrostatic interactions between hard acids and hard bases are entropy-stabilized. The accompanying enthalpy changes are usually small and endothermic, reflecting the energy required to remove the coordinated water molecules from the hydration spheres of the ions. In such cases the tendency of the system to go to the most random state outweighs the strength of the bonds formed and hence such complexes are entropy-stabilized.

Complexes formed between soft acids and soft bases, where coordinate bonds with a high covalent character are formed, are enthalpy-stabilized. This is to be expected since the enthalpy change is the quantity most directly related to the changes in the numbers and strengths of the bonds. In such cases the entropy change becomes increasingly negative as the softness of the interacting species increases (12). This effect is exhibited by metal-polyamine complexes with successive steps of complex formation.

It is interesting to note that polyamines do not form stable complexes with hard cations (e.g. Ca^{2+}) in aqueous solution. Nevertheless when nitrogen donors are combined with carboxylate groups the resulting aminocarboxylate ligands can form complexes with both hard and soft cations. For example,

TABLE 1.7

Thermodynamic data for the formation of various metal-carboxylate complexes. ($M^{2+} + L^{2-} \rightleftharpoons ML$)

(All data have been taken from reference 12 and are valid at μ = 0 mol dm^{-3} and t = 25°C.)

L^{2-}	M^{2+}	$\Delta G^{\ominus}$/kJmol^{-1}	$\Delta H^{\ominus}$/kJmol^{-1}	$T\Delta S^{\ominus}$/kJmol^{-1}
Oxalate	Co^{2+}	-27.36	2.47	29.81
	Ni^{2+}	-29.50	0.63	30.19
	Cu^{2+}	-35.52	- 0.21	35.30
Malonate	Co^{2+}	-21.46	12.13	33.56
	Ni^{2+}	-23.43	7.87	31.19
	Cu^{2+}	-32.17	11.92	44.16
Succinate	Co^{2+}	-12.67	13.18	25.82
	Ni^{2+}	-13.41	10.29	23.70
	Cu^{2+}	-18.49	19.08	37.55

ethylenediamine forms complexes with Ni^{2+} but not with Ca^{2+}, yet edta forms complexes with both Ni^{2+} and Ca^{2+}.

As in the case of the enthalpy changes, steric considerations also appear to affect entropy changes. For example (19), in the complexes of Zn^{2+} with the linear ligand trien and the tripod-like ligand tren, one would expect the $Zn(tren)^{2+}$ complex to have the more positive entropy change since the ligand molecule is attached to the metal ion in a more 'natural' configuration, i.e. less change has occurred in the conformation of this ligand on complex formation. The thermodynamic data for the formation of these two complexes are given in Table 1.8. A larger exothermic enthalpy change is observed for the $Zn(tren)^{2+}$ complex than for $Zn(trien)^{2+}$. This is due to the lower energy required to overcome the mutually repulsive forces between the donor groups of tren. The higher enthalpy change reflects the greater strength of the coordinate bonds formed. This greater strength reduces the ligand vibrational and rotational entropy, and thereby accounts for the surprisingly low value of the entropy change for $Zn(tren)^{2+}$ (19).

Thermodynamic data have been used as evidence in favour of proposed stereochemistries for various complex ions (42,50). For example, from a comparison of the $\Delta S^{\ominus}$ values for the complexes of Co^{2+} with the two ligands trien and tren it has been suggested (42) that the complex formed with trien is octahedral and that that formed with tren is penta-coordinated, since in the latter compound at least one more molecule of water would be liberated and this would be expected to increase the translational entropy and the overall entropy change.

Similarly the collection of thermodynamic data has made possible the rationalisation of the formation of protonated and hydroxo-metal-polyamine complexes (42).

It has been observed that the complexes of metal ions, e.g. Ni^{2+}, with cyclised polyamines such as cyclam (1,4,8,11-tetraazacyclotetradecane) are very much more stable than their open-chain analogues. This observation has been termed the macrocyclic effect (and is really a special case of the chelate effect).

TABLE 1.8

Thermodynamic data for the formation of the complexes of Zn^{2+} with the ligands 1,2-diamino-N,N'-di-(2-aminoethyl)ethane (trien) and tri(2-aminoethyl)amine (tren). (All data are at μ = 0.1 mol dm^{-3} and t = 25°C, and have been taken from reference 4.)

Reaction	$\Delta G^{\ominus}$/kJmol^{-1}	$\Delta H^{\ominus}$/kJmol^{-1}	$T\Delta S^{\ominus}$/kJmol^{-1}
Zn^{2+} + trien $\rightleftharpoons$ $Zn(trien)^{2+}$	-68.61	-37.24	31.2
Zn^{2+} + tren $\rightleftharpoons$ $Zn(tren)^{2+}$	-82.65	-57.95	24.3

Fabbrizzi *et al.* (51) have shown (in the case of cyclam) that this increased stability is due in equal parts to enthalpy and entropy effects.

It is generally accepted that the higher entropy changes observed are due to the smaller configurational entropy of the macrocycle. That is, the open-chain ligand loses entropy in going from a state in which the ligand has many possible configurations to one in which it has a fixed configuration. The macrocycle, on the other hand, is already in a rigid configuration prior to complexation and so no such loss of entropy occurs.

Various explanations have been put forward for the increased enthalpy change observed. Hinz *et al.* (52) suggested that it arose because of steric hindrance to solvation of the nitrogen donor atoms. McDougall *et al.* (47) have suggested that because the macrocycle has an almost identical configuration to that which it assumes in the complex, the unfavourable increase in strain energy of the ligand on complex formation is much smaller, i.e. the macrocycle is 'prestrained'.

Hancock and McDougall (53,54) have extended their empirical force-field calculations for Ni-polyamine complexes to include complexes of Ni with macrocycles. They calculated the difference $\Delta U_{cyclic} - \Delta U_{noncyclic}$, where ΔU_{cyclic} and $\Delta U_{noncyclic}$ refer to the increase in U on complex formation for the complexes $Ni(cyclam)(H_2O)_2^{2+}$ and $Ni(2,3,2\text{-tet})(H_2O)_2^{2+}$ respectively. They found that this difference agreed fairly well with the difference in $\Delta H^{\ominus}$ between these two complexes. The predicted difference had however been corrected for the presence of secondary nitrogen donors (since it had previously been assumed (29), on the basis of empirical force-field calculations, that a Ni-secondary nitrogen bond is 7.1 kJ mol^{-1} more exothermic than a Ni-primary nitrogen bond). Thus they postulated that the main contributors to the enthalpy changes accompanying the formation of macrocycle complexes are the presence of a large number of secondary nitrogen donor atoms and the abovementioned high value of the conformational potential energy of the macrocyclic ligand.

Table 1.9 summarizes the various factors which influence the chelation process.

TABLE 1.9

Enthalpy and entropy factors influencing solution stabilities of chelate complexes. (This table is taken from Table 1 in reference 32.)

Enthalpy Effects	Entropy Effects
Variation of bond strength with electronegativities of metal ions and ligand donor atom.	Number of chelate rings.
Ligand field effects.	Size of chelate ring.
Steric and electrostatic repulsion between ligand donor groups in the complex.	Changes of solvation on complex formation.
Enthalpy effects related to the conformation of the uncoordinated ligand.	Arrangement of chelate rings.
Other coulombic forces involved in chelate ring formation.	Entropy variations in uncoordinated ligands.
Enthalpy of solution of ligands.	Effects resulting from differences in configurational entropies of the ligand in complex compounds.
Change of bond strength when ligand is changed (same donor and acceptor atom).	Entropy of solution of ligands.
	Entropy of solution of coordinated metal ions.

1.1.5. Attempts to estimate enthalpy changes

As previously mentioned (see page 20), it is of considerable interest to estimate the enthalpy contribution to the chelate effect. Attempts have therefore been made to predict and perhaps explain the enthalpy changes for complex formation reactions and we now discuss several such attempts.

Barbucci and Barone (55) have put forward an equation for calculating the enthalpies of protonation of polyamines. The enthalpies are calculated as the sum of E_B, the enthalpy for the formation of the new N^+-H bond, and E_S, the solvation energy. The values of $\Delta H^{\ominus}$ for the first protonation of en and (2,3-tri) are set equal to their experimental values. Hence the stepwise protonation enthalpies for all diamines are calculated from

$$\Delta H^{\ominus}(\text{diamine}) = \Delta H_1^{\ominus}(\text{en}) + E_B + E_S, \qquad (1.25)$$

and for all other polyamines from

$$\Delta H^{\ominus}(\text{polyamine}) = \Delta H_1^{\ominus}(\text{2,3-tri}) + E_B + E_S \ . \qquad (1.26)$$

In the calculation of E_B and E_S only inductive and electrostatic effects are taken into account. This model seems to reproduce the experimental heats of protonation of di-, tri-, tetra-, penta- and hexa-amines fairly well.

Previously Paoletti *et al.* (56) had suggested an empirical formula for the prediction of enthalpies of protonation of amines. The formula had the form

$$-\Delta H = \alpha + \Sigma\, \delta_i, \qquad (1.27)$$

where α has an experimentally determined fixed value depending on whether the nitrogen atom being protonated is primary, secondary or tertiary, and the δ_i's are the effects of the carbon and nitrogen atoms on the protonation of the amine. Satisfactory agreement was found between the calculated and experimental stepwise and overall heats of protonation of monoamines and symmetric diamines. For asymmetric diamines and polyamines only the predicted overall enthalpy change was in reasonable agreement with the experimentally determined value. Hence an explanation based on a tautomeric equi-

librium between a species protonated on the primary nitrogen and one protonated on the secondary or tertiary nitrogen was invoked to explain this deviation. However it was later shown (57) that there is no tautomeric equilibrium in the protonation of triamines.

Christensen *et al.* (58) also proposed an empirical formula for the estimation of enthalpy and entropy changes of protonation of primary and secondary aliphatic monoamines. Their equation arose through the observation that $\Delta H^{\ominus}$ and $\Delta S^{\ominus}$ values for proton ionization of primary and secondary protonated monoamines increase in a regular, additive way as more methyl groups are added to the carbon chain. The equation has the form

$$\Delta X^{\ominus} = \Delta X^{\ominus}_{m} + n_{\alpha} X_{\alpha} + n_{\beta} X_{\beta} + n_{\gamma} X_{\gamma} , \qquad (1.28)$$

where X can represent either H or S. The value of $\Delta X^{\ominus}_{m}$ is the appropriate value for protonated methylamine or dimethylamine depending on whether a primary or a secondary amine is being considered. n_{α}, n_{β} and n_{γ} are the numbers of carbon atoms in the α, β and γ positions relative to the carbon atom adjacent to the protonated amine group. X_{α}, X_{β} and X_{γ} are the increases in the appropriate quantities caused by the addition of methyl groups on the said positions. These values were calculated from selected experimental data. The values calculated for proton ionization of the monoamines were found to be in fair agreement with the experimental values except in the case of cyclopropylamine. This discrepancy was thought to be the result of ring strain effects which were not present in the other amines considered.

Degischer and Nancollas (59) have interpreted the enthalpy changes for the formation of a variety of metal complexes with nitrogen- and carboxylate oxygen-containing ligands. Since $\Delta H^{\ominus}$ values reflect the changes in the numbers and strengths of bonds made and broken during the reactions, the authors related the $\Delta H^{\ominus}$ values to the type of bonding between the metal ion and the ligand, and to the structural features of the complex.

They applied the idea (first suggested by Gurney (60)) of separating the work required for the dissociation of a metal complex into those contributions due to electrostatic forces depending on the environment and the temperature, and those contributions due to covalent interactions and independent of temperature. They then related these two quantities to

the total free energy change for dissociation of the complex. Hence they obtained an expression for the enthalpy change due to electrostatic interactions:

$$\Delta H_e = (T - \upsilon)\ (\Delta S + \Delta n\ R\ \ell n\ 55.5)\,, \qquad (1.29)$$

and one for the enthalpy change due to covalent interactions:

$$\Delta H_c = \Delta H - \Delta H_e$$

$$= \Delta H - (T - \upsilon)\ (\Delta S + \Delta n\ R\ \ell n\ 55.5)\,, \qquad (1.30)$$

where υ is a temperature characteristic of the solvent and has a value of 219 K for water, and Δn is the decrease in the number of solute particles.

These authors have calculated ΔH_c values for a number of nitrogen- and carboxylate oxygen-donor ligands with the metal ions Ni^{2+}, Co^{2+}, Cu^{2+} and Zn^{2+}.

From these values various trends were observed. It was noted that the nitrogen donors form much stronger covalent bonds than do carboxylate oxygen donors, and that where both donors are present in the ligand the former donors make the major contribution to ΔH_c. The values of ΔH_c also reflect the decrease in stability as one goes from a five-membered chelate ring to a seven-membered chelate ring. (This latter effect is not observed in the values of ΔH_c for Co^{2+}.)

In order to correct the ΔH_c values for the varying number (p) of nitrogen donor atoms per ligand, values of $-\Delta H_c/p$ were calculated.

From these latter values the authors realised that structural/strain effects could not be ignored. Hence they devised a simple equation for interpreting ΔH_c in terms of the additive contributions due to M^{2+}-N and M^{2+}-O bonds, and a term for structural effects, i.e.

$$\Delta H_c = \Delta H(M^{2+}\text{-}N) + \Delta H(M^{2+}\text{-}O) + \Delta H(\text{structure})\,. \qquad (1.31)$$

Values of ΔH(structure) were calculated for various Ni^{2+} complexes from this equation by substituting the enthalpies of formation of the monoammine and

monoacetate complexes for $\Delta H(M^{2+}\text{-}N)$ and $\Delta H(M^{2+}\text{-}O)$ respectively.

Some of the trends previously mentioned in this chapter were found to be reflected in the values of ΔH(structure). For example, ΔH(structure) was found to have fairly large endothermic values in complexes in which strain existed or six-membered (or larger) chelate rings were present. These ΔH(structure) values were exothermic in the case of aminocarboxylate complexes, which indicates a stabilizing contribution to chelate ring formation when both nitrogen and oxygen donors (as opposed to only nitrogen donors) are coordinated to the metal ion. This bears out Schwarzenbach's conclusion that 'when ligand molecules contain more than two potential donor atoms, the presence of a nitrogen atom enables the special structural requirements to be met for the formation of relatively strain-free chelate rings' (12).

Hancock *et al.* (29) have proposed that the enthalpy change for metal-polyamine complex formation be estimated from the corresponding metal-ammonia heat of formation by use of the following equation:

$$\Delta H(\text{polyamine}) = nf\ \Delta H_1(NH_3) + \frac{n}{2}(n - 1)\ \lambda_H \ . \qquad (1.32)$$

This equation was derived by analogy with a previously reported equation (28)(equation (1.17)) used for the estimation of the stability constants of metal-polyamine complexes (with five-membered chelate rings) from the stability constants of the analogous ammonia complexes.

In these equations n is the number of nitrogen donor atoms. The factor of 1.152 in equation (1.17) used to account for the inductive effect of the ethylene bridges is paralleled by the factor f in equation (1.32). The value of f cannot be determined in a manner analogous to that used for equation (1.17), i.e. from an LFER (linear free energy relationship), because LER's (linear enthalpy relationships) do not pass through the origin. From an LER involving non-heterocyclic nitrogen donors a value of 1.16 was estimated for the inductive effect factor f for Ni^{2+}. However it was found empirically that a better value of f was 1.19 for both Ni^{2+} and Co^{2+}.

The term (n-1) log 55.5 in equation (1.17) accounts for the asymmetry of

the standard state, but since this is an entropy term it does not appear in equation (1.32).

In equation (1.17) the term in λ was introduced to account for the steady decrease in log $K_n(NH_3)$ as more ligands are added. In ammonia complexes this decrease manifests itself in unfavourable entropy changes. However, in polyamine complexes, the decrease in log K_1(polyamine) with an increase in the number of chelate rings is an enthalpy effect. Thus the term in λ has, for polyamine complexes, been interpreted (29) as being of largely steric origin, and relating to steric strain developed in the polyamine ring system. From strain energy calculations (47,48) it appeared that there were large increases in U (the conformational potential energy) on complex formation with polyamines, and it was suggested that the term in λ allowed for this fact. Hence a term of this form was retained in equation (1.32), which relates to energy changes taking place on complex formation.

It was found empirically that a best-fit value for λ_H was 2.47 kJ mol^{-1} for both Co^{2+} and Ni^{2+}. With this value of λ_H, equation (1.32) was used (29) to generate values of $\Delta H^{\ominus}$ which were in fair agreement with experimentally determined $\Delta H^{\ominus}$ values for polyamine complexes containing five-membered chelate rings.

The value of the term in λ_H was interpreted as a measure of the decrease in $\Delta H^{\ominus}$ per nitrogen atom as more chelate rings are added to the complex. This decrease was thought to be the result of steric effects. To test this hypothesis Hancock *et al.* (29) calculated ΔU as defined by the following equations:

$$\begin{array}{ccccc} & & \Delta U & & \\ M & + & L & \rightarrow & ML \\ U_M & & U_L & & U_{ML} \end{array}$$

$$\Delta U = U_{ML} - U_M - U_L \ ,$$

for the complexes of Ni^{2+} with en, dien, trien, tetren and penten, and compared the values of ΔU thus obtained with the corresponding term in λ_H used in equation (1.32).

It was found that the value of ΔU increased with an increase in the number of chelate rings, as did the corresponding value of the term in λ_H, and that the values of ΔU were higher than those of the term in λ_H. The authors attributed this discrepancy to the differences in bonding capacity of primary, secondary and tertiary nitrogen donors. It was felt that in the absence of steric effects Ni-secondary nitrogen bonds should be stronger than Ni-primary nitrogen bonds. Since steric effects had already been taken into account, a correction of 7.1 kJ mol^{-1} for this increased exothermicity was made. After this correction had been made, good agreement between the values of ΔU and the term in λ_H was obtained.

The idea that the bond between a metal ion and a secondary nitrogen atom should be stronger than the bond between a metal ion and a primary nitrogen atom (if steric effects are absent) is reinforced by the following arguments. A similar tendency is observed in the heats of protonation of amines such as methylamine, dimethylamine and trimethylamine in the gas phase. For these amines the strength of bonding to nitrogen increases along the series $CH_3NH_2 < (CH_3)_2NH < (CH_3)_3N$ (61). This basicity order is not observed in aqueous solution, apparently because of solvation and steric effects (62, 29). The work of Drago *et al.* (63) has also lent support to the idea that Ni-secondary nitrogen bonds should be stronger than Ni-primary nitrogen bonds. Of the Lewis acids considered by Drago *et al.* (63), the one which most closely resembles Ni^{2+} is $Cu(hfac)_2$ (where hfac denotes the hexafluoroacetylacetonate anion). With Drago's E and C equation, the heats of reaction of $Cu(hfac)_2$ with the methylamines CH_3NH_2, $(CH_3)_2NH$ and $(CH_3)_3N$ can be calculated as -52.9, -66.6 and -79.1 kJ mol^{-1} respectively, after one has excluded the influence of steric effects (64). These figures seem to justify the conclusion that Ni-secondary nitrogen bonds are more exothermic than Ni-primary nitrogen bonds (and Ni-tertiary nitrogen bonds are more exothermic than Ni-secondary nitrogen ones).

As stated earlier, the argument that secondary nitrogen donors form stronger bonds than do primary donors has also been used to explain why the macrocyclic ligand cyclam, with four secondary nitrogen donors, forms complexes that are enthalpically more stable than those of its open-chain analogue 2,3,2-tet, which has two primary and two secondary nitrogen donors (53,54).

Hancock *et al.* (29) also calculated ΔH values for the various polyamine

complexes, evidently by using an equation of the form:

$$\Delta H = n_p \Delta H_p + n_s \Delta H_s + \Delta U \ . \qquad (1.33)$$

Here n_p and n_s are the numbers of primary and secondary nitrogen donors respectively, and ΔH_p and ΔH_s are the enthalpy contributions per primary and secondary nitrogen donor atom present. The value of -20.1 kJ mol^{-1} used for ΔH_p was obtained as follows. For $[Ni(en)(H_2O)_4]^{2+}$, ΔH is -37.7 kJ mol^{-1} and ΔU is 2.55 kJ mol^{-1}. A "strain-free" ΔH can therefore be expected to equal -40.2 kJ mol^{-1}, and ΔH_p half this value. (The ΔH value for the ammonia complex was not used as it lacks the inductive effect of the ethylene bridges.) The value used for ΔH_s was -27.2 kJ mol^{-1} i.e. 7.1 kJ mol^{-1} less than ΔH_p. The ΔU value for each complex was calculated as described previously. The agreement between the observed ΔH values and the values calculated in this fashion was good.

The fact that the same form of term in λ works for predicting free energy changes and enthalpy changes was not thought to be significant. In equation (1.17) the term in λ was introduced to account for the statistical (and hence entropy) effect involved in the addition of an increasing number of monodentate ligands to the complex. In equation (1.32) the term in λ represents an unfavourable enthalpy contribution composed of two opposing terms:

1. the cumulative ring strain obtained on adding successively more rings to the complex as the polyamine ligand becomes larger (producing a decrease in exothermicity); and

2. the increase in exothermicity produced by increasing the number of secondary nitrogen donors as the number of rings is increased.

1.2. Outline of the project

The aim of this project is to test experimentally the assertion that, in the absence of ring strain effects, the formation of Ni-secondary nitrogen bonds in aqueous solution is enthalpy-stabilized, compared with Ni-primary nitrogen bonds, by some 7.1 kJ mol^{-1} (29). To this end, $\Delta G^{\ominus}$, $\Delta H^{\ominus}$ and $\Delta S^{\ominus}$ were determined for the formation of the complexes of Ni^{2+} with the fol-

lowing two ligands: 2,2'-oxybisethanamine [oden ≡ $(H_2NCH_2CH_2)_2O$] and 2-(2-aminoethyl)aminoethanol [etolen ≡ $HO(CH_2)_2NH(CH_2)_2NH_2$], which have the structures shown in Figure 1.3.

The proposed comparison to be made of oden and etolen was extended to include the metal ions Co^{2+} and Zn^{2+}, in order to test whether the assertion is also valid for different metal ions.

These two ligands differ principally in that oden has two primary nitrogen atom donors, whereas etolen has a secondary nitrogen atom as well as a primary nitrogen atom donor. (They also differ in that oden has an ethereal oxygen donor atom, whereas etolen has an alcoholic oxygen donor atom.)

The proposed measurements were also to be made on the complexes of Ni^{2+} with another two ligands, viz. 2-aminoethoxyacetate [$aea^- \equiv H_2N(CH_2)_2O CH_2COO^-$] and N-(2-hydroxyethyl)glycinate [$heg^- \equiv HO(CH_2)_2NHCH_2COO^-$], which are also depicted in Figure 1.3.

These two ligands differ from oden and etolen in that one $-CH_2NH_2$ group has been replaced by a $-COO^-$ group and they differ from each other in the nature of the nitrogen and oxygen donor atoms in the same way as do oden and etolen.

From the measurements to be made on the complexes of aea^- and heg^- with Ni^{2+}, the effect of a carboxylate group on the difference between the coordinating properties of primary and secondary nitrogen atoms could be shown. This information would be of value in assisting the interpretation of the observed enthalpies of formation of complexes of metal ions with polyamine-carboxylate ligands. Such data would be useful in determining whether an equation similar to equation (1.32) could be used to predict the enthalpy changes of such complexes.

It was felt that the $Ni\text{-}O\begin{smallmatrix}R\\R\end{smallmatrix}$ and $Ni\text{-}O\begin{smallmatrix}R\\H\end{smallmatrix}$ bonds would be fairly similar in strength, since Everhart *et al.* (65) had shown that the $\Delta H^{\ominus}$ for replacement of a water molecule by either an ethereal (R-O-R) or an alcoholic (R-O-H) oxygen is zero. Also, provided that these pairs of complexes have similar structures, one would expect the total strain energies developed in the ring systems to be very similar. Thus, from the difference between the en-

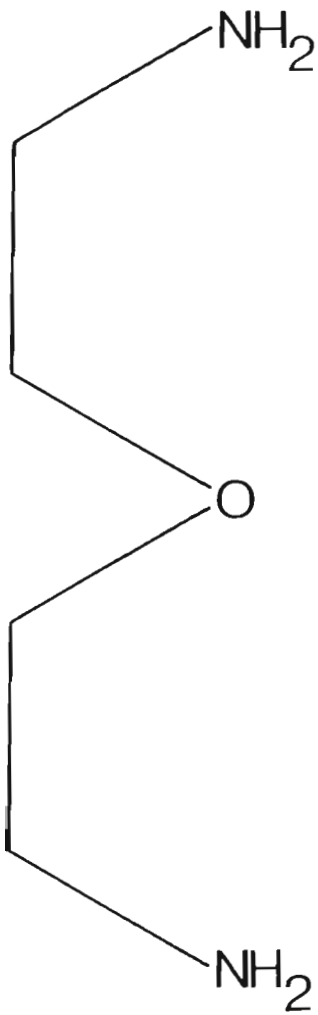

oden

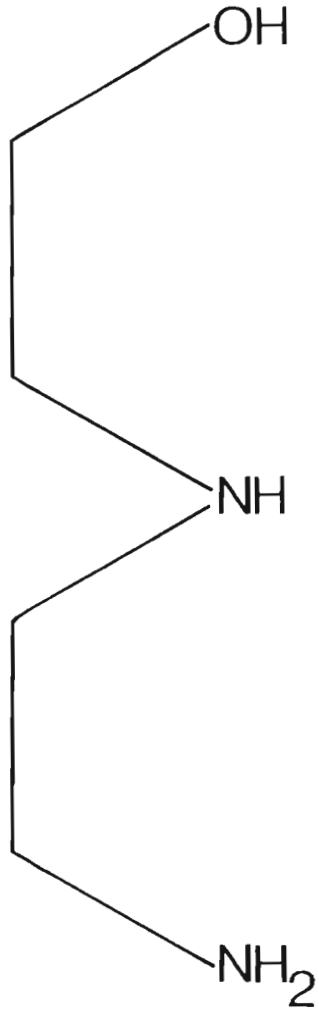

etolen

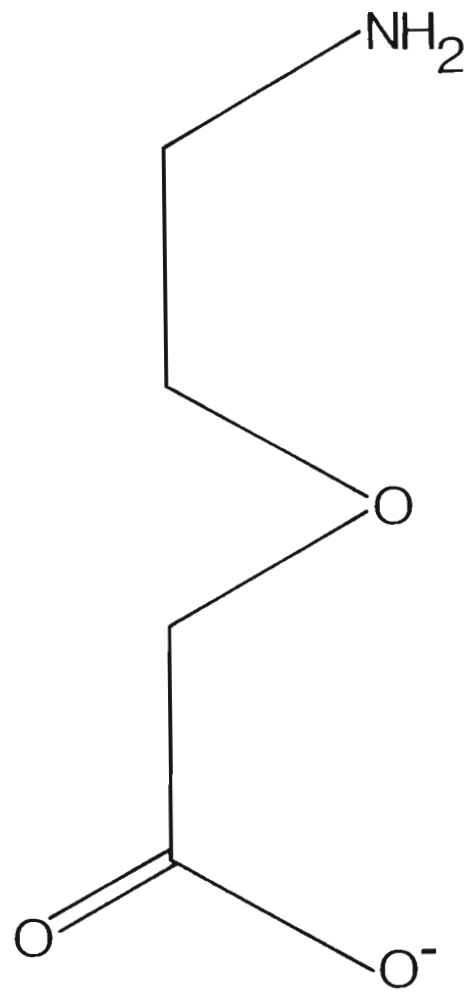

aea$^-$

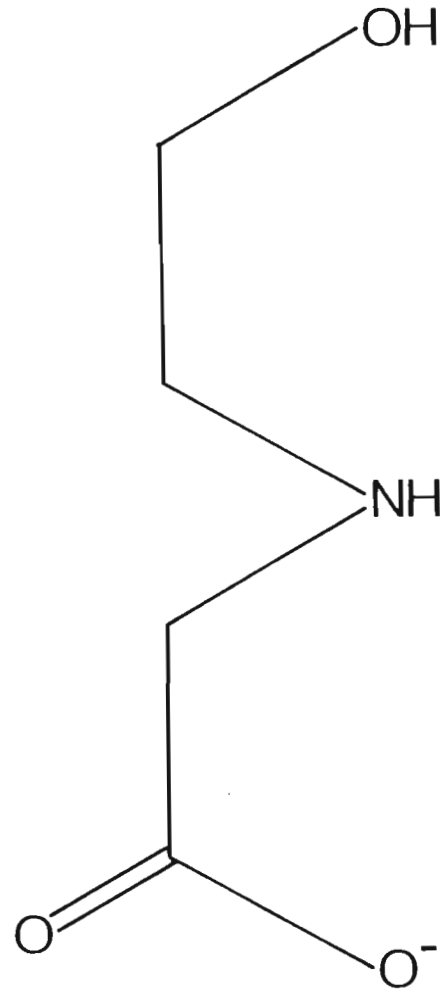

heg$^-$

Figure 1.3 The ligands studied.

thalpies of formation of the complexes of Ni^{2+} with oden and etolen, it should be possible to determine whether secondary nitrogen donors do in fact form stronger bonds than do primary nitrogen donors - and to what extent.

Paoletti *et al.* (42) showed that, in the gas phase, the energy of a coordinate bond depends not only on the nature of the donor atoms but also on the coordination number and geometry of the complex. Evidence is available that when oden and etolen are coordinated to Ni^{2+} they are both tridentate ligands and the resulting complexes are octahedral in geometry.

Evilia *et al.* (66) concluded from n.m.r. contact shift studies that the ethereal oxygen atom in oden was coordinated to Ni^{2+}. They also found that at 300 K the facial isomer of the complex $Ni(oden)(H_2O)_3^{2+}$ is 1.05 kJ mol^{-1} more stable (in free energy terms) than the meridional isomer, and that $\Delta H^{\ominus}$ is positive for the isomerisation reaction facial $\rightleftharpoons$ meridional. The greater stability of the facial isomer was thought to be due to stabilization by coordinated water molecules.

Much controversy has raged in the literature as to whether etolen coordinates as a bi- or a tridentate ligand.

In 1948 Breckenridge (67) reported the isolation of $Ni(etolen)_3Cl_2$. He thought that the Ni^{2+} was hexacoordinated, i.e. the two amino groups in each of the ligand molecules were coordinated to the metal ion while the alcoholic OH-groups were not. Although such a structure suggests the possibility of isomerism no evidence of such isomerism was found.

Harvey *et al.* (68) later carried out spectrophotometric studies and found that Ni^{2+} forms the complexes $Ni(etolen)^{2+}$ and $Ni(etolen)_2^{2+}$ in solution. They found no evidence for the existence in solution of a compound similar to that found by Breckenridge in the solid state.

Keller and Edwards (69) reported the preparation of the compounds $Ni(etolen)_3Br_2$ and $Co(etolen)_3X_3$ (where X = Cl or Br). They assumed that in these compounds the alcoholic OH-group was left free for further reaction. However they found that the latter compound was extremely unreactive towards reagents which normally react with free OH-groups, a fact

which they could not explain.

When this work was repeated by Drinkard *et al.* (70) these authors could obtain only $Co(en)_3Cl_3$, which resulted from a cleavage of C-N bonds during the oxidation of Co^{2+}.

To avoid this cleavage the compound was reprepared, this time using $Co(NH_3)_6(NO_3)_3$ as the starting material (71). The compound obtained was thought to be $Co(etolen^-)_2^+$, i.e. the compound was formulated as

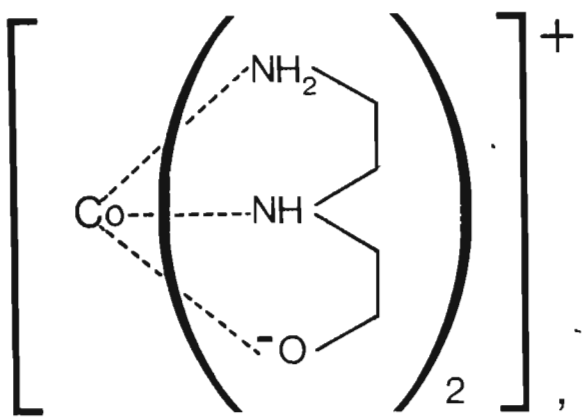

in which etolen behaves as a tridentate ligand with a proton lost from the hydroxyl group.

Das Sarma and Bailar (72) showed that under varying conditions etolen can behave as a tridentate or a bidentate ligand. They found that etolen$^-$ (etolen which has had a proton removed from the OH-group) is tridentate, attaching itself through two nitrogen and one O^- donor atoms. The ligand etolen can behave as a tridentate ligand, but is bidentate when the other coordination sites are already occupied by strongly coordinating groups such as tridentate etolen, NO_2^-, etc. These authors report the preparation of various Co^{3+} complexes with the ligand etolen as well as that of $Ni(etolen)_2Br_2$, in which complexes etolen is bidentate. This was ascertained through a study of the electrical conductivities and reflectance, i.r. and n.m.r. spectra of the complexes.

Bassett *et al.* (73,74) found that etolen acts as a bidentate ligand in the following solid tris complexes: $Ni(etolen)_3Cl_2$ and $Ni(etolen)_3Br_2$; but acts as a tridentate ligand in the following solid bis complexes: $Ni(etolen)_2I_2$, $Ni(etolen)_2(NCS)_2$, $Ni(etolen)_2(NO_3)_2$ and $Ni(etolen)_2(ClO_4)_2$. In the bis nickel sulphate complex $Ni(etolen)_2SO_4$, etolen is bidentate and the sulphate anion is covalently linked to the metal ion. It was thought that the formation of another five-membered ring would introduce a great deal of strain into the molecule, and hence that coordination with the anion occurs instead.

Rustagi and Rao (75) concluded from infrared spectral studies of solid metal complexes with the ligand etolen that in all cases the NH_2, NH and OH-groups participated in complex formation, i.e. etolen acts as a tridentate ligand. They also found that in the complexes containing sulphate as the anion it was not coordinated to the metal ion. For the nickel complexes $Ni(etolen)_2Cl_2$ and $Ni(etolen)_2SO_4$, the absorption spectra were found to be very similar to the reflectance spectra, which indicated that the complexes retained their octahedral geometry in both the solution and the solid state.

From infrared spectral data Nasanen *et al.* (76) have shown that, in the solid state complex $Ni(etolen)_2(NO_3)_2$, etolen is tridentate.

Barbucci (77) determined the stability constants of Ni-etolen complexes in order to ascertain whether or not the hydroxy group is coordinated to the metal ion. From a comparison of the ΔS° values obtained for the complexes of Ni^{2+} with dien and those with etolen he concluded that in the $Ni(etolen)_2^{2+}$ case not all the six donor atoms were coordinated, but that one ethylenic branch containing an alcohol group was free.

Subsequently Everhart *et al.* (65) have shown by means of n.m.r. contact shifts that alcoholic and ethereal oxygen donors can successfully compete with water for metal coordination sites, provided that the other donor groups in the ligand form bonds sufficiently strong to ensure the stability of the complex. In the case of the $Ni(etolen)(H_2O)_3^{2+}$ complex, they found that a substantial amount of oxygen coordination occurred. Furthermore ΔH° for the replacement of a coordinated water molecule by the R-OH group on etolen is zero, and ΔS° is about 6.3 J $K^{-1}mol^{-1}$. A significant amount

of oxygen coordination was also observed for the complex $Co(etolen)(H_2O)_3^{2+}$. However for Co^{2+} it was not possible to make quantitative measurements.

On balance of the evidence available, it therefore appears that both oden and etolen are tridentate and their complexes with Ni^{2+} are octahedral in aqueous solution. Comparison of the results for these two ligands should therefore constitute a fairly direct measure of the coordinating properties of primary and secondary nitrogen atom donors in complexes of this type.

Values of $\Delta G^{\ominus}$, $\Delta H^{\ominus}$ and $\Delta S^{\ominus}$ for the formation of complexes involving oden and etolen with Ni^{2+} have been reported with a view to evaluating the coordinating properties of the oxygen atom (77,78). However these values are in poor accord with previously reported values (1,2) for the same quantities. Thus the experimental data relating to the metal ion Ni^{2+} with the ligands oden and etolen needed to be checked.

Before the thermodynamic measurements for each pair of oden and etolen complexes can be compared, various assumptions should, if possible, be confirmed. Although the total strain energies developed in the ring systems for oden and etolen are expected to be rather similar, this could be confirmed with the aid of conformational strain energy calculations. UV-visible spectra of the complexes were recorded to investigate whether the d-d electronic energy level spacing increases or decreases when primary nitrogen atom donors are replaced by secondary nitrogen atom donors. (This spacing is a measure of the metal-ligand interaction for complexes having the same geometry.)

The stability constants (and hence $\Delta G^{\ominus}$) of the reactions studied were determined by glass electrode potentiometry (see Section 1.3), and the enthalpy changes by titration calorimetry (see Section 1.4). All the measurements were made at an ionic strength of 0.5 mol dm^{-3} using KNO_3 as the background electrolyte, and at a temperature of 25°C.

1.3. The potentiometric method of determining stability constants

Although various methods are available for the determination of stability constants, the one which seemed most suitable for the systems under investigation was glass electrode potentiometry. Before discussing this method

we shall describe the various types of complex which can be formed, and define some of the quantities frequently used in discussions of complex equilibria.

Various types of complex species are known. The simplest species formed are the mononuclear complexes. These can include oligomers M_q which form by self-association, such as Hg_2^{2+}, acids H_pL_r, and complexes ML_r. If more than one central metal ion is contained in the complex (M_qL_r, $q > 1$), then the species is termed a polynuclear complex. Polynuclear complexes may be homo- or hetero-nuclear, depending on whether the central metal ions are the same or different. Species can also exist in which more than one type of ligand is attached to the metal ion ($M_qL_rX_p$). These are called mixed ligand or ternary complexes. X may be a second type of ligand, the hydroxyl ion (in which case the complexes are usually described as 'hydrolysed'), or a hydrogen ion (a protonated complex).

The reactions which lead to the formation of metal complexes are really substitution reactions, i.e. one or more solvent molecules are substituted by a ligand molecule. There may also be interaction of the species of interest with the bulk electrolyte. However for simplicity it is assumed that the concentrations of the solvent and bulk electrolyte remain constant, and their contributions are ignored.

We shall now consider the formation of mononuclear metal complexes ML_r. In aqueous solution, a metal ion M (or more generally any Lewis acid, i.e. an electron acceptor) can react with a ligand L (or Lewis base, i.e. an electron donor) to form a series of complexes generally represented by the following reversible reaction:

$$M(aq) + rL(aq) \rightleftharpoons ML_r(aq); \quad r > 0. \qquad (1.34)$$

The resulting complexes can be cations, anions or uncharged molecules, but for the sake of simplicity charges have been omitted.

The activities (a) of the species present at equilibrium are related to the thermodynamic (activity) equilibrium constant ${}_a\beta_{ir}$ at a given temperature as follows:

$$ {}_a\beta_{1r} = \frac{a_{ML_r}}{a_M \; a_L^r} \; . \qquad (1.35) $$

However the activity of a species Z is simply related to its concentration ([Z]) by the activity coefficient, γ_Z:

$$ a_Z = \gamma_Z \, [Z]. \qquad (1.36) $$

Hence equation (1.35) can be rewritten as

$$ {}_a\beta_{1r} = \frac{\gamma_{ML_r}[ML_r]}{\gamma_M[M] \; \gamma_L^r[L]^r} $$

$$ = \frac{\gamma_{ML_r}}{\gamma_M \; \gamma_L^r} \; . \; \frac{[ML_r]}{[M][L]^r} $$

$$ = \frac{\gamma_{ML_r}}{\gamma_M \; \gamma_L{}^r} \; . \; \beta_{1r} \; . \qquad (1.37) $$

If reaction (1.34) is carried out in a medium of constant ionic strength μ, the activity coefficients of the various species present in solution will remain approximately constant. Hence ${}_a\beta_{1r}$ will be proportional to β_{1r}, since the activity coefficient quotient is a constant.

Hence the concentration quotient

$$ \beta_{1r} = \frac{[ML_r]}{[M][L]^r} \qquad (1.38) $$

will also be a constant. β_{1r} is known as the (cumulative) stability constant and is a constant for a given reaction at a given temperature and ionic strength.

Reaction (1.34) can alternatively be expressed as a series of r steps:

$$M + L \rightleftharpoons ML$$

$$ML + L \rightleftharpoons ML_2$$

$$\vdots$$

$$ML_{r-1} + L \rightleftharpoons ML_r,$$

and equilibrium constants or stepwise stability constants for each of these steps can be written as follows:

$$K_{11} = \frac{[ML]}{[M][L]},$$

$$K_{12} = \frac{[ML_2]}{[ML][L]},$$

$$\vdots$$

$$K_{1r} = \frac{[ML_r]}{[ML_{r-1}][L]}.$$

Thus it follows that the cumulative stability constants are obtained from the product of the stepwise stability constants:

$$\beta_{11} = K_{11}$$

$$\beta_{12} = K_{11}.K_{12}$$

$$\vdots$$

$$\beta_{1r} = K_{11}.K_{12}..... K_{1r}$$

$$= \prod_{i=1}^{r} K_{1i}.$$

In this work a third species besides M and L, viz. the hydrogen ion, was considered. Hence the reaction analogous to reaction (1.34) is

$$pH(aq) + qM(aq) + rL(aq) \rightleftharpoons H_pM_qL_r(aq), \qquad (1.39)$$

where p is an integer and q and r are nonnegative integers. If $p < 0$ coordination by hydroxide instead of hydrogen ions is indicated. The corresponding cumulative stability constant is defined as

$$\beta_{pqr} = \frac{[H_pM_qL_r]}{[H]^p[M]^q[L]^r}. \qquad (1.40)$$

It is seldom possible to determine the equilibrium concentrations of all the species present in a solution in which complexes are formed. However it is possible to measure the concentration of one species and relate it to the reactions occurring and the associated stability constants (see Section 4.3). Potentiometry is a particularly useful technique for measuring the said equilibrium concentration, since the concentration changes caused by complex formation are reflected in the potential of a sensing electrode.

In this work a potentiometric titration method was used in which the concentration of the free (uncomplexed) hydrogen ion was followed. This was possible because the reactions being studied involved competition between the hydrogen ion and the metal ion for the ligand.

The cell used to follow the hydrogen ion concentration was

reference electrode	‖	test solution	glass electrode

.

The details of this cell, as well as the various methods used to calibrate it, will be described in Section 5.1.

The actual titration experiments can be designed in a number of ways (see Chapter 6). If possible, though, they should be designed so as to furnish as much information as possible from a single titration.

It is imperative that a good choice of background electrolyte should be made so as to upset the measurements as little as possible. Beck (79) lists the qualities of a good electrolyte. The salts most commonly used are $NaCl O_4$ and KNO_3.

Once the potentiometric data have been collected they have to be processed. The first step is to obtain a graphical representation of the numerical data in the form of formation curves. From these plots one can detect 'dud' experimental data, as well as deduce the presence of complicated species such as polynuclear complexes etc. One is able also to see whether the collection of additional data is necessary. The second step is to deduce the nature of the species present and to calculate the corresponding stability constants. In this work the stability constants were calculated from the

potentiometric data by the use of the computer programs MINIQUAD (see Section 4.4.4.) and ESTA (see Section 4.4.5.).

For simple systems in which up to three stability constants are unknown, graphical methods can be used to obtain these stability constants. There are two main types of graphical method: linear, non-logarithmic plots, and curve-fitting methods. Graphical techniques have the advantage that errors are more easily estimated than from a computer print-out, although the results obtained may be less precise. Graphical methods of determining the stability constants were not used in this work.

There are a number of references (79 - 84) which elaborate on the points summarized here, and describe the various techniques by which stability constants may be determined.

1.4. The titration calorimetric method of determining enthalpy changes

Titration calorimetry provides a convenient and rapid method for the determination of enthalpy changes and, in some cases, values of the stability constants as well. In this work the technique was applied only to the determination of enthalpy changes. Since this method gives a direct measure of the quantity desired, it is to be preferred over such methods as temperature variation of stability constants for the purpose of accurate determination of enthalpy changes.

In titration calorimetry one reactant is titrated into another, and the temperature of the system is measured as a function of the amount of titrant added. The temperature change may be the result of a chemical reaction or of physical interaction between the titrate and titrant. The resulting data, i.e. temperature versus volume of titrant added (or time), can be analyzed to give information on the types and numbers of reactions taking place, as well as values of $\Delta H^{\ominus}$ and (for incomplete reactions) values of the corresponding stability constants.

Titration calorimeters come in two types - incremental and continuous - depending on the mode of titrant delivery. In the former type the titrant is added in increments, and the temperature is recorded after the addition of each portion of titrant. Before the next increment of titrant is added the temperature is readjusted to the initial value. In this way a series

of points, each corresponding to the addition of an increment of titrant, is obtained. In the latter type the titrant is added at a constant rate and the temperature is recorded continuously. This produces a continuous plot of temperature versus volume of titrant added. Incremental titration calorimetry has the advantage that temperature dependent corrections are small. Nonetheless, the method is laborious for the collection of a large volume of data, and errors are introduced in that a separate run has to be performed for each data point. Continuous titration calorimeters have the advantage that in one run an amount of data can be collected that would take very many runs by the other method. However the continuous method does require that the reactions being studied occur rapidly.

In this work a continuous titration calorimeter was used. A description of this calorimeter will be given in Section 3.2.

The data obtained from a typical titration calorimetric run are in the form of potential difference (which is linearly related to temperature) versus time (or moles of titrant added). A plot of such data is called a thermogram. Such a thermogram consists of various regions in which different heat effects predominate. This will be described in Section 4.2., together with the calculation procedure required to correct the data for extraneous heat effects, heat of dilution, etc.

Data corrected in this way are then processed by the computer program LETAGROP KALLE (see Section 4.4.10.). This program corrects the data for the contributions made by reactions other than those of interest (provided that their $\Delta H^{\ominus}$ values are known), and hence calculates values of $\Delta H^{\ominus}$ for the reactions of interest.

The shape of the thermogram is dependent on the equilibrium constant(s) and $\Delta H^{\ominus}$ value(s) of the reaction(s) occurring in the calorimeter. For titration calorimetry to be successful in the determination of enthalpy changes, the reaction of interest must produce a temperature change of at least 0.04°C (for the calorimeter used here), although a temperature change of about 0.4°C is to be preferred. If the technique were to be used to determine stability constants as well as enthalpy changes, the equilibrium constant for the overall reaction occurring in the calorimeter would have to lie between 1 and 10^4, so that a measurable amount of reaction takes place and also so

that the heat evolved or absorbed depends on the value of the equilibrium constant as well as on the value of $\Delta H^{\ominus}$.

Christensen *et al.* (85) have shown that $\Delta G^{\ominus}$, $\Delta H^{\ominus}$ and $\Delta S^{\ominus}$ can, under certain conditions, be determined from a single titration.

From a thermogram it is also possible to check on the stoichiometry of an incomplete reaction (86, 87). This is possible because the $\Delta H^{\ominus}$ value calculated must be constant throughout the titration. If the value of $\Delta H^{\ominus}$ is found to vary with different total concentrations of titrate and titrant, then the reaction postulated is incorrect and perhaps the presence of other species has to be assumed.

Barthel (88) lists various metal-complex systems for which the enthalpy changes have been determined by titration calorimetry. Christensen, Eatough, Izatt and Ruckman have published a series of three papers (89, 90, 91) and a later review (92) in which the determination of equilibrium constants by titration calorimetry is described. Hansen, Izatt and Christensen (93) have reviewed the use of titration calorimetry as an analytical procedure for the accurate and rapid standardization of solutions.

CHAPTER TWO

MATERIALS

Throughout this work only A-grade volumetric glassware and twice deionized water were used. Unless otherwise stated the solutions used for the measurements were prepared by dilution of the appropriate standardised stock solutions.

2.1. Preparation and standardisation of stock solutions of strong acid

Stock solutions of nitric acid (ca. 5 mol dm^{-3}) were prepared by diluting MERCK p.a. HNO_3 (min. 65 % pure, sp. gr. 1.40) to the required concentration and standardised by titration against freshly recrystallized borax (94).

2.2. Preparation and standardisation of stock solutions of strong base

Stock solutions of sodium hydroxide (ca. 1 mol dm^{-3}) were prepared from MERCK TITRISOL concentrated volumetric solutions and were made up with water which had been twice deionized and freshly boiled to expel CO_2. When these ampoules were not available the stock solutions were prepared by dilution of a 50 % NaOH solution, as described by Vogel (95). In both cases, the solutions prepared from these stock solutions were standardised by potentiometric titration against a standard HNO_3 solution, and application of the Gran method of end-point detection (see Section 4.1.1.).

2.3. Preparation and standardisation of stock solutions of background electrolyte

Potassium nitrate was used as the background electrolyte in these measurements. A stock solution (ca. 2 mol dm^{-3}) was prepared by mass from BDH ANALAR KNO_3 (99.5 % pure) and standardised by passing a 5.00 cm^3 aliquot through a cation exchange resin. A column was packed with BDH AMBERLITE IR-120 (H), which is an analytical grade ion-exchange resin supplied in the protonated form with a strongly acidic active group, viz. $-SO_3H$. Prior to use the resin was converted to the Na^+ form (by eluting with a 10 % solution of NaCℓ) and then converted back to the H^+ form (by treating it with a 6 % solution of HCℓ). This was done to ensure that

the resin was completely in the H^+ form, and also to clean, and improve the effective capacity of, the resin. After each treatment the column was washed with deionized water until a neutral eluate was obtained. The aliquot of KNO_3 was then passed through the column and the HNO_3 collected was titrated against a freshly prepared and standardised NaOH solution, by using methyl orange as the indicator.

It was found that the concentration of KNO_3 obtained in the above way differed from that calculated by mass by only 0.4 %, which is not a significant difference for a background electrolyte. Hence from then onwards the KNO_3 stock solutions were prepared from the pure reagent by mass.

2.4. Preparation and standardisation of stock solutions of metal nitrates

The nickel nitrate stock solutions (ca. 0.2 mol dm^{-3}) were prepared from MERCK p.a. $Ni(NO_3)_2.6H_2O$ (min. 99 % pure), and standardised by direct titration against a standard solution of EDTA (MERCK p.a., min. 99 % pure) with murexide as the indicator (96). For the standardisation a ca. 0.05 mol dm^{-3} $Ni(NO_3)_2$ solution was used.

MERCK p.a. $Co(NO_3)_2.6H_2O$ (min. 99 % pure) was used in the preparation of the stock solutions of cobalt nitrate. Again, for the standardisation the stock solution was diluted to ca. 0.05 mol dm^{-3} and this dilute solution was standardised by EDTA titration with murexide as the indicator (97).

The zinc nitrate stock solutions (ca. 0.2 mol dm^{-3}) were prepared from MERCK p.a. $Zn(NO_3)_2.4H_2O$ (min. 98.5 % pure). For standardisation purposes the stock solution was diluted to 0.05 mol dm^{-3}. This dilute solution was standardised by direct titration against a standard solution of EDTA with Eriochrome Black T as the indicator (98).

2.5. Preparation and standardisation of ligand solutions

2.5.1. Preparation and standardisation of solutions of 2-(2-aminoethyl)aminoethanol (etolen)

The 2-(2-aminoethyl)aminoethanol (etolen) used was purchased from RIEDEL-DE HAËN (Prosynth grade, 99 % pure) and was purified by fractional distillation under reduced pressure. The fractional distillation equipment used consisted of a liquid dividing fractional distillation head (QUICKFIT SH 30/42) and a vacuum-jacketed column of approx. 50 cm effective length. This column was wrapped with aluminium foil and packed with 9 x 9 mm Raschig rings (QUICKFIT FC 8/09) using a QUICKFIT EX 13/25 packing support. The apparatus was connected to a rotary high vacuum pump. It was found that smaller Raschig rings, viz. 6 x 6 mm (QUICKFIT FC 8/06), could not be used because the high viscosity of the ligand caused them to retain too much of the liquid phase.

The fraction used distilled over at 89°C at 0.9 mmHg. The refractive index of this fraction, as measured by a Hilger and Watts Abbé refractometer, was found to be 1.4888 at 20.0°C, as compared to a published value of 1.4861 at 20.0°C (99). This distillation procedure succeeded in removing the yellow colour of the ligand.

Earlier, etolen had been fractionally distilled under reduced pressure through a 30 cm-long vacuum-jacketed Vigreux column having eight sets of points. However this procedure did not remove the yellow colour of the ligand. The fractions collected by this method distilled over at 135°C at 15 mmHg and had a refractive index of 1.4878 at 22.1°C.

The purity of the distilled etolen was also checked by running a thin layer chromatographic plate. The plates used were MERCK pre-coated silica gel $60F_{254}$ aluminium-backed sheets of 0.2 mm thickness and the solvent system was: 96 % aq. ethanol/25 % aq. ammonia in the ratio 4:1. The plate was sprayed with MERCK 0.1 % ninhydrin solution. Only one spot appeared on the plate, and it had an R_f value of 0.33.

An infrared spectrum of neat etolen (between KBr plates) was recorded by using a BECKMAN ACCULAB 8 infrared spectrophotometer. The spectrum obtained (shown in Figure 2.1) showed essentially the same features as

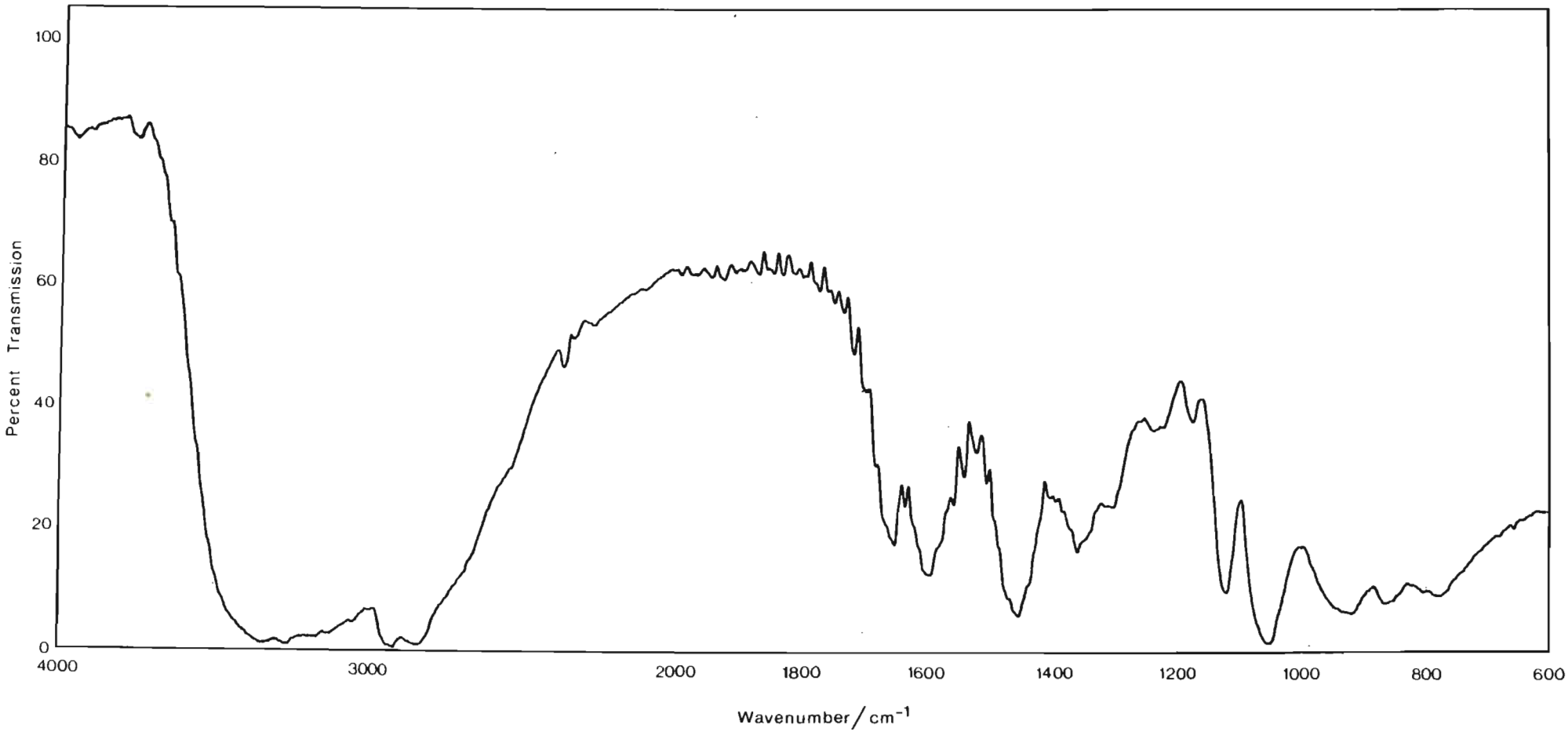

Figure 2.1 The infrared spectrum of 2-(2-aminoethyl)aminoethanol (etolen).

previously reported infrared spectra of etolen (100, 101).

Solutions of this amine were prepared by using freshly boiled doubly deionized water, and standardised a day before use. The concentrations of the solutions were determined by potentiometric titration against a standard nitric acid solution. The equivalence points were determined by using an "extended" Gran plot method as described in section 4.1.3.

2.5.2. Preparation and standardisation of solutions of 2,2'-oxybisethanamine (oden)

The ligand 2,2'-oxybisethanamine (oden) was purchased as the dihydrochloride from ALDRICH. The melting point of the unpurified compound, measured on a GALLENKAMP MF-370 melting point apparatus, was found to be 224 - 226°C, which did not agree with the melting point of 232 - 235°C stated on the label of the bottle.

The material was purified by recrystallizing it three times in the following manner: the solid was dissolved in the minimum amount of hot water, and an equal volume of ethanol was added. It was then dried to constant mass under high vacuum in a drying pistol by using carbon tetrachloride (which boils at 76.5°C) as the heating medium and phosphorus pentoxide as the drying agent. The melting point of the recrystallized material was found to be 226 - 226.5°C, which compared well with the published value (102) of 226 - 227°C.

An elemental analysis (in duplicate) was performed on the solid by PASCHER. The sample was dried at 60°C under high vacuum. There was no loss in mass and the following results were obtained: C: 25.54 %, H: 7.375 %, N: 14.77 %, O: 8.74 %, Cℓ: 40.40 %. As can be seen, these percentages leave 3.18 % unaccounted for. On the assumption that the material contained some NaCℓ, the formulation $C_4H_{12}N_2O.xHC\ell.yNaC\ell$ was fitted to the experimental results by a least squares technique. The results obtained were x = 1.88 and y = 0.26. A comparison of the experimental and

calculated percentages for each element is shown in Table 2.1. As can be seen, the calculated results agree fairly well with the experimental results.

An infrared spectrum of the same material as sent for elemental analysis was obtained on a BECKMAN ACCULAB 8 spectrophotometer. The spectrum (shown in Figure 2.2) was taken as a Nujol mull between KBr plates. The wavenumbers of the absorptions were found to correspond fairly well with those reported in the literature (103).

Solutions of oden.2HCℓ were prepared fresh as required, by using boiled decarbonated doubly deionized water. They were standardised by potentiometric titration against a standard NaOH solution using the Gran plot method of end-point detection for dibasic acids (see Section 4.1.2). The standardisation of the NaOH titrant solution was carried out 'in situ' beforehand. In this way the excess acid that remained after this preliminary standardisation enabled one to check whether any 'dirt' acid was present in the oden.2HCℓ solutions. (Of course the possibility of 'dirt' acid does not arise if indeed it is correct to assume x = 1.88, i.e. the formulation proposed.) The plot of e.m.f. versus volume for the standardisation of oden.2HCℓ gives only one point of inflection, since log K_{101} and log K_{201} are fairly similar for oden.2HCℓ (log K_{101} = 9.77, log K_{201} = 9.17). In this respect oden differs from etolen.

2.6. Ligand syntheses

The ligands aea and heg were not available commercially and had to be synthesized.

2.6.1. Synthesis of the ligand N-(2-hydroxyethyl)glycine (heg)

A number of syntheses for the ligand N-(2-hydroxyethyl)glycine (heg) have been reported (104 - 107). The synthesis by Kipriyanov and Kipriyanov (104) was not tried, as it seemed to be more involved than that of Farbenind (105) and it was anticipated that removal of the by-products would be difficult. The methods of Stewart (106) and of Benedikovic *et al.* (107) make use of hydroxyacetonitrile ($HOCH_2CH_2CN$) as a starting material and this chemical was too expensive to buy in the quantities required. The latter two methods also require the dehydration in vacuum at 90°C of

TABLE 2.1

A comparison of experimental and calculated elemental percentages for oden.

Element	Percentage found	Percentage calculated assuming $C_4H_{12}N_2O.1.88HC\ell.0.26NaC\ell$
C	25.54 ± 0.07	25.57
H	7.375 ± 0.005	7.45
N	14.77 ± 0.07	14.91
O	8.74 ± 0.11	8.52
Cℓ	40.40 ± 0.02	40.38
Na	3.19 ± 0.12	3.18

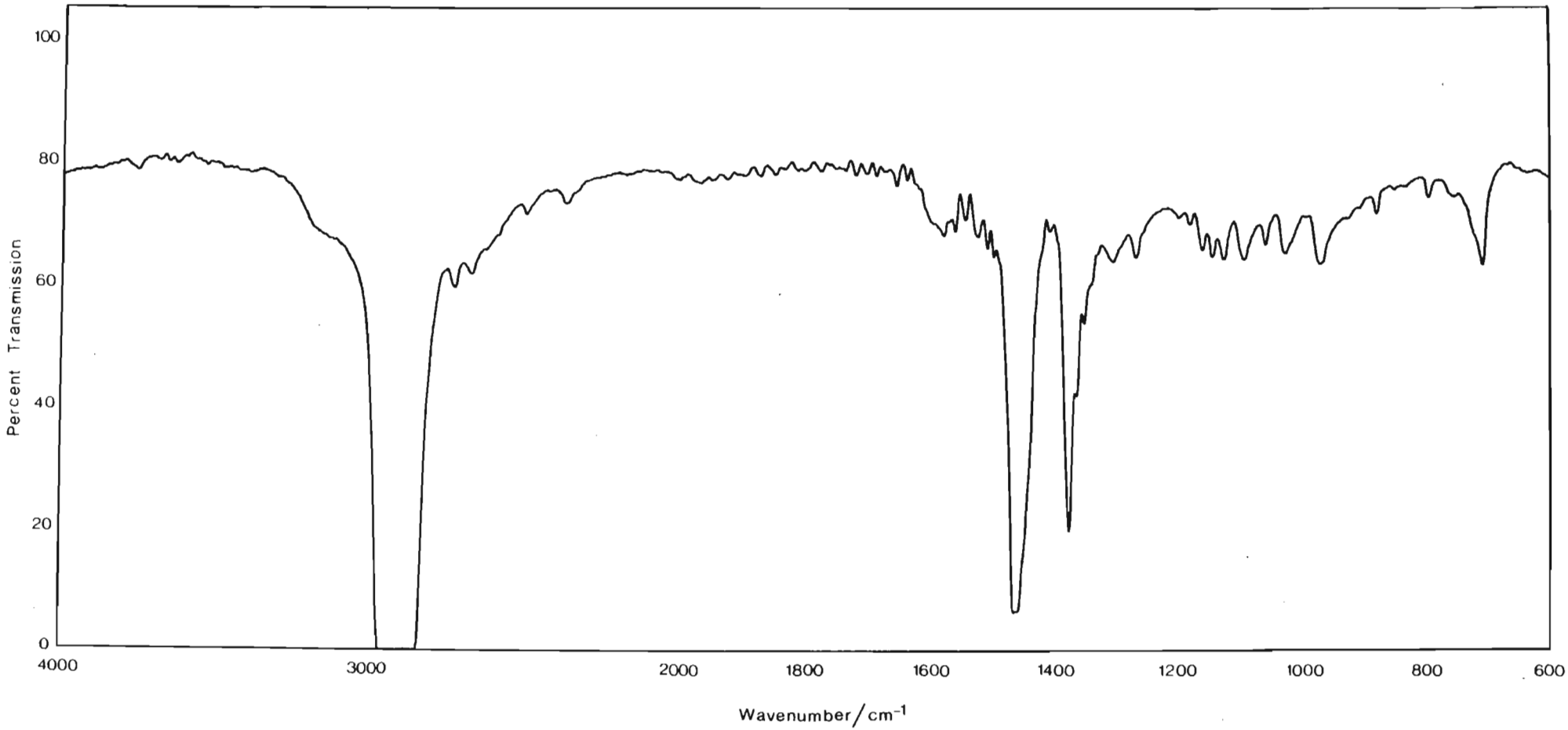

Figure 2.2 The infrared spectrum of 2,2'-oxybisethanamine dihydrochloride (oden.2HCℓ).

the reaction mixture. This appears to be a particularly violent reaction and, according to advice obtained, should not be attempted (108). Thus the synthesis of heg was attempted by using the method published in a French patent by I.G. Farbenind (105). This synthesis, however, yields the by-product Na_2CO_3 in addition to the sodium salt of heg. Hence the synthesis was modified in that the reaction products were passed through an ion-exchange resin in order to replace the Na^+ by H^+ and so remove the by-product. A summary of the synthesis is shown in Scheme 2.1.

The first step in the synthesis is the formation of oxazolidine. Therefore 75 g (1.0 mole) of methanal solution (BDH lab. reagent, 37 - 41 % w/v) was added dropwise, with stirring, to 61 g (1.0 mole) of 2-aminoethanol (BDH lab. reagent, 99 % pure) contained in a three-necked round-bottomed flask. The two clear liquids were miscible and on reacting liberated much heat (as expected, since this is a dehydration reaction), and formed a pale yellow mixture.

The next step of the synthesis involved the opening of the ring structure of oxazolidine by the addition of HCN to form a nitrile. To do this, 56 g (1.1 moles) of NaCN (BDH lab. reagent, 97 % pure) in the solid form was then added to the mixture and washed down with 20 - 30 cm^3 of water. The mixture was kept well stirred and at a temperature of 40 - 50°C while gaseous CO_2 was bubbled through the solution. Two gas traps, the first containing a concentrated solution of potassium permanganate and the second a 30 % NaOH solution, and a beaker of concentrated $KMnO_4$ were used to absorb any HCN that might have formed and escaped. As the reaction proceeded, the mixture became a viscous pale yellow liquid. Carbon dioxide was bubbled through for approx. one hour or until no further change was visible in the mixture. At this stage the reaction mixture was alkaline.

A volume of 30 cm^3 of a 20 % solution of NaOH was added and the mixture was refluxed for two hours. The mixture became a pale brown/orange colour during the hydrolysis and NH_3 was liberated.

The reaction product consisted of a white solid at the bottom of the flask and a pale-brown syrupy upper layer. The syrupy layer was separated from the solid by decantation. The white solid was found to dissolve in water and, when acid was added to an aqueous solution thereof, CO_2 was

SCHEME 2.1

Summary of the synthesis of heg undertaken.

$$HOCH_2CH_2NH_2 + CH_2O \xrightarrow{-H_2O}$$

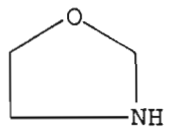

oxazolidine

$$\xrightarrow[CO_2]{NaCN} \text{40 - 50 °C}$$

$$HOCH_2CH_2NHCH_2CN + Na_2CO_3 \xrightarrow[\text{reflux}]{NaOH}$$

$$HOCH_2CH_2NHCH_2COO^-Na^+ + NH_3\uparrow + Na_2CO_3 \xrightarrow[N_2]{H^+ \text{ cation-exchange resin}}$$

$$HOCH_2CH_2NHCH_2COOH + CO_2\uparrow + H_2O$$

heg

liberated. It was therefore concluded that the solid was Na_2CO_3.

To remove the sodium ions present in the syrupy layer it was decided to pass the mixture through a cation-exchange resin in the H^+ form. The resin used was BDH AMBERLITE IR-120(H). The resin was conditioned before use as described in Section 2.3. The resin was then placed in a three-necked round-bottomed flask with just enough water to cover it. The flask was fitted with a nitrogen inlet and an outlet leading to the same gas traps as before. The third inlet was fitted with a dropping funnel containing the syrupy material (approx. pH 10) referred to above. The material was released drop by drop onto the resin while the resin was kept well stirred, with nitrogen bubbling through all the time so as to sweep off the CO_2 that formed and possibly any HCN that might have formed from any unreacted NaCN present in the reaction mixture. Once this procedure was completed the aqueous phase was filtered off from the resin by suction and the resin was washed with water. The washings were combined with the reaction product.

The reaction product was then tested for the presence of CN^- by standard tests, as described by Vogel (109), to ensure that it could safely be treated in the open without further precautions. The test results proved to be negative.

To ensure that all the sodium ions had been removed the reaction product was again treated with resin but this time in an open beaker. Again the washings were combined with the reaction product and the mixture was evaporated by means of a rotary evaporator to a volume of approx. 400 cm^3. The product was then passed through a column packed with regenerated resin in the H^+ form, to secure the benefits of a chromatographic separation. The column was washed down with water. The mixture, now presumably containing heg, was again evaporated by means of a rotary evaporator until it was thick and syrupy. After treatment with resin, the reaction product had a pH value of 3.

On standing, the reaction product formed white crystals. These were filtered off by suction and washed with ethanol. Further crystals were obtained from the mother liquor by adding an equal volume of ethanol. The crystals obtained were then recrystallized by dissolving them in the minimum amount of hot water and adding an equal volume of ethanol. The

product was recrystallized four times in this manner. The yield was 30 g, which represented a yield of 25 % if the product was heg.

A small sample of this material was dried to constant mass under high vacuum in a drying pistol, by using trichloromethane (boiling point 61.7°C) as the heating medium and phosphorus pentoxide as the drying agent. The dried material was found to have a melting point of 174 - 175°C.

An elemental analysis was performed by the Council for Mineral Technology on a sample of this material. The results obtained were: C: 40.45%, H: 6.44%, N: 7.76%. The results calculated for $C_4H_9NO_3$, i.e. heg, are C: 40.33 %, H: 7.62 %, N: 11.76 %, O: 40.29 %. It can be seen that the values obtained for N and H are too low.

A mass spectrum of the product, recorded at 70 eV and with a mass range of 600, is shown in Figure 2.3. The molar mass was found to be 177 g mol^{-1} which is not the value expected for heg, viz. 119 g mol^{-1}. Prominent peaks occur at the following m/e values: 18, 28, 42, 56, 60, 74, 86, 88, 101, 102, 114, 132, 146, 159 and 177.

From this evidence it seems that the compound formed is most probably N-(2-hydroxyethyl)-iminodiacetic acid [$HOCH_2CH_2N(CH_2COOH)_2$] (molar mass 177 g mol^{-1}). The calculated composition percentages for this compound ($C_6H_{11}NO_5$) are: C: 40.68, H: 6.26, N: 7.91 and O: 45.16, which fit the elemental analysis results fairly well.

An infrared spectrum of the reaction product (shown in Figure 2.4) was recorded on a BECKMAN ACCULAB 8 infrared spectrophotometer. The spectrum was taken as a Nujol mull between KBr plates. The spectrum obtained was compared with a reported spectrum for N-(2-hydroxyethyl)iminodiacetic acid (110) and found to agree very well.

A p.m.r. spectrum of this material in D_2O was recorded on a VARIAN CFT-20 NMR spectrophotometer and is shown in Figure 2.5. Relative to an internal standard of acetone the following absorptions occurred:

δ: 1.22, 1.27, 1.31, 1.34; quartet; 2H; C-$C\underline{H}_2$-N

δ: 1.66, 1.70, 1.73, 1.79; quartet; 2H; HO-$C\underline{H}_2$-C

δ: 1.86; singlet; 4H; N-$C\underline{H}_2$-COOH

δ: 2.46; singlet; H_2O.

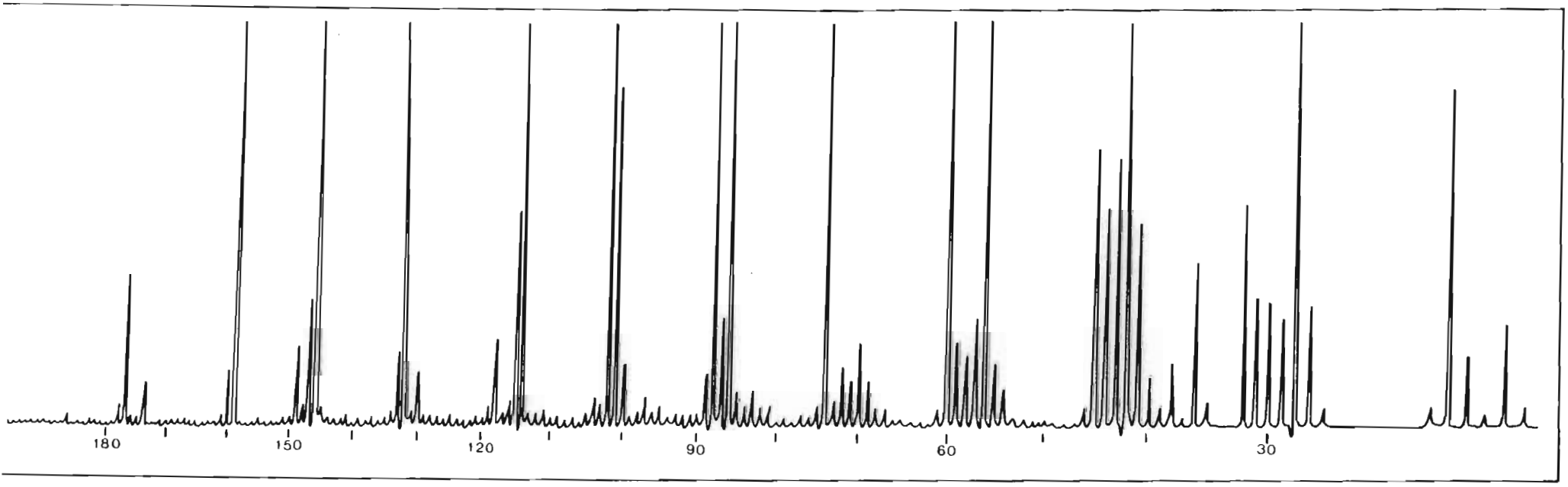

igure 2.3 Mass spectrum of the compound obtained from the attempted synthesis of heg.

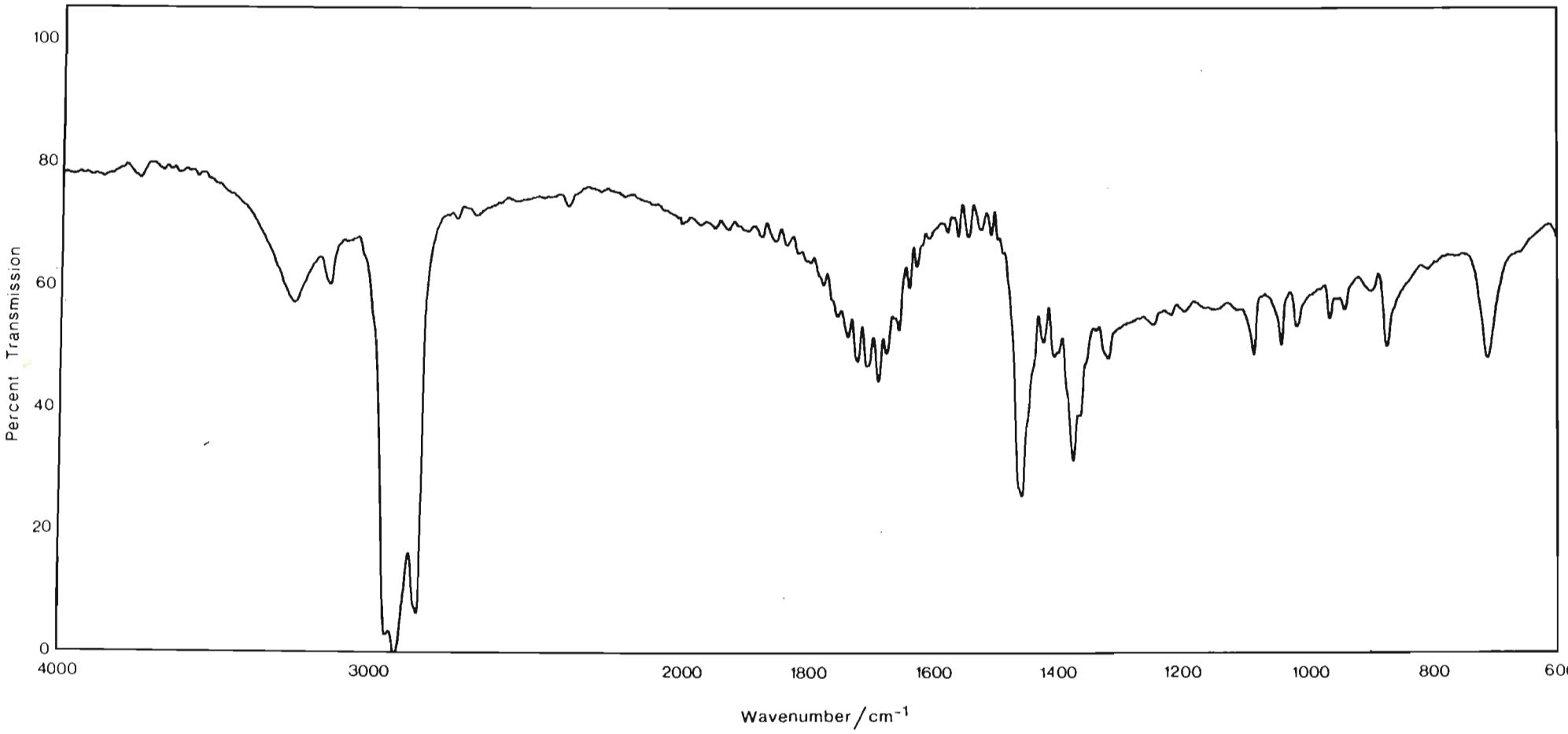

Figure 2.4 The infrared spectrum of the compound obtained from the attempted synthesis of heg.

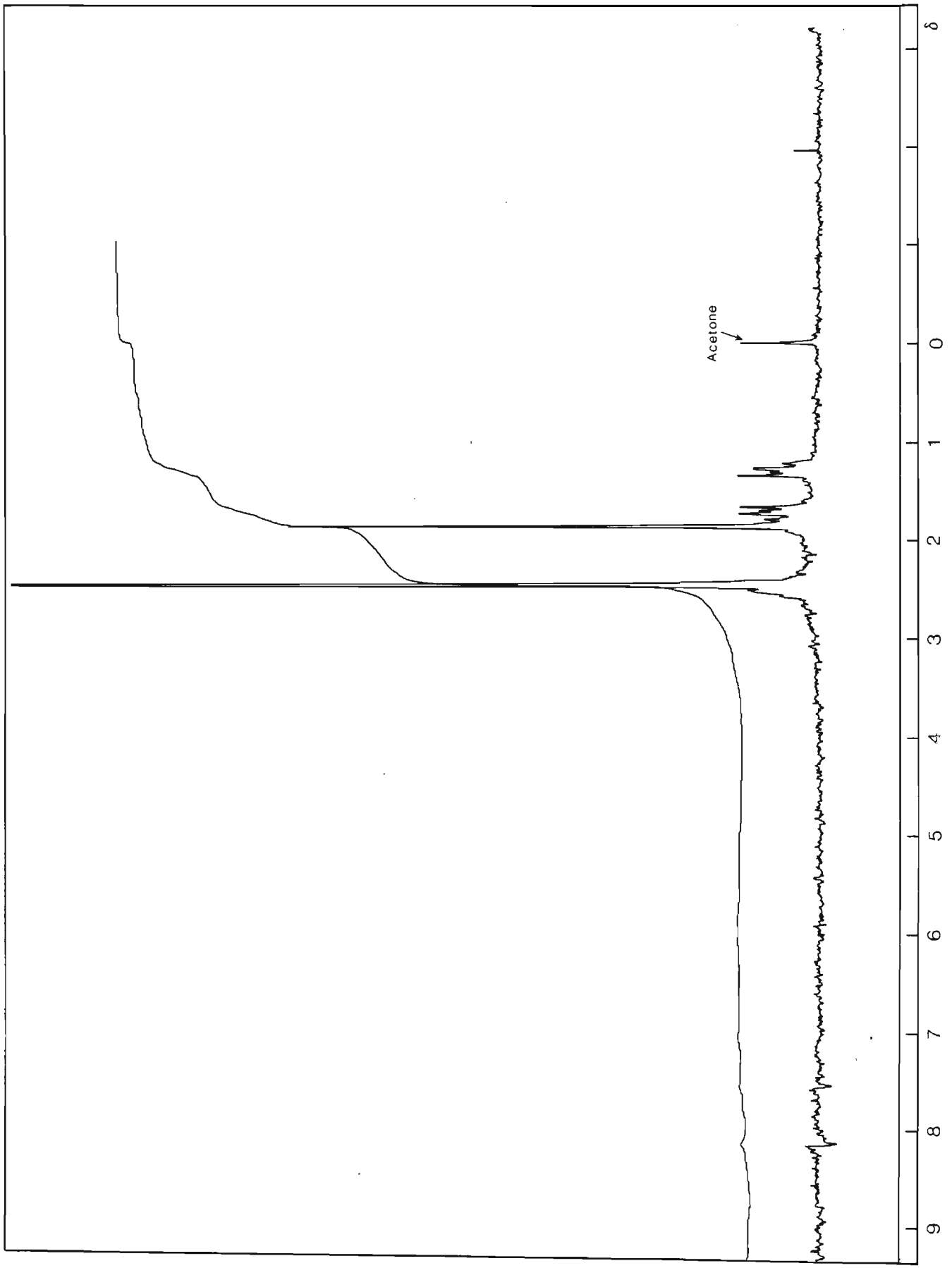

Figure 2.5 P.m.r. spectrum of the product obtained from the attempted synthesis of heg.

All the above evidence seems to indicate that N-(2-hydroxyethyl)-iminodiacetic acid was formed rather than heg.

A modified version of the synthesis was attempted, in which the amount of 2-aminoethanol used was increased threefold in order to force the reaction with methanal to the right, and to prevent any possibility of two methanal molecules attaching themselves to one molecule of 2-aminoethanol. It was found difficult to obtain any crystals on addition of ethanol to the reaction product. On the addition of some diethyl ether pale blue crystals formed. However the yield was very low. Surprisingly, the melting point of the product was found to decrease instead of increase on recrystallization. It was surmised that the compound obtained was undergoing a chemical change on recrystallization, since the melting point changed with recrystallization but not with time, as shown in Table 2.2.

A mass spectrum was run on the product obtained, and a peak at m/e = 177 was obtained, showing that N-(2-hydroxyethyl)-iminodiacetic acid was probably present. Hence the following disproportionation reaction was suggested:

$$2HOCH_2CH_2NHCH_2COOH \longrightarrow HOCH_2CH_2N(CH_2COOH)_2 + HOCH_2CH_2NH_2$$

There is therefore some doubt as to whether the published syntheses for heg are valid. Farbenind (105) do not describe any characterization of their product, and so it is difficult to ascertain whether they actually did synthesize heg. Kipriyanov and Kipriyanov (104) claim that the melting point of their product was 174 - 175°C (i.e. the same as obtained in this work), which is not in agreement with Benedikovic *et al.* (107), who report a melting point of 190 - 191°C for the same compound. Jankowski and Berse (111) report yet another melting point for heg, 141°C. Stewart (106) reports the same melting point as Kipriyanov and Kipriyanov. Both Benedikovic *et al.* and Kipriyanov and Kipriyanov determine the nitrogen content of their compound. The former authors obtain 11,74 %, and the latter 11,61 %, as compared to the calculated value of 11,76 % N. Although these nitrogen content figures agree fairly well with the calculated result, the last three papers (104, 106, 107) do not provide any

TABLE 2.2

Change of melting point on recrystallization of reaction product.

Date	Description of Sample	Melting Point/°C
Day 1	Crude	185
Day 1	Once recrystallized	181
Day 4	Twice recrystallized	178 - 178.5
Day 7	Twice recrystallized	178 - 178.5

further characterizations of the compounds, and therefore it is difficult to decide what compounds actually were prepared.

Takagi *et al.* (112) claim to have extracted heg from Petalonia fascia (Formosan seaweed) and they claim that heg decomposes at 182 - 184°C. Thus there is some controversy over the melting point of heg.

A rather different possible synthetic route for heg involves an addition reaction as shown in Scheme 2.2.

This synthesis was however not attempted because it had been decided by this time that heg was not sufficiently stable in aqueous solution for use in thermodynamic measurements, and this part of the project was discontinued. A very similar synthesis, in which H_2NCH_2COOH was heated with 2-chloroethanol in the presence of alkali and water at 90 - 100°C, has recently been published in a U.S.S.R. patent (113).

2.6.2. Synthesis of the ligand 2-aminoethoxy acetic acid (aea)

Syntheses for this ligand have been reported in the literature (114 - 117). The first stage in the synthesis of 2-aminoethoxy acetic acid (aea) is the production of the cyclic compound, 3-morpholone. This compound was prepared by the method of Vièles and Séguin (115, 116). A summary of the synthesis is shown in Scheme 2.3.

The first step in the production of 3-morpholone is the formation of the sodium salt of 2-aminoethanol. For this, 100 cm^3 of anhydrous dioxane (MERCK - dried, max. 0.01 % H_2O, min. 99.5 % pure) was placed in a round-bottomed flask. A mass of 35 g (0.57 moles) of 2-aminoethanol (BDH lab. reagent, min. 99 % pure) was then dissolved in the dioxane. To this was added, with stirring, 11.5 g (0.5 moles) of sodium metal in small portions. Much heat was liberated. On completing the addition of Na the mixture was refluxed until as much Na as possible had dissolved. When the mixture had cooled the remaining unreacted Na was removed. By now the mixture had a pale yellow colour.

A mass of 63 g (0.51 moles) of ethylchloroacetate (MERCK, 99 % pure) was then added dropwise to the solution, which was kept well stirred and cool.

SCHEME 2.2

Suggested synthesis for heg.

$$HOCH_2CH_2C\ell + H_2NCH_2COOH \xrightarrow[\text{using methanol or ethanol as solvent}]{\text{reflux}}$$

$$HOCH_2CH_2NHCH_2COOH + HC\ell \xrightarrow[\text{separate on a column which will retain } C\ell^-\text{, elute with methanol perhaps}]{} HOCH_2CH_2NHCH_2COOH$$

heg

SCHEME 2.3

Summary of the synthesis of 3-morpholone.

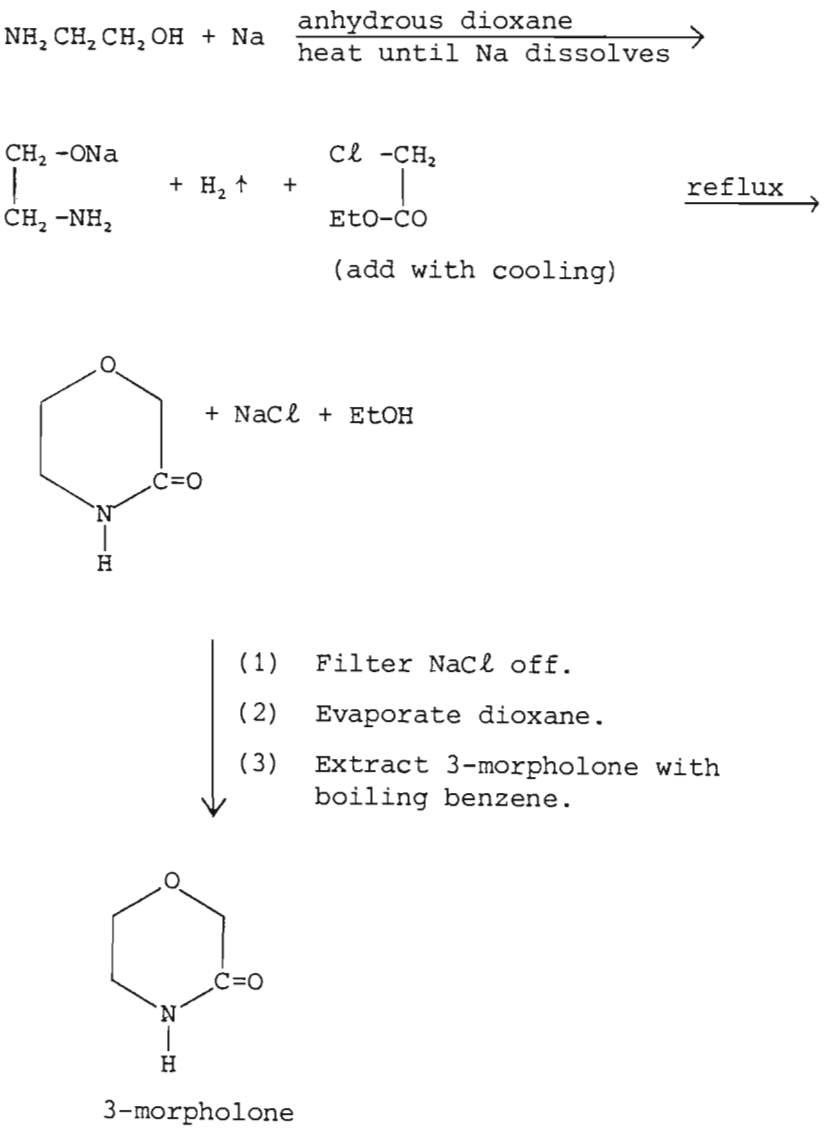

3-morpholone

A white precipitate formed. The mixture was then refluxed for two hours. Again the mixture was kept well stirred during the whole operation. After refluxing, the solution had become pale brown and the white solid remained.

The white solid, which was sodium chloride, was filtered off by suction and washed with boiling ethanol. The washings were combined with the filtrate and the solution was evaporated to dryness using a rotary evaporator. A viscous dark brown syrup remained.

The next step involved the extraction of the 3-morpholone with boiling benzene. The syrupy mixture was placed in a large beaker and to it was added approximately one third of its volume of benzene. This was then heated while being kept well stirred. The benzene was allowed to boil for a short while (< 5 minutes) and then was decanted from the hot mixture. When the benzene extract had cooled slightly an equal volume of diethyl ether was added. White needle-shaped crystals formed. The crystals were filtered off and recrystallized twice from the minimum volume of benzene and diethyl ether. The syrupy substance was extracted with boiling benzene a number of times in order to obtain an appreciable quantity of product.

The melting point of the recrystallized product was found to be ~100°C, as compared to the published values of 104 - 105.5°C (117) and 105°C (116) for 3-morpholone.

The final step in the synthesis was to hydrolyse the 3-morpholone (116, 117) to obtain the ligand required. This step was not carried out since, by this time, the attempted synthesis of heg had been abandoned and it had been decided that this section of the project should not be pursued.

CHAPTER THREE

APPARATUS

In this work stability constants were determined potentiometrically by measuring hydrogen ion concentrations with a glass electrode, and enthalpy changes were determined by titration calorimetry.

3.1. The Potentiometric Cell

The potentiometric cell was assembled as follows.

The test solution was placed in a METROHM No. EA 876-50 jacketed glass reaction vessel thermostatted at 25.00 $\pm$ 0.05°C by water circulating from a HETOFRIG cooling bath type CB7 fitted with a HETO heating unit type 03 T 623. The plastic lid of the reaction vessel was fitted with a glass electrode, nitrogen bubbler, thermometer and the reference electrode/salt bridge assembly. The remaining hole in the lid was covered with a teflon stopper and was used for the introduction of the titrant solution via a burette or an automatic burette. The glass electrodes employed were of the RADIOMETER G202B (low sodium error) type. These electrodes were conditioned before use by allowing the bulb of the electrode to soak for at least eight hours in 0.1 mol dm^{-3} $HC\ell$ at room temperature. The bulb was then rinsed with doubly deionized water and soaked for several hours in pH 7 buffer solution. This conditioning procedure was repeated at frequent intervals and always performed after the electrodes had been stored dry for a fairly long interval. During use, the glass electrodes were stored by soaking the bulb in pH 7 buffer solution. The reference electrode and salt bridge were assembled by using two INGOLD liquid junction tubes type 303/95/T/NS. The liquid junction tubes were later modified in that the upper halves were provided with water jackets, which enabled the reference electrode/salt bridge assembly to be thermostatted at the same temperature as the reaction vessel. The solution in the reference electrode was 0.01 mol dm^{-3} $KC\ell$ + 0.49 mol dm^{-3} KNO_3, and that in the salt bridge was 0.50 mol dm^{-3} KNO_3. A drop of $AgNO_3$ solution was added to the reference electrode solution before inserting the Ag, $AgC\ell$ electrode, to ensure that the solution was saturated with $AgC\ell$ and thus prevent dissolution of the $AgC\ell$ coating on the

reference electrode. METROHM type EA-275 silver-silver chloride reference electrodes were used. The reference electrode/salt bridge assembly is shown in Figure 3.1. The e.m.f. of the cell was measured to $\pm$ 0.1 mV with RADIOMETER PHM 64 and PHM 84 research pH meters.

The titrant solutions were dispensed from grade 'A' burettes or, if they were sodium hydroxide solutions, from a METTLER DV210 automatic piston burette of 10 cm^3 capacity fitted on a METTLER DV10 burette drive. The solution reservoir of this automatic burette was modified to enable the solution therein to be kept under an atmosphere of nitrogen. (This precaution was taken when working with sodium hydroxide titrant solutions to prevent the absorption of CO_2 by the solution.) A nitrogen inlet was fitted onto the solution reservoir. Before the nitrogen came into contact with the solution it passed through a U-tube containing an absorbent for CO_2 and, in the last third of the tube, an absorbent for water. A drying-tube containing the same two absorbents was fitted to the nitrogen outlet of the reservoir in order to prevent atmospheric CO_2 from entering the reservoir in the event of an interruption in the nitrogen flow. The CO_2 absorbent used was HOPKIN AND WILLIAMS soda-lime INDICARB (self-indicating, 5 - 10 mesh), and the absorbent for water was BDH lab. reagent anhydrous calcium sulphate. A water absorbent was needed because the absorption of CO_2 by soda-lime produces water as follows:

$$2NaOH + CO_2 \rightleftharpoons Na_2CO_3 + H_2O.$$

Figure 3.2 shows the solution reservoir assembly.

A stream of high-purity nitrogen, which had been freed from acid and alkaline impurities by passage through 10 % NaOH and 10 % H_2SO_4 solutions respectively, and then presaturated with 0.5 mol dm^{-3} KNO_3, was bubbled through the test solution during the entire duration of the experiment. The solution in the cell was stirred by using a magnetic bar stirrer at all times. The cell assembly is shown in Figure 3.1. The potentiometric titrations were performed in a room thermostatted at 25 $\pm$ 1°C.

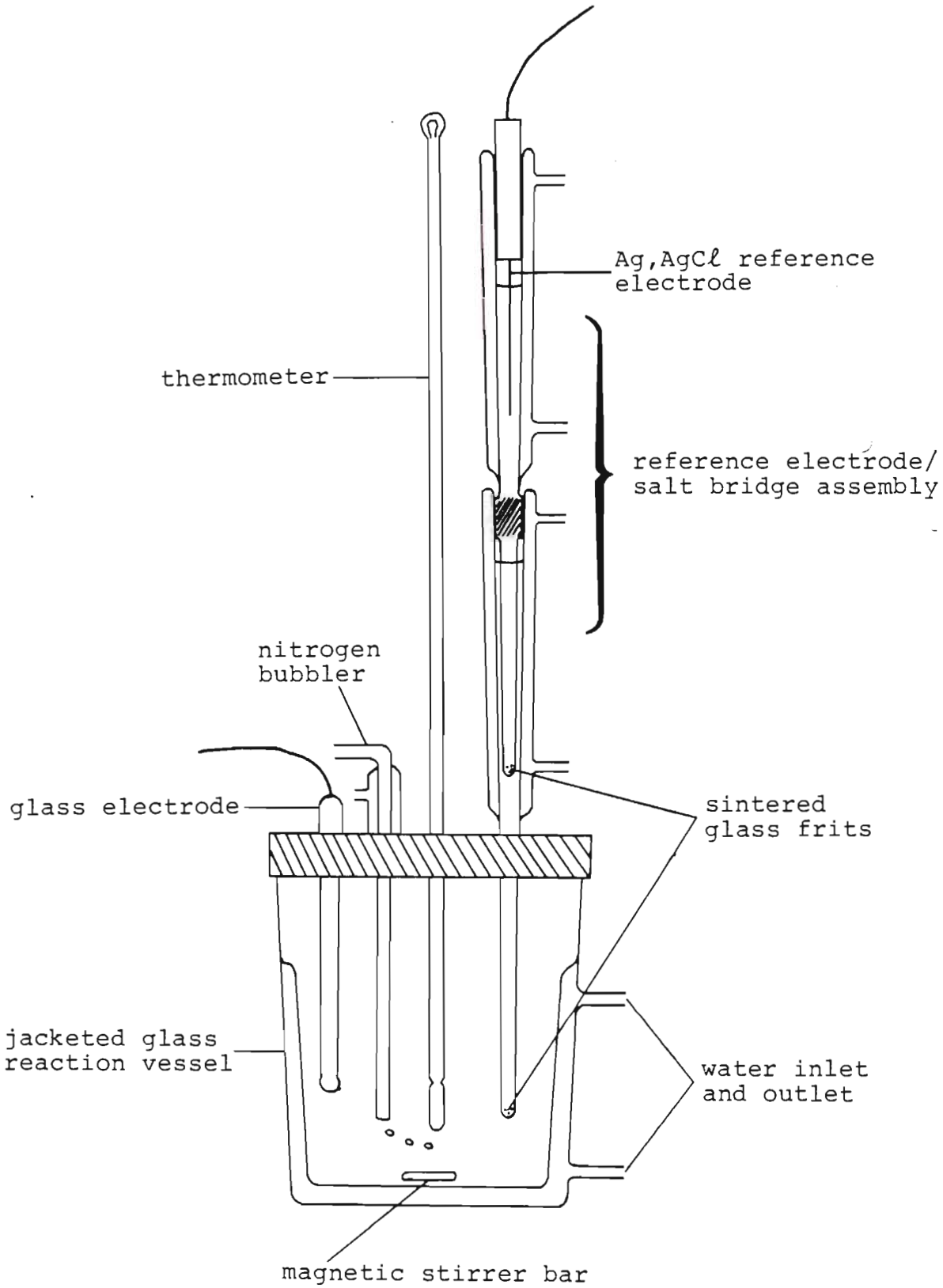

Figure 3.1 The potentiometric cell assembly.

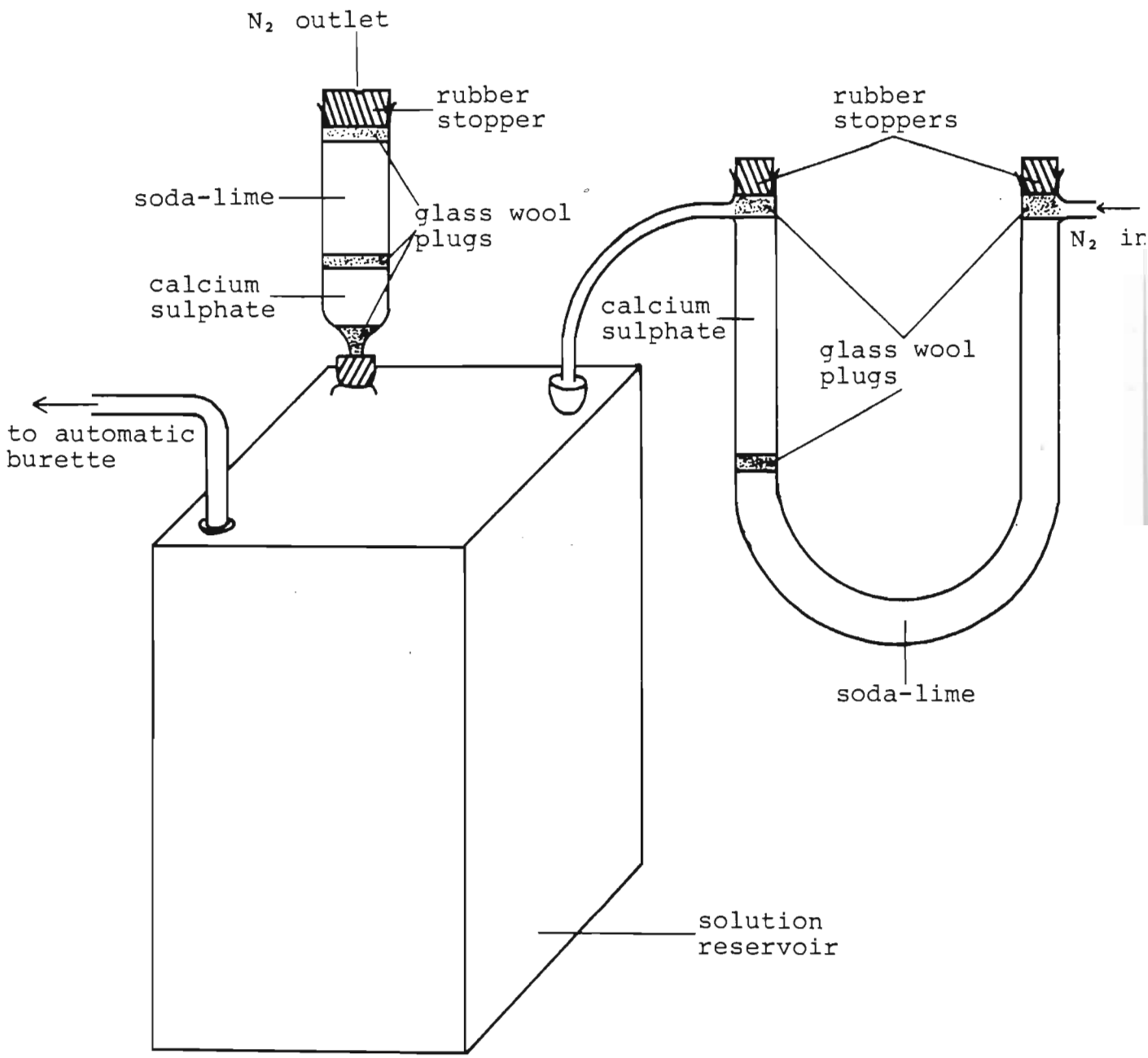

Figure 3.2 Solution reservoir modified to prevent CO_2 absorption.

3.2. The Titration Calorimeter

The enthalpy changes were measured by means of a precision titration calorimeter which the Department of Chemistry, University of Natal, Durban has on loan from the Council for Mineral Technology. The construction and testing of the calorimeter have been described in a N.I.M. Report (118).

The titration calorimeter consists essentially of the LKB 8721-2 titration calorimeter assembly (i.e. a precision thermostatic bath type 7603A, a proportional controller type 7602A, a calorimeter unit type 8721-2 and a stirrer driver unit type 8723) with an electronic system designed and constructed by the Council for Mineral Technology (then the National Institute for Metallurgy). (See Plates 1 and 2.) Since the report on the construction of the calorimeter was published some changes have been made to the electronic assembly. The measuring instrument is no longer the EMT type 213 MK2 six-digit voltmeter but a Fluke model 8810A 5½-digit digital multimeter. The Moduprinter has also been replaced by a Fluke model 2030A programmable printer. The calorimeter is housed in a room thermostatted at 25 ± 1°C.

All the calorimetric measurements are carried out in a cylindrical stainless steel water bath. This bath is in turn contained in a second cylinder of stainless steel. Water from an auxiliary bath maintained at 25,00 ± 0.05°C is circulated between the two cylinders. The temperature of the water in the inner bath is maintained at 25.000 ± 0.001°C by a proportional controller. The whole water bath assembly is surrounded by polystyrene (to prevent heat loss to the surroundings) and placed in a metallic case.

The calorimeter reaction vessel consists of a glass bottle of about 110 cm^3 capacity. Within the vessel are three glass fingers. The first finger contains the heater, the second the thermistor, and the third may be filled from the outside with cooling material. The vessel also contains a glass delivery tip which is connected to the titrant-delivery system via thin tubing.

The glass reaction vessel has a metallic screw-thread at the neck. This is used to attach the vessel to the underside of the stainless steel

Plate 1 The titration calorimeter assembly. From left to right: the proportional controller, thermostatic bath, calorimeter unit, stirrer driver unit and automatic burette.

Plate 2 The titration calorimeter electronic assembly.

cover-plate of the reaction vessel assembly. The heater and thermistor are also connected, via gold contacts, to the underside of this plate. (See Plate 3.) This plate forms the cover of a cylindrical air-tight stainless steel container in which the glass reaction vessel is placed. Above the stainless steel cover-plate is coiled the tubing of the titrant-delivery system. This ensures that the titrant tubing is immersed in the water of the inner bath and that the titrant is held at the temperature of the water bath. Above the titrant coils is a plastic cover. When the calorimeter assembly is placed in the water bath this plastic cover seals off the water bath.

The contents of the glass reaction vessel are stirred by means of a glass screw propeller. The propeller shaft is attached to the bottom of the stainless steel cover-plate. (See Plate 3.) The stirrer is driven by a three-speed stirrer motor.

The titrant is delivered by means of a METTLER DV 10 automatic burette drive fitted with a METTLER DV210 automatic piston burette of 10 cm^3 capacity. The titrant-delivery system was checked and found to be accurate to within 1×10^{-5} cm^3 s^{-1} (118).

The temperature changes occurring in the reaction vessel are measured by means of a thermistor which makes up one arm of a Wheatstone bridge. The other components of the bridge are two equal resistors and a variable resistor. The variable resistor is set in such a way as to balance the bridge at the temperature of the constant-temperature bath. As the temperature in the reaction vessel changes, measurements of the off-balance potential of the bridge are made. (It has been found that the off-balance potential is proportional to the change in temperature (118).)

The digital multimeter is the bridge detector. Readings of the off-balance potential in μV are printed out by the printer at fixed time intervals. The time interval is set on an electronic timer or on the timer incorporated in the printer.

The off-balance potential is related to the actual temperature by means of a calibration experiment (see Section 5.2.1).

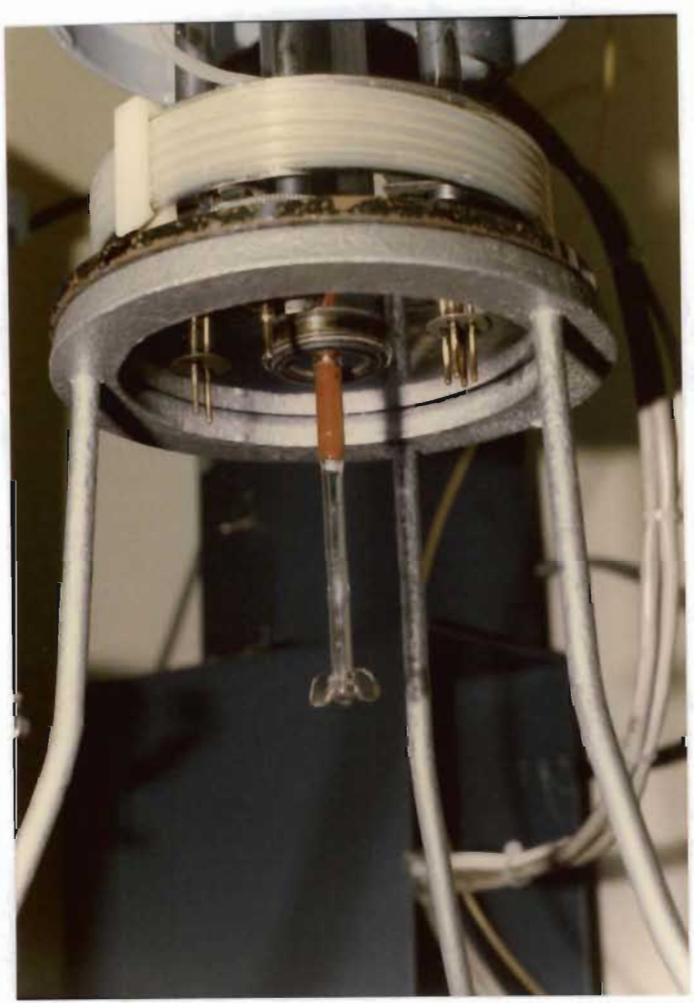

Plate 3 The cover-plate of the reaction vessel assembly, seen from below. Note the stirrer and gold contacts.

There are three modes of operation of the titration calorimeter:

1) Burette mode - this switches on the burette drive and a titration can be performed.

2) Heater mode - this switches on the heater to enable a heat capacity to be determined.

3) Ampoule mode - this activates the ampoule smasher. (This last function was not used in this work.)

For the first two modes of operation a time interval of length up to 999 seconds, during which the burette or heater is operative, must be selected. When that pre-set interval has elapsed the burette or heater automatically switches off.

An accurately known current passes through the reaction vessel heater when one sets a potential of 1.000 00 V across any one of a set of standard resistors built into the circuit. If one then measures the voltage drop across the heater corresponding to the current flowing through it, one can calculate the power dissipated by the heater for a particular nominal power setting. (Values of the current flowing through the heater at particular power settings have been tabulated (118).)

Further details of the operation of the calorimeter will be given in Chapter 7.

CHAPTER FOUR

CALCULATION TECHNIQUES

In this chapter the various computational techniques employed in this work will be described. These will include the Gran plot method for equivalence point determination in potentiometric titrations, the various corrections which have to be applied to the 'raw' calorimetric data before ΔH° values can be calculated, and a description of how formation curves can be derived from potentiometric data. The use of various computer programs to process potentiometric and calorimetric data will also be described.

4.1. Gran Plots

Gran plots provide an easy and accurate means of determining the equivalence point of a potentiometric titration. The equivalence point of a potentiometric titration can, in principle, be determined by plotting values of the cell potential against the volume of titrant added and finding the point of inflection (or maximum slope) of the titration curve. This method presents problems when there is only a small potential change at the end-point, e.g. in the titration of weak acids by strong bases. In such cases it has been customary to plot the curve of $\Delta E/\Delta v$ against the volume v of titrant added. These methods can be criticized in that they do not use the data points which are far from the point of inflection. Furthermore, if the titration curve is not symmetrical about the equivalence point, the results obtained may be erroneous.

Gran (119, 120) and later others (121) devised a way of linearizing the titration curve in such a way that all the points in the titration are used, and not only those in the vicinity of the equivalence point. In his first paper (119) Gran showed that curves of $\Delta v/\Delta pH$ or $\Delta v/\Delta E$ against v have two branches which intersect at the equivalence point. Although for weak electrolyte systems these branches are parabolic they can be transformed into straight lines, and this makes it possible to determine the equivalence point very accurately. Later Gran (120) developed the idea first proposed by Sørensen that, if one plots the antilogarithm of the pH as a function of the volume of titrant added, one can also transform potentiometric titration curves into straight lines.

The plots obtained are called Gran plots and consist of two straight lines which, in theory, intersect each other and the volume axis at the equivalence point. The straight line before the equivalence point shows the titrate concentration decreasing and has a negative slope, whilst that after the equivalence point has a positive slope and shows the excess titrant concentration increasing.

The Gran plot method of determining the equivalence point in a potentiometric titration has several advantages:

1. The titrant solution can be added in regular increments, which is not the case in conventional titrations, where a large number of readings have to be taken near the equivalence point. In this way one may avoid the difficulty of obtaining many points in a region in which the electrode potentials are unstable and drift readily.

2. It provides a simple way of determining the equivalence point in systems in which the end-point break is poor, e.g. weak acid-strong base titrations.

3. Since the plots consist of straight lines, one need only obtain points in a region in which the electrode response is Nernstian or near-Nernstian.

4. The calculations are simple and quick and can be computed and plotted during the actual titration while one is waiting for steady potential readings to be attained.

5. The presence of carbonate in alkali solutions is easily detected and the concentration thereof easily computed.

6. The equivalence point can be determined accurately, even in cases where the titration curve is asymmetrical.

The Gran plot method has the limitation that when the protonation constant of the weak acid is greater than about 10^7 the method no longer gives straight lines, but instead produces curves which do not intersect the

volume axis at the true equivalence point. This is due to the neglect of minor components in the equilibria involved in the titration reactions. Ingman and Still (122) have shown that, if the protonation constant of the weak acid is known, an expression can be derived which, when plotted against the titrant volume, does yield a straight line. This latter method was tried on the standardisations of the ligands used here and will be discussed in the relevant sections. The method also has the limitation that it neglects variations in activity coefficients. This effect can be minimized by the use of a constant ionic medium.

In this work the Gran plot method was used in the analysis of acid-base neutralization titrations. The potentiometric readings for these titrations were obtained by measuring the e.m.f. of the following cell:

(-)RE |salt bridge |titration solution |glass electrode (+) (I)

where RE (reference electrode) = Ag |AgCℓ |0.01 mol dm^{-3} $Cℓ^-$, 0.49 mol dm^{-3} NO_3^-, 0.50 mol dm^{-3} K^+ and salt bridge = 0.50 mol dm^{-3} KNO_3.

The potential of cell (I) is (in theory) given by

$$E = E^{\ominus} + s \log([H^+]\gamma_{H+}) + E_J. \qquad (4.1)$$

Here $E^{\ominus}$ incorporates the standard potential of the glass electrode half-cell and the potential of the reference half-cell, E_J is the liquid junction potential between the salt bridge and the test solution, γ_{H+} is the activity coefficient of H^+ and s represents 2.3026 RT/nF - i.e. we assume that the electrode response is Nernstian. As the ionic strength was kept almost constant, $E^{\ominus}$, E_J and γ_{H+} were considered to remain constant during a potentiometric titration. Equation (4.1) can thus be simplified to

$$E = E^{\ominus *} + s \log([H^+]\gamma_{H+}), \qquad (4.2)$$

where $E^{\ominus *} = E^{\ominus} + E_J$.

Although the Gran plot method has been described in some detail in the literature (119 - 121, 123), a discussion of three cases of the method is included for completeness. In the case of the titration of a strong base

with a strong acid it is of interest to show how the method was used to estimate the carbonate contamination in the strong base solution. The application of Ingman and Still's extended Gran plot method (122) to the titration of a weak diprotic base with a strong acid is described in detail because that case was not treated by them.

In passing, it may be worth noting that,besides acid-base neutralisation titrations, the Gran plot method can also be applied to precipitation, complex formation and redox titrations and the multiple standard addition technique. These applications are discussed in the review article by Mascini (123) and also in Gran's papers (119, 120). A modified Gran plot technique has been described for the determination of activity coefficients and junction potentials (124).

4.1.1. Titration of a strong base with a strong acid

If v_0 cm^3 of strong base, of initial concentration C_B, is titrated with a strong acid of concentration C_A, the concentration of hydroxide ions after the addition of v cm^3 of acid will be:

$$[OH^-] = \frac{C_B v_0 - C_A v}{V_0 + v} , \qquad (4.3)$$

where V_0 is the total initial volume, i.e. besides v_0 it includes the volume of background electrolyte added at the start of the titration.

Setting $v = v_e$, the volume of acid added at the equivalence point, we see that

$$C_B v_0 = C_A v_e . \qquad (4.4)$$

Hence, substituting equation (4.4) into equation (4.3), we obtain

$$[OH^-] = \frac{C_A (v_e - v)}{V_0 + v} . \qquad (4.5)$$

Now

$$[H^+] = \frac{K_W}{[OH^-]} , \qquad (4.6)$$

where K_W is the ionic product of water.

Thus

$$[H^+] = \frac{K_W(V_0 + v)}{C_A(v_e - v)} \quad . \tag{4.7}$$

If the above expression is substituted into equation (4.2) we obtain the following:

$$E = E^{\ominus *} + s \log \left(\frac{\gamma_{H^+} K_W (V_0 + v)}{C_A (v_e - v)} \right) , \tag{4.8}$$

which is a nonlinear relationship between E and v containing the quantity v_e which one wishes to determine. The relationship can be linearized if one considers the following:

$$10^{pH} = 1/a_{H^+}$$

$$= 1/(\gamma_{H^+}[H^+])$$

$$= \frac{C_A(v_e - v)}{\gamma_{H^+} K_W (V_0 + v)}$$

$$= 10^{(E^{\ominus *} - E)/s}$$

(where a_{H^+} is the activity of the hydrogen ion). On rearrangement one obtains the function ϕ given by

$$\phi(v) = (V_0 + v)\ 10^{-E/s} \tag{4.9a}$$

$$= \frac{C_A}{\gamma_{H^+} K_W}\ 10^{-E^{\ominus *}/s}\ (v_e - v) \ , \tag{4.9b}$$

which is linear in v.

After the equivalence point has been passed

$$[H^+] = \frac{C_A v - C_B v_0}{V_0 + v} \ , \tag{4.10}$$

since we are now in the region of excess acid. Again, substituting equation (4.4) into equation (4.10), we obtain

$$[H^+] = \frac{C_A(v - v_e)}{V_0 + v} \quad . \tag{4.11}$$

Equation (4.2) for the cell potential now becomes

$$E = E^{\ominus *} + s \log\left(\frac{\gamma_{H^+} C_A (v - v_e)}{V_0 + v}\right). \tag{4.12}$$

One can then linearize as before:

$$10^{-pH} = a_{H^+}$$

$$= \gamma_{H^+}[H^+]$$

$$= \frac{\gamma_{H^+} C_A (v - v_e)}{V_0 + v}$$

$$= 10^{(E - E^{\ominus *})/s},$$

and

$$\phi'(v) = (V_0 + v)\ 10^{E/s} \tag{4.13a}$$

$$= \gamma_{H^+} C_A\ 10^{E^{\ominus *}/s}(v_e - v). \tag{4.13b}$$

If the ionic strength is kept quite high and almost constant during the titration, then γ_{H^+} and K_w do not change appreciably and the functions ϕ and ϕ' are linear functions of v. The functions ϕ and ϕ', given by equations (4.9a) and (4.13a) respectively, can be plotted and extrapolated to intersect the horizontal axis at the point v_e, since both functions assume the value zero when $v = v_e$.

An example of a Gran plot for the titration of a strong base with a strong acid is shown in Figure 4.1. In this example a mixture of 5.00 cm^3 of approx. 0.1 mol dm^{-3} NaOH and 50.00 cm^3 of 0.50 mol dm^{-3} KNO_3 was titrated with 0.0999 mol dm^{-3} HNO_3 in a cell containing a glass electrode and a silver-silver chloride reference electrode as shown in cell (I). All the solutions used were made up to an ionic strength of 0.50 mol dm^{-3} by using KNO_3. The data collected and the calculations performed to obtain the Gran plot are shown in Table 4.1.

From Figure 4.1 one obtains v_e = 4.87 cm^3, whence the concentration of

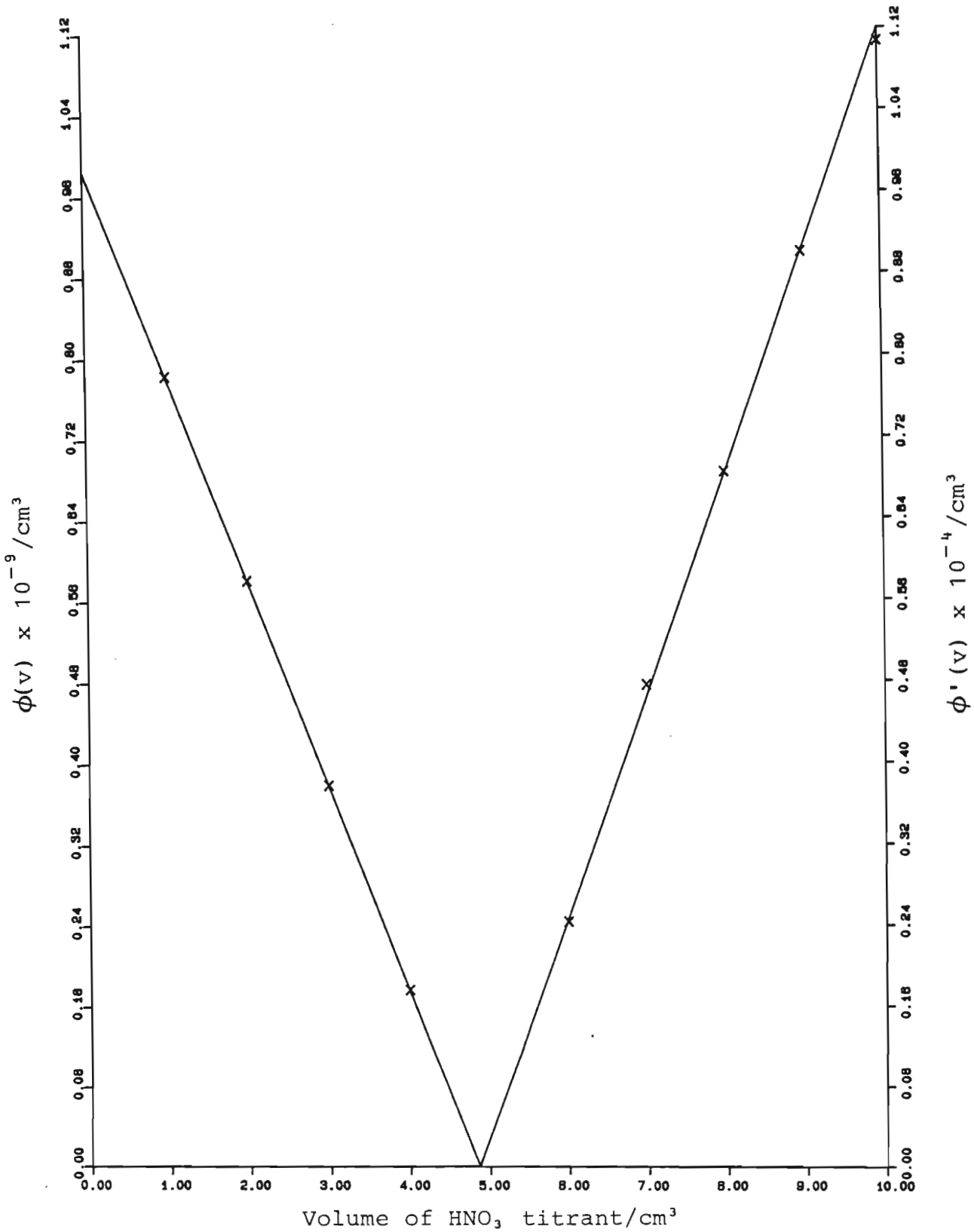

Figure 4.1 Gran plots ϕ and ϕ' for the titration of a strong base with a strong acid.

TABLE 4.1

Titration of a mixture of 5.00 cm^3 of approx. 0.1 mol dm^{-3} NaOH + 50.00 cm^3 of 0.50 mol dm^{-3} KNO_3 with 0.0999 mol dm^{-3} HNO_3 (V_0 = 55.00 cm^3 and t = 25.00°C).

v/cm^3	$(V_0 + v)/cm^3$	E_{cell}/mV	$\phi(v) \times 10^{-9}/cm^3$*
1.00	56.00	-422.7	0.783
2.00	57.00	-414.6	0.581
3.00	58.00	-403.2	0.379
4.00	59.00	-383.2	0.177
			$\phi'(v) \times 10^{-4}/cm^3$*
6.00	61.00	94.8	0.244
7.00	62.00	111.6	0.477
8.00	63.00	120.5	0.686
9.00	64.00	127.1	0.901
10.00	65.00	132.0	1.107

*$\phi(v)$ and $\phi'(v)$ may be multiplied by any constants to make plotting more convenient as this changes only the slopes of the lines and not their point of intersection.

the sodium hydroxide solution can be calculated to be 0.0973 mol dm^{-3}.

The functions ϕ and ϕ' do sometimes deviate from linearity because of one or more of the following factors.

1. If curvature of the Gran plots at values of v remote from v_e occurs it suggests that the activity coefficient and junction potential are not constant at extreme values of hydrogen and hydroxide ion concentrations. If such plots are linear near the equivalence point the value of v_e must be obtained from this region alone.

2. If the strong base is contaminated with carbonate, ϕ, the function on the alkaline side of the equivalence point v_e, is curved in the vicinity of that point, and ϕ', the function on the acidic side, now cuts the horizontal axis at some point $v_e' > v_e$. (An example of this is shown in Figure 4.2.) In this case

$$v_e' = v_0 C_B / C_A, \qquad (4.14)$$

where $C_B = [OH^-] + 2[CO_3^{=}]$, the total concentration of base. If the function ϕ is linear over an appreciable range of v it may be extrapolated to cut the horizontal axis at the point

$$v_e = v_0 [OH^-] / C_A, \qquad (4.15)$$

i.e. from this point the concentration of hydroxide ions in the strong base can be obtained. Thus the concentration of carbonate in the base can be estimated from the difference between v_e' and v_e. Symbolically

$$[CO_3^{=}] = \frac{(v_e' - v_e) C_A}{2 v_0}. \qquad (4.16)$$

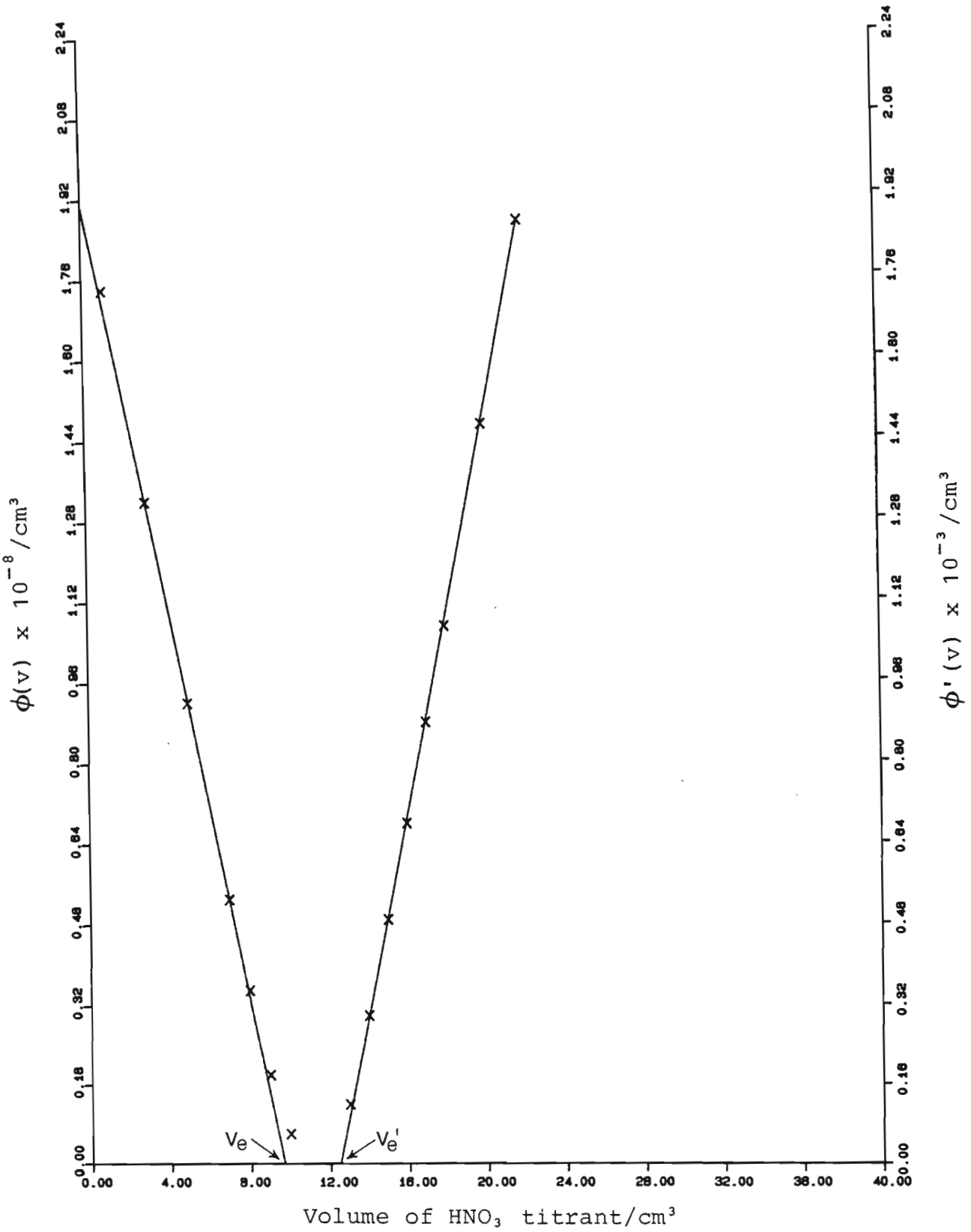

Figure 4.2 Gran plots ø and ø' for the titration of a strong base solution containing both carbonate and hydroxide with a strong acid.

4.1.2. Titration of a weak dibasic acid with a strong base

If v_0 cm^3 of a weak dibasic acid, BH_2^{2+}, having an overall concentration C_A, is titrated with a strong base of concentration C_B, then before the first equivalence point we have the following reaction:

$$BH_2^{2+} + OH^- \rightleftharpoons BH^+ + H_2O$$

with the associated equilibrium constant

$$K_1 = \frac{[BH^+]}{[BH_2^{2+}][OH^-]} . \qquad (4.17)$$

Hence

$$[H^+] = K_w K_1 [BH_2^{2+}]/[BH^+], \qquad (4.18)$$

where

$$[BH_2^{2+}] = \frac{C_A v_0 - C_B v}{V_0 + v} \qquad (4.19)$$

and

$$[BH^+] = \frac{C_B v}{V_0 + v} . \qquad (4.20)$$

(Note that equations (4.19) and (4.20) are only approximations. We have neglected the dissociation of BH^+ and we are assuming that $[B] \ll [BH^+]$ and $[BH_2^{2+}]$.)

Thus

$$[H^+] = \frac{K_w K_1 (C_A v_0 - C_B v)}{C_B v} . \qquad (4.21)$$

By setting $v = v_{e1}$, the volume of base added by the first equivalence point, we see that

$$C_A v_0 = C_B v_{e1}, \qquad (4.22)$$

and so equation (4.21) becomes

$$[H^+] = K_w K_1 (v_{e1} - v)/v. \qquad (4.23)$$

The cell potential for the region before the first equivalence point is therefore given by:

$$E = E^{\ominus *} + s \log(\gamma_{H^+} K_w K_1 (v_{e1} - v)/v). \qquad (4.24)$$

Equation (4.24) is a non-linear relationship between E and v which can be linearized as follows:

$$10^{-pH} = a_{H^+}$$

$$= \gamma_{H^+}[H^+]$$

$$= \gamma_{H^+} K_w K_1 (v_{e1} - v)/v$$

$$= 10^{(E - E^{\ominus *})/s} ,$$

and

$$\phi_1(v) = v\, 10^{E/s} \qquad (4.25a)$$

$$= \gamma_{H^+} K_w K_1 10^{E^{\ominus *}/s} (v_{e1} - v). \qquad (4.25b)$$

After the first equivalence point v_{e1} has been passed the following reaction occurs:

$$BH^+ + OH^- \rightleftharpoons B + H_2O$$

with the associated equilibrium constant

$$K_2 = \frac{[B]}{[BH^+][OH^-]} . \qquad (4.26)$$

The hydrogen ion concentration can be calculated as follows:

$$[H^+] = K_w K_2 [BH^+]/[B] , \qquad (4.27)$$

where

$$[BH^+] = \frac{2C_A v_0 - C_B v}{V_0 + v} \qquad (4.28)$$

and

$$[B] = \frac{C_B v - C_A v_0}{V_0 + v} \quad . \tag{4.29}$$

(Again, equations (4.28) and (4.29) are only approximate.)

Thus

$$[H^+] = \frac{K_w K_2 (2C_A v_0 - C_B v)}{C_B v - C_A v_0} \quad . \tag{4.30}$$

From $v = v_{e1}$ we already have

$$C_A v_0 = C_B v_{e1}, \tag{4.31}$$

and by setting $v = v_{e_2}$, the volume of base added by the second equivalence point, we get

$$2C_A v_0 = C_B v_{e_2} \quad . \tag{4.32}$$

Substituting equations (4.31) and (4.32) into equation (4.30) gives

$$[H^+] = \frac{K_w K_2 (v_{e_2} - v)}{(v - v_{e1})} \quad . \tag{4.33}$$

Therefore

$$E = E^{\ominus *} + s \log(\gamma_H + K_w K_2 (v_{e_2} - v)/(v - v_{e1})) . \tag{4.34}$$

Equation (4.34) can be linearized as follows for the region after the first equivalence point but remote from the second equivalence point:

$$10^{pH} = 1/a_{H+}$$

$$= 1/(\gamma_H + [H^+])$$

$$= \frac{(v - v_{e1})}{\gamma_H + K_w K_2 (v_{e_2} - v)}$$

$$= 10^{(E^{\ominus *} - E)/s} ,$$

and

$$\phi_1'(v) = (v_{e_2} - v)\ 10^{-E/s} \qquad (4.35a)$$

$$= (\gamma_H + K_w K_2)^{-1} 10^{-E^{\ominus *}/s} (v - v_{e_1}). \qquad (4.35b)$$

For the region just before the second equivalence point equation (4.34) can similarly be linearized:

$$\Psi_1(v) = (v - v_{e_1})\ 10^{E/s} \qquad (4.36a)$$

$$= \gamma_H + K_w K_2\ 10^{E^{\ominus *}/s}\ (v_{e_2} - v). \qquad (4.36b)$$

The function to be plotted after the first equivalence point, given by equation (4.35a), presupposes knowledge of v_{e_2} which, for this purpose, can be estimated from the plot of cell potential against volume of titrant added. By the time the Gran function for the region before the second equivalence point is calculated (by means of equation (4.36a)) v_{e_1} will have been determined.

After the second equivalence point has been passed excess base is present. Thus

$$[OH^-] = \frac{C_B v - 2C_A v_0}{V_0 + v}, \qquad (4.37)$$

and since equation (4.32) holds we have

$$[OH^-] = \frac{C_B(v - v_{e_2})}{V_0 + v}. \qquad (4.38)$$

Now

$$[H^+] = \frac{K_w(V_0 + v)}{C_B(v - v_{e_2})}, \qquad (4.39)$$

which can be substituted into equation (4.2) to give the cell potential for the region after the second equivalence point:

$$E = E^{\ominus *} + s \log\left(\frac{\gamma_H + K_w(V_0 + v)}{C_B(v - v_{e_2})}\right). \qquad (4.40)$$

Equation (4.40) can be linearized to:

$$\Psi_1'(v) = (V_0 + v)\ 10^{-E/s} \qquad (4.41a)$$

$$= \frac{C_B}{\gamma_{H^+}K_w}\ 10^{-E^{\ominus *}/s}(v - v_{e_2}). \qquad (4.41b)$$

Provided, then, that γ_{H^+}, K_w, K_1 and K_2 are constant, which can approximately be achieved by keeping the ionic strength constant, the functions ϕ_1, ϕ_1', Ψ_1 and Ψ_1' are linear functions of v. The first equivalence point is the point v_{e_1} such that $\phi_1(v_{e_1}) = \phi_1'(v_{e_1}) = 0$, and the second equivalence point, v_{e_2}, is obtained similarly from Ψ_1 and Ψ_1'.

To illustrate the Gran plot method for the titration of a weak dibasic acid with a strong base the titration of 20.00 cm^3 of approx. 0.044 mol dm^{-3} oden.2HCℓ with 0.0996 mol dm^{-3} NaOH will be considered. All the solutions used were made up to an ionic strength of 0.50 mol dm^{-3} using KNO_3. An estimate of v_{e_1} was arrived at by halving the estimate of v_{e_2} obtained from the titration curve shown in Figure 4.3. A Gran plot could be drawn only for the determination of the second equivalence point of oden.2HCℓ because the first equivalence point is not distinct. The plot is shown in Figure 4.4. The data and calculations performed to obtain these Gran plots are shown in Table 4.2. From the intersection of Ψ_1' with the horizontal axis, as shown in Figure 4.4, we see that v_{e_2} = 16.6 cm^3. Hence the concentration of oden can be calculated to be 0.0413 mol dm^{-3}.

An attempt was made to apply Ingman and Still's extension (122) of Gran's method to the standardisation of solutions containing oden. For the titration described above, i.e. the titration of oden.2HCℓ with a strong base, the functions plotted were:

$$\phi_2(v) = v_{e_1} - v$$

$$= vK_{201}b + (1 + K_{201}b)(b - K_w b^{-1})(V_0 + v)/C_B \qquad (4.42)$$

before the first equivalence point, and

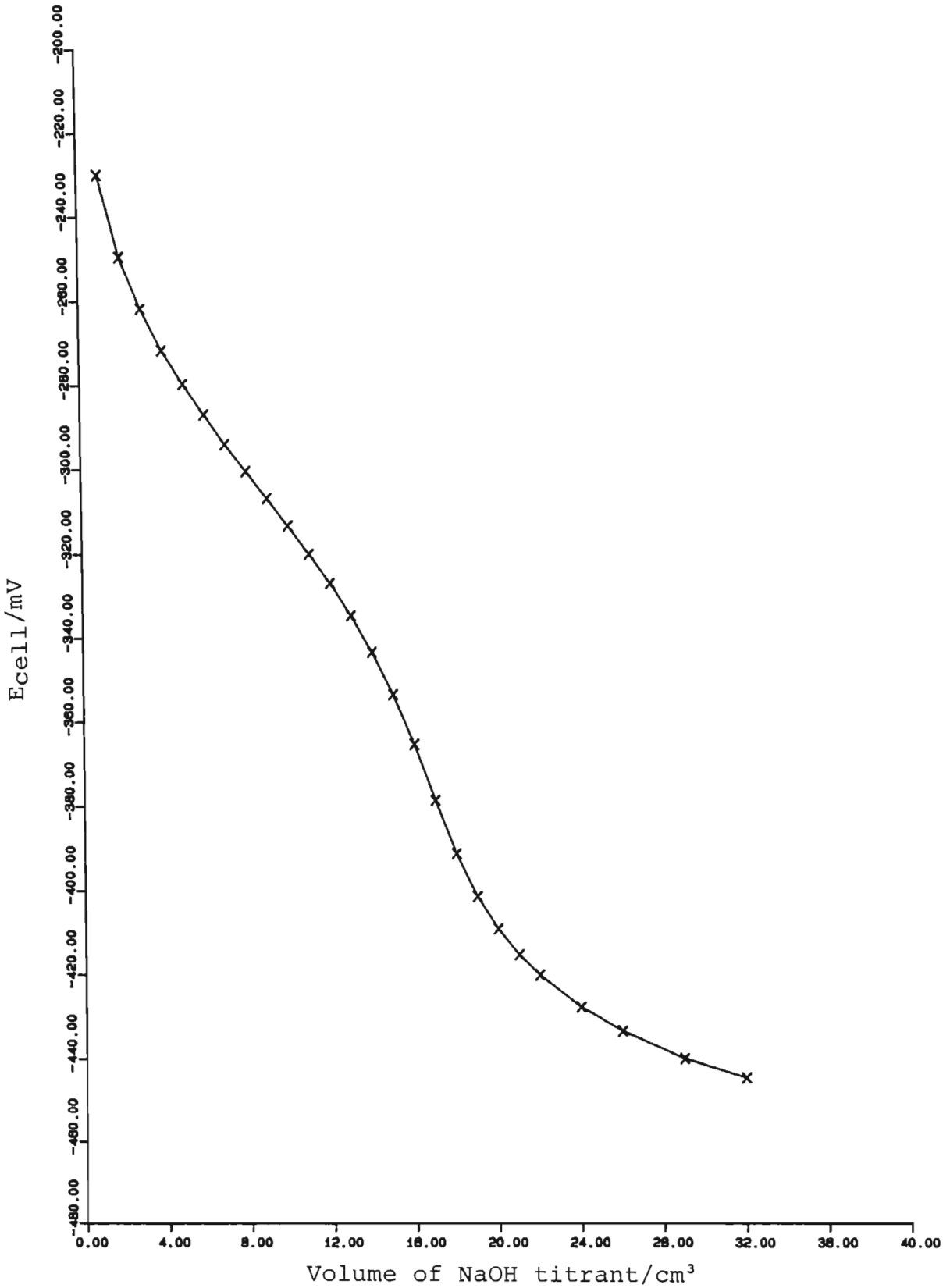

Figure 4.3 Titration curve for the titration of a weak dibasic acid (oden.2HCℓ) with a strong base (NaOH).

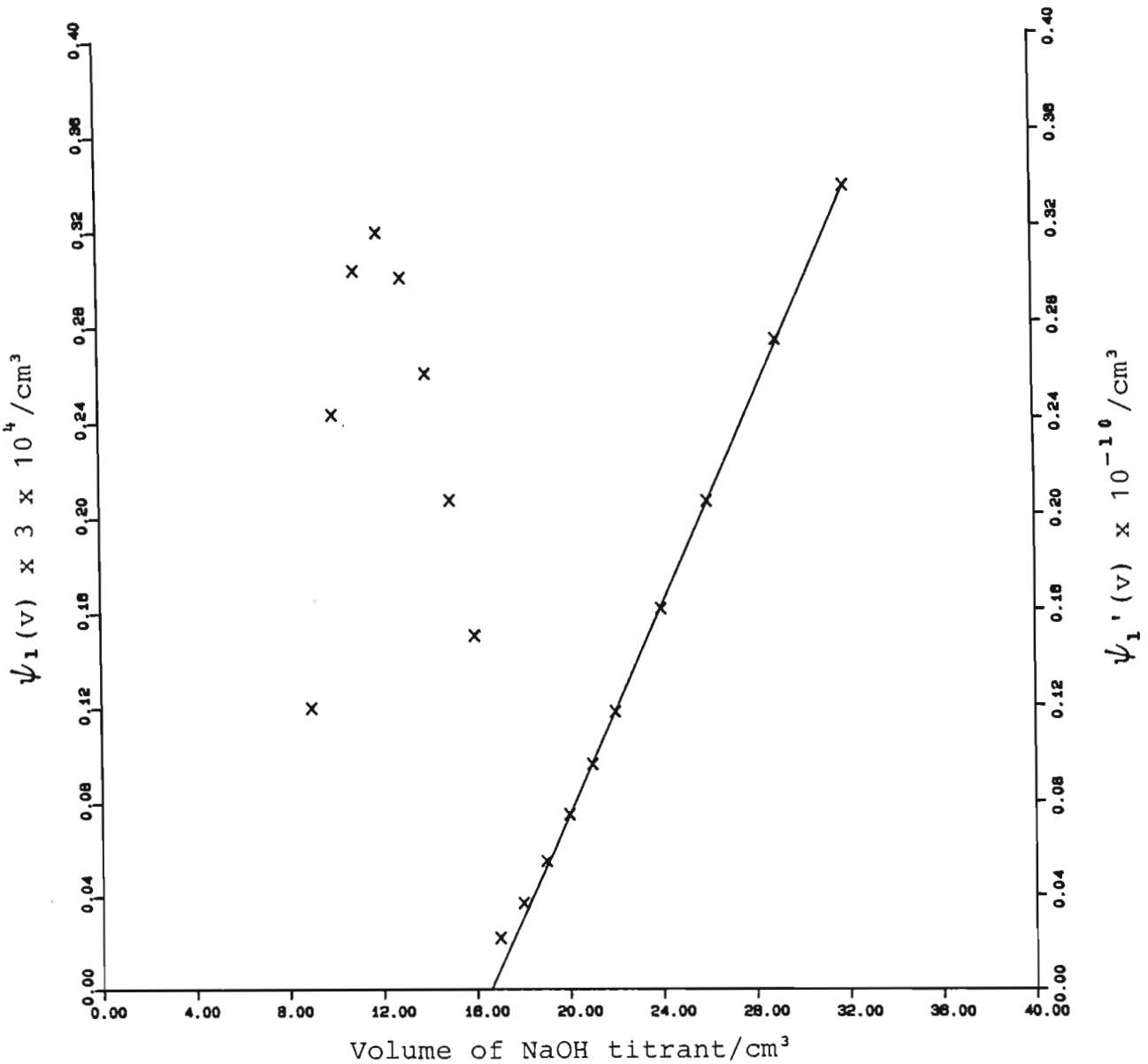

Figure 4.4 Gran plots Ψ_1 and Ψ_1' for the determination of the second equivalence point in the titration of a weak dibasic acid with a strong base.

TABLE 4.2

Titration of 20.00 cm^3 of approx. 0.044 mol dm^{-3} oden.2HCℓ with 0.0996 mol dm^{-3} NaOH (V_0 = 70.00 cm^3).

(a) Before the second equivalence point:

v/cm^3	$(v - v_{el})/cm^3$	E_{cell}/mV	$\Psi_1(v) \times 3 \times 10^4/cm^3$
9.00	0.62	-307.1	0.120
10.00	1.62	-313.6	0.243
11.00	2.62	-320.3	0.303
12.00	3.62	-327.3	0.319
13.00	4.62	-335.1	0.300
14.00	5.62	-343.8	0.260
15.00	6.62	-353.9	0.207
16.00	7.62	-365.7	0.150

where v_{el} = 8.38 cm^3.

(b) After the second equivalence point:

v/cm^3	$(V_0 + v)/cm^3$	E_{cell}/mV	$\Psi_1'(v) \times 10^{-10}/cm^3$
17.00	87.00	-379.0	0.022
18.00	88.00	-391.6	0.037
19.00	89.00	-401.8	0.055
20.00	90.00	-409.5	0.075
21.00	91.00	-415.6	0.096
22.00	92.00	-420.4	0.118
24.00	94.00	-428.0	0.161
26.00	96.00	-433.7	0.206
29.00	99.00	-440.2	0.273
32.00	102.00	-444.8	0.337

$$\Psi_2(v) = v_{e_2} - v$$

$$= (v - v_{e_1})K_{101}b + (1 + K_{101}b)(b - K_w b^{-1})(V_0 + v)/C_B \qquad (4.43)$$

before the second equivalence point.

(The meanings of the symbols used in equations (4.42) and (4.43) are described in Section 4.1.3.) It was found that the difference between log K_{101} and log K_{201} for oden is too small (i.e. < 1) for straight lines to be obtained even by this method. This is because no simple expressions can be obtained to describe the concentrations of BH_2^{2+}, BH^+, B and H^+ adequately. Hence the concentration of oden was calculated as described previously.

4.1.3. Titration of a weak diprotic base with a strong acid

In the case of the titration of the weak diprotic base etolen with a strong acid, it turns out that the "ordinary" Gran plot method can be inaccurate because it does not take into account minor species involved in the equilibria. If often happens that one does not get a pair of straight lines intersecting on the horizontal axis. More important, however, is that there is considerable variation between repeat titrations in the equivalence points as calculated by this method. The following method, similar to that of Ingman and Still (122), was therefore developed and applied to the etolen standardisation data in an attempt to obtain more reliable and reproducible estimates of the equivalence points. The expressions to be plotted against the titrant volume for the titration of a weak diprotic base with a strong acid can be derived as follows.

If v_0 cm^3 of a weak diprotic base, B, of concentration C_B is titrated with a strong acid of concentration C_A the reversible reaction occurring before the first equivalence point is

$$B + H_3O^+ \rightleftharpoons BH^+ + H_2O,$$

with the associated equilibrium constant

$$K_{101} = \frac{[BH^+]}{[B][H^+]} \cdot \qquad (4.44)$$

The following expressions can be written for the concentrations of BH^+ and B in solution:

$$[BH^+] = \frac{C_A v}{V_0 + v} - [H^+] + [OH^-] \qquad (4.45)$$

and

$$[B] = C_B - [BH^+]$$

$$= \frac{C_B v_0 - C_A v}{V_0 + v} + [H^+] - [OH^-] , \qquad (4.46)$$

where V_0 is the total initial volume. (The equations analogous to (4.45) and (4.46) appearing in Gran's method are:

$$[BH^+] = \frac{C_A v}{V_0 + v} \quad \text{and}$$

$$[B] = \frac{C_B v_0 - C_A v}{V_0 + v} , \text{ respectively.}$$

We see that these two equations neglect the terms in $[H^+]$ and $[OH^-]$. In other words, Gran's method ignores the fact that protonation of the base B is a reversible reaction - i.e. a reaction that does not necessarily proceed quantitatively to completion - and that the base B is capable of generating BH^+ in solution through hydrolysis reactions.)

At the first equivalence point, v_{e1}, we have

$$C_B v_0 = C_A v_{e1} . \qquad (4.47)$$

Substitution of equations (4.45), (4.46) and (4.47) into the equilibrium constant expression (equation (4.44)) and subsequent rearrangement yield

$$v_{e1} - v = \frac{v}{K_{101}[H^+]} + \frac{V_0 + v}{C_A K_{101}[H^+]} ([OH^-] - [H^+])(1 + K_{101}[H^+]) . \qquad (4.48)$$

Now the cell potential is given by

$$E = E^{\ominus\prime\prime} + s \log [H^+], \qquad (4.49)$$

where $E^{\ominus\prime\prime}$ incorporates the standard potential of the probe half-cell, the potential of the reference half-cell, the liquid junction potential and the activity coefficient of H^+. $E^{\ominus\prime\prime}$ was considered to remain constant during a titration because the ionic strength was kept almost constant.

Hence

$$[H^+] = 10^{(E - E^{\ominus\prime\prime})/s} \qquad (4.50)$$

and since

$$[OH^-] = \frac{K_W}{[H^+]}\ , \qquad (4.51)$$

equation (4.48) can be rewritten to define a function ϕ_3 as follows:

$$\phi_3(v) = v_{e1} - v$$

$$= v/(bK_{101}) + (K_W b^{-1} - b)(1 + K_{101}b)(V_0 + v)/(bK_{101}C_A) \qquad (4.52)$$

where b represents $10^{(E - E^{\ominus\prime\prime})/s}$.

ϕ_3 is a linear function of v and intersects the horizontal axis at v_{e1}. The only disadvantage of this method is that the value of K_{101} at the ionic strength being used must be known.

After the first equivalence point, v_{e1}, has been passed we have the following reaction occurring:

$$BH^+ + H_3O^+ \rightleftharpoons BH_2^{2+} + H_2O$$

with the associated equilibrium constant

$$K_{201} = \frac{[BH_2^{2+}]}{[BH^+][H^+]}\ . \qquad (4.53)$$

Again, expressions for the reactant concentrations can be written:

$$[BH_2^{2+}] = \frac{C_A v - C_B v_0}{V_0 + v} - [H^+] + [OH^-] \qquad (4.54)$$

and

$$[BH^+] = \frac{2C_B v_0 - C_A v}{V_0 + v} + [H^+] - [OH^-]. \qquad (4.55)$$

(The expressions appearing in Gran's method are:

$$[BH_2^{2+}] = \frac{C_A v - C_B v_0}{V_0 + v}$$

and

$$[BH^+] = \frac{2C_B v_0 - C_A v}{V_0 + v} .)$$

When $v = v_{e1}$ we have the following relationship:

$$C_B v_0 = C_A v_{e1}, \qquad (4.56)$$

whereas when $v = v_{e2}$, the volume of acid added at the second equivalence point, we have

$$2C_B v_0 = C_A v_{e2}. \qquad (4.57)$$

After substitution of equations (4.54), (4.55), (4.56) and (4.57) into equation (4.53) and subsequent rearrangement, we obtain

$$v_{e2} - v = \frac{v - v_{e1}}{K_{201}[H^+]} + \frac{V_0 + v}{K_{201}[H^+]C_A}([OH^-]-[H^+])(1 + K_{201}[H^+]). \qquad (4.58)$$

Again equations (4.50) and (4.51) hold, and we can define a function Ψ_3 as follows:

$$\Psi_3(v) = v_{e2} - v$$

$$= (v - v_{e1})/(bK_{201}) + (K_w b^{-1} - b)(1 + K_{201}b)(V_0 + v)/(bK_{201}C_A) \qquad (4.59)$$

which is again linear in v. Equation (4.59) presupposes knowledge of the first equivalence point, v_{e1}, but this is usually determined before the second equivalence point.

In conclusion, we see that the plots of $\phi_3(v)$ and $\Psi_3(v)$ against v are linear provided $E^{\ominus}$", K_w, K_{101} and K_{201} are constant, i.e. if the ionic strength is kept constant. One obtains v_{e_1} from $\phi_3(v_{e_1}) = 0$ and v_{e_2} from $\Psi_3(v_{e_2}) = 0$.

To illustrate this method the titration of a mixture of 20.00 cm^3 of approx. 0.1 mol dm^{-3} etolen and 50.00 cm^3 of 0.50 mol dm^{-3} KNO_3 with 0.09992 mol dm^{-3} HNO_3 will be considered. All the solutions used in this titration were made up to an ionic strength of 0.50 mol dm^{-3} by using KNO_3. The resulting titration curve is shown in Figure 4.5, and the data and calculations performed to obtain the extended Gran plots are shown in Table 4.3. The value of $E^{\ominus}$" required for these calculations was determined experimentally by calibrating the potentiometric cell as described in Section 5.1.1 prior to standardising the ligand solution. For those standardisations in which the value of $E^{\ominus}$" was not determined experimentally it was estimated from log $[H^+]$ values obtained from a species distribution calculation. The computer program HALTAFALL (see Section 4.4.1) was used to calculate the required species distribution. The program was provided with the protonation constants of the ligand, an estimate of the ligand concentration obtained from the titration curve, and the titrant acid concentration. From the calculated log $[H^+]$ and the experimental cell potential values an estimate for $E^{\ominus}$" could be obtained through use of the Nernst relationship (equation (4.49)).

Figure 4.6 depicts the extended Gran plot obtained for the determination of the first equivalence point, v_{e_1}, of etolen. As can be seen, a curve was obtained instead of a straight line. It seems that the difference between log K_{101} and log K_{201} is insufficient (being < 3) to prevent partial overlap of the two protonation equilibria. However a straight line was obtained for the second equivalence point, v_{e_2}. From Figure 4.7 we see that the extended Gran plot gives v_{e_2} = 40.80 cm^3. In plotting $\Psi_3(v)$ an estimate for v_{e_1} is required. This was obtained from the graph of cell potential against volume of titrant added. It was found that the value of v_{e_2} obtained was not very sensitive to the estimate of v_{e_1} used. The concentration of etolen was calculated from the value of v_{e_2} alone. In this example the concentration of etolen was found to be 0.1019 mol dm^{-3}.

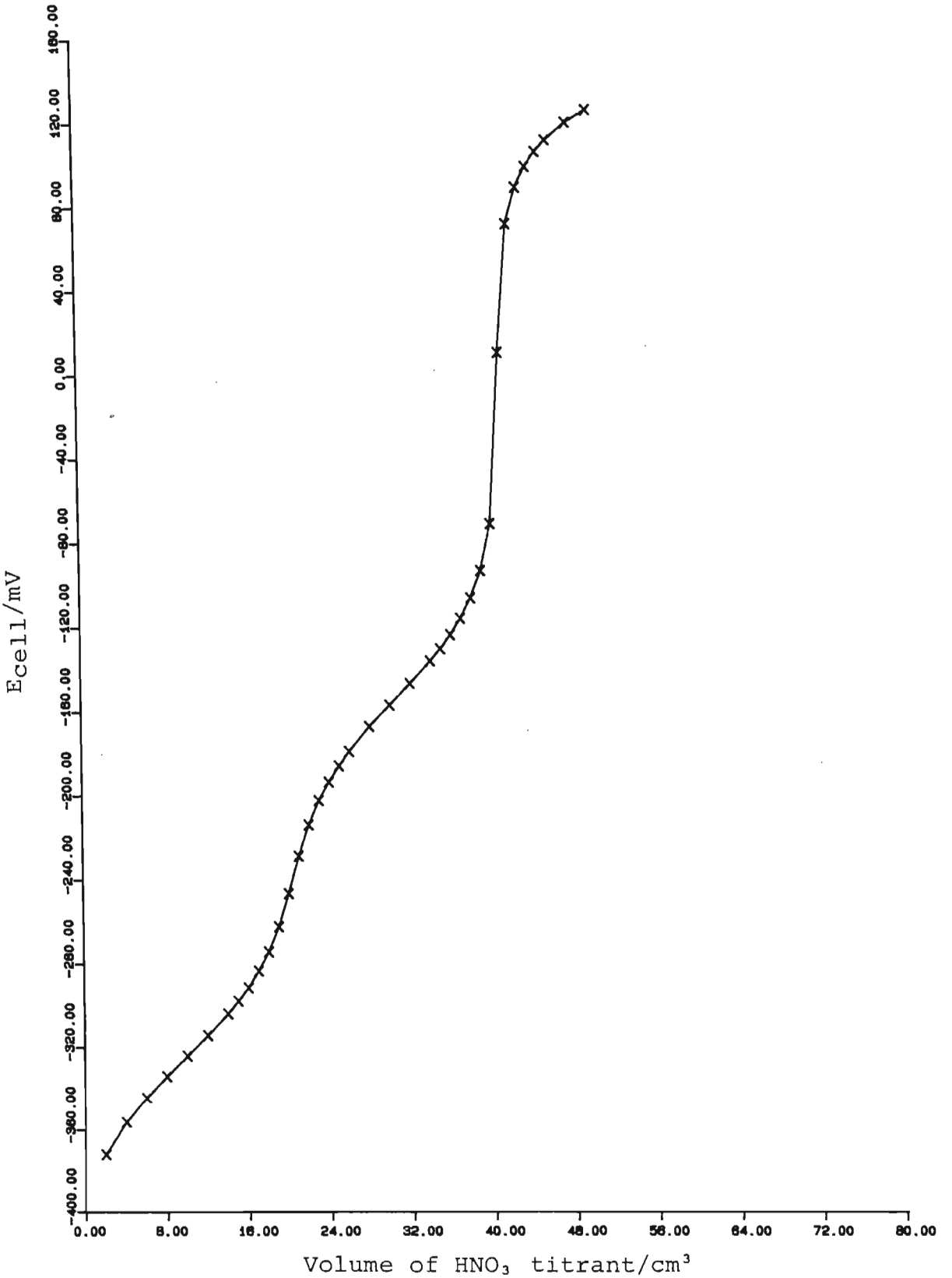

Figure 4.5 Titration curve for the titration of a weak diprotic base (etolen) with a strong acid (HNO_3).

TABLE 4.3

Titration of a mixture of 20.00 cm^3 of approx. 0.1 mol dm^{-3} etolen + 50.00 cm^3 of 0.50 mol dm^{-3} KNO_3 with 0.09992 mol dm^{-3} HNO_3 (V_0 = 70.00 cm^3).

(a) Determination of the first equivalence point, v_{e1}:

v/cm^3	E_{cell}/mV	$\phi_3(v)/cm^3$
2.00	-372.0	16.60
4.00	-356.3	15.37
6.00	-344.3	13.87
8.00	-333.9	12.14
10.00	-324.3	10.36
12.00	-314.4	8.42
14.00	-303.9	6.51
15.00	-298.1	5.56
16.00	-291.5	4.58
17.00	-283.6	3.58
18.00	-274.4	2.65
19.00	-262.3	1.74
20.00	-246.6	1.00
21.00	-229.1	0.53
22.00	-214.3	0.31
23.00	-202.8	0.21
24.00	-194.0	0.15
25.00	-186.4	0.12
26.00	-179.5	0.09

Values of constants used to evaluate ϕ_3:

$K_W = 1.8197 \times 10^{-14}$

$K_{101} = 5.4954 \times 10^{9}$

$E^{\ominus}_{II} = 252.4$ mV

(b) Determination of the second equivalence point, v_{e_2} :

v/cm^3	E_{cell}/mV	$\Psi_3(v)/cm^3$
30.00	-157.6	11.50
32.00	-147.4	9.35
34.00	-136.7	7.23
35.00	-131.0	6.22
36.00	-124.4	5.14
37.00	-116.8	4.07
38.00	-107.2	2.97
39.00	- 94.4	1.91
40.00	- 72.3	0.85
41.00	8.9	-0.05
42.00	69.5	-0.90
43.00	86.8	-1.79
44.00	96.7	-2.66

Values of constants used to evaluate Ψ_3 :

$K_W = 1.8197 \times 10^{-14}$

$K_{201} = 7.0795 \times 10^{6}$

$E^{\ominus}{}'' = 252.40$ mV

$v_{e1} = 20.45\ cm^3$

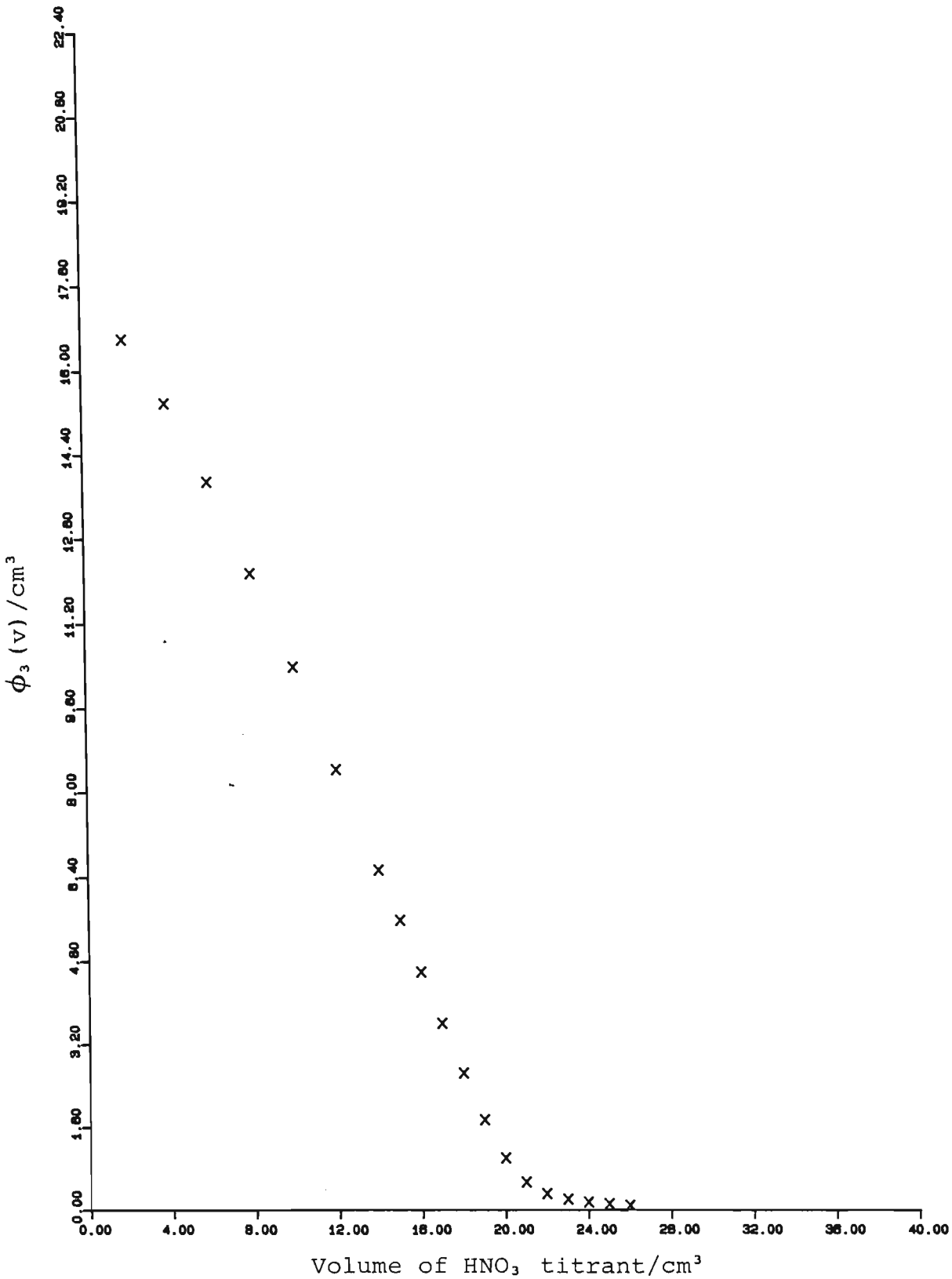

Figure 4.6 Extended Gran plot ϕ_3 for the determination of the first equivalence point in the titration of a weak diprotic base with a strong acid.

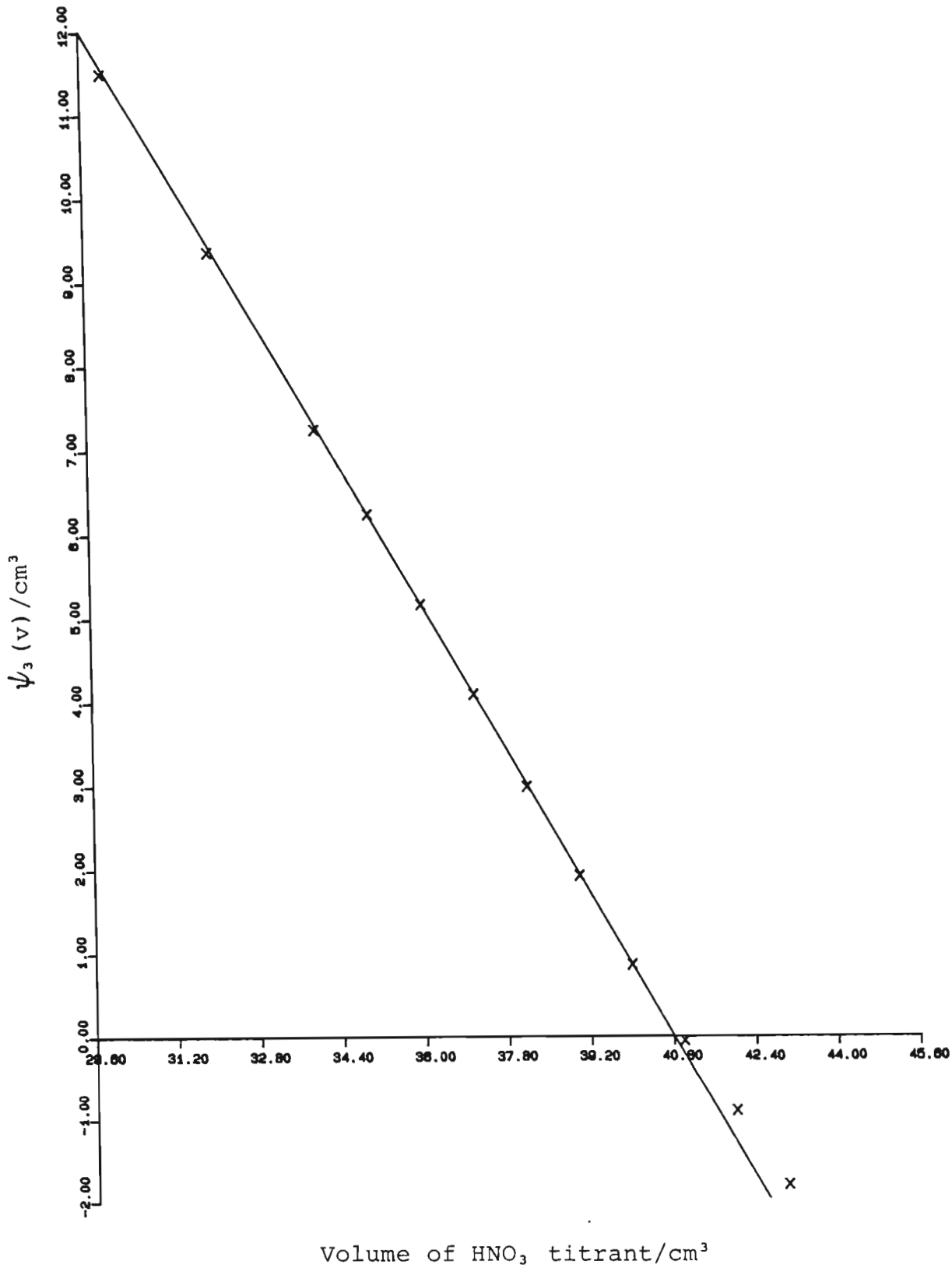

Figure 4.7 Extended Gran plot Ψ_3 for the determination of the second equivalence point in the titration of a weak diprotic base with a strong acid.

In spite of the problems associated with the first equivalence point, this method did indeed overcome the irreproducibility encountered in the "ordinary" Gran plot method.

4.2. Calculation of 'non-chemical' heat corrections for titration calorimetric data

The gross heat liberated in the reaction vessel during a titration calorimetric run not only consists of the heats of the reactions being studied but is also the result of extraneous heat effects operating during the experiment. Thus, in general, the determination of $\Delta H^{\ominus}$ values from titration calorimetric data involves four main steps:

(1) the experimental determination of the gross heat liberated in the reaction vessel as a function of titrant added,

(2) the calculation of all correction terms for 'non-chemical' heat effects occurring in the reaction vessel,

(3) the evaluation of heat effects contributed from reactions other than the ones being studied, and

(4) the calculation of the energy changes due to the reactions in question and, finally, the $\Delta H^{\ominus}$ values.

In this section the first two points will be considered.

Continuous titration calorimeters (such as the one used in this study) produce data consisting of times of titrant delivery and the corresponding temperature of the system. (In the calorimeter used in this work the Wheatstone bridge off-balance potentials were measured. Over a small temperature interval such potentials are linearly related to temperature (90). This relationship is determined by calibrating the Wheatstone bridge - see Section 5.2.1.) Plots of such data are called thermograms. In essence a thermogram consists of three parts: a lead (or initial) period, a titration period, and a trail (or final) period. There are two basic types of thermogram. The first type is obtained for reactions that proceed to completion, i.e. every aliquot of titrant added is almost completely consumed up to the end-point, and further addition of titrant

merely results in dilution of the titrant. Thus the titration period is divided into two parts: a reaction period before the end-point and a dilution period after the end-point. A thermogram for such a titration is shown in Figure 4.8. The second type of thermogram, shown in Figure 4.9, is observed for incomplete reactions, in which no amount of titrant added is ever used up completely. Thus there is no division of the titration period in such a thermogram.

The regions shown in Figures 4.8 and 4.9 will now be discussed in terms of the predominant heat effects occurring within them. Region 'a' shows a rise in temperature of the reaction vessel and its contents before the titration begins. Such heat gain is due to stirring, resistive heating across the thermistor, conduction, convection and radiation to or from the surroundings, and evaporation. Region 'b' is the reaction period, in which the heat rise is largely due to the reaction occurring in the calorimeter but also partly due to the dilution of titrant and titrate, the difference in temperature between the titrate and titrant, and the 'non-chemical' effects mentioned for region 'a'. Region 'c' is the post-reaction region, in which the temperature change is due to continued addition of titrant after the reaction is complete. That is, the same effects as in region 'b', apart from the reaction of interest, result in the temperature change observed in region 'c'. For incomplete reactions 'c' does not exist and it is necessary to measure the heat of dilution produced on addition of the titrant to a blank titrate (i.e. one not containing the reacting species of interest). This is done by means of a separate experiment. Region 'd' is the post-reaction or trail period, where no titrant is added and the slope is a function of the same effects as those mentioned for region 'a'.

Thus a thermogram consists of a series of bridge off-balance potentials read at various points in time or, equivalently, a plot of temperature against time. From each reading the total heat liberated or absorbed in the reaction vessel, from the beginning of the titration to that point, can be calculated. Once this quantity has been corrected for extraneous heat effects, all that remains is the heat due to the reaction of interest, and $\Delta H^{\ominus}$ for the reaction can be calculated. However, before analyzing such data, one must calibrate the calorimetric equipment - see Section 5.2.

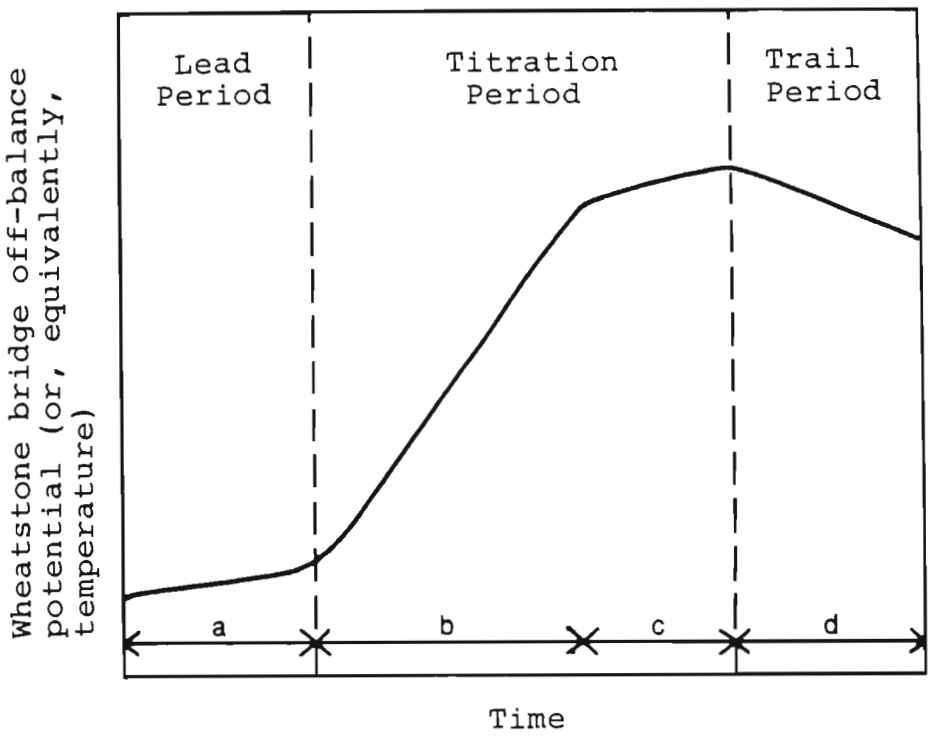

Figure 4.8 Thermogram of a titration with complete reaction.

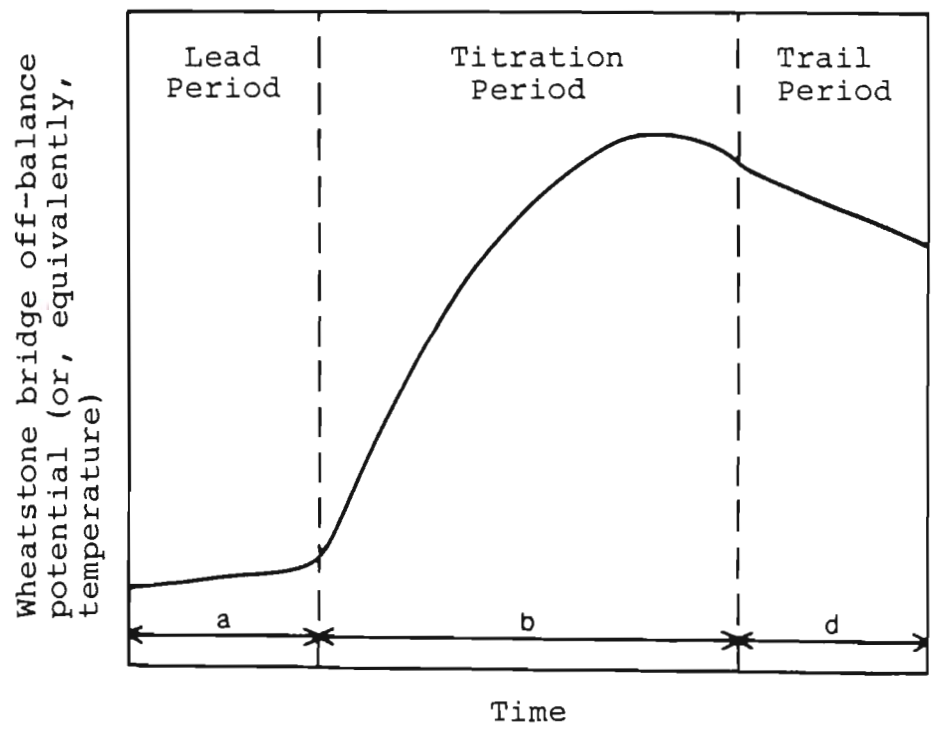

Figure 4.9 Thermogram of a titration with incomplete reaction.

In calculating the various corrections to be applied to the gross heat liberated in the reaction vessel one first determines the heat capacities of all the solutions used in the experiment. Experimentally one actually measures Cp, the heat capacity of the reaction vessel plus its contents. This quantity is made up of two parts, as shown in the following equation:

$$Cp = Cp^r + Cp^s. \qquad (4.60)$$

Here Cp^r is the heat capacity of the empty reaction vessel plus the various parts of the calorimeter (such as the stirrer, thermistor, heater and burette tip) which are immersed in the reaction solution and heated with it, and Cp^s is the heat capacity of the solution in the reaction vessel. (For the determination of Cp^r see Section 5.2.3.) A typical thermogram for the determination of the heat capacity of a filled reaction vessel is shown in Figure 4.10.

One can relate Q_E, the electrical heat introduced into the reaction vessel during a heat capacity determination, to the temperature rise observed, ΔT_{obs}, by means of

$$Cp = Q_E/\Delta T_{obs}. \qquad (4.61)$$

This equation is however an oversimplification, as it does not take into account the heat effects such as heat of stirring, resistive heating of the thermistor and heat exchange with the surroundings. A procedure for correcting for these effects can be developed by making use of the fact that these are the only effects occurring in regions 'a' and 'd' of the thermogram, and this is done as follows.

If one takes N points, equally spaced in time along the heating section of the thermogram, one can calculate for each time point the rate of change in bridge off-balance potential attributable at that point to the abovementioned effects. The rate of change, r_k, at the k-th time point, t_k, is obtained as follows by interpolation between S_i and S_f, the slopes of the lead and trail sections respectively of the thermogram:

$$r_k = S_i + (S_f - S_i)\,\frac{E_k - E_x}{E_y - E_x}, \quad \text{for } k = 1, 2, \ldots, N. \qquad (4.62)$$

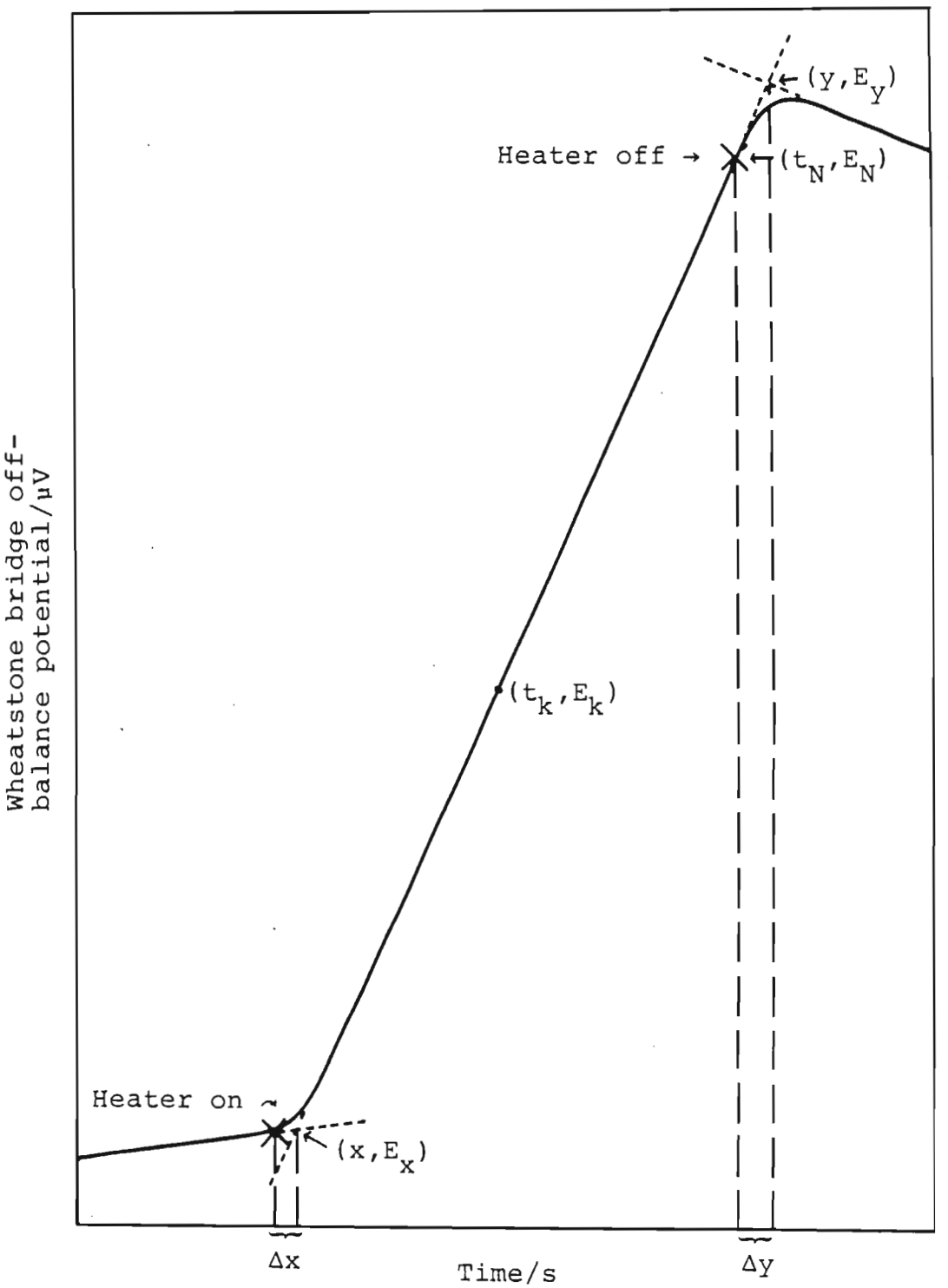

Figure 4.10 Thermogram for the determination of the heat capacity of a filled reaction vessel.

Here E_k is the off-balance potential at the time point t_k.(x, E_x) is the point of intersection of the (extensions of the) straight lines observed in the lead and heating sections of the thermogram, and (y, E_y) is defined similarly by the heating and trail sections. (See Figure 4.10.) One can now integrate these rates r_k by means of the trapezoidal rule to obtain a correction (ΔT_{corr}) to the total temperature rise observed (ΔT_{obs}) during a determination of heat capacity. The result is:

$$\Delta T_{corr} = \{(h - \Delta x)(S_i + r_1) + h \sum_{k=2}^{N} (r_{k-1} + r_k) + \Delta y\ (r_N + S_f)\}/2b, \quad (4.63)$$

where the N points chosen are spaced at intervals of h seconds, and Δx is the time elapsed from the moment the heater is switched on to time x. Time x may be regarded as the time at which the off-balance potential begins to rise in response to heating, if one replaces the observations by the piecewise linear approximation depicted in Figure 4.10. Similarly Δy represents the time elapsed from the moment the heater is switched off to the time y, which may be regarded as the approximate time at which the off-balance potential ceases to rise. b is the slope of the Wheatstone bridge calibration line (see Section 5.2.1), which relates the off-balance potential measured, E, to the temperature T, as follows:

$$E = a + bT. \quad (4.64)$$

(If the points (t_k, E_k) lie exactly on the straight line joining (x, E_x) to (y, E_y), the correction term reduces to the simple formula $(S_i + S_f)(y - x)/2b$, which is, mutatis mutandis, the same as the correction term in equation (15) of the paper of Eatough *et al.* (90). Detailed examination of the data from several heat capacity determinations suggests that there is in fact very little difference between the values of ΔT_{corr} produced by the two methods.)

In any case a more explicit expression for Cp is given by the following equation:

$$Cp = Q_E/(\Delta T_{obs} - \Delta T_{corr}), \quad (4.65)$$

where Q_E is found by multiplying the calibration heater power by the total time for which the heater was in use during the run, and ΔT_{obs} is taken to be $(E_y - E_x)/b$.

A computer program called CALCAL has been written by Prof. F. Marsicano to calculate such heat capacity values. The use of this program will be described in Section 4.4.7.

If one now considers a reaction run, as distinct from a heat capacity determination, one can calculate for each of the N equally spaced time points t_k the total heat capacity of the reaction vessel and its contents at that point, Cp_k. For a given volume $V_{T,k}$ of titrant added at point t_k we have:

$$Cp_k = Cp^r + V_0.Cp^S + V_{T,k}.Cp^T + V_{T,k}(dCp^r/dV) \quad k = 1, 2, \ldots, N, \tag{4.66}$$

where V_0 is the initial volume of the titrate, and Cp^S and Cp^T are, in $J\ K^{-1}\ cm^{-3}$, the specific heats (per unit volume) of the titrate and titrant solutions respectively. The derivative dCp^r/dV is the rate of increase of the heat capacity of the reaction vessel with increase in volume above V_0. This increase in heat capacity occurs because further parts of the vessel and stirrer paddle come into contact with solution. The additivity of the heat capacities in the above equation is a reasonable assumption because one is here considering dilute aqueous solutions.

The gross heat produced in going from t_{k-1} to t_k can be calculated as follows:

$$\begin{aligned} Qp_k &= -(Cp_{k-1} + Cp_k)(T_k - T_{k-1})/2 \\ &= -(Cp_{k-1} + Cp_k)(E_k - E_{k-1})/2b \quad k = 2, 3, \ldots, N. \end{aligned} \tag{4.67}$$

T_k and T_{k-1} are the temperatures in the reaction vessel at times t_k and t_{k-1} respectively. Qp_1, the gross heat produced between time x and time t_1, is calculated as follows:

$$Qp_1 = -(Cp_x + Cp_1)(E_1 - E_x)/2b. \tag{4.68}$$

Thus for each of the N points on the thermogram a corresponding Qp_k value

can be determined which represents the total heat produced in the reaction vessel from t_{k-1} to t_k. These Qp_k values therefore have to be corrected for all the heat effects other than the reaction of interest before the ΔH° values can be obtained.

Among the heat effects which must be corrected for are the heat generated by stirring of the solution, resistive heating by the thermistor, and the heat exchange due to the temperature difference between the reaction vessel and its surroundings. For a suitably constructed calorimeter it can be assumed that the power derived from the thermistor and stirrer, w, is a constant.

For each of the N points of the titration one can calculate the rate of heat loss of the reaction vessel by assuming that it obeys Newton's law of cooling, i.e. this rate is proportional to the difference in temperature between the reaction vessel and its surroundings. Therefore the net rate of heat loss, $q_{HL,k}$, at the kth point is:

$$q_{HL,k} = -w - c(\theta - T_k), \qquad (4.69)$$

where w and c are positive constants and θ is the temperature of the surroundings. To obtain the rates of heat loss at points x and y we can make use of S_i and S_f, the slopes of the initial and final portions of the thermogram. The results we get are:

$$q_{HL,x} = -S_i Cp_x/b$$

$$= -w - c(\theta - T_x) \qquad (4.70)$$

and

$$q_{HL,y} = -S_f Cp_y/b$$

$$= - w - c(\theta - T_y), \qquad (4.71)$$

where Cp_y is given by

$$Cp_y = Cp^r + V_0 Cp^s + V_{T,y} Cp^T + V_{T,y}(dCp^r/dV), \qquad (4.72)$$

and $V_{T,y}$ represents the total volume of titrant added. The relationships involving θ given in (4.69) - (4.71) are difficult to use because of the difficulty of obtaining values for θ. By combining equations (4.69) to

(4.71) we can however arrive at an expression for $q_{HL,k}$ not involving θ, w, or c:

$$q_{HL,k} = q_{HL,x} + (q_{HL,y} - q_{HL,x}) \frac{E_k - E_x}{E_y - E_x} . \qquad (4.73)$$

To obtain $Q_{HL,k}$, the total contribution of the non-chemical heat effects from time t_{k-1} to time t_k, we assume that q_{HL} is a linear function of time between t_{k-1} and t_k. (This is why it is desirable to choose a sufficiently large number, N, of data points so that the interval between points is small.) Thus one arrives at:

$$Q_{HL,k} = \frac{h}{2} (q_{HL,k-1} + q_{HL,k}) \quad k = 2, 3, \ldots, N \qquad (4.74)$$

and

$$Q_{HL,1} = \frac{(h - \Delta x)}{2} (q_{HL,x} + q_{HL,1}) . \qquad (4.75)$$

The second correction which must be applied is one that takes account of the difference in temperature between the titrate and the titrant. Since the titrant is kept at the temperature of the water bath, heat appears to be liberated or absorbed according to whether the titrate in the reaction vessel is at a temperature lower or higher than that of the constant temperature bath. The correction for this effect over the interval from t_{k-1} to t_k is given by

$$Q_{TC,k} = -Cp^T(hV_{T,y}/Nh)(T_{bath} - T_k) \quad k = 2, 3, \ldots, N, \qquad (4.76)$$

where T_k is obtained from E_k by means of equation (4.64), and T_{bath} is the temperature of the thermostatic bath. In the case of the first time interval one has to allow for the time lag occurring at the start of the titration, hence the temperature correction term is

$$Q_{TC,1} = -Cp^T[(h - \Delta x)V_{T,y}/Nh][T_{bath} - T_1] . \qquad (4.77)$$

The next correction which must be applied is that which allows for the dilution of the titrant as it is added to the titrate. This heat effect occurs as a result of solvation and ion-pairing, and its magnitude changes according to the relative concentrations of the species present in the

titrate solution. Usually the concentrations and concentration changes of the species present in the titrate solution are small enough so that their contribution to the heat of dilution is negligible. However this is not true in the case of the titrant solution, which undergoes dilution by a factor of about twenty during a typical calorimetric titration. In this work the heat of dilution for each titration was determined experimentally by adding the titrant to a blank titrate solution (i.e. to a titrate solution which differs from the usual one only in that the reacting species of interest has been replaced by an equivalent amount of background electrolyte). In each determination the 'raw' heats obtained are corrected for the non-chemical heat effects. To obtain the heat of dilution H_D (in J mol^{-1}) for the titrant of concentration C_T into the appropriate titrate solution, we proceed as follows. The corrected heats liberated or absorbed between t_{k-1} and t_k are averaged and divided by Δv, the incremental volume, and by the concentration C_T. The heat of dilution correction is calculated as follows for the interval from t_{k-1} to t_k:

$$Q_{D,k} = C_T(V_{T,y}/Nh)(h/1000)H_D \qquad k = 2, 3, \ldots, N. \qquad (4.78)$$

(The factor of 1000 in the denominator accommodates the usual practice of expressing C_T in mol dm^{-3} and $V_{T,y}$ in cm^3.) However the value of $Q_{D,1}$ must be corrected for the usual time lag observed at the beginning of the titration. Hence

$$Q_{D,1} = C_T(V_{T,y}/Nh)((h - \Delta x)/1000)H_D. \qquad (4.79)$$

Once all these corrections have been calculated the gross heat liberated or absorbed from time t_{k-1} to t_k can be corrected appropriately. Thus $Q_{c,k}$, the corrected gross heat produced between t_{k-1} and t_k, is given by:

$$Q_{c,k} = Qp_k - Q_{HL,k} - Q_{TC,k} - Q_{D,k} \qquad k = 1, 2, \ldots, N. \qquad (4.80)$$

A computer program called CALCOR has been written by Prof. F Marsicano to correct calorimetric data for 'non-chemical' heat effects. The use of this program will be described in Section 4.4.8.

Once these $Q_{c,k}$ values have been obtained they can be supplied to a published computer program such as LETAGROP KALLE (see Section 4.4.10), which then corrects these values for the heats contributed from side reactions and finally calculates $\Delta H^{\ominus}$ values for the reactions of interest.

Christensen *et al.* have published three papers describing titration calorimetry (89), the calculation techniques used therein (90), and applications of the method (91). The above discussion of corrections for non-chemical heat effects is based partly on their treatment of this issue, and partly on the work of Prof. F Marsicano as implemented in the programs CALCAL and CALCOR. Barthel (125) also gives a mathematical description of the heat processes involved during a calorimetric titration.

4.3. Formation Curves

Before one calculates stability constants by computerised methods it is advisable to perform a simple exploratory graphical analysis in order to obtain a general view of the behaviour of the system and detect the presence of errors. For this purpose plots of formation curves are extremely useful. Such curves can also be used for species selection and the determination of numerical values of stability constants (79 - 81). Formation curves were however not used for this last purpose. The construction of formation curves and their interpretation will now be discussed. The ligands used in this study are diprotic bases. Hence the theory outlined in Sections 4.3.1. and 4.3.2. will be for such ligands only.

4.3.1. $\bar{j}(\log[H])$ plots

Since the stability constants of the complexes studied in this work were determined by a method involving competition between metal ions and hydrogen ions for the ligand L, the protonation constants of these ligands had to be measured first.

Fora diprotic base there are two protonation reactions:

$$H + L \rightleftharpoons HL \qquad (4.81)$$

and

$$2H + L \rightleftharpoons H_2L, \tag{4.82}$$

for which we can write the following stability constants respectively:

$$\beta_{101} = \frac{[HL]}{[H][L]} \tag{4.83}$$

and

$$\beta_{201} = \frac{[H_2L]}{[H]^2[L]} \cdot \tag{4.84}$$

(Charges have been omitted for the sake of clarity.)

We may express the total concentrations of the ligand and hydrogen ion as

$$[L]_t = [L] + [HL] + [H_2L] \tag{4.85}$$

and

$$[H]_t = [H] + [HL] + 2[H_2L] - [OH]. \tag{4.86}$$

Since the equilibrium concentrations of HL, H_2L and OH can be given in terms of the equilibrium concentrations of H and L and the appropriate stability constants, we get:

$$[L]_t = [L] + \beta_{101}[H][L] + \beta_{201}[H]^2[L] \tag{4.87}$$

and

$$[H]_t = [H] + \beta_{101}[H][L] + 2\beta_{201}[H]^2[L] - K_w[H]^{-1}. \tag{4.88}$$

The extent of protonation is expressed by means of the quantity $\bar{j}$, defined as the average number of hydrogen ions bound to each ligand. Thus

$$\bar{j} = \frac{\text{bound H}}{\text{total L}}$$

$$= \frac{[H]_t - [H] + [OH]}{[L]_t}$$

$$= \frac{[H]_t - [H] + K_w[H]^{-1}}{[L]_t} , \qquad (4.89)$$

and therefore, by using equations (4.88) and (4.87), we arrive at

$$\bar{j} = \frac{\beta_{101}[H] + 2\beta_{201}[H]^2}{1 + \beta_{101}[H] + \beta_{201}[H]^2} . \qquad (4.90)$$

By means of equation (4.89), values of $\bar{j}$ can be calculated from the experimental values of $[H]_t$, $[L]_t$ and $[H]$. From equation (4.90) we see that $\bar{j}$ is a function only of $[H]$ and is independent of $[H]_t$ and $[L]_t$. The way in which $\bar{j}$ varies with $[H]$ depends on the values of β_{101} and β_{201}.

Plots of $\bar{j}$ against log $[H]$ can therefore be drawn to show this variation with $[H]$. Such plots are called 'formation curves'. The formation curve of a diprotic ligand has the following characteristics:

1. The points plotted form a single curve for all values of $[H]_t$ and $[L]_t$.

2. The curve is horizontal near $\bar{j} = 0$ and $\bar{j} = 2$.

3. The only other plateau is at $\bar{j} = 1$.

4. The formation curve is symmetrical under rotation through 180° about its mid-point.

If any deviations from the above characteristics occur, then there is an error either in the measurements or in the species assumed to be present. An error in the measurements can arise through use of an incorrect value for $[L]_t$ or $[H]_t$ due to faulty standardisation of a stock solution. A description of how one can deduce the types of species present in solution from formation curves will be given in the following section.

4.3.2. $\bar{Z}$(log[L]) plots

For equilibrium systems involving a metal ion the formation curves of interest are plots of $\bar{Z}$ against log (concentration of free ligand, L), where $\bar{Z}$ is the average number of ligands bound to each metal ion and is given by

$$\bar{Z} = \frac{\text{conc. of ligand bound to metal}}{\text{total metal ion concentration}} \quad . \qquad (4.91)$$

In this study metal complex formation was followed by measuring the hydrogen ion concentration by means of a glass electrode. The ligands used can complex with both metal ions and hydrogen ions. These considerations must therefore be borne in mind when deriving mass balance expressions for the total concentrations of metal ion, ligand and hydrogen ion. Thus, if we assume that only the mononuclear species ML to ML_N are present, and that there is no hydrolysis of the metal aquo ion, we obtain equations (4.92) - (4.94) for the total concentrations.

$$[M]_t = \sum_{i=0}^{N} [ML_i]$$

$$= \sum_{i=0}^{N} \beta_{01i}[M][L]^i \quad , \qquad (4.92)$$

where $\beta_{01i} = \dfrac{[ML_i]}{[M][L]^i}$ and $\beta_{010} = 1.$

$$[L]_t = \sum_{i=1}^{N} i[ML_i] + \sum_{j=0}^{2} [H_jL]$$

$$= \sum_{i=1}^{N} i\,\beta_{01i}\,[M][L]^i + \sum_{j=0}^{2} \beta_{j01}[H]^j[L], \qquad (4.93)$$

where $\beta_{001} = 1.$

$$[H]_t = [H] - [OH] + \sum_{j=1}^{2} j\,[H_jL]$$

$$= [H] - K_w[H]^{-1} + \sum_{j=1}^{2} j\,\beta_{j01}[H]^j[L]. \qquad (4.94)$$

Equation (4.91) may be expressed as

$$\bar{Z} = \frac{\sum_{i=1}^{N} i\,[ML_i]}{\sum_{i=0}^{N} [ML_i]} = \frac{\sum_{i=1}^{N} i\,\beta_{01i}[L]^i}{\sum_{i=0}^{N} \beta_{01i}\,[L]^i} \quad . \qquad (4.95)$$

Using (4.92) and (4.93) we obtain the following expressions for $\bar{Z}$:

$$\bar{Z} = \frac{[L]_t - \sum_{j=0}^{2} [H_jL]}{[M]_t}$$

$$= \frac{[L]_t - [L] - \beta_{101}[H][L] - \beta_{201}[H]^2[L]}{[M]_t} \quad . \qquad (4.96)$$

From equation (4.94)

$$[L] = \frac{[H]_t - [H] + K_w[H]^{-1}}{\beta_{101}[H] + 2\beta_{201}[H]^2} \quad . \qquad (4.97)$$

Substituting equation (4.97) into equation (4.96) and using equation (4.90) we obtain

$$\bar{Z} = \frac{[L]_t - \bar{j}^{-1}([H]_t - [H] - K_w[H]^{-1})}{[M]_t} \quad . \qquad (4.98)$$

Thus $\bar{Z}$ can easily be calculated since $[M]_t$, $[L]_t$ and $[H]_t$ are usually known, $[H]$ is measured experimentally, and β_{101} and β_{201} have usually been determined previously.

The derivation of the expressions (4.95), (4.96) and (4.98) for the quantity $\bar{Z}$ assumes that no polynuclear or ternary species are present. Under these assumptions $\bar{Z}$ is identical to the quantity $\bar{n}$ used by various other authors. If such species are present, these expressions are no longer exact: exact calculation of $\bar{Z}$ would require knowledge of the stability constants for these species.

From equation (4.95) we see that $\bar{Z}$ is a function of the stability constants and the free ligand concentration if only mononuclear species ML_i

are present. If polynuclear species are present $\bar{Z}$ (as given by equation 4.96) will depend on [M] in addition to [L] and the stability constants. If however the complexes are mononuclear but include hydrolysed or protonated complexes, $\bar{Z}$ will be independent of [M] but will vary according to $[H]_t$, $[L]_t$ and the stability constants.

Thus, if plots of $\bar{Z}$ against log [L] are superimposable for differing values of $[M]_t$, polynuclear species are absent. If the formation curve plots are superimposable for widely differing values of $[H]_t$ and $[L]_t$, the possibility of protonated or hydroxo- complexes may be ruled out (126, 127). Thus formation curves give an indication of the types of complexes present in the system being studied.

If the highest value of $\bar{Z}$ obtained (say N) lies on a plateau and is an integer then the highest mononuclear complex formed is ML_N. However it is sometimes not possible to obtain a complete formation curve. Nevertheless some information can be obtained in that case. For instance, if the highest value of $\bar{Z}$ obtained is slightly greater than 1, the highest complex present is at least ML_1, whereas if a maximum value of $\bar{Z}$ just below 2 is obtained but there is no decrease in slope, then the presence of at least ML_3 can tentatively be assumed.

Caution must be exercised when using the procedures described in the above paragraph, because, at high $p[H^+]$ values, $\bar{Z}(\log[L])$ curves seem to exhibit 'shoot-up'. (That is, after some stage $\bar{Z}$ increases very steeply relative to $\log[L]$.) It seems that, in the presence of excess hydroxide, $\bar{Z}$ becomes very sensitive to small changes in $[H]_t$, and so this 'shoot-up' effect could merely reflect experimental error (see Section 8.3). Another feature exhibited by formation curves is a 'curl-back' effect (see Section 8.4). This feature seems to indicate the presence of ternary hydroxy metal complexes (128).

In practice formation curves obtained from experimental measurements are compared with theoretical formation curves obtained for the various models postulated. The model which best reproduces the experimental formation curve is then accepted as giving a satisfactory description of the system. (For the calculation of experimental and theoretical formation curves see Sections 4.4.1, 4.4.3, and 4.4.5.)

Formation curves can also reveal the presence of various kinds of errors. This enables 'bad' points (i.e. outliers) to be discarded, and some systematic errors, e.g. those due to incorrect solution concentrations, to be detected.

4.4. Computer Programs Used

A number of computer programs were used in order to process the potentiometric and calorimetric data. Their use will now be described.

4.4.1. HALTAFALL

The computer program HALTAFALL (129) is a general program for calculating the concentrations of species in an equilibrium mixture. It can treat a mixture of several components which can form a number of complexes and solid phases. The calculations can be carried out if one specifies the overall concentrations of the components, the relevant equilibrium constants (known or estimated, expressed as stability constants), and a description of the composition of the mixture.

In this study the program was used to simulate titrations in a single solution phase. In order to do this, values of the unknown stability constants were estimated. From the species distribution tables obtained for various reagent concentrations it could be decided under what conditions (e.g. $p[H^+]$ range) the experiments should be performed in order to optimize the formation of the species desired without interference from side reactions. The program was also used to determine which experimental procedure would result in the greatest sensitivity of the measured quantity, in this case $[H^+]$, to the stability constant/s being determined. To do this the estimate of the stability constant under consideration was changed by one log unit at a time and the effect on the estimated $p[H^+]$ was noted.

A modified version of the standard HALTAFALL program, viz. HALTA1, was developed in order to calculate the ionic strength at each point of a titration. The only additional input information required is the concentration of the inert electrolyte and the charges of all the components present. This version of the program is useful in verifying that an approximately constant ionic medium is present during a titration. This modification to the standard HALTAFALL program was carried out by L. Biggs

in December 1979.

The program HALTAFALL was also used to calculate species distributions once the stability constants for a particular system were known (e.g. see Section 4.1.3). These species distributions can be used to calculate theoretical values of $\bar{Z}$, denoted $\bar{Z}$(calc), which can then be compared with the observed values, denoted $\bar{Z}$(obs).

4.4.2. MAGEC

The computer program MAGEC (130) uses potentiometric glass electrode cell calibration data to set up and solve a set of equations for the values of $E^{\ominus}{}''$, K_w, the protonation constants of the calibrant, and the slope of the electrode calibration line. It can also refine estimates of solution concentrations if so required. The titrate and titrant solutions can consist of a strong acid, a strong base, a ligand, or any combination of these.

In addition it contains a subprogram called CALIBT which analyses calibration data from potentiometric acid-base neutralisation titrations involving monobasic reactants only. It determines the electrode calibration line by least squares. It can also scan pK_w and adjust the reagent concentrations in order to improve the fit. It also provides a Gran plot analysis for comparison.

MAGEC is useful when weak acids or weak bases are used as calibrants, since their protonation constants can be determined at the same temperature and ionic strength as the rest of the experiment while one is calibrating the potentiometric cell. In practice, however, the use of MAGEC for the simultaneous determination of the cell calibration line and the ligand protonation constants is limited. If correlation of errors between two or more of the parameters occurs the program may give a false solution. The authors advise the use of MAGEC in conjunction with MINIQUAD (131) in a cycling procedure (130).

Various problems were encountered with the use of the program MAGEC. These are described in Section 5.1.3. Despite its advantages, this program was in fact not used in the final analysis of the data.

MAGEC was used via the program FORMAT which will be described briefly in Section 4.4.6.

4.4.3. ZBAR

A FORTRAN program called ZBAR was written to calculate $\bar{Z}$(obs) (as given by equation 4.96) from e.m.f. data. This program was tested on Ni^{2+}-etolen data which had previously been used in hand calculations of $\bar{Z}$(obs).

4.4.4. MINIQUAD

The stability constants of the complex species in solution were calculated from the potentiometric data by making use of the computer program MINIQUAD (131), which is specifically written for the purpose. In this work the original version of MINIQUAD, with the modifications made by Leggett (132) to the subroutine ML, was used. The program used incorporated another change which made it possible to specify a non-Nernstian slope for the electrode calibration line.

A further modified version of the MINIQUAD program called MINIQUAD 75 (133) also exists. It is claimed by the authors that this latter program is more efficient and produces more reliable convergence, and is thus better suited for use in model selection, where a number of possibilities have to be tested. However it was found by Leggett (132) that MINIQUAD 75 produced slower execution times than MINIQUAD, especially for systems having more than one metal and one ligand. Leggett showed that the efficiency of program execution depended largely on the algorithm used to compute the equilibrium concentrations. He found that the method employed by MINIQUAD, viz. a modified Newton-Raphson approach, was the most satisfactory of those he surveyed.

MINIQUAD arose from further development of the Gauss-Newton variant of the LEAST program (134), and uses the Gauss-Newton method for refinement of stability constants. The version used in this study can treat data from systems containing up to 5 reactants, 20 complexes, 3 electrodes and 600 data points. However these dimensions can easily be changed by the user. The complexes specified can be mononuclear, polynuclear or hydrolysed species. Fuller information, including a listing of the program, can be found in the original paper by Sabatini *et al.* (131).

4.4.5. ESTA

Towards the end of this work a new general program for the analysis of potentiometric titration data called ESTA (135, 136) became available. ESTA is actually a suite of five programs which perform various calculations used in the analysis of potentiometric data. However only those options used in this work will be discussed.

This program (as well as MINIQUAD) was used to calculate the stability constants for the various complexes studied. The Gauss-Newton method is used to minimize the objective function, which may be one of two possibilities. Either the sum of squared e.m.f. residuals is used, or the sum of squares of residuals of the total analytical concentrations. In both cases weighted or unweighted residuals can be selected. It was decided to use the objective function based on weighted e.m.f. residuals. To determine the weights the program was supplied with the estimated random errors in the titre volumes (0.01 cm^3) and observed e.m.f. (0.10 mV). This is in contrast to MINIQUAD (131), where the unweighted sum of squared residuals of total analytical concentrations is used. The facility for correcting for changes in the ionic strength during a titration was used. For this purpose ESTA uses the extended Debye-Hückel expression for the calculation of activity coefficients. This facility was especially useful for those titrations in which part of the background electrolyte had been replaced by a significant amount of protonated ligand. In order to perform such corrections the ionic size parameter å and the empirical parameter c are required. These values were obtained from Kielland (137), or estimated as described by Linder and Murray (138).

This program was also used to calculate values of $\bar{Z}$(calc) for various postulated models of the species present in solution. These were then compared with $\bar{Z}$(obs) values. Species distribution plots for the various systems were obtained by means of the SPEC task in the program.

The BETA simulation task was used to provide clues as to the identity of the minor species present in the various systems. To use this facility the program is supplied with estimates of the stability constants of the major species assumed present. A list of likely minor species is then added to the model and the program calculates, at each titration point,

the stability constant for the minor species. Each minor species is regarded as the only remaining complex required to produce agreement between calculated and observed data at each titration point. The use of this facility for model selection will be described in more detail in Section 4.5.

Further details of this program can be found in the ESTA Users Manual (139).

4.4.6. FORMAT

FORMAT is a program designed to assist the entering of potentiometric data to a wide range of programs used for the analysis of such data sets. It was developed at the University of Wales Institute of Science and Technology during 1978, and instructions for its use were provided by Prof. P.W. Linder of the University of Cape Town.

As already mentioned, FORMAT was used in this work as a 'front-end' to MAGEC.

4.4.7. CALCAL

The computer program CALCAL was written by Prof. F. Marsicano. It calculates the heat capacity of the calorimeter reaction vessel and its contents from data of the Wheatstone bridge off-balance potential and time. The theory employed by the program is described in Section 4.2. A listing of the program appears in Appendix II.

4.4.8. CALCOR

CALCOR was also written by Prof. Marsicano. This program corrects the gross heat change between the (k - 1)th and k-th points for 'non-chemical' heat effects, the temperature difference between the titrate and titrant, and the heat of dilution of the titrant. The corrections are made as described in Section 4.2. The program is also used to calculate heats of dilution from experimental data. The program produces output in the form of a table of the quantities Q_p, Q_{HL}, Q_{TC}, Q_D and Q_C for each of the titration points considered. (For the definitions of these symbols see Section 4.2.) The text of this program can be found in Appendix III.

4.4.9. PREKAL

The computer program PREKAL is an input program for the program LETAGROP KALLE (140), which calculates values of $\Delta H^{\ominus}$ from titration calorimetric data. The data supplied to PREKAL are converted into a form compatible with the input requirements of LETAGROP KALLE and stored in a data file accessed by LETAGROP KALLE. The data required by PREKAL consist of:

1. the concentrations of the reagents in the titrate and titrant,

2. the initial volume of the titrate,

3. the titration data in the form of total volume of titrant added up to the k-th point and (corrected) heat liberated between (k - 1)th and k-th points,

4. the complexes assumed present,

5. the known or estimated values of the cumulative enthalpy changes for the abovementioned complexes, and

6. the stability constants for the complexes assumed present.

4.4.10. LETAGROP KALLE

In this work the computer program LETAGROP KALLE (140) was used to calculate values of $\Delta H^{\ominus}$ from titration calorimetric data. LETAGROP KALLE is one of a suite of programs known as LETAGROPVRID (141) that use the 'pit-mapping' minimisation technique to provide the least-squares estimates of the parameters of interest.

The necessary inputs are provided via PREKAL (see Section 4.4.9). LETAGROP KALLE corrects the data for the effect of side reactions and then produces values of $\Delta H^{\ominus}$ for the reactions of interest.

In addition to calculating $\Delta H^{\ominus}$ values from calorimetric data, this program can also calculate the stability constants of the species present and adjust the solution concentrations. However the stability constants obtained from calorimetric titration data are less accurate than those determined by, say, potentiometry. In this work LETAGROP KALLE was used

to calculate ΔH° values only, because all the stability constants were determined by potentiometry.

The version of the program used in this work has some limitations. It can handle data sets containing up to 3 reactants, 3 titrations and 20 data points per titration. It also cannot deal with data obtained from experiments which use pre-reacted components in the titrant. If one wishes to use more than one reactant in the titrant, a separate burette must be used for each component. However, in the titration calorimeter used in this work, only one burette was available. This meant that protonated ligand species could be introduced for buffering purposes only in the titrate.

4.5. Species Selection

One of the major problems in solution chemistry is still that of identifying the chemical model for a particular equilibrium mixture. A number of authors (142 - 147) have dealt with the problem of species selection but, as pointed out by Gans (148), 'the development of a sound model selection procedure presents the greatest challenge to the computational chemist interested in solution equilibria'.

The choice of a chemical model entails finding the set of pqr triples and corresponding stability constants β_{pqr} that best reproduce the experimental data. One cannot exhaustively try all sets of pqr triples, so some degree of chemical intuition must be applied. The model ultimately chosen is the one that gives the most satisfactory account of the data from chemical and statistical points of view. Of course, when judging the adequacy of the model chosen, one must keep in mind any likely systematic errors in the experimental data. These errors can transmit themselves to the model (136, 149) and thereby make it difficult to decide when to stop adding species to the model.

In this work the likely major species present in any system were chosen by inspection of the $\bar{Z}(\log[L])$ plots obtained from the experimental data. Then a likely set of minor species was chosen. These were included in the model either singly, in pairs, or triples. The likely models were tested by making use of the BETA task in the ESTA program (see Section

4.4.5). With the BETA task one can test a number of these models at the same time. From the output provided by BETA one can consider for inclusion in the model the minor species which best fits the following description (139).

1. The minor species is present at a large number of titration points.

2. The stability constant of the minor species does not vary much.

3. The percentage component of the minor species changes appreciably from point to point, and lies between 15 % and 85 %.

The most likely models were then submitted to a program which calculates stability constants, e.g. ESTA or MINIQUAD. The adequacy of each model was evaluated by looking at the value of the objective function. That model which yields the lowest value of the objective function gives the best fit to the experimental data. Where several models had similar values for the objective function the simplest model was chosen, in keeping with Occam's Razor. In addition the program MINIQUAD provides two statistics to judge the adequacy of a model, viz. the R factor and a χ^2 value. If the value of R is less than the value of R_{lim}, as defined by Vacca *et al.* (146), then the postulated model is acceptable. The value of χ^2 gives a measure of the randomness of the experimental error. This value should be less than about 12.6 for an 'acceptable' model.

The adequacy of the models eventually selected to describe the solution equilibria was also tested visually by comparing plots of $\bar{Z}$(calc) and $\bar{Z}$(obs). If any serious discrepancies occurred then other models were tried.

CHAPTER FIVE

INSTRUMENT CALIBRATION

Both of the main experimental techniques employed, viz. potentiometry and titration calorimetry, entail as a first step the calibration of the instrumentation. In this chapter a description is given of the various methods used in this work for calibration of electrochemical cells and the titration calorimeter.

5.1. Calibration of an electrochemical cell having a glass indicating electrode

The general technique for potentiometric determination of stability constants involves setting up an electrochemical cell which has an indicator electrode reversible to one of the ions in the system, and a reference electrode of fixed potential. In this work the glass electrode was chosen as the indicator electrode in order to monitor the hydrogen ion concentration. This was possible because the ligands used can act as Lewis bases and complex with the metal ion, in addition to acting as Brønsted bases and combining with hydrogen ions. Thus the reactions studied entailed competition between the metal ions and hydrogen ions for the ligand. The silver-silver chloride electrode was chosen as the reference electrode of fixed potential.

The electrochemical cell used in these titrations to determine the equilibrium hydrogen ion concentration can be written as follows:

$$(-)\ \mathrm{RE}\,|\,\underset{j}{\text{salt bridge}}\,|\,\underset{J}{\text{test solution}}\,|\,\text{glass electrode}\ (+) \qquad (\mathrm{I})$$

where RE (reference electrode) = $Ag|AgC\ell|0.01$ mol dm^{-3} $C\ell^-$, 0.49 mol dm^{-3} NO_3^-, 0.50 mol dm^{-3} K^+ and salt bridge = 0.50 mol dm^{-3} KNO_3. This is thus an electrochemical cell with two liquid junctions - one between the reference electrode and the salt bridge (j) and one between the salt bridge and the test solution (J). The e.m.f. of cell (I) is given by (150):

$$E_{cell} = E_+ - E_- + E_j + E_J \qquad (5.1)$$

$$= E^{\ominus}_+ - E_- + d + E_j + s \log a_{H^+} + E_J$$

$$= E^{\ominus} + s \log a_{H^+} + E_J, \qquad (5.2)$$

where the term $E^{\ominus}$ is a constant which includes the potential of the reference half-cell (E_-), the standard potential and asymmetry potential of the glass electrode ($E^{\ominus}_+$ and d, respectively), and the diffusion potential at the junction between the reference electrode and the salt bridge (E_j). (E_j is unaffected by changes in the test solution and should remain constant.) The term E_J is the diffusion potential generated at the liquid junction between the salt bridge and the test solution. The electrode calibration slope, s, is in theory 2.3026 RT/nF (i.e. Nernstian), but may in practice depart slightly from this value. As pointed out by Mascini (123) 'very few electrodes have a truly Nernstian value of the calibration slope, but all electrodes have a very large range in which the slope is constant'.

In this work the activity coefficients were kept near-constant by use of a constant ionic medium. Hence equation (5.2) then relates cell potential to hydrogen ion concentration as follows (82):

$$E_{cell} = E^{\ominus\prime} + s \log [H^+] + E_J, \qquad (5.3)$$

where $E^{\ominus\prime} = E^{\ominus} + s \log \gamma_{H^+}$. (5.4)

The asymmetry potential, d, of a glass electrode arises because the two sides of the glass membrane do not behave exactly alike. Although this quantity varies with time it can usually be assumed that it will remain effectively constant during the periods required to make measurements (151). Nevertheless it is necessary that the value of $E^{\ominus\prime}$ be determined afresh for each set of measurements and that it should remain constant during the period over which an experiment is performed. For this electrochemical cell, then, the composition of the reference half-cell remains constant (as required) while that of the other half-cell varies as the titration proceeds.

The liquid junction potential E_J arises from the diffusion of ions across the liquid junction between two solutions in contact, from a region of high activity to one of low activity. E_J becomes large if the two adjoining solutions differ greatly in the concentration, mobility or charge of one or more ions. This is especially true if the adjoining solutions contain appreciably different concentrations of hydrogen or hydroxyl ions, both of which have very high mobilities. In such cases it is best to determine E_J experimentally. Methods of estimating the value of E_J, and methods of eliminating the liquid junction potential, have been discussed by a number of authors (82, 152 - 155). Thus, in order to keep the value of E_J as low as possible, gross concentration gradients between two solutions in contact must be avoided. The use of a high concentration of the same background electrolyte in the two half-cell solutions and the salt bridge helps to minimize the junction potential or keep it constant. E_J can then be added to the term $E^{\ominus}{}'$ (156). If

$$E^{\ominus}{}'' = E^{\ominus}{}' + E_J = \text{constant}, \qquad (5.5)$$

equation (5.3) becomes

$$E_{cell} = E^{\ominus}{}'' + s \log [H^+] \ . \qquad (5.6)$$

Hence the concentration of hydrogen ions in a solution of unknown acidity can easily be calculated from the cell potential, provided that values of $E^{\ominus}{}''$ and s can be obtained.

A number of ways of determining $E^{\ominus}{}''$ exist. Molina *et al.* (157) discuss various methods, including one of their own, for calibrating glass electrodes in cells with liquid junctions, and demonstrate the effect of different calibration methods on the determination of stability constants. Four methods of cell calibration were used in this work. These will now be described, as well as tests for the validity of equation (5.6) and a verification of the constancy of the liquid junction potential, E_J.

5.1.1. Calibration using a strong acid

The simplest method of determining $E^{\ominus}{}''$ is by titrating known volumes of a solution of known hydrogen ion concentration (such as a 0.01 mol dm^{-3}

solution of strong acid like nitric acid), made up to the required ionic strength with the background electrolyte, into an aliquot of a solution of the background electrolyte at the same ionic strength (in this work 50.00 cm^3 of 0.5 mol dm^{-3} KNO_3). The e.m.f. of the cell is measured after each addition of titrant. Hence $E^{\ominus}$" can be calculated by rearranging equation (5.6), if one assumes that the glass electrode has a Nernstian slope:

$$E^{\ominus}" = E_{cell} - \frac{2.3026\ RT}{F} \log [H^+]. \qquad (5.7)$$

Assuming a Nernstian slope here is probably more reliable than determining s from a narrow range of values of $[H^+]$. The values of $E^{\ominus}$" obtained for each addition are then averaged provided that they are approximately constant. (Constancy of $E^{\ominus}$" is in accordance with the assumption that the activity coefficients and the liquid junction potentials are constant and the glass electrode responds in Nernstian or near-Nernstian fashion. When variations in $E^{\ominus}$" occur at high acidity, changes in E_J become significant.) This average $E^{\ominus}$" value is used in all subsequent calculations.

This calibration procedure was used in those potentiometric titrations performed to determine the protonation constants of etolen, and in some of the titrations performed on the Ni^{2+}-etolen system.

It was also used to verify the validity of equation (5.6), and to determine the $p[H^+]$ region in which changes in the junction potential term, E_J, became significant. In this experiment four titrant solutions of known hydrogen ion concentration were used, instead of just one, in order to cover a somewhat wider $p[H^+]$ range. Data collected from one such titration are given in Table 5.1. The corresponding plot of cell potential against $p[H^+]$ is shown in Figure 5.1.

It was found that, for $p[H^+]$ values from 2.0 to 3.3, the response of the glass electrode with respect to $\log[H^+]$ was linear. This is in agreement with the comment made by Linder and Torrington (158) that strong acid calibrants should be used only in the $p[H^+]$ region 2.0 to 3.0. At $p[H^+]$ values lower than 2.0 the liquid junction potential becomes significant and must be taken into account. However, in the experiments performed in this work, there was no necessity to work at such low $p[H^+]$ values

TABLE 5.1

Data obtained from the calibration of a cell containing a glass electrode by using strong acid. (t = 25.00°C and μ = 0.50 mol dm^{-3})

Concentration of hydrogen ions in the titrate, $[H^+]_0$, and the titrant, $[H^+]_T$, initial volume V_0	Volume of titrant solution added/cm^3	$p[H^+]$	E_{cell}/mV
$[H^+]_0$ = 0	1.00	4.008	19.6
	2.00	3.716	37.5
$[H^+]_T$ = 5.003 x 10^{-3} mol dm^{-3}	3.00	3.548	47.4
	4.00	3.431	54.5
	5.00	3.342	59.8
V_0 = 50.00 cm^3	6.00	3.271	64.1
	7.00	3.212	67.6
$[H^+]_0$ = 6.144 x 10^{-4} mol dm^{-3}	1.00	2.834	89.8
	2.00	2.640	101.4
$[H^+]_T$ = 5.003 x 10^{-2} mol dm^{-3}	3.00	2.511	108.9
	4.00	2.414	114.7
	5.00	2.337	119.2
V_0 = 57.00 cm^3	6.00	2.274	122.9
$[H^+]_0$ = 5.321 x 10^{-3} mol dm^{-3}	1.00	2.167	129.0
	2.00	2.084	133.9
$[H^+]_T$ = 1.001 x 10^{-1} mol dm^{-3}	3.00	2.016	137.8
	4.00	1.960	141.1
V_0 = 63.00 cm^3	5.00	1.911	143.8
	6.00	1.868	146.3

TABLE 5.1 continued

$[H^+]_0 = 1.356 \times 10^{-2}$ mol dm^{-3}	1.00	1.688	156.1
	2,00	1.564	162.9
$[H^+]_T = 5.001 \times 10^{-1}$ mol dm^{-3}	3.00	1.471	167.7
	4.00	1.396	171.7
$V_0 = 69.00$ cm^3	5.00	1.333	174.7

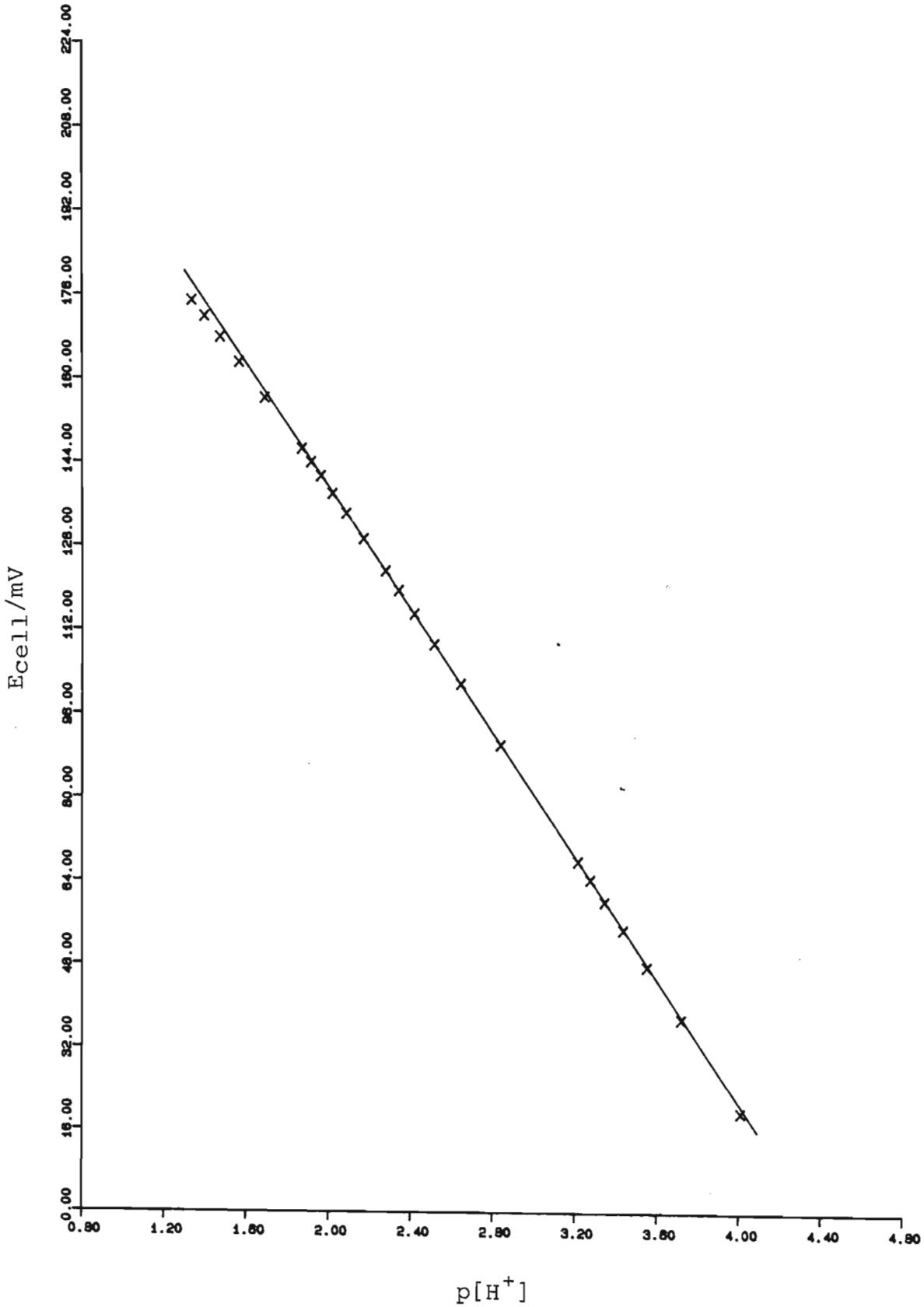

Figure 5.1 Plot obtained when a solution of the background electrolyte is titrated with a strong acid.

and this term was not considered. According to Corrie and Williams (128), the solution is not buffered above a $p[H^+]$ of 3.0, and so deviations from linearity occur there. In all stability constant measurements the systems are buffered and such deviations should not occur. The points in the linear region of (e.g.) Figure 5.1 were then used to obtain least squares estimates of $E^{\ominus}$" and s. For the data of Table 5.1 the estimates were $E^{\ominus}$" = 256.77 mV and s = 58.91 mV. The values of s obtained for the different titrations were found to range between 58.4 and 59.6 mV, which is in fair agreement with the theoretical Nernstian value of 59.16 mV. Hence we see that our use of equation (5.6) is justified.

This method of calibrating the cell suffers from the drawback that $E^{\ominus}$" is determined over a rather narrow range of $p[H^+]$, viz. 2.0 - 3.3, and it is unlikely that the measurements to be made will fall entirely within this range. Furthermore, rather few experimental points can be obtained within this range, which makes it difficult to obtain reliable values for $E^{\ominus}$" and s by analysis of the linear region of the data. An improvement of this calibration procedure is easily achieved by using both strong acid and strong base as calibrants.

5.1.2. Calibration using a strong acid and a strong base

This calibration technique entails titrating a solution containing background electrolyte and a strong base such as sodium hydroxide, with a standardised solution of a strong acid such as nitric acid. All the solutions used are made up to the same ionic strength with the background electrolyte, in this case KNO_3. For each addition of acid the cell potential is measured. If cell potentials are obtained before and after the equivalence point, the Gran plot method of equivalence point determination (see Section 4.1.1) can be applied to determine the concentration of the NaOH solution and that of any carbonate contamination present in it.

The concentrations of acid, base and carbonate in the titrate and titrant, together with the value of K_w and the protonation constants of carbonate, are supplied to a computer program such as HALTAFALL (see Section 4.4.1) in order to calculate the $p[H^+]$ at each point during the titration. The $p[H^+]$ values thus calculated are then plotted against the corresponding cell potential values. The points lying on the linear part of the curve are then used to obtain least-squares estimates of $E^{\ominus}$" and s. Table 5.2

shows typical data for such a cell calibration. Figure 5.2 is a plot of E_{cell} against calculated $p[H^+]$, from which $E^{\ominus}$" and s were obtained. For these data $E^{\ominus}$" = 252.63 mV and s = 58.41 mV.

Various authors (159) in this field use a different calculation technique when dealing with strong acid - strong base calibration of an electrochemical cell using a glass electrode. Instead of assuming a constant value of K_W, as was done here, they assume that the glass electrode has a perfectly Nernstian calibration slope. They then determine (from their observations in the alkaline region of the calibration) that value of K_W which is most consistent with this assumption. In the present work, however, the assumption of a perfectly Nernstian slope was not made, in keeping with the ideas of workers in the field of ion-selective electrodes (123). Instead the single value of 1.8197×10^{-14} (160) was used throughout for K_W, and the calibration slope determined as described above.

The above calibration method was used mainly for measurements involving the ligand oden. It has the advantage over the method of Section 5.1.1 that a wider range of $p[H^+]$ values is spanned, i.e. the calibration procedure includes points both in the high and the low $p[H^+]$ regions, and $E^{\ominus}$" and s can be obtained with greater accuracy. The response of the electrode in the high $p[H^+]$ region is linear, but (as in the case of acid calibration) only over a limited range of $p[H^+]$ values, viz. 10.3 - 11.0. However, since the measurements made in this study did not involve $p[H^+]$ values greater than 11, correction for junction potential effects was not necessary.

This method has the drawback that $p[H^+]$ values in the intermediate range, 4 - 9, cannot be reached. For such purposes calibration with a strong acid and a weak base is preferable. (See Section 5.1.3.)

5.1.3. Calibration using a strong acid and a weak base

The cell calibration procedure can be adapted to cover a more appropriate range of $p[H^+]$ values by using the ligand (a weak base) instead of the strong base hydroxide, to obtain readings at intermediate $p[H^+]$ values, which cannot be obtained by using hydroxide alone.

TABLE 5.2

Data obtained in the calibration of a cell containing a glass electrode, with strong acid and strong base used as calibrants. (t = 25.00 °C and μ = 0.50 mol dm^{-3})

Concentrations of reactants in the titrate, $[]_0$, and the titrant, $[]_T$, initial volume V_0	Volume of titrant solution added/cm^3	$p[H^+]$, as calculated by HALTAFALL*	E_{cell}/mV
$[OH^-]_0$ = 1.567 x 10^{-3} mol dm^{-3}	1.00	10.88	-382.9
	3.00	10.75	-375.5
	4.00	10.67	-370.8
$[CO_3^{=}]_0$ = 7.000 x 10^{-5} mol dm^{-3}	5.00	10.58	-365.2
	6.00	10.46	-358.4
	7.00	10.30	-348.4
	8.00	10.09	-333.2
$[H^+]_T$ = 9.999 x 10^{-3} mol dm^{-3}	9.00	9.70	-302.0
	11.00	3.97	22.1
V_0 = 60.00 cm^3	12.00	3.61	41.3
	13.00	3.42	52.3
	14.00	3.29	60.1
	15.00	3.20	65.9

*Values of constants used by HALTAFALL:

K_w = 1.820 x 10^{-14}

$\beta_1(HCO_3^-)$ = 6.180 x 10^9

$\beta_2(H_2CO_3)$ = 7.482 x 10^{15}

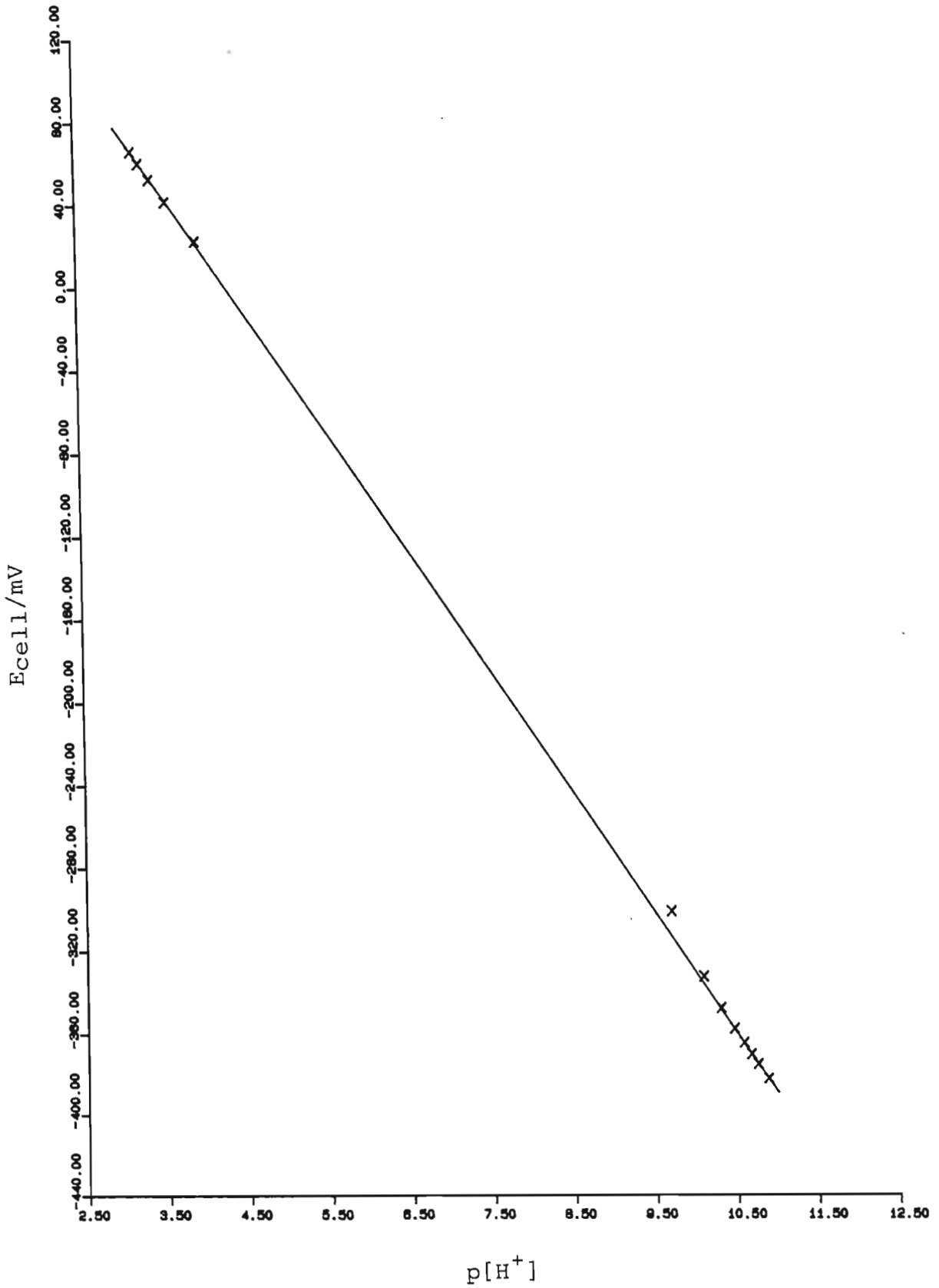

Figure 5.2 Plot of data obtained in the calibration of a cell containing a glass electrode, with strong acid and strong base used as calibrants.

The calibration method adopted was the following:

1. About 5 points were obtained in the $p[H^+]$ range 2.0 to 3.3 by adding a solution of known hydrogen ion concentration (0.01 mol dm^{-3} HNO_3) to an aliquot of background electrolyte solution (50 cm^3 of 0.50 mol dm^{-3} KNO_3).

2. A further aliquot of strong acid (5 cm^3 of 0.1 mol dm^{-3} HNO_3) was then added. The mole ratio of acid present at this stage to ligand eventually to be added was of the order of 1 : 2.5. The aliquot of strong acid solution mentioned above is added in one step and no e.m.f. readings are taken, since they would be in a region in which the liquid junction potential comes into effect.

3. This acidic solution was then titrated with the ligand solution (24 cm^3 of 0.05 mol dm^{-3} ligand solution). Readings of the cell potential were taken after each addition. One must ensure that sufficient ligand is added to cover the intermediate $p[H^+]$range, since these are the points of interest. Ligand added at this stage of the procedure also acts as protonated ligand in the background later in the experiment. This is especially useful when one wants to lower the $p[H^+]$ of the reaction mixture.

4. The above procedure was then reversed by adding a solution of strong acid (21 cm^3 of 0.1 mol dm^{-3} HNO_3). Again, readings of the cell potential were taken after each addition of acid. Sufficient acid was added so that, at the end of the calibration, all of the ligand present was protonated to saturation.

   As always, all the solutions used in the calibration were made up to the same ionic strength (0.5 mol dm^{-3}) by using the background electrolyte. The volumes and concentrations of the solutions used in the procedure described above serve merely as an illustration. The actual values used in each experiment depended on such requirements as the metal to ligand ratio and metal ion concentration needed.

5. The $p[H^+]$ value of each of the data points was then calculated as follows. For those points obtained in part 1., the $p[H^+]$ was cal-

culated directly from the concentration and volumes of the strong acid solution added. The $p[H^+]$ values for the points obtained in parts 3. and 4. of the procedure were calculated by using the computer program HALTAFALL (see Section 4.4.1). The program was provided with K_w, the protonation constants of the ligand, and the concentrations of the reactants in the titrate and titrant solutions. The output produced was the hydrogen ion concentration for each titration point. A plot of cell potential against $-\log[H^+]$ was then drawn. This plot was used as a visual indication of the linearity of the data and to discard any 'dud' points. A simple linear regression was then performed on the data to find $E^{\ominus}$" and s. Typical data obtained in a calibration of this sort are shown in Table 5.3, and plotted in Figure 5.3. The values of $E^{\ominus}$" and s found were 242.66 mV and 58.56 mV respectively.

This calibration technique, involving the use of a strong acid and a weak base, was used for most of the potentiometric titrations performed in this work. This calibration technique has the advantage that one determines $E^{\ominus}$" and s under conditions (e.g. $p[H^+]$) similar to those encountered in the actual potentiometric titration. The method has the disadvantage that the protonation constants of the ligand must be known under the same conditions of ionic strength and temperature as used in the experiment.

The abovementioned disadvantage can be overcome with the use of a computer program such as MAGEC (see Section 4.4.2). The program MAGEC can simultaneously determine the calibration constants of the cell and the protonation constants of the ligand. This makes it unnecessary to determine the protonation constants of the ligand in a separate experiment.

Various attempts were made to use the program MAGEC to determine simultaneously the protonation constants of the ligand and the cell calibration constants. The program was supplied with the following information:

a) the concentrations of the reactants in the titrate and titrant solutions;

b) an estimate of $E^{\ominus}$" obtained from the data collected in part 1. of the calibration and calculated in the same way as for the

TABLE 5.3

Data obtained from the calibration of a cell containing a glass electrode, with strong acid and the weak base etolen used as calibrants.
(t = 25.00°C and μ = 0.50 mol dm^{-3})

Concentrations of reactants in the titrate, $[]_0$, and the titrant, $[]_T$, initial volume V_0	Volume of titrant solution added/cm^3	Calculated $p[H^+]$*	E_{cell}/mV
$[H^+]_0$ = 0	1.00	3.708	26.3
	2.00	3.415	43.8
$[H^+]_T$ = 9.990 x 10^{-3} mol dm^{-3}	4.00	3.131	60.7
	6.00	2.971	70.2
V_0 = 50.00 cm^3	8.00	2.861	76.7
	10.00	2.779	81.4
$[H^+]_0$ = 9.222 x 10^{-3} mol dm^{-3}	6.00	5.530	-82.0
	7.00	6.531	-139.8
$[etolen]_T$ = 5.110 x 10^{-2}	8.00	6.907	-162.3
mol dm^{-3}	9.00	7.206	-179.8
V_0 = 65.00 cm^3	10.00	7.512	-197.6
	11.00	7.905	-220.9
	12.00	8.435	-251.8
	13.00	8.818	-273.6
	14.00	9.039	-286.7
	15.00	9.189	-295.5
	16.00	9.300	-302.0
	17.00	9.389	-307.2
	18.00	9.463	-311.4
	20.00	9.581	-318.3
	24.00	9.748	-327.9
$[H^+]_0$ = 6.735 x 10^{-3} mol dm^{-3}	1.00	9.610	-319.7
	2.00	9.465	-310.9
$[etolen]_0$ = 1.378 x 10^{-2}	3.00	9.302	-301.2
mol dm^{-3}	4.00	9.107	-289.7
$[H^+]_T$ = 9.990 x 10^{-2} mol dm^{-3}	5.00	8.845	-274.1
	6.00	8.436	-249.8
V_0 = 89.00 cm^3	7.00	7.943	-221.7
	8.00	7.611	-202.8
	9.00	7.384	-189.8
	10.00	7.206	-179.7
	11.00	7.051	-170.8
	12.00	6.907	-162.5
	13.00	6.766	-154.4
	14.00	6.620	-145.8
	15.00	6.459	-136.4
	16.00	6.269	-125.4
	17.00	6.011	-110.2

	18.00	5.526	-82.4
	19.00	3.379	41.6
	20.00	2.877	73.6
	21.00	2.653	87.3

*Values of constants used by HALTAFALL:

$K_W = 1.820 \times 10^{-14}$

$\beta_{101} = 5.495 \times 10^{9}$

$\beta_{201} = 3.890 \times 10^{16}$

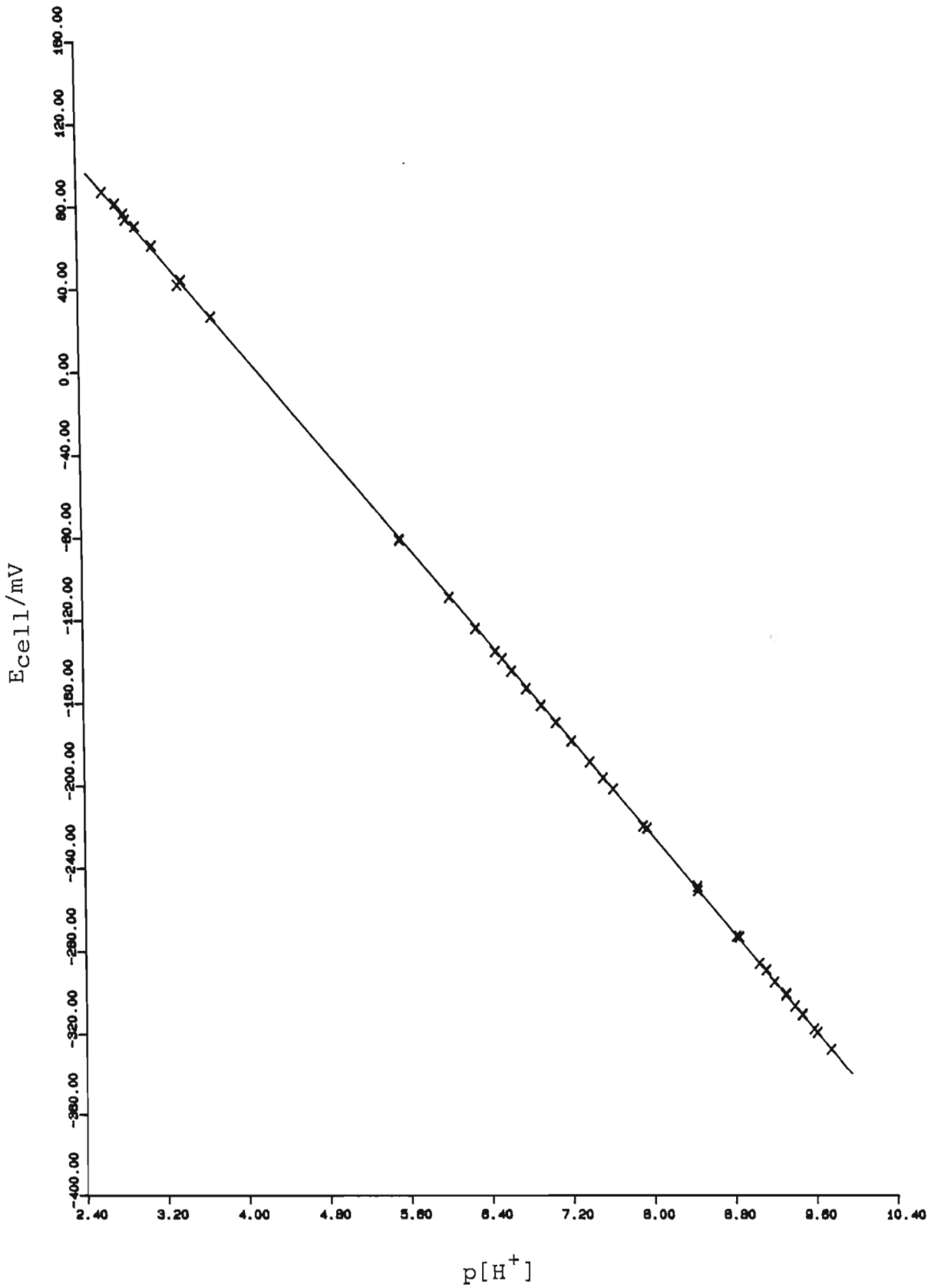

Figure 5.3 Calibration line for a cell containing a glass electrode, obtained by using a strong acid and a weak base as calibrants.

strong acid calibration of the cell (see Section 5.1.1);

c) the Nernstian value for s; and

d) the titration data obtained in the intermediate $p[H^+]$ region, i.e. the titration points obtained in parts 3. and 4. of the calibration procedure.

Care was taken when carrying out the calibration that not too much acid was added at step 2., because the $p[H^+]$ of the solution would then no longer have been a sensitive function of the protonation constants of the ligand. The sensitivity of the measured $p[H^+]$ to the protonation constants of the ligand, as well as the $p[H^+]$ range covered during the calibration, were previously investigated by using HALTAFALL to do a species distribution calculation.

Some problems were encountered with MAGEC which made it impossible to determine simultaneously both the protonation constants and the cell calibration constants. It was found that the values of E°", s and the protonation constants to which MAGEC converged depended considerably on the initial approximations supplied. This is perhaps due to ill-conditioning of the numerical problem solved by MAGEC. Furthermore, the protonation constants obtained from several similar calibration experiments differed considerably. This made it difficult to choose a single set of protonation constants to supply as input to the programs MINIQUAD and ESTA. These constants were required when several sets of titration data were being refined simultaneously to determine the metal-ligand stability constants. The values of the calibration constants obtained for the forward and backward parts of the calibration run also differed. This latter problem could not be solved by refining the data from the forward and backward runs simultaneously, as the program cannot deal with the change in the titrant solution. Hence it was decided not to use MAGEC but to use the calculation procedure described earlier.

These attempts to use the program MAGEC took place prior to publication of the paper by May *et al.* (130) on its use. It is there stated that MAGEC can be used in a cycling procedure with MINIQUAD. These authors do point out that when MAGEC is used alone to determine both the cell calibration constants and the protonation constants of the ligand, a false

solution can be obtained if correlation of errors between two or more parameters occurs.

A modified version of the strong acid-weak base calibration technique exists. In this version the calibration is performed over a whole day and many points are taken. The titration vessel is then cleaned. On the following day one calibration point is taken in order to establish the intercept of the calibration line, and then the rest of the experiment is performed. It was felt that this version was not as reliable as one in which the calibration and actual experiment are performed on the same day.

5.1.4. Calibration using a strong acid, a strong base and a weak acid

In an attempt to find a calibration technique which included points in the $p[H^+]$ range 4 to 10 it was decided to use acetic acid in addition to HNO_3 and NaOH. It was claimed by Linder and Torrington (161) that 'plots of E_{cell} versus log $[H^+]$ for acetic acid are usually fairly linear over quite an extended range of log $[H^+]$ values'. They were unhappy with the use of strong acid and strong base calibrants because they 'found that plots of E_{cell} against log $[H^+]$ for such systems are only very approximately linear over a very limited range of log $[H^+]$ values', and they concluded that acetic acid was a better calibrant.

There is a problem associated with using acetic acid as a calibrant, which is that in the systems studied here the acetate ion can act as a ligand. That is, if it is present during the actual experiment, it will coordinate to the metal ion and thus complicate the equilibria being studied, which is of course not desired. To determine whether acetic acid could indeed be used as a calibrant it was decided to test the assumption that the cell calibration constants remained the same after the calibrating solutions had been discarded. If so, then it would be reasonable to calibrate the cell, rinse out the calibrating solutions, and perform the main experiment separately: the glass electrode would no longer be calibrated in situ.

To test the above assumption two calibration runs were carried out on the same day, with the cell being rinsed out after the completion of the first run. The calibrations were carried out as follows. First a solution of known HNO_3 concentration was titrated into an aliquot of background elec-

trolyte to obtain points in the low $p[H^+]$ region. Then a solution of known NaOH concentration was titrated into the mixture in order to neutralize the acid present and obtain cell potential readings at high $p[H^+]$ values. Finally a solution of known acetic acid concentration was titrated into the mixture to obtain points in the intermediate region. All the solutions used were made up to the appropriate ionic strength by using KNO_3.

The $p[H^+]$ values for the strong acid and strong base points were obtained from the analytical concentrations of H^+ and OH^-, whereas the $p[H^+]$ values for the acetate points were obtained from a species distribution calculation carried out by the program HALTAFALL. A value of $pK_a = 4.50$ for acetic acid at an ionic strength of 0.5 mol dm^{-3} and a temperature of 25°C was obtained from the literature (162). Table 5.4 contains the data collected in these trial calibrations. A plot of E_{cell} against the calculated value of $p[H^+]$ is given in Figure 5.4. For the sake of clarity only points obtained from run 1 are shown in the figure. $E^{\ominus}$" and s were obtained, as usual, by simple linear regression and are shown in Table 5.5.

From these results it appears that the calibration line has shifted somewhat between runs. It was therefore thought to be unwise to go to the considerable extra effort involved in the acetic acid technique, since it would quite possibly produce results less accurate than those of an in situ calibration method. A comparison of Figures 5.3 and 5.4 suggests that the strong acid - weak base technique is in any case capable of producing a far better fit to a straight line than is the acetic acid technique. This latter calibration technique was therefore not adopted.

TABLE 5.4

Data obtained from the calibration of a cell containing a glass electrode, with strong acid, strong base and acetic acid used as calibrants. (t = 25.00°C and μ = 0.50 mol dm^{-3})

Concentrations of reactants in the titrate, $[]_0$, and the titrant, $[]_T$, initial volume V_0	Volume of titrant solution added/cm^3	Calculated $p[H^+]$	E_{cell}/mV Run 1	E_{cell}/mV Run 2
$[H^+]_0 = 0$	4.00	3.431	49.1	49.4
	8.00	3.161	65.7	66.8
$[H^+]_T = 5.000 \times 10^{-3}$ mol dm^{-3}	12.00	3.014	74.8	75.9
	16.00	2.916	80.2	81.5
$V_0 = 50.00$ cm^3	20.00	2.845	84.7	86.1
$[H^+]_0 = 1.429 \times 10^{-3}$ mol dm^{-3}	12.00	10.123	-340.1	-341.7
	14.00	10.416	-356.8	-357.9
$[OH^-]_T = 9.986 \times 10^{-3}$ mol dm^{-3}	16.00	10.582		-366.8
	17.00	10.644	-369.5	
	18.00	10.697	-371.8	-372.9
$V_0 = 70.00$ cm^3	20.00	10.785	-376.3	-376.2
$[OH^-]_0 = 1.108 \times 10^{-3}$ mol dm^{-3}	12.00	5.207	- 62.6	- 63.0
	14.00	4.912	- 42.3	- 41.3
$[HAc]_T = 1.000 \times 10^{-2}$ mol dm^{-3}	16.00	4.740	- 31.0	
	17.00	4.675		- 26.0
	18.00	4.619	- 23.3	
$V_0 = 90.00$ cm^3	20.00	4.526	- 17.5	- 16.5

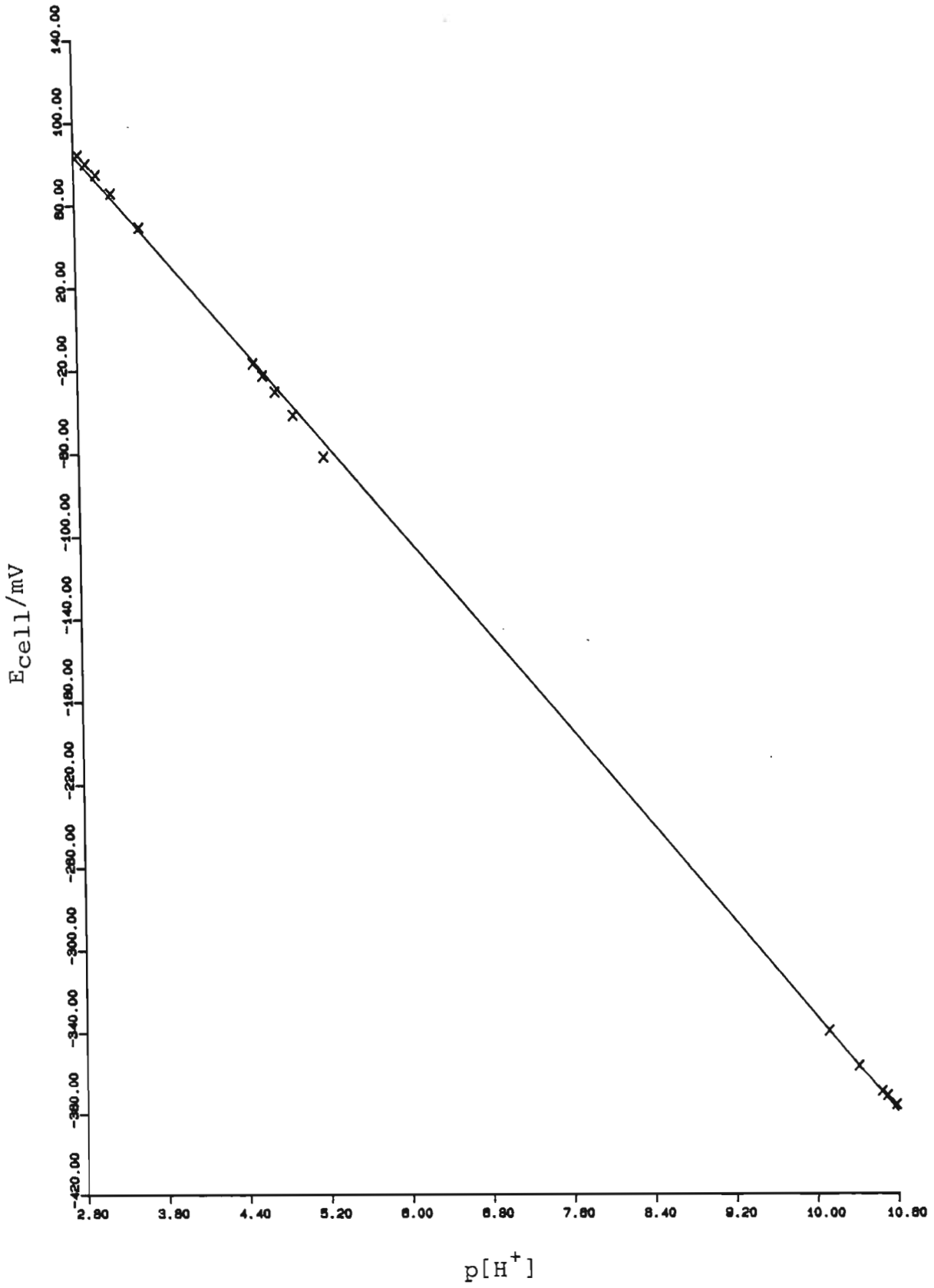

Figure 5.4 Calibration line for a cell containing a glass electrode, obtained by using a strong acid, a strong base and acetic acid as calibrants.

TABLE 5.5

Values of $E^{\ominus}$" and s obtained from the data shown in Table 5.4.

Run No.	$E^{\ominus}$"/mV	s/mV
1	246.23	57.91
2	248.43	58.20

5.2. Calibration of the titration calorimeter

Before the data obtained from the titration calorimetric experiments can be analyzed, the calorimeter must be calibrated. Such calibration entails the following:

1. calibration of the Wheatstone bridge containing the reaction vessel thermistor, in order to establish the relation between the temperature in the reaction vessel and the measured off-balance potential of the bridge;

2. determination of the temperature rise caused by heat generated by the stirrer;

3. determination of the heat capacity of the reaction vessel as a function of the volume of liquid contained;

4. testing of the accuracy of the titrant-delivery system; and

5. calibration of the reaction vessel heater.

The last two tasks were carried out by Lowe *et al.* (163), and we now consider the remaining three aspects in detail. The procedures described below were performed each time a set of calorimetric experiments was undertaken, usually over a period of about two months. It was assumed that the characteristics of the calorimeter were sufficiently stable for this to be reasonable.

5.2.1. Calibration of the Wheatstone bridge containing the thermistor

The Wheatstone bridge was calibrated by measuring the off-balance potential corresponding to small, accurately measured changes in the temperature of the water bath surrounding the calorimeter assembly. The value of the variable resistor in the bridge was set at 1979.0 Ω, so that the bridge was balanced at approximately 25°C and all experiments were carried out in the linear response region of the thermistor. The changes in the temperature of the water bath were measured with a 1°C Beckmann thermometer (GALLENKAMP TJ 525). Measurements were performed as follows, at intervals

within the range 25°C - 26°C. The reaction vessel was filled with 95.00 cm^3 of doubly deionized water, encapsulated in the calorimeter assembly, and placed in the water bath. The stirrer was switched on with its speed set on 'high', and the thermistor was switched into the bridge circuit. The temperature of the water bath was set at the desired level by adjusting the setting on the proportional controller. The whole assembly, including the 1°C Beckmann thermometer, was then allowed to equilibrate for 24 hours. Once the system had equilibrated, the bridge off-balance potential was recorded for 5 minutes and the reading on the Beckmann thermometer noted. The absolute temperature scale was fixed by means of a standard mercury-in-glass thermometer calibrated for the range 24°C to 35°C. For each temperature selected, the readings of off-balance potential were averaged and corrected for the temperature rise caused by the heat of stirring (see Section 5.2.2). A plot of corrected off-balance potential against the temperature in the water bath (and reaction vessel) was then drawn. A typical plot is shown in Figure 5.5.

As mentioned in Section 4.2, the temperature in the reaction vessel (T) is related to the off-balance potential (E) by an equation of the form $E = a + bT$. Simple linear regression applied to the data plotted in Figure 5.5 yields the result

$$E/\mu V = -195825 + 7739.83\ (T/°C). \qquad (5.8)$$

It can be seen from the figure that this straight line fits the data very well, and thereby provides the relation needed in this case to convert readings of off-balance potential into temperature values.

5.2.2. Determination of the temperature rise caused by the heat of stirring

In the calibration of the Wheatstone bridge the water in the reaction vessel was kept stirred throughout the course of the measurements. In calculating the results of this calibration, one must correct for the steady-state rise in temperature resulting from the heat generated by stirring. This correction must be made to obtain an accurate relationship between the temperature sensed in the reaction vessel by the thermistor and the temperature actually measured by the thermometer, i.e. that of the water

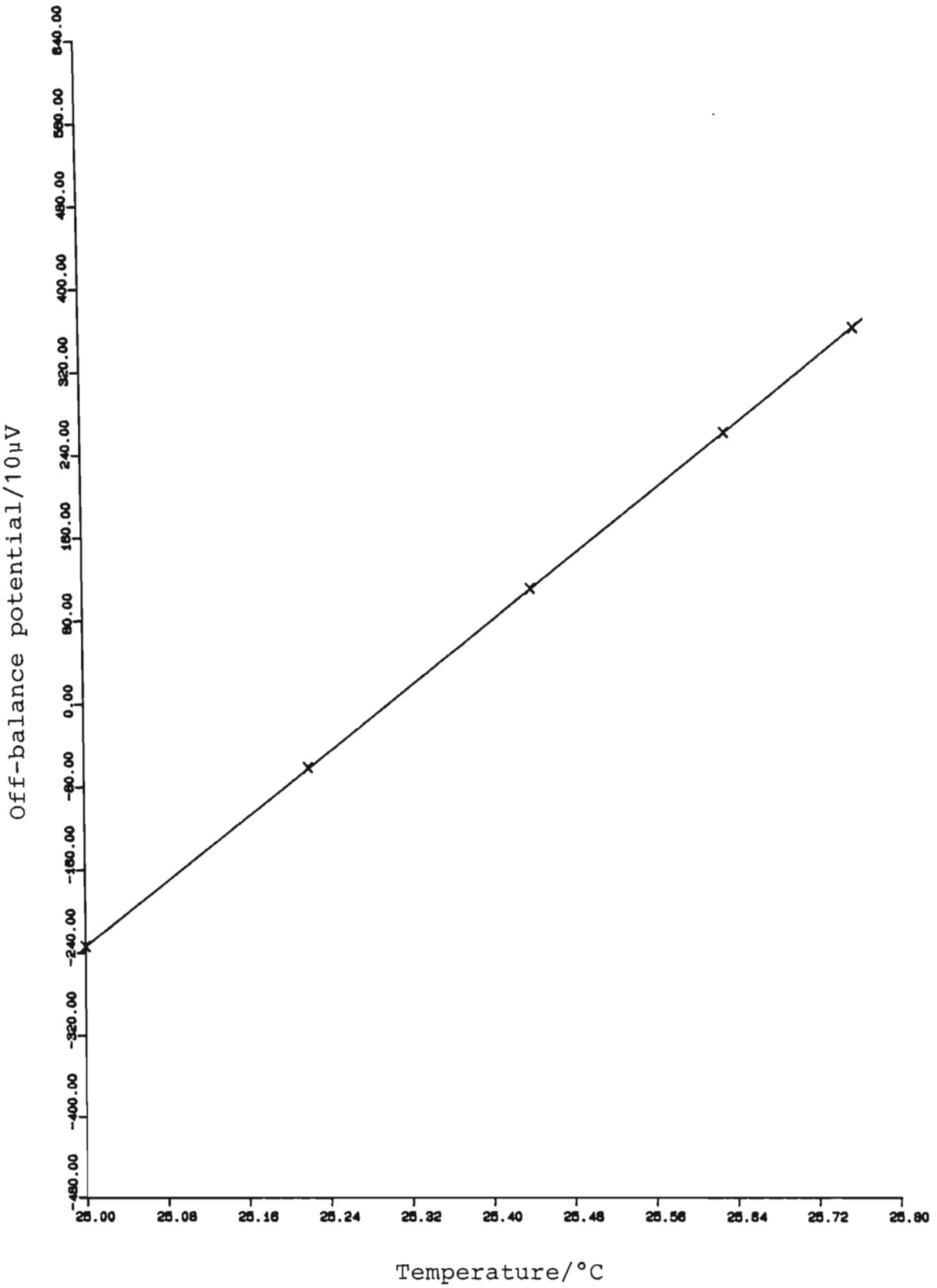

Figure 5.5 The Wheatstone bridge calibration line.

surrounding the calorimeter assembly. Since the rate of stirring is kept constant, it is assumed that the rate of generation of heat by stirring is constant.

The steady-state temperature rise resulting from the stirring action, ΔT_{stir}, was determined as follows. The reaction vessel, containing 95.00 cm^3 of water and placed within the calorimeter assembly, was left for about 72 hours to come to temperature equilibrium with the water (in the bath) surrounding the assembly. During this period the stirrer was left off and the thermistor isolated from the Wheatstone bridge circuit. Then the stirrer was switched on at 'high', and simultaneously the thermistor was switched into the bridge circuit. (The high stirring rate is the most efficient rate for removing build-up of heat in the vicinity of the thermistor, and also the rate used in all subsequent measurements.) The off-balance potential was recorded every 4 seconds for a period of 10 minutes after switch-on, and then again for 5 minutes 24 hours after switch-on.

Figure 5.6 shows a plot of the off-balance potential recorded over the full 24-hour period in one case. Figures 5.7 and 5.8 show expanded versions of the intial and final portions of the curve displayed in Figure 5.6. It was concluded that the thermistor attained its steady-state operating temperature at the point marked 'a' in Figure 5.7. This stage was always reached within one minute of switch-on. It was thought that the heat dissipated by the thermistor in such a short period would have a negligible effect on the overall temperature of the vessel, and similarly that the amount of heat generated by the stirrer would be insignificant. The gradual rise in off-balance potential taking place after point 'a' is assumed to result from the stirring action. The levelling-off in off-balance potential by point 'b' in Figure 5.8, 24 hours after switch-on, is an indication that the system has attained steady state. Furthermore, the off-balance potential was steady after 48 hours at the same value as was reached after 24 hours, viz. -1803 μV.

The difference in off-balance potential between points 'a' and 'b' was, in general, taken to represent ΔT_{stir}. The value of ΔT_{stir} thus calculated was then subtracted from the off-balance potential reading obtained at each point of the calibration of the Wheatstone bridge. ΔT_{stir} was found

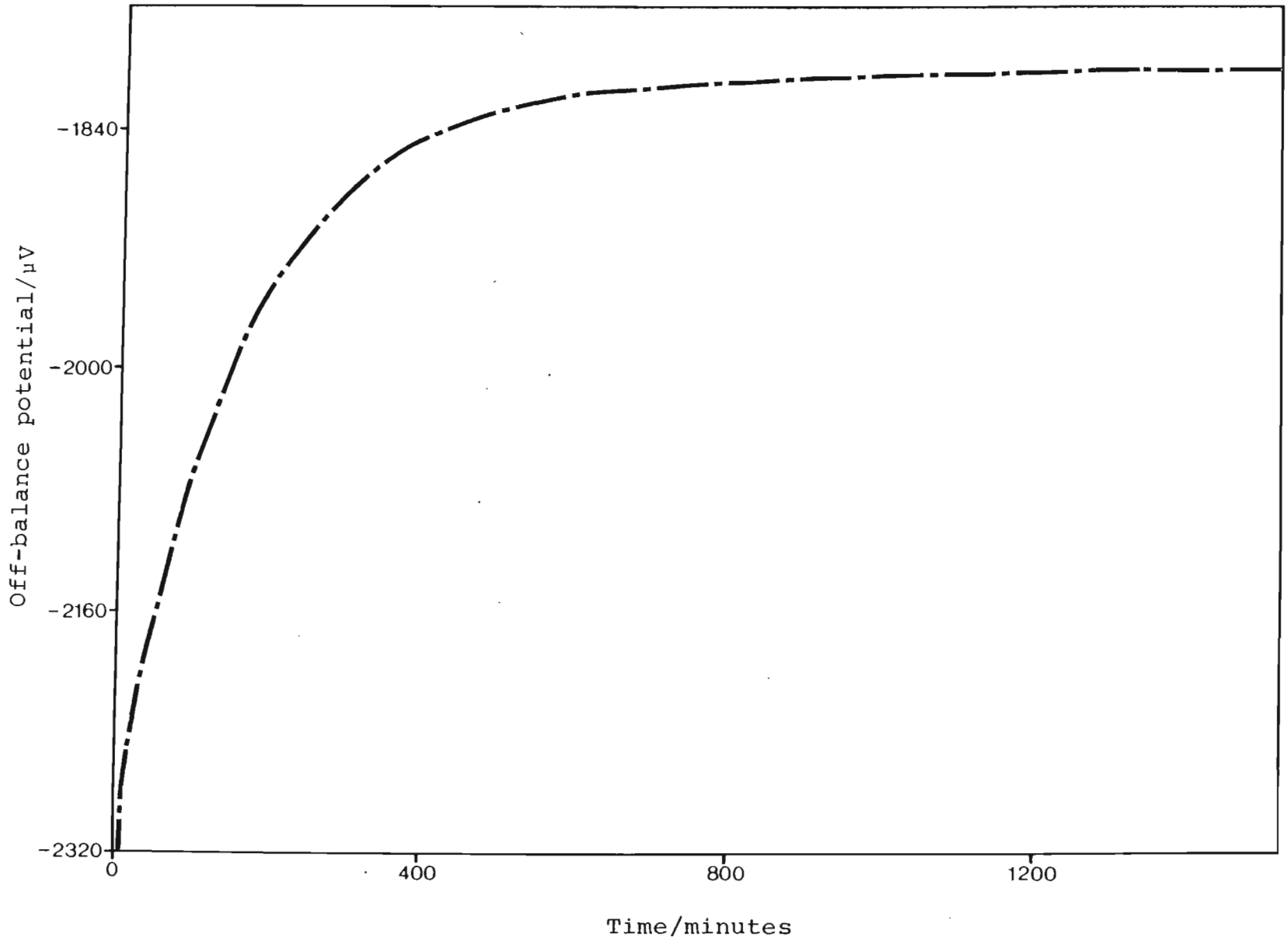

Figure 5.6 Plot of the off-balance potential of the Wheatstone bridge recorded over 24 hours for one of the points on the bridge calibration line, viz. that at 25.00°C.

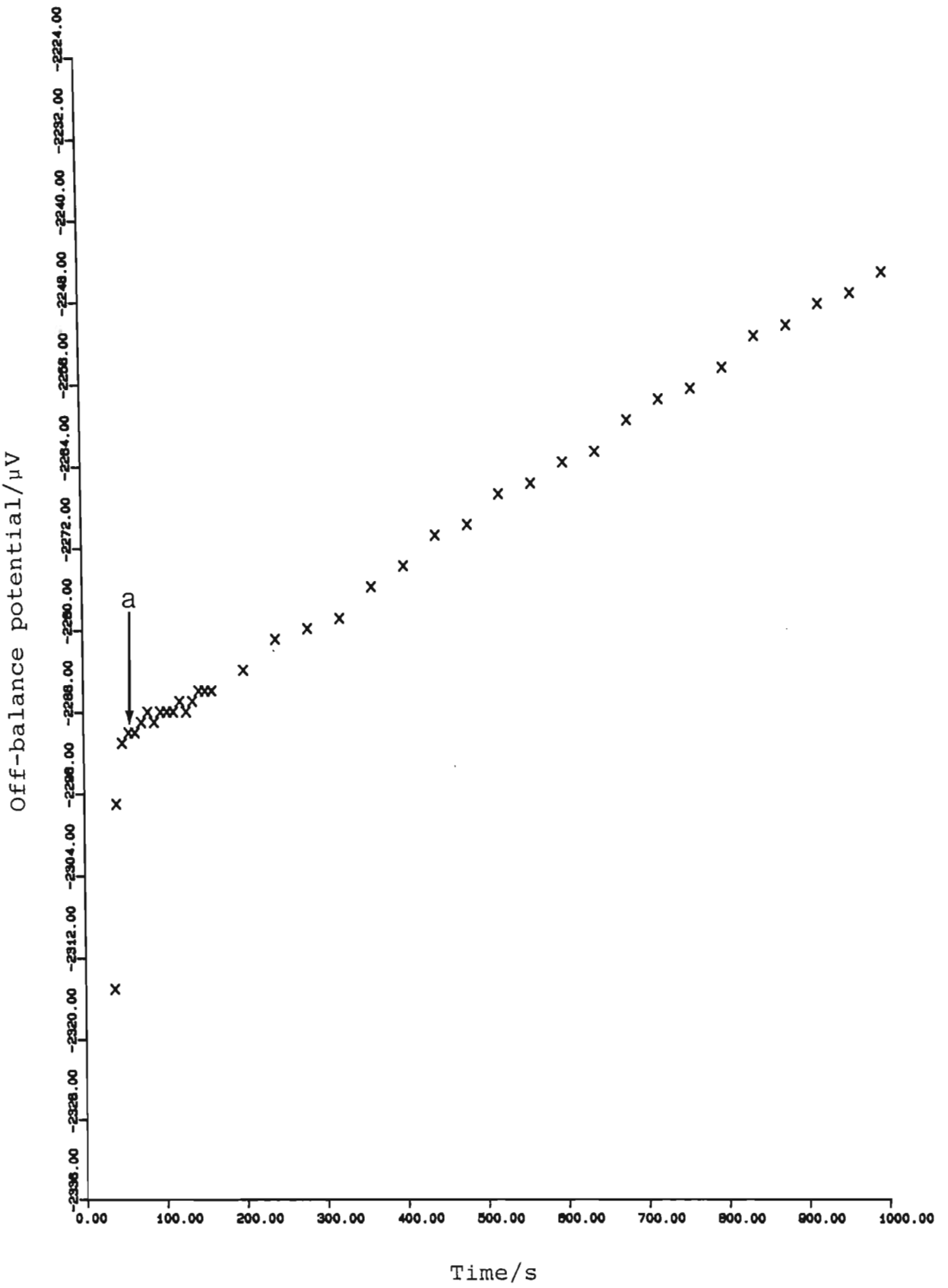

Figure 5.7 Initial period for the determination of the 25.00°C point on the Wheatstone bridge calibration line.

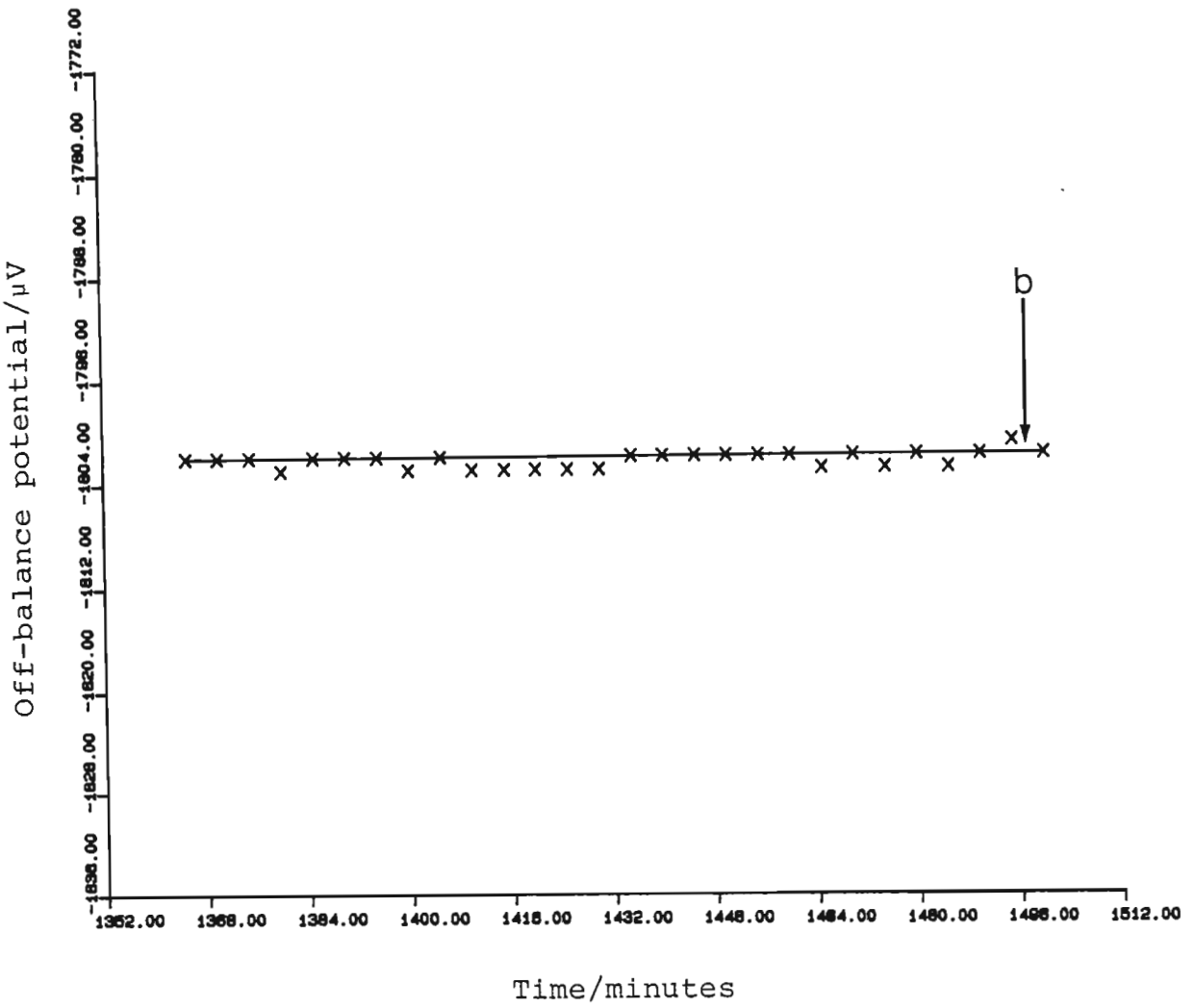

Figure 5.8 Final period for the determination of the 25.00°C point on the Wheatstone bridge calibration line.

to have a value in the range 484 ± 4 μV. This represents a temperature range of 0.063 ± 0.001°C.

It should be pointed out that the procedure described in Section 5.2.1., for obtaining readings of off-balance potential at different temperatures, is in fact a quicker way than the above of obtaining points such as 'b'.

Before 1982, however, ΔT_{stir} was determined by the procedure described in the N.I.M. Report (164), a procedure which (unlike that described above) does not yield reproducible results, and appears to be incorrect. If one looks at Figure 5 of that report (165), it will be seen that the difference found (i.e. ΔT_{stir}) is negative. This of course contradicts the reasonable assumption that heat is generated by stirring. The explanation appears to be the following. The liquid in the vicinity of the thermistor is at a higher temperature than the rest of the liquid in the reaction vessel, as a result of resistive heating of the thermistor. Stirring serves to dissipate this heat from the vicinity of the thermistor, which therefore registers a lower temperature. (The greater the rate of stirring, the greater is the drop in temperature caused by such dissipation.) This dissipation of heat from the vicinity of the thermistor can, it seems, mask the heat generated by stirring.

The measurements made before 1982 to calibrate the Wheatstone bridge were therefore corrected by using a value for ΔT_{stir} determined by the new procedure. A slight complication was caused by the fact that the low stirring rate was originally the rate used in the calibration of the bridge. (This rate had been used for calibration because it was thought that this would minimise the heat generated by stirring, but the high rate had been used for all other measurements.) It was, however, decided not to re-calibrate the bridge at the high rate. Hence the readings originally taken at the low rate were converted so that they represented equivalent readings taken at the high rate. To do this, the position of one of the calibration points, viz. that at 25.000°C, was re-determined at high and low rates. The difference between the two readings of off-balance potential was taken to be the difference between the ΔT_{stir} values corresponding to high and low stirring rates. This difference was found to be 445 ± 27 μV (or 0.057 ± 0.003°C).

5.2.3. Determination of the heat capacity of the reaction vessel

The heat capacity of the reaction vessel, containing a known volume of doubly deionized water, was determined by the dissipation of a known quantity of electrical energy and measurement of the resulting temperature rise. Water was used in the reaction vessel because its heat capacity is accurately known as a function of temperature.

The reaction vessel, containing the known volume of doubly deionized water and positioned in the calorimeter assembly, was placed in the water bath at 25.000°C in order to equilibrate. Once the equilibration period (> 45 minutes) was over, the off-balance potential was recorded for approximately 5 minutes to obtain the lead period of the thermogram. The heater was then switched on for the selected time period, and once again the off-balance potential was followed. Observation of the off-balance potential for 5 minutes after the heater was switched off provided the trail period of the thermogram. The resulting thermogram was plotted and the data were corrected for heat exchange effects, etc., with the aid of the computer program CALCAL (see Section 4.4.7), which also calculates the heat capacity of the reaction vessel and its contents. The heat capacity of the empty reaction vessel, Cp^r, was then found by subtracting the contribution of the water to the total heat capacity.

Cp^r is constant for a given volume of liquid in the reaction vessel, but varies as this volume changes. This change results from more of the reaction vessel and stirrer coming into contact with the liquid as its volume increases. Therefore Cp^r was determined as a function of the volume of water in the reaction vessel, for volumes between 95.00 and 100.00 cm^3.

Care was taken during these, and subsequent, heat capacity measurements to ensure that the stirrer was always attached in exactly the same position, so as not to change the area in contact with the liquid and thereby introduce an error in the heat capacity determinations. As a further precaution the capillary tube, through which the titrant solution is normally added into the vessel, was kept filled throughout the heat capacity measurements.

A typical set of results obtained for the various heat capacity determinations performed in order to calculate Cp^r is shown in Table 5.6. The result of a simple linear regression performed on this set of volume-Cp^r data is the relationship:

$$Cp^r/JK^{-1} = 28.82 + (0.2884\ cm^{-3})(V - 95). \qquad (5.9)$$

A plot of the data leading to equation (5.9) is shown in Figure 5.9.

TABLE 5.6

Heat capacity of the reaction vessel as a function of volume of water contained, at 25.000°C.

Volume of water contained in the reaction vessel/ cm^3	Heat capacity of the reaction vessel + water/ JK^{-1}	Heat capacity of water*/JK^{-1}	Cp^r/JK^{-1}
95.00	424.8	395.9	28.9
96.00	429.2	400.1	29.1
97.00	433.6	404.2	29.4
99.00	442.2	412.6	29.6
100.00	447.3	416.7	30.6

*Values obtained from reference 166.

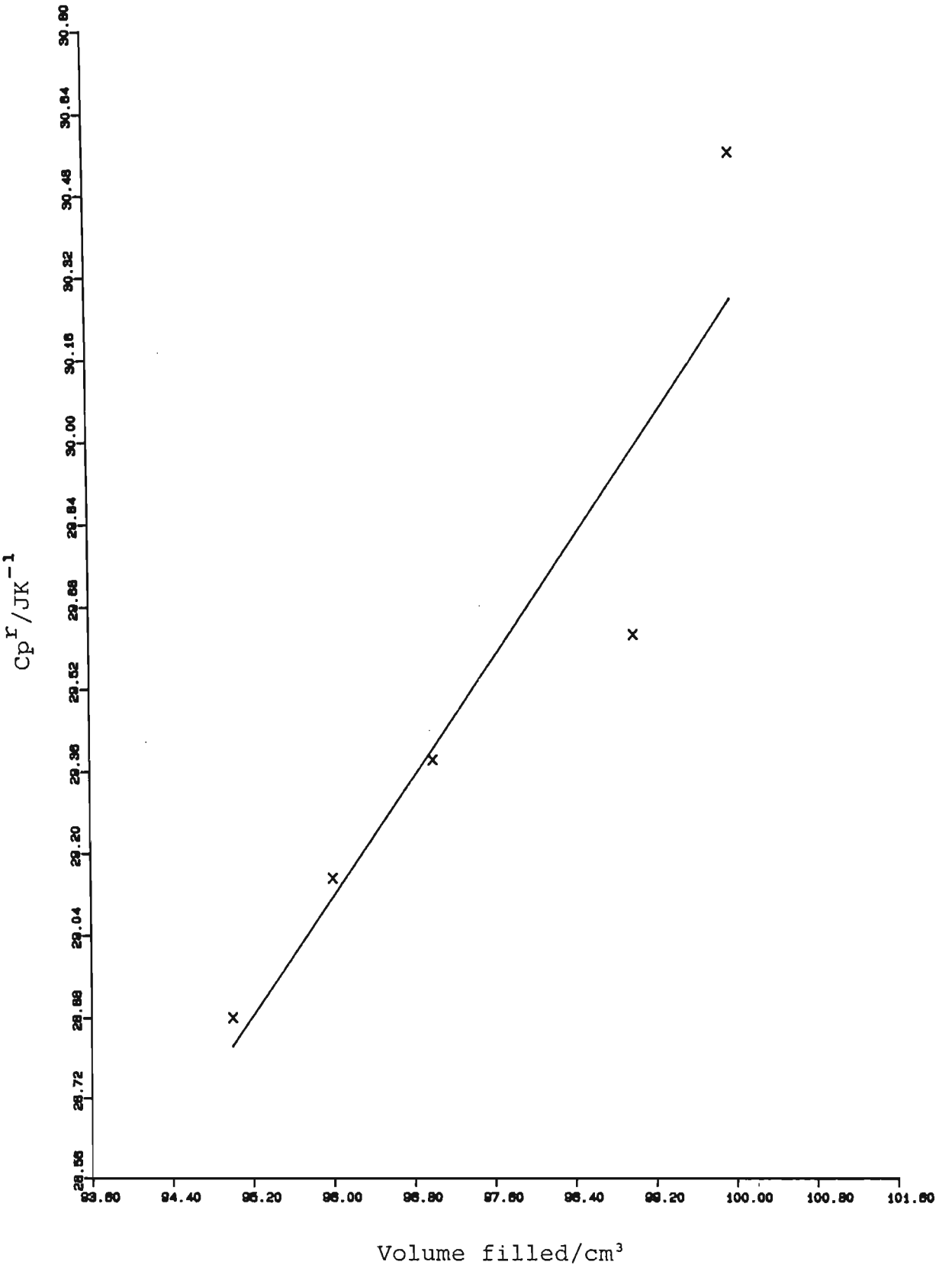

Figure 5.9 Heat capacity of the reaction vessel as a function of the volume filled with liquid.

CHAPTER SIX

SELECTION OF EXPERIMENTAL CONDITIONS

When selecting the conditions for an experiment, one must consider the relationship between the desired thermodynamic quantity and the measured quantity so as to choose the conditions that will enable the maximum amount of useful information to be extracted from the measurements.

6.1. General approach to the selection of experimental conditions

First the considerations arising in the choice of conditions for a potentiometric titration will be discussed. If reliable values of the stability constants are to be determined, such experiments must be well designed and the measurements made as accurately as possible.

In choosing the conditions for determining a particular stability constant, one must ensure that the quantity being measured, in this case the hydrogen ion concentration, quantitatively reflects the effects of complex formation: that is, the measured quantity must be a sensitive function of the stability constant being determined.

If several species coexist to a significant extent, this will cause a decrease in the precision of the stability constants extracted from the experimental data. Hence it is advisable that the species of interest predominates over an appreciable part of the concentration range covered by the titration. In particular, if one wishes to study mononuclear complexes (as in this case) one should if possible avoid conditions under which mixed or polynuclear species predominate. If on the other hand one wishes to study polynuclear or mixed complexes, measurements should of course be made under conditions where such complexes are more likely to occur, e.g. high metal-ion concentrations or high $p[H^+]$. Nevertheless, one should always test for the presence of unwanted species through the use of $\bar{Z}(\log[L])$ plots. For this reason the potentiometric titrations should be carried out at several metal ion concentrations. (See Section 4.3.2.)

Since one is studying systems at equilibrium, one should ensure that equilibrium (as indicated by a steady potential reading) has indeed been

attained after each addition of titrant. Reversibility of the reaction should also be checked, by carrying out a reverse titration. That is, if the addition of titrant has caused an increase in $p[H^+]$, then at the end of this titration the titrant is changed so that further titration causes a decrease in $p[H^+]$ to its initial value. If the $\bar{Z}(\log[L])$ plots for the forward and reverse titrations are superimposable, the reaction is reversible.

One should always ascertain that the results obtained are reproducible. This need not be checked by repeating a titration if the formation curves obtained by using different concentrations of reactants are superimposable. Should the formation curves not coincide, however, then it is best to repeat one of the titrations and use fresh stock solutions.

The experiments should be planned in such a way that the concentration of each of the reactants is varied over as wide a range as is practically possible. In this way one facilitates the attainment of reliable stability constants. (The upper limit of the concentrations which can be used is controlled by such factors as the variation of activity coefficients and limited solubility, whereas the lower limit is reached when the equilibria being studied are swamped by the dissociation equilibria within the medium, or by experimental error.) Another advantage of covering a wide range of concentrations is that the stability constant for a particular species can be extracted from a selected region where other, interfering species appear to be absent.

In titration calorimetry the general considerations are somewhat different, since here one wishes, for reasons of accuracy, to maximise the amount of heat liberated for a given amount of titrant added. With the instrument used in this work the desirable change in off-balance potential is 3000 μV, which is equivalent to about 0.4°C. Again it is important that the species of interest predominates in the concentration range covered, so that most of the heat liberated can be ascribed to the reaction of interest and not to interfering reactions. The calorimetric experiments for each system should be carried out under similar conditions, i.e. within roughly the same $p[H^+]$ and $\bar{Z}$ regions, as the potentiometry. This ensures that the stability constants of all the species present are known. Such knowledge greatly simplifies the calculation procedure used to determine the enthalpy changes of complex formation (see Section 4.4.10). Unfortunately the

computer program LETAGROP KALLE (used to calculate the enthalpy changes) cannot in its present form deal with more than one reacting component in the titrant. This fact limits somewhat the range of experimental conditions available.

In selecting experimental conditions for both the potentiometric and the calorimetric titrations much use was made of the program HALTAFALL (see Section 4.4.1). The program was used to arrive at species distribution diagrams, from which one could determine which concentration combinations give the optimum formation of a certain species. From HALTAFALL-calculated $p[H^+]$ values it could be decided whether the $p[H^+]$ changes occurring in a particular potentiometric titration were sensitive to changes in the stability constant being determined. In order to perform these calculations HALTAFALL requires as inputs the reagent concentrations, and the stability constants for the species assumed present. The former inputs were chosen by the author, while the latter were either obtained directly from the literature, or estimated from knowledge of similar systems previously studied.

Throughout this work the measurements were undertaken at an ionic strength of 0.5 mol dm^{-3} by using KNO_3 as the background electrolyte, and at a temperature of 25°C. This ionic strength was chosen mainly because of calorimetric considerations. At this strength reagent concentrations could be kept sufficiently high so that adequate amounts of heat were liberated for the enthalpy changes to be determined precisely. In addition, the higher the ionic strength in comparison with reagent concentrations, the more likely it is that the activity coefficients will remain constant. The background electrolyte was chosen to be KNO_3 mainly because the NO_3^- anion is small in size and therefore unlikely to form precipitates with protonated polyamine ligands or with metal-polyamine complexes. Also, NO_3^- has no affinity in aqueous solution for Ni^{2+}, Co^{2+} or Zn^{2+}. Finally, the cation K^+ has a very low tendency to form complexes. It was therefore hoped that this background electrolyte would have no unwanted effect on the equilibria being studied. The working temperature was chosen to be 25°C because this is the temperature most often used for thermodynamic measurements.

In some of the measurements care was needed to prevent hydrolysis of the metal-ligand complexes. In an attempt to overcome this potential problem it was decided to replace some of the cation in the background electrolyte

with protonated ligand, as this would lower the $p[H^+]$. However, this method of lowering the working $p[H^+]$ can cause loss of sensitivity if $[M]_t$ is much lower than $[L]_t$, especially in the case of potentiometric measurements. On the other hand, reagent concentrations must not be too high in comparison with the concentration of background electrolyte, as this would cause fluctuations in the ionic strength and resultant changes in activity coefficients. A compromise technique was therefore adopted. The program HALTA1 (see Section 4.4.1) was used to calculate the ionic strength at each point of the titrations to ensure, if possible, that an approximately constant ionic strength would be maintained.

In both potentiometry and calorimetry the formation of precipitates is undesirable. In some cases the experimental conditions can be chosen in such a way as to avoid their formation. For instance, the problem can often be overcome in potentiometry by the use of more dilute solutions. This option is not always available in titration calorimetry, however, as it can result in insufficient heat liberation and hence poor determination of the enthalpy change for the reaction of interest. Lowering the $p[H^+]$ of the reaction mixture as described in the previous paragraph can also help to prevent precipitation of metal hydroxides.

What now follows is a discussion of how the experimental conditions for each of the different types of measurement undertaken were chosen. An example will be given for each case discussed.

6.2. Choice of experimental conditions for potentiometric measurements

There were three methods available for the determination of the stability constants of the metal-ligand complexes:

1. addition of acid to a solution containing the metal-ligand complexes, i.e. decomposing the metal-ligand complexes with acid;

2. addition of a hydroxide solution to a solution containing the metal ion plus protonated ligand, i.e. deprotonating the ligand so that it can then complex with the metal ion; and

3. addition of deprotonated ligand to a solution containing metal ion and protonated ligand.

For practical convenience and because of the form in which the ligands were available, methods 1. and 3. were used for the complexes of etolen, and methods 2. and 3. used for oden.

Four methods were available for the determination of the protonation constants of oden and etolen. These were:

1. titration of acid into a solution containing deprotonated ligand;

2. titration of a solution of deprotonated ligand into an acid solution;

3. titration of hydroxide into a solution containing protonated ligand; and

4. titration of protonated ligand into a solution containing hydroxide.

It must however be noted that the $p[H^+]$ readings which are sensitive to the values of the protonation constants lie in the range from $pK_a - 1$ to $pK_a + 1$. Readings outside this range are not useful. Therefore, in using any of the above four methods, one must ensure that $p[H^+]$ readings are taken in the appropriate range. For the sake of convenience method 2. was used for determination of the protonation constants of etolen, since this ligand was available in deprotonated form. Method 3. was used for oden because the ligand was purchased and purified in protonated form.

For the metal-ligand systems the working $p[H^+]$ was kept fairly low in order to suppress hydrolysis of the metal-ligand complexes. This was achieved largely by introducing some protonated ligand as part of the background electrolyte.

As an example, the selection of the reagent concentrations for the potentiometric measurements involving etolen and Ni^{2+} will be described. In these titrations the cell was calibrated with strong acid and with the ligand as base (see Section 5.1.3). Hence, on completion of the calibration, part of the background electrolyte consisted of doubly protonated etolen. The following stability constants, obtained from the literature and valid

at an ionic strength of 0.5 mol dm^{-3} and a temperature of 25°C, were used in the calculations:

$$K_w = 1.8197 \times 10^{-14} \quad (160)$$
$$\beta_{101} = 5.495 \times 10^{9} \quad (167)$$
$$\beta_{201} = 3.890 \times 10^{16} \quad (167)$$
$$\beta_{011} = 9.333 \times 10^{6} \quad (167)$$
$$\beta_{012} = 6.310 \times 10^{12} \quad (167)$$
$$\beta_{-110} = 9.120 \times 10^{-11} \quad (168).$$

Table 6.1 shows the various reagent concentrations used to calculate the species distributions. As stated previously, the aim is to obtain conditions such that each species in solution predominates over some region of the titration, and to ensure that the measured $p[H^+]$ is a sensitive function of the stability constants being determined. From the species distribution curves obtained for the various metal-to-ligand ratios (and shown in Figure 6.1), we see that each of the species assumed present does indeed predominate over some region of the $p[H^+]$ range covered by the experiments. The sensitivity of the measured $p[H^+]$ to the stability constants being determined was tested by changing the values of β_{011} and β_{012} by one log unit in turn. The results of this calculation for experiment 1 are plotted in Figure 6.2. A calculated change of 3 mV in the cell potential, corresponding to approximately 0.05 $p[H^+]$ units, was taken as the lowest acceptable level of sensitivity.

Similar considerations and calculations were used to select the reagent concentrations for the titrations involving the other metal ion-ligand systems and the hydrogen ion-ligand systems.

6.3. Choice of experimental conditions for calorimetric measurements

In the calorimetric measurements all the same titration methods as previously described were possible, but some were found more suitable than the others for reasons specific to calorimetry.

In titration calorimetry it is best to use a method which involves a minimum of side reactions interfering with the reaction of interest. For example, in the hydrogen ion-ligand systems titration methods 3. and 4.

TABLE 6.1

Reagent concentrations chosen for the potentiometric titrations involving Ni^{2+} and etolen.

Experiment Number	1	2	3
Concentrations of reactants in the titrate/mol dm^{-3}			
$[H^+]_0$	2.25×10^{-2}	2.25×10^{-2}	2.35×10^{-2}
$[etolen]_0$	1.00×10^{-2}	1.00×10^{-2}	1.04×10^{-2}
$[Ni^{2+}]_0$	3.33×10^{-3}	2.50×10^{-3}	1.74×10^{-3}
Concentrations of reactants in the titrant/mol dm^{-3}			
$[H^+]_T$	0	0	0
$[etolen]_T$	5.00×10^{-2}	5.00×10^{-2}	5.00×10^{-2}
$[Ni^{2+}]_T$	0	0	0
Initial Volume, V_0/cm^3	120.00	120.00	115.00
Initial metal-to-ligand ratio	1:3	1:4	1:6

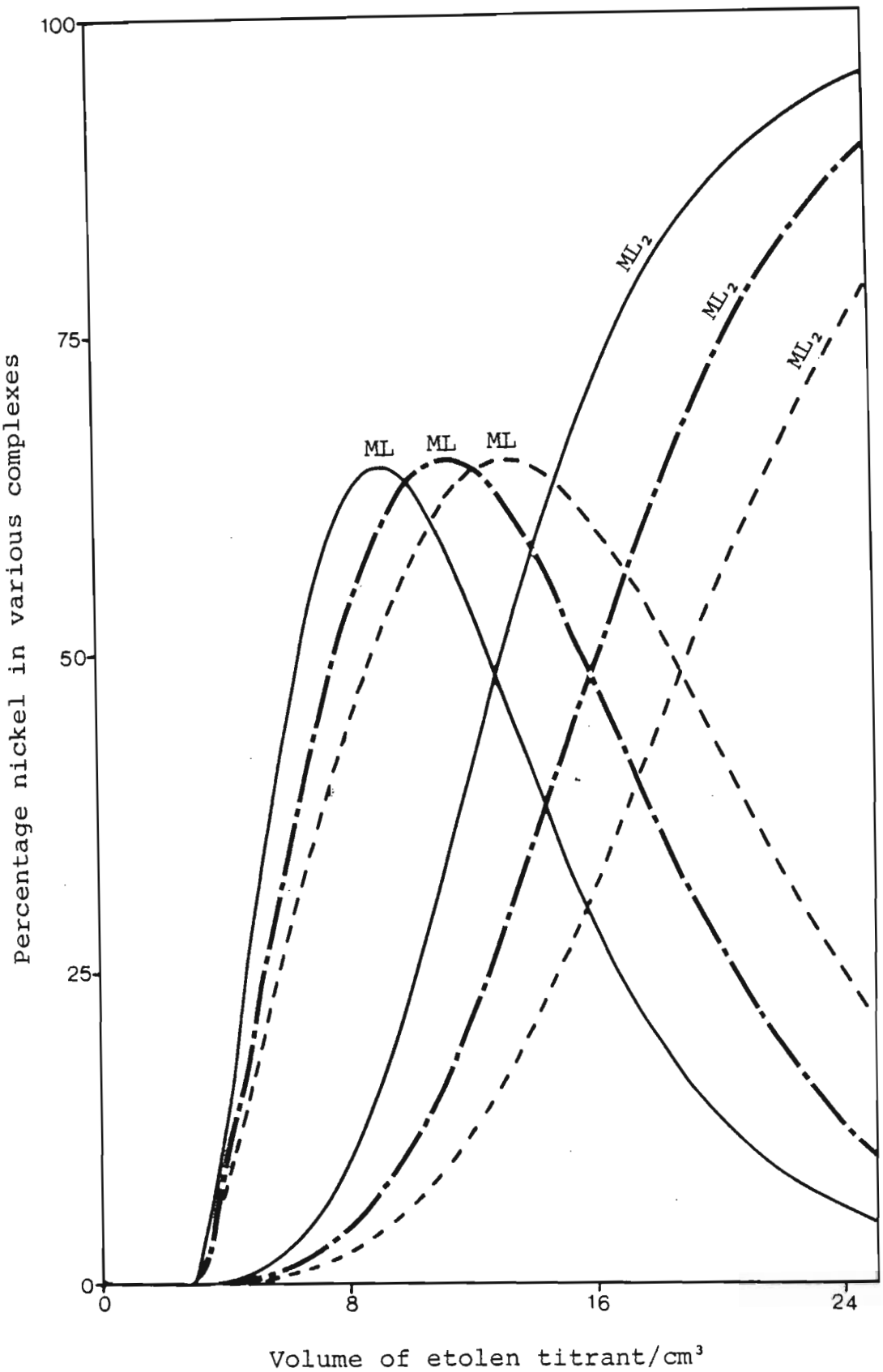

Figure 6.1 Species distribution curves for the Ni^{2+}-etolen potentiometric titrations showing the variation that occurs on changing the metal to ligand ratio. The lines — — — — , —·—·— and ———— represent experiments 1, 2 and 3 respectively.

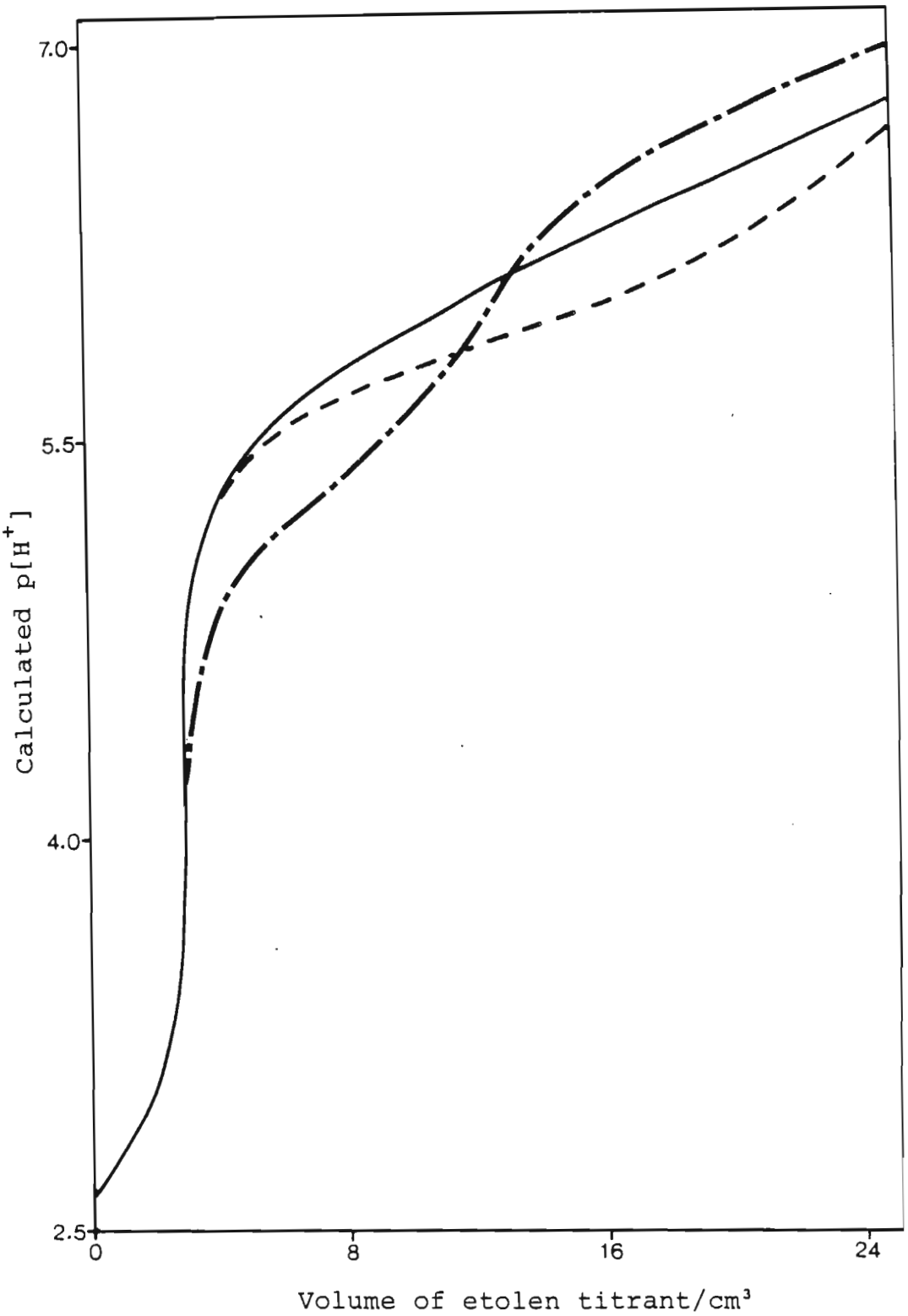

Figure 6.2 Plot illustrating the sensitivity of the calculated $p[H^+]$ to the stability constants being determined. The line ———— is based on the literature values of the stability constants. The lines -·-·- and — — — — result when log β_{011} and log β_{012} respectively are increased by one unit.

have the disadvantage that the heat associated with the reaction of interest is overshadowed by the heat liberated by the formation of water. Hence these two methods are not the best for accurate determination of the heats of protonation.

Another consideration to bear in mind is that in this calorimetry the titrant solution should be very much more concentrated than the titrate solution. Hence for convenience titration method 1. (titration of acid into a solution containing deprotonated ligand) was chosen for the determination of the enthalpy changes of protonation for both etolen and oden. Similarly method 3., the titration of deprotonated ligand into a solution containing metal ion and protonated ligand, was chosen for the metal ion systems involving etolen. The high cost of oden prevented its use in concentrated ligand titrant solutions. Therefore measurements of the heats of reaction of the various metal ions with oden were performed by titrating a solution of metal ion into a solution containing a mixture of ligand and protonated ligand.

As an example, the selection of the reagent concentrations for the calorimetric measurements involving Co^{2+} and etolen will now be described. Reagent concentrations for the other systems were chosen similarly.

The calorimetric experiments had to be carried out under conditions similar to those used for the potentiometric experiments, to ensure that the solution equilibria were adequately described. In practice this meant that the $p[H^+]$ and $\bar{Z}$ regions covered during the calorimetric titrations should lie within those covered during the potentiometric titrations. Hence the experiments were designed in such a way that the titrate contained the metal ion and some protonated ligand. The latter was included in order to lower the $p[H^+]$ of the resulting solution. The titrant consisted solely of the ligand etolen made up to the correct ionic strength with KNO_3. Only one reacting species could be used in the titrant solution, because of the limitation of the program LETAGROP KALLE already mentioned in Section 6.1. In addition, the solutions had to be sufficiently concentrated to produce an acceptable change in temperature (i.e. about 0.4°C). The required enthalpy changes were estimated from the enthalpy changes for the Ni^{2+}-etolen system and other systems involving Ni^{2+} and Co^{2+} with polyamine ligands. Table 6.2 shows the reagent concentrations chosen. A species distribution for these reagent concentrations was cal-

TABLE 6.2

Reagent concentrations chosen for the calorimetric measurements involving Co^{2+} and etolen.

Reactants	Concentrations of reactants in the titrate/mol dm^{-3}	Concentrations of reactants in the titrant/mol dm^{-3}
H^+	1.1×10^{-1}	0
etolen	5.0×10^{-2}	1.3
Co^{2+}	3.0×10^{-2}	0

culated (by HALTAFALL) to ensure that the different species of interest would predominate over roughly equal portions of the titration.

CHAPTER SEVEN

EXPERIMENTAL PROCEDURE AND DATA

This chapter describes a series of potentiometric and calorimetric titrations performed in order to obtain the stability constants and enthalpy changes of complex formation for each system studied. Numerical data obtained from these experiments are included. Also reported here are the preparations of various solid complexes and the recording of the electronic spectra of some of these complexes. All the titrations were carried out at an ionic strength of 0.5 mol dm^{-3} with KNO_3 as the background electrolyte and at a constant temperature of 25.00 $\pm$ 0.05°C for the potentiometry and 25.0 $\pm$ 0.2°C for the calorimetry. All the solutions mentioned here were made up by dilution of the appropriate stock solution or as described in Chapter 2.

In the potentiometric measurements, the whole assembly was allowed to come to equilibrium over a period of at least 2 - 3 hours after the first addition of calibrating titrant solution. After each subsequent addition of titrant solution, sufficient time was allowed to ensure that the system had come to equilibrium. An equilibration period of 10 to 15 minutes was allowed for points in the low $p[H^+]$ region, whereas for points in the high $p[H^+]$ region 30 or more minutes were allowed. When successive cell e.m.f. readings differed by less than 3 mV the volume of titrant solution added was doubled.

In the calorimetric titrations the heats of reaction were measured as follows. First the automatic burette and the titrant tubing were filled with the titrant solution. Then 95.00 cm^3 of the titrate solution were placed in the reaction vessel. The vessel was attached to the calorimeter assembly and the stirrer was switched on at the high stirring speed. The capillary tube through which the titrant enters the vessel was then filled. However, a small air gap was left to separate the titrant from the titrate in order to avoid premature mixing of the two solutions. The temperature of the reaction vessel and its contents was brought to approximately 25°C, either by warming the contents of the vessel by means of the calibration heater, or by cooling the outside of the vessel with

iced water. When the required temperature had been attained, the outside surface of the reaction vessel was wiped clean with tissue paper to ensure the reproducibility of the heat capacity of the reaction vessel. The calorimeter assembly was clamped closed and placed in the constant temperature water bath maintained at 25.000 $\pm$0.001°C.

A period of at least 45 minutes was allowed for thermal stabilisation of the calorimeter assembly. (The stirrer was switched on to 'high' and the thermistor switched into the Wheatstone bridge circuit throughout these operations.) The off-balance potential was then recorded for a period of approximately 5 minutes to obtain the lead period of the thermogram. The automatic burette and timer were then switched on simultaneously and again the off-balance potential was followed, to obtain the titration curve. The titration period continued for the length of time selected. Once this was over the trail period of the thermogram was obtained in the same way as the lead period. The volume of titrant solution dispensed by the automatic burette was noted.

The heats of dilution were measured in the same way as the heats of reaction, except that the titrate solution was replaced by the corresponding blank titrate solution.

The operational procedure for determination of the heat capacities of the various solutions is described in Section 5.2.3. Before each heat capacity determination a potential difference of 1.0000 V was set across one of the standard resistors in order to maintain the design-specified current value through the heater for the power setting selected (169). The heat capacity of each of the solutions used was measured. In each case the vessel was filled with 95.00 cm^3 of solution. During these measurements the capillary tube through which the titrant solution enters the reaction vessel was kept filled with the titrant solution. A small air gap was left at the tip to prevent mixing of the solutions. The length of time for which the calibration heater was activated was selected in such a way as to yield approximately the same temperature change as occurred during the reaction runs. At the end of each heat capacity determination the potential difference across the calibration heater was recorded.

The data collected from the potentiometric experiments are listed in full in Table 7.1 of Section 7.9, together with the solution concentrations used. The calorimetric titration data, together with the corresponding solution concentrations, are presented in Table 7.2 of Section 7.9. Unless otherwise stated, the calorimetric data have been corrected for non-chemical heat effects by the method described in Section 4.2.

7.1. The hydrogen ion - etolen system

The protonation constants for etolen were determined potentiometrically by the addition of a titrant solution containing ligand to a titrate solution containing acid. First the cell was calibrated by using a strong acid, as described in Section 5.1.1. Deviations of the $E^{\ominus}$" values from constancy could usually be traced to contamination of the apparatus. The addition of acid was discontinued at a $p[H^+]$ of 2.7. After the determination of $E^{\ominus}$" a solution of the ligand was added in small increments. After each addition the system was allowed to come to equilibrium and the cell e.m.f. noted. The experiment was carried out in triplicate.

The calorimetric titrations for the determination of the heats of protonation of etolen were carried out by the addition of a 0.5 mol dm^{-3} nitric acid solution to a solution containing 0.01 mol dm^{-3} etolen. The specific heat capacities of the titrant, titrate and blank titrate were measured in duplicate, as was the heat of dilution of the titrant into the blank titrate. The heat of reaction for addition of the titrant to the titrate was measured in triplicate.

7.2. The hydrogen ion - oden system

The potentiometric titrations for this system were carried out by the addition of a titrant solution containing hydroxide to a titrate solution containing oden.2HCℓ. In these titrations the cell was calibrated by using strong acid and strong base. A solution of 0.01 mol dm^{-3} HNO_3 was added in small increments to a mixture of 50.00 cm^3 of 0.50 mol dm^{-3} KNO_3 and 5.00 cm^3 of the NaOH solution later to be used as the titrant. The concentrations of hydroxide and carbonate, as well as the constants $E^{\ominus}$" and s, were calculated from the cell potential readings as described in Section 5.1.2. Once the cell had been calibrated, a 10.00 cm^3 aliquot

of a solution of oden·2HCℓ was pipetted into the reaction mixture. This was then titrated with the solution of NaOH, whose concentration had been determined in the first part of the experiment. The experiment was carried out in quadruplicate. (Note that in Table 7.1 each titration is split into two parts: (a) and (b). This was done because the carbonate present in the hydroxide solution was taken into account only at $p[H^+]$ values greater than 10. At $p[H^+]$ values below 10 the total base concentration is used. See Section 8.2.)

The heats of protonation for oden were determined by the addition of a titrant solution containing acid to a titrate solution containing oden. The heat capacity of each of the solutions used, the heat of dilution and the heat of reaction were all measured in duplicate.

7.3. The nickel ion - etolen system

Some of the potentiometric titrations for this system (titrations 1 - 3) were performed by starting with the complex ion in solution and stripping the ligand off the metal ion with acid. In these titrations the potentiometric cell was calibrated with strong acid alone, as described in Section 5.1.1. The addition of acid was discontinued at a $p[H^+]$ of 2.7. Once $E^{\ominus}$" had been determined, appropriate aliquots of Ni^{2+} and deprotonated ligand solutions were added to the reaction mixture in order to obtain the required initial metal to ligand ratio. This mixture was then titrated with a solution of HNO_3 and Ni^{2+} (the latter to keep the total metal ion concentration constant) in order to strip the ligand off the metal ion.

In the rest of the titrations (nos. 4 - 7) the cell was calibrated with strong acid and ligand, as described in Section 5.1.3. Once the cell had been calibrated and metal ion added, a titrant solution containing ligand was added to the reaction mixture. At the completion of the calibration the reaction mixture in these titrations was approximately 0.01 mol dm^{-3} in doubly protonated ligand. This helped to lower the working $p[H^+]$, and possibly to suppress hydrolysis of the metal-ligand complexes.

In the first three titrations the total concentration of Ni^{2+} was kept constant. In the rest of the titrations, however, neither the total

concentration of Ni^{2+} nor that of etolen was kept constant. In titrations 2 and 3 the reversibility of the equilibria was tested by performing both forward (decreasing $p[H^+]$) and reverse (increasing $p[H^+]$) titrations. (The titrations were reversed by titrating the reaction mixture with a solution of NaOH.) One titration (no. 4) was carried out in duplicate in order to check the reproducibility of the results obtained. The repeat titration is no. 7. The total initial concentrations of Ni^{2+} and etolen were varied within the limits $5.0 \times 10^{-4} \leq [Ni^{2+}]_0 \leq 3.3 \times 10^{-3}$ mol dm^{-3} and $4.2 \times 10^{-3} \leq [\text{etolen}]_0 \leq 1.1 \times 10^{-2}$ mol dm^{-3}. The following initial metal to ligand ratios were studied: 1:2.2, 1:3.1, 1:3.6, 1:4.1, 1:4.5, 1:6.1, 1:8.5 and 1:11.1.

The calorimetric titrations involving etolen and Ni^{2+} were designed so that a titrant solution containing ligand was added to a titrate solution containing metal ion, some doubly protonated ligand and some surplus acid. In this way approximately 30 % of the background electrolyte was replaced by the nitrate salt of the doubly protonated ligand, which lowered the $p[H^+]$ and suppressed hydrolysis of the metal-ligand complexes. For this system all the calorimetric measurements were carried out in triplicate. The raw calorimetric data were processed as described in Section 4.2, apart from two modifications.

First, the heat of dilution of the titrant into the titrate for this system was not calculated in exactly the way previously described. This was because the heat liberated during the determination was due not only to dilution of the titrant, but also to some reaction between the ligand titrant solution and the excess acid which was present in the titrate solution. The heat of dilution was therefore calculated as follows. First the raw data from the heat of dilution titrations were corrected for non-chemical heat effects by using CALCOR. The calorimetric data obtained (i.e. $V_{T,k}, Q_{c,k}$ pairs) were then corrected for ligand protonation by using LETAGROP KALLE. This program was supplied with the concentrations of each of the components, the protonation constants and the heats of protonation of the ligand, and the calorimetric data. The first set of output from LETAGROP KALLE gives the differences between the heat observed and the heat calculated on the basis of the concentrations and enthalpy changes provided. These differences, which are the heats arising from the dilution process, were used to calculate H_D, the heat of dilution,

by the same method as before.

The second modification was made as follows. The titrate solution used in the heat of reaction experiments contained excess acid to ensure that the ligand forming part of the background electrolyte was completely protonated. However this meant that at the beginning of each titration there was an end-point, i.e. this excess acid protonated the ligand added from the titrant. This is not desirable since it introduces errors into the LETAGROP KALLE calculations. Hence the concentrations of the components in the titrate were modified to include the volume of titrant added up to just after the end-point. The heat liberated from the beginning of the titration up to this point was disregarded. This modification was carried out only after the heats had been corrected for non-chemical heat effects by using CALCOR.

The calorimetric data for this system listed in Table 7.2 reflect these modifications.

7.4. The nickel ion - oden system

Some of the potentiometric titrations for this system (nos. 1 - 3) were carried out by adding a titrant solution containing hydroxide to a titrate containing Ni^{2+} and oden.2HCℓ. In these titrations the potentiometric cell was calibrated with strong acid and strong base, as described in Sections 5.1.2 and 7.2. (In these calibrations the HNO_3 concentration was 0.02 mol dm^{-3} and the NaOH concentration was 0.04 mol dm^{-3}.)

In the remainder of the titrations (nos. 4 - 7) a titrant solution containing ligand was added to a reaction mixture containing Ni^{2+}, doubly protonated ligand and surplus acid. In these titrations the cell was calibrated with strong acid and ligand. At the completion of the calibration the reaction mixture in these titrations was approximately 0.01 mol dm^{-3} in doubly protonated ligand, except in titration no. 6, where the concentration was approximately 6.7×10^{-3} mol dm^{-3}. Once the cell had been calibrated, an appropriate aliquot of the metal ion solution was added and the titration commenced.

In titration 1 the total concentration of Ni^{2+} was kept constant at 1.0×10^{-3} mol dm^{-3}. In the rest of the titrations neither the metal ion concentration nor that of the ligand was kept constant. In the first titration the reversibility of the reactions was tested by performing a reverse titration (decreasing $p[H^+]$) once the forward titration had been completed. This was achieved by adding a titrant solution containing hydrogen ion. One titration (no. 4) was carried out in duplicate in order to check the reproducibility of the results obtained. The repeat titration was no. 7. The initial concentrations of Ni^{2+} and oden were varied within the limits $5.0 \times 10^{-4} \leq [Ni^{2+}]_0 \leq 5.0 \times 10^{-3}$ mol dm^{-3} and $1.7 \times 10^{-3} \leq [oden]_0 \leq 1.0 \times 10^{-2}$ mol dm^{-3}. The following initial metal to ligand ratios were studied: 1:1.7, 1:2.0, 1:2.2, 1:4.0, 1:4.5, 1:6.0 and 1:9.0.

The high cost of oden prevented the use of concentrated ligand solutions in the calorimetric titrations. These titrations were therefore performed by titrating a solution of the metal ion into a solution containing a mixture of ligand and protonated ligand. The heat capacities of the solutions and the heat of dilution were determined in triplicate. The heat of reaction titration was carried out in quadruplicate.

When the calorimetric experiments for this system were first carried out, a solution of the metal ion (0.1667 mol dm^{-3}) was titrated into a dilute solution of the deprotonated ligand (0.0083 mol dm^{-3}) made up to the correct ionic strength with KNO_3. When the first heat of reaction titration was carried out, a turquoise-coloured precipitate formed. Three options were open to overcome this problem:

1. addition of a known quantity of protonated ligand to the titrate in order to lower the $p[H^+]$;

2. reduction of the ligand concentration in the titrate; and

3. reduction of the reaction time.

At the time option 1. was not feasible, as no further quantities of ligand were available. (However this option was subsequently adopted. By the replacement of some of the background electrolyte with protonated ligand

it was possible to lower the $p[H^+]$ sufficiently so that the heats of reaction could be measured successfully with the total avoidance of any precipitation.) The second option was not feasible because, if the ligand concentration had been reduced further, insufficient heat would have been liberated for an accurate determination of the heats of complexation with the titration calorimeter available. Reduction of the reaction time would avoid the formation of a precipitate, since it was ascertained that precipitation occurred towards the end of the titration. This option would however reduce the amount of information obtainable, especially in respect of the ML complex, which formed towards the end of the titration. Although this option was tried, it never completely succeeded in avoiding the precipitation problem. Hence these titrations were abandoned and subsequently repeated as already described.

7.5. The cobalt ion - etolen system

Two potentiometric titrations (nos. 1 and 2) were performed in which a titrant solution containing hydroxide was added to a titrate solution containing Co^{2+} and etolen.H_2^{2+}. In these two titrations the cell was calibrated with strong acid and strong base. (In these calibrations a 10.00 cm^3 aliquot of approximately 0.023 mol dm^{-3} NaOH was titrated with 0.02 mol dm^{-3} HNO_3.) Once the calibration of the cell was completed, appropriate aliquots of solutions containing Co^{2+}, etolen and HNO_3 were placed in the vessel and titrated with a titrant solution containing hydroxide.

The rest of the titrations (nos. 3 - 9) involved the use of protonated ligand as part of the background electrolyte, and calibration of the cell with strong acid and ligand. The reaction mixture was approximately 0.024 or 0.05 mol dm^{-3} in doubly protonated ligand at the start of the titration, i.e. after completion of the cell calibration. Depending on the initial concentration of Co^{2+} desired, an appropriate aliquot of a solution containing Co^{2+} was added to the mixture in the reaction vessel, and this was then titrated with a solution containing etolen.

In all these titrations neither the metal ion concentration nor that of the ligand was kept constant. The initial concentrations of Co^{2+} and etolen were varied within the limits $5.0 \times 10^{-4} \leq [Co^{2+}]_0 \leq 1.4 \times 10^{-2}$

mol dm^{-3} and $1.5 \times 10^{-3} \leq [etolen]_0 \leq 5.3 \times 10^{-2}$ mol dm^{-3}. The initial metal to ligand ratios studied were: 1:1.7, 1:1.8, 1:3.0, 1:3.3, 1:3.6, 1:3.9, 1:5.9 and 1:7.2. The reproducibility of the measurements was tested by carrying out one of the titrations in duplicate (see nos. 6 and 9).

It was noticed that, in the Co^{2+} - etolen potentiometric titrations in which the background electrolyte had been partially replaced by protonated ligand, the reaction mixture obtained after completion of the experiment turned dark brown on standing overnight exposed to the atmosphere. Hence it was decided to undertake a UV-visible spectrophotometric study of the system to ensure that no oxidation of the Co^{2+} complexes or ligand decomposition occurred during the potentiometric titrations.

First a potentiometric titration was set up under the same experimental conditions as were employed in titration 4. The reaction mixture was kept well stirred and high purity nitrogen was bubbled through it continuously. Samples of the reaction mixture were taken after 0, 12 and 22 cm^3 of 0.29 mol dm^{-3} etolen titrant solution had been added (samples 1 to 3 respectively). The decrease in volume on withdrawing the samples was disregarded. UV-visible spectra of these samples were recorded on a Pye Unicam SP1800 UV-visible spectrophotometer. The samples collected were kept in stoppered cuvettes and the spectra were re-run at several different times.

Although the reaction vessel was flushed with nitrogen, no such precaution was taken in the case of the cuvettes or the syringe used to withdraw the samples. It was noticed that, when the samples were left to stand in the cuvettes, the portion of the solution in contact with the vapour phase became brown. This was especially noticeable in the case of sample 3, but was also noticeable, to a lesser extent, in sample 2. A peak was observed at approximately 500 nm in the spectra of all the samples. In the case of samples 2 and 3, it was found to shift some 6 - 8 nm in the direction of lower wavelength as time passed and the samples became browner. In these cases there was also a build-up of the background with time. A spectrum showing this effect can be seen in Figure 7.1. In the spectrum obtained from the first sample the peak at 515 nm remained unchanged with time, which was consistent with the visual observations.

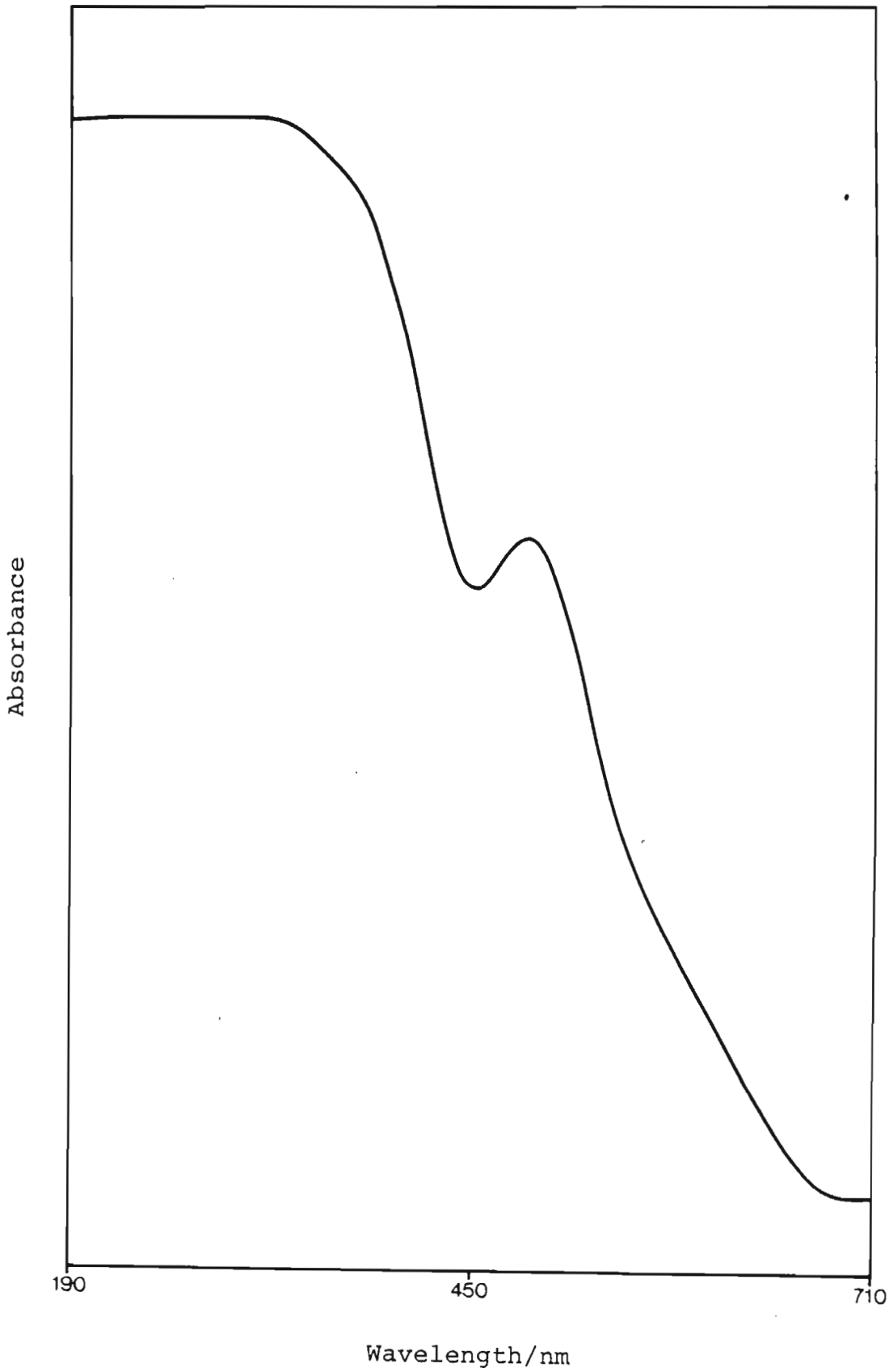

Figure 7.1 A typical UV-visible spectrum for a sample of Co^{2+} and etolen not kept completely under an atmosphere of nitrogen.

This experiment thus indicated that oxidation of the Co-etolen complexes occurred when the samples were in contact with air. It still remained to be seen whether or not oxidation or decomposition occurred when the reaction mixture was kept under an atmosphere of nitrogen. Hence the experiment was repeated, but this time the cuvettes and syringe were flushed out with nitrogen beforehand. The sample was placed in the cuvette in such a way that no vapour space remained, and nitrogen was flushed over the solution before the cuvette was stoppered.

Three potentiometric titration vessels were set up. In each of these was placed the same titrate solution as was used for titration 4. No titrant was added to the first vessel, but 12.5 and 25.0 cm^3 of 0.29 mol dm^{-3} etolen titrant solution were added to the others (2.2 and 4.4 moles etolen to 1 mole Co^{2+} respectively). One sample was taken from each of the three vessels in the manner described and UV-visible spectra were recorded at hourly intervals for a total of five hours. The spectra obtained from these samples remained unchanged with time. A typical spectrum is shown in Figure 7.2. A fourth potentiometric titration vessel was set up containing the same titrate solution. In this experiment a mock titration was performed and samples were taken at hourly intervals. The purpose of this experiment was to see whether decomposition occurred under the conditions prevailing during an actual titration. The spectra obtained at various stages during the experiment compared well with the corresponding spectra obtained in the three experiments described above.

Hence it was concluded that no significant oxidation or decomposition occurred during the course of the titration, provided that the reaction mixture was kept under an atmosphere of nitrogen.

The calorimetric titrations involving etolen and Co^{2+} were performed in much the same way as those for the Ni^{2+} - etolen system. The only difference was that a higher cobalt ion concentration was used because it was anticipated that the values of $\Delta H^{\ominus}$ would be lower for this system than for Ni^{2+} and etolen. All the calorimetric measurements were carried out in triplicate. The data were corrected as described in the case of Ni^{2+} and etolen.

Because the calorimeter reaction vessel is not equipped with a nitrogen inlet, there was some doubt as to whether the Co^{2+} - etolen system,

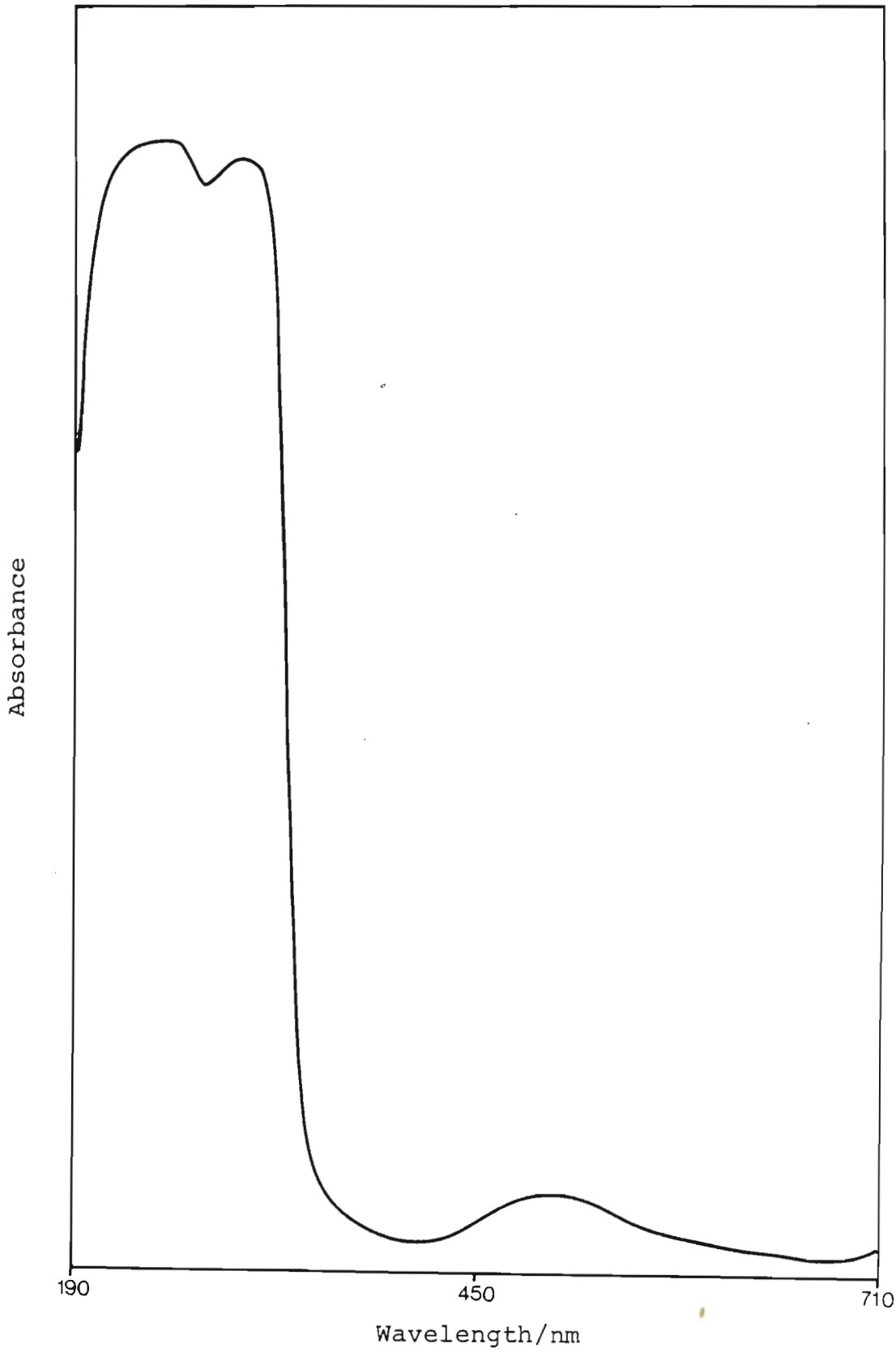

Figure 7.2 A typical UV-visible spectrum of the Co^{2+} - etolen reaction mixture in the absence of air.

which oxidises easily, could be studied calorimetrically. Hence a mock calorimetric run was performed to ascertain whether oxidation occurred even if the titrate solution was flushed out with nitrogen before the start of the titration.

The mock titration was carried out as follows. The calorimeter reaction vessel was filled with 95.00 cm^3 of the titrate solution. The titrate solution was not kept under an atmosphere of nitrogen at this stage, because it had been observed in the previous UV-visible study that, when the ligand is in a protonated state, no oxidation occurs. The stirrer shaft and stirrer were then removed from the calorimeter and the reaction vessel attached. A nitrogen inlet tube was inserted in the space left by the stirrer shaft and the vapour space above the titrate solution in the reaction vessel was flushed out with nitrogen. As soon as the nitrogen inlet had been removed, the stirrer shaft and stirrer were screwed into place. After the solution had been left for approximately one hour to simulate equilibration, the titration was performed. Five minutes after completion of the titration a sample of the solution in the reaction vessel was withdrawn with a syringe flushed out with nitrogen. The sample was withdrawn by undoing the vessel's burette tube from the burette, attaching a piece of heat shrink tubing to the syringe in place of a needle, and inserting one tube into the other.

When the first sample was withdrawn, the air in the burette tube and syringe oxidised the top part of the sample solution. This sample was forced back into the vessel and so diluted, as the solution in the reaction vessel was stirred continuously. A fresh sample was then withdrawn and placed in a cuvette previously flushed out with nitrogen, and the cuvette was stoppered.

A UV-visible spectrum of the reaction mixture was recorded, but it was difficult to ascertain, by comparison with the previous spectra, whether oxidation had occurred. It was decided to repeat the calorimetric titration under conditions in which there was certainty that no oxidation occurred, i.e. repeat it in a potentiometric titration vessel flushed out with nitrogen. From a comparison of the spectra obtained, it appeared that if oxidation did occur during the calorimetric titration it was slight and did not progress with time. If was felt that this small degree

of oxidation (if any) would introduce negligible error into the calorimetric measurements. Furthermore there was no evidence of any continuing reaction at the end of any of these titrations. That is, no further heat was absorbed or liberated, which would have happened if continuous oxidation were taking place.

Accordingly, it was concluded that the enthalpy changes for this system could be determined calorimetrically.

7.6. The cobalt ion - oden system

For this system some of the potentiometric titrations (nos. 1 - 4) involved the addition of a titrant solution containing hydroxide to a titrate containing Co^{2+} and oden.2HCℓ. In these titrations the cell calibration constants were obtained by using strong acid and strong base. After the cell had been calibrated, appropriate aliquots of solutions of Co^{2+} and oden.2HCℓ were placed in the vessel to achieve the desired metal to ligand ratio. This mixture was then titrated with a titrant solution containing hydroxide. In titrations 1 and 2 a precipitate formed before a significant concentration range had been covered. Hence in the subsequent titrations performed in this manner (nos. 3 and 4) a more dilute hydroxide titrant solution was used. However this meant that a smaller range of $p[H^+]$ was covered than originally intended.

The remainder of the potentiometric titrations for this system (nos. 5 - 8) were performed in the same manner as titrations 4 - 7 for the Ni^{2+} - oden system (see Section 7.4). The presence of some protonated ligand in the background electrolyte helped to lower the $p[H^+]$ sufficiently to avoid any further precipitation problems.

The concentrations of Co^{2+} and oden were not kept constant during any of these eight titrations. The initial metal to ligand ratios studied were: 1:2.0, 1:2.2, 1:4.0, 1:4.5, 1:6.0 and 1:9.0. The initial concentrations of Co^{2+} and oden were varied within the limits $5.0 \times 10^{-4} \leq [Co^{2+}]_0 \leq 5.0 \times 10^{-3}$ mol dm^{-3} and $2.2 \times 10^{-3} \leq [oden]_0 \leq 1.0 \times 10^{-2}$ mol dm^{-3}. One titration (no. 5) was carried out in duplicate in order to check the reproducibility of the results obtained. The repeat titration was no. 8.

The calorimetric titrations for this system were performed in the same manner as those for the Ni^{2+} - oden system. The heat capacities of the solutions and the heat of dilution were measured in triplicate. The heat of reaction titration was carried out in quadruplicate.

The first time the calorimetric measurements for this system were carried out, a 0.1667 mol dm^{-3} Co^{2+} solution was titrated into a 0.0083 mol dm^{-3} oden solution. When the first titration was performed, an olive-green precipitate formed. On reduction of the quantity of titrant added a pink precipitate formed. Attempts were then made to find concentration conditions that would obviate precipitation, but without replacement of any background electrolyte by protonated ligand. It was found that precipitates formed under all the concentration conditions suitable for calorimetric measurements. It was thought that the size of the anion possibly had some influence on the incidence of precipitation. Experiments were performed with $CoC\ell_2$ instead of $Co(NO_3)_2$, but precipitates formed as before. Once again the use of protonated ligand as part of the background electrolyte succeeded in overcoming this problem.

7.7. The zinc ion - etolen system

All the potentiometric titrations carried out for this system involved the use of protonated ligand as part of the background electrolyte. The potentiometric cell was calibrated by using strong acid and ligand. At the completion of the calibration the reaction mixture in these titrations was approximately either 0.01 or 0.02 mol dm^{-3} in doubly protonated ligand. The titrations were then carried out by titrating a titrant solution containing ligand into a reaction mixture containing Zn^{2+}, doubly protonated ligand and surplus acid.

The initial concentrations of Zn^{2+} and etolen were varied within the limits $1.7 \times 10^{-3} \leq [Zn^{2+}]_0 \leq 1.0 \times 10^{-2}$ mol dm^{-3} and $1.0 \times 10^{-2} \leq [\text{etolen}]_0 \leq 2.1 \times 10^{-2}$ mol dm^{-3}. The following initial metal to ligand ratios were studied: 1:2.0, 1:4.0 and 1:6.0. The reproducibility of the results was checked by performing one titration (no. 2) in duplicate (repeat titration: no. 6).

The calorimetric titrations were carried out by titrating a titrant solution containing ligand into a titrate containing metal ion, some doubly

protonated ligand and some surplus acid. For this system all the calorimetric measurements were carried out in quadruplicate. The calorimetric data were treated as described in the case of Ni^{2+} and etolen.

7.8. The zinc ion - oden system

This system was not studied experimentally as both the stability constants and the enthalpy changes of complex formation had previously been reported (78).

7.9. Experimental Data

The potentiometric titration data collected in this work are presented in Table 7.1 and the corrected titration calorimetric data in Table 7.2. In both of these tables the descriptions of the titrations performed begin with a listing of the concentrations of the components in the titrate solution (denoted $[\ ]_0$) and titrant solution (denoted $[\ ]_T$), and the initial volume (V_0) of the titrate solution. The concentration of the background electrolyte has been omitted for simplicity. For the potentiometric titration data, i.e. Table 7.1, the cell calibration constants (E°" and s) have also been included.

In Table 7.1 the description of the solutions is followed by a listing of the volume and cell e.m.f. data and several derived quantities, for each point in the titration under discussion. For the protonation titrations, i.e. systems 1 and 2, the data are given as groups of four numbers, viz. (in order): volume of titrant solution added/cm^3, cell e.m.f./mV, $-\log\{[H^+]/\text{mol dm}^{-3}\}$, and $\bar{j}$. For the metal ion - complexation titrations involving one titrant the data listed are: volume of titrant solution added/cm^3, cell e.m.f./mV, $-\log\{[H^+]/\text{mol dm}^{-3}\}$, $\log\{[L]/\text{mol dm}^{-3}\}$, and $\bar{Z}$. For those titrations involving more than one titrant, these are referred to as titrant A and titrant B. The data for such titrations are given as: volume of titrant solution A added/cm^3, volume of titrant solution B added/cm^3, cell e.m.f./mV, $-\log\{[H^+]/\text{mol dm}^{-3}\}$, $\log\{[L]/\text{mol dm}^{-3}\}$, and $\bar{Z}$.

In Table 7.2 the solution description is followed by pairs of numbers, the first being the total volume (in cm^3) of titrant solution added up to

that point, and the second being the corrected incremental heat (in J). A minus sign in the second position indicates liberation of heat.

TABLE 7.1

Potentiometric titration data for the various systems. (Those points marked with an asterisk were not used in the calculation of stability constants.)

1. System: H^+ + etolen

Titration No. 1

$E^{\ominus\prime\prime}$ = 255.13 mV, s = 59.158 mV,
$[H^+]_0 = 1.667 \times 10^{-3}$ mol dm^{-3}, $[etolen]_0 = 0$,
$[H^+]_T = 0$, $[etolen]_T = 1.009 \times 10^{-2}$ mol dm^{-3},
$V_0 = 60.00$ cm^3.

* 1.00	84.7	2.881	1.961
* 2.00	76.6	3.018	2.008
* 3.00	64.9	3.216	2.038
* 4.00	44.2	3.566	2.048
5.00	-75.8	5.594	1.980
6.00	-135.2	6.598	1.652
7.00	-159.3	7.006	1.417
8.00	-180.4	7.362	1.240
9.00	-205.6	7.788	1.103
10.00	-240.0	8.370	0.995
11.00	-263.7	8.770	0.908
12.00	-277.0	8.995	0.837
13.00	-285.7	9.142	0.777
14.00	-291.8	9.245	0.725
15.00	-296.8	9.330	0.680
16.00	-301.0	9.401	0.641
17.00	-304.3	9.457	0.607
19.00	-309.8	9.550	0.548
21.00	-314.4	9.627	0.502
23.00	-317.9	9.687	0.463
25.00	-321.1	9.741	0.430

Titration No. 2

$E^{\ominus\prime\prime}$ = 259.13 mV, s = 59.158 mV,
$[H^+]_0 = 1.667 \times 10^{-3}$ mol dm^{-3}, $[\text{etolen}]_0 = 0$,
$[H^+]_T = 0$, $[\text{etolen}]_T = 1.009 \times 10^{-2}$ mol dm^{-3},
V_0 = 60.00 cm^3.

*1.00	87.9	2.895	2.205
*2.00	80.0	3.028	2.077
*3.00	68.8	3.217	2.043
*4.00	49.9	3.537	2.018
6.50	-142.4	6.788	1.525
8.00	-174.3	7.327	1.240
9.00	-198.0	7.727	1.102
10.00	-230.9	8.284	0.994
11.00	-257.5	8.733	0.908
12.00	-272.2	8.982	0.837
13.00	-281.7	9.142	0.777
14.00	-288.5	9.257	0.726
15.00	-293.7	9.345	0.681
16.00	-298.0	9.418	0.642
17.00	-301.6	9.479	0.608
19.00	-307.6	9.580	0.550
21.00	-312.1	9.656	0.504
23.00	-315.8	9.719	0.465
25.00	-319.0	9.773	0.433

Titration No. 3

$E^{\ominus\prime\prime}$ = 255.0095 mV, s = 59.1577 mV,
$[H^+]_0 = 1.667 \times 10^{-3}$ mol dm^{-3}, $[\text{etolen}]_0 = 0$,
$[H^+]_T = 0$, $[\text{etolen}]_T = 1.009 \times 10^{-2}$ mol dm^{-3},
V_0 = 60.00 cm^3.

*1.00	84.5	2.882	1.984
*2.00	76.5	3.018	2.006
*3.00	64.6	3.219	2.047
*4.00	43.4	3.577	2.059
5.00	-80.0	5.663	1.980
6.00	-136.0	6.610	1.652
7.00	-159.9	7.014	1.417
8.00	-181.3	7.375	1.240
9.00	-206.8	7.806	1.103
10.00	-241.4	8.391	0.995
11.00	-264.1	8.775	0.908
12.00	-276.9	8.991	0.837
13.00	-285.1	9.130	0.776
14.00	-291.4	9.237	0.725
15.00	-296.1	9.316	0.680

16.00	-300.3	9.387	0.641
18.00	-306.7	9.495	0.575
20.00	-311.5	9.576	0.523
22.00	-315.6	9.646	0.480
25.00	-320.4	9.727	0.429

2. System: H^+ + oden

Titration No. 1 (a)

$E^{\ominus}$" = 254.85 mV, s = 58.72 mV,

$[H^+]_0 = 5.726 \times 10^{-3}$ mol dm^{-3}, $[\text{oden}]_0 = 2.300 \times 10^{-3}$ mol dm^{-3},

$[OH^-]_T = 2.440 \times 10^{-2}$ mol dm^{-3}, $[\text{oden}]_T = 0$,

$V_0 = 87.00$ cm^3.

*1.00	73.6	3.087	2.008
*2.00	62.6	3.274	2.009
*3.00	43.6	3.598	2.010
5.00	-230.0	8.257	1.882
6.00	-249.8	8.594	1.761
7.00	-262.2	8.805	1.642
8.00	-271.9	8.971	1.522
9.00	-279.9	9.107	1.403
10.00	-287.0	9.228	1.285
11.00	-293.6	9.340	1.168
12.00	-299.7	9.444	1.051
13.00	-305.6	9.544	0.936
15.00	-317.2	9.742	0.712
17.00	-328.7	9.938	0.499

Titration No. 1 (b)

$E^{\ominus}$" = 254.85 mV, s = 58.72 mV,

$[H^+]_0 = 6.571 \times 10^{-4}$ mol dm^{-3}, $[CO_3^{=}]_0 = 0$,

$[\text{oden}]_0 = 1.913 \times 10^{-3}$ mol dm^{-3},

$[OH^-]_T = 1.780 \times 10^{-2}$ mol dm^{-3}, $[CO_3^{=}]_T = 3.300 \times 10^{-3}$ mol dm^{-3},

$[\text{oden}]_T = 0$,

$V_0 = 104.60$ cm^3.

1.40	-341.0	10.147	0.347
3.40	-353.8	10.365	0.257
*5.40	-365.8	10.570	0.222
*8.40	-379.9	10.810	0.247

Titration No. 2 (a)

$E^{\ominus\prime\prime}$ = 250.84 mV, s = 58.22 mV,
$[H^+]_0 = 6.014 \times 10^{-3}$ mol dm^{-3}, $[oden]_0 = 2.382 \times 10^{-3}$ mol dm^{-3},
$[OH^-]_T = 1.700 \times 10^{-2}$ mol dm^{-3}, $[oden]_T = 0$,
V_0 = 84.00 cm^3.

*1.00	77.6	2.976	1.991
*2.00	71.8	3.075	1.993
*3.00	64.5	3.201	1.996
*4.00	54.5	3.372	1.998
*5.00	38.5	3.647	2.000
*6.00	10.2	4.133	1.982
7.00	-214.9	8.000	1.931
14.00	-283.9	9.185	1.349
20.00	-310.0	9.633	0.866

Titration No. 2 (b)

$E^{\ominus\prime\prime}$ = 250.84 mV, s = 58.22 mV,
$[H^+]_0 = 7.355 \times 10^{-4}$ mol dm^{-3}, $[CO_3^{=}]_0 = 0$,
$[oden]_0 = 1.836 \times 10^{-3}$ mol dm^{-3},
$[OH^-]_T = 1.530 \times 10^{-2}$ mol dm^{-3}, $[CO_3^{=}]_T = 8.500 \times 10^{-4}$ mol dm^{-3},
$[oden]_T = 0$,
V_0 = 109.00 cm^3.

1.00	-334.8	10.059	0.437
7.00	-359.7	10.487	0.184

Titration No. 3 (a)

$E^{\ominus\prime\prime}$ = 250.94 mV, s = 58.21 mV,
$[H^+]_0 = 6.042 \times 10^{-3}$ mol dm^{-3}, $[oden]_0 = 2.382 \times 10^{-3}$ mol dm^{-3},
$[OH^-]_T = 1.658 \times 10^{-2}$ mol dm^{-3}, $[oden]_T = 0$,
V_0 = 84.00 cm^3.

*3.00	66.5	3.169	1.993
*6.00	19.3	3.979	1.992
7.00	-192.9	7.625	1.957
8.00	-228.0	8.228	1.875
10.00	-253.6	8.668	1.712
12.00	-267.9	8.913	1.549
14.00	-278.6	9.097	1.388
17.00	-292.1	9.329	1.147

20.00	-305.2	9.554	0.913
25.00	-324.9	9.893	0.542

Titration No. 3 (b)

$E^{\ominus}{}''$ = 250.94 mV, s = 58.21 mV,

$[H^+]_0 = 6.168 \times 10^{-4}$ mol dm^{-3}, $[CO_3^{=}]_0 = 0$,

$[oden]_0 = 1.811 \times 10^{-3}$ mol dm^{-3},

$[OH^-]_T = 1.316 \times 10^{-2}$ mol dm^{-3}, $[CO_3^{=}]_T = 1.712 \times 10^{-3}$ mol dm^{-3},

$[oden]_T = 0$,

$V_0 = 110.50$ cm^3.

3.50	-345.6	10.248	0.286
8.50	-364.9	10.580	0.183
*13.50	-378.1	10.806	0.165
*18.50	-387.7	10.971	0.213

Titration No. 4 (a)

$E^{\ominus}{}''$ = 249.52 mV, s = 57.88 mV,

$[H^+]_0 = 5.697 \times 10^{-3}$ mol dm^{-3}, $[oden]_0 = 2.300 \times 10^{-3}$ mol dm^{-3},

$[OH^-]_T = 2.497 \times 10^{-2}$ mol dm^{-3}, $[oden]_T = 0$,

$V_0 = 87.00$ cm^3.

4.00	-124.3	6.459	1.978
5.00	-230.0	8.285	1.855
6.00	-249.3	8.618	1.732
7.00	-261.4	8.827	1.609
9.00	-278.9	9.130	1.366
10.00	-285.4	9.242	1.244
11.00	-291.6	9.349	1.124
13.00	-303.9	9.562	0.888
14.00	-309.7	9.662	0.772
15.00	-315.1	9.755	0.658
17.00	-326.3	9.949	0.439

Titration No. 4 (b)

$E^{\ominus}{}''$ = 249.52 mV, s = 57.88 mV,

$[H^+]_0 = 5.488 \times 10^{-4}$ mol dm^{-3}, $[CO_3^{=}]_0 = 0$,

$[oden]_0 = 1.914 \times 10^{-3}$ mol dm^{-3},

$[OH^-]_T = 1.932 \times 10^{-2}$ mol dm^{-3}, $[CO_3^{=}]_T = 2.823 \times 10^{-3}$ mol dm^{-3},

$[oden]_T = 0$,

$V_0 = 104.55$ cm^3.

1.45	-338.5	10.159	0.280
3.45	-351.4	10.382	0.180

3. System: $H^+ + Ni^{2+}$ + etolen

Titration No. 1

$E^{\ominus\prime\prime}$ = 259.59 mV, s = 59.158 mV,

$[H^+]_0 = 1.251 \times 10^{-3}$ mol dm^{-3}, $[Ni^{2+}]_0 = 2.501 \times 10^{-3}$ mol dm^{-3},

$[\text{etolen}]_0 = 5.569 \times 10^{-3}$ mol dm^{-3},

Titrant A : $[H^+]_T = 4.001 \times 10^{-2}$ mol dm^{-3},

Titrant B : $[Ni^{2+}]_T = 5.001 \times 10^{-3}$ mol dm^{-3},

V_0 = 80.00 cm^3.

1.00	1.00	-168.8	7.24	-5.524	1.642
2.00	2.00	-156.8	7.04	-5.731	1.505
3.00	3.00	-147.8	6.89	-5.898	1.379
4.00	4.00	-140.6	6.76	-6.040	1.261
5.00	5.00	-134.1	6.65	-6.178	1.151
6.00	6.00	-128.1	6.55	-6.314	1.048
7.00	7.00	-122.8	6.46	-6.437	0.949
8.00	8.00	-117.7	6.38	-6.562	0.855
9.00	9.00	-113.2	6.30	-6.673	0.763
10.00	10.00	-108.7	6.23	-6.789	0.676
11.00	11.00	-104.5	6.15	-6.900	0.591
12.00	12.00	-100.2	6.08	-7.016	0.510
13.00	13.00	-95.9	6.01	-7.136	0.432
14.00	14.00	-91.7	5.94	-7.254	0.357
15.00	15.00	-87.1	5.86	-7.388	0.285
16.00	16.00	-81.9	5.77	-7.544	0.217
17.00	17.00	-76.1	5.67	-7.721	0.151
18.00	18.00	-67.9	5.54	-7.980	0.089
19.00	19.00	-54.6	5.31	-8.413	0.032
20.00	20.00	4.0	4.32	-10.378	-0.008
21.00	21.00	55.4	3.45	-12.121	-0.010
22.00	22.00	72.0	3.17	-12.690	-0.009
23.00	23.00	81.7	3.01	-13.025	-0.008
24.00	24.00	88.3	2.90	-13.254	-0.010
25.00	25.00	93.5	2.81	-13.436	-0.011

Titration No. 2

(a) Forward titration (decreasing $p[H^+]$)

$E^{\ominus\prime\prime}$ = 256.94 mV, s = 59.158 mV,

$[H^+]_0 = 7.496 \times 10^{-3}$ mol dm^{-3}, $[Ni^{2+}]_0 = 2.501 \times 10^{-3}$ mol dm^{-3},

$[\text{etolen}]_0 = 1.119 \times 10^{-2}$ mol dm^{-3},

$[H^+]_T$ = 6.250 x 10^{-2} mol dm^{-3}, $[Ni^{2+}]_T$ = 2.501 x 10^{-3} mol dm^{-3},

$[etolen]_T$ = 0,

V_0 = 80.00 cm^3.

1.00	-167.0	7.17	-4.955	1.950
2.00	-156.5	6.99	-5.194	1.876
3.00	-148.3	6.85	-5.390	1.784
4.00	-141.0	6.73	-5.571	1.686
5.00	-135.0	6.63	-5.723	1.573
6.00	-129.0	6.52	-5.881	1.464
7.00	-123.5	6.43	-6.028	1.350
8.00	-118.2	6.34	-6.174	1.235
9.00	-113.1	6.26	-6.317	1.117
10.00	-108.0	6.17	-6.462	1.001
11.00	-102.9	6.08	-6.610	0.884
12.00	-97.9	6.00	-6.758	0.766
13.00	-93.0	5.92	-6.903	0.647
14.00	-87.8	5.83	-7.061	0.530
15.00	-82.2	5.73	-7.233	0.415
16.00	-76.0	5.63	-7.426	0.301
17.00	-68.1	5.49	-7.678	0.192
18.00	-55.8	5.29	-8.078	0.088
19.00	-12.0	4.55	-9.544	0.004
20.00	64.2	3.26	-12.121	-0.008

(b) Reverse Titration (increasing $p[H^+]$)

$E^{\ominus}$" = 256.94 mV, s = 59.158 mV,

$[H^+]_0$ = 1.850 x 10^{-2} mol dm^{-3}, $[Ni^{2+}]_0$ = 2.501 x 10^{-3} mol dm^{-3},

$[etolen]_0$ = 8.954 x 10^{-3} mol dm^{-3},

Titrant A: $[OH^-]_T$ = 7.995 x 10^{-2} mol dm^{-3},

Titrant B: $[Ni^{2+}]_T$ = 5.001 x 10^{-3} mol dm^{-3},

V_0 = 100.00 cm^3.

1.00	1.00	-34.7	4.93	-8.795	0.023
2.00	2.00	-63.9	5.42	-7.841	0.135
3.00	3.00	-75.2	5.61	-7.493	0.256
4.00	4.00	-83.0	5.75	-7.264	0.376
5.00	5.00	-89.6	5.86	-7.077	0.492
6.00	6.00	-95.3	5.95	-6.922	0.605
7.00	7.00	-100.7	6.05	-6.779	0.714
8.00	8.00	-105.9	6.13	-6.645	0.818
9.00	9.00	-111.0	6.22	-6.518	0.918
10.00	10.00	-116.1	6.31	-6.395	1.015
11.00	11.00	-121.3	6.39	-6.273	1.108
12.00	12.00	-126.4	6.48	-6.159	1.199
13.00	13.00	-131.6	6.57	-6.048	1.289
14.00	14.00	-137.3	6.66	-5.929	1.375
15.00	15.00	-143.2	6.76	-5.813	1.462

16.00	16.00	-149.9	6.88	-5.686	1.547
17.00	17.00	-157.6	7.01	-5.548	1.633
18.00	18.00	-167.0	7.17	-5.387	1.720
19.00	19.00	-179.7	7.38	-5.180	1.811
20.00	20.00	-201.1	7.74	-4.843	1.908
21.00	21.00	-251.8	8.60	-4.073	2.012
22.00	22.00	-296.6	9.36	-3.558	2.108
23.00	23.00	-323.1	9.81	-3.655	2.288
24.00	24.00	-341.9	10.12	-	-

Titration No. 3

(a) Forward Titration (decreasing $p[H^+]$)

$E^{\ominus}{}''$ = 257.34 mV, s = 59.158 mV,

$[H^+]_0 = 1.251 \times 10^{-3}$ mol dm^{-3}, $[Ni^{2+}]_0 = 5.011 \times 10^{-4}$ mol dm^{-3},

$[etolen]_0 = 5.569 \times 10^{-3}$ mol dm^{-3},

$[H^+]_T = 3.995 \times 10^{-2}$ mol dm^{-3}, $[Ni^{2+}]_T = 5.001 \times 10^{-4}$ mol dm^{-3},

$[etolen]_T = 0$,

$V_0 = 80.00$ cm^3.

7.00	-208.1	7.87	-4.308	2.111
8.00	-185.1	7.48	-4.750	2.072
9.00	-171.0	7.24	-5.045	1.978
10.00	-159.6	7.05	-5.303	1.889
11.00	-150.3	6.89	-5.527	1.752
12.00	-141.8	6.75	-5.742	1.599
13.00	-134.0	6.62	-5.948	1.414
14.00	-126.0	6.48	-6.169	1.229
15.00	-117.8	6.34	-6.404	1.028
16.00	-109.3	6.20	-6.655	0.809
17.00	-100.0	6.04	-6.938	0.575
18.00	-89.2	5.86	-7.275	0.330
19.00	-73.2	5.59	-7.789	0.095
20.00	-15.5	4.61	-9.715	-0.081
21.00	54.2	3.43	-12.072	-0.108
22.00	72.8	3.12	-12.706	-0.103
23.00	83.3	2.94	-13.065	-0.099
24.00	90.5	2.82	-13.312	-0.101
25.00	95.9	2.73	-13.499	-0.112

(b) Reverse Titration (increasing $p[H^+]$)

$E^{\ominus}$" = 257.34 mV, s = 59.158 mV,

$[H^+]_0 = 1.046 \times 10^{-2}$ mol dm^{-3}, $[Ni^{2+}]_0 = 5.009 \times 10^{-4}$ mol dm^{-3},

$[etolen]_0 = 4.243 \times 10^{-3}$ mol dm^{-3},

Titrant A: $[OH^-]_T = 7.995 \times 10^{-2}$ mol dm^{-3},

Titrant B: $[Ni^{2+}]_T = 1.000 \times 10^{-3}$ mol dm^{-3},

V_0 = 105.00 cm^3.

*1.00	1.00	81.8	2.97	-13.029	-0.081
*2.00	2.00	51.0	3.49	-11.996	-0.079
3.00	3.00	-74.7	5.61	-7.789	0.074
4.00	4.00	-100.5	6.05	-6.988	0.487
5.00	5.00	-117.1	6.33	-6.509	0.871
6.00	6.00	-132.1	6.58	-6.105	1.195
7.00	7.00	-146.7	6.83	-5.744	1.487
8.00	8.00	-164.3	7.13	-5.346	1.711
9.00	9.00	-191.8	7.59	-4.793	1.861
10.00	10.00	-255.5	8.67	-3.703	1.994
11.00	11.00	-292.7	9.30	-3.199	2.234
12.00	12.00	-315.1	9.68	-2.998	2.562
13.00	13.00	-334.4	10.00	-2.934	3.195
14.00	14.00	-352.6	10.31	-3.092	4.639
16.00	16.00	-379.7	10.77	-	-
18.00	18.00	-394.4	11.02	-	-
20.00	20.00	-403.7	11.17	-	-

Titration No. 4

$E^{\ominus}$" = 244.10 mV, s = 58.330 mV,

$[H^+]_0 = 2.248 \times 10^{-2}$ mol dm^{-3}, $[Ni^{2+}]_0 = 3.334 \times 10^{-3}$ mol dm^{-3},

$[etolen]_0 = 1.022 \times 10^{-2}$ mol dm^{-3},

$[H^+]_T = 0$, $[Ni^{2+}]_T = 0$,

$[etolen]_T = 5.110 \times 10^{-2}$ mol dm^{-3},

V_0 = 120.00 cm^3.

3.00	-56.8	5.16	-8.238	0.045
4.00	-72.5	5.43	-7.706	0.143
5.00	-81.0	5.57	-7.422	0.247
6.00	-87.1	5.68	-7.219	0.351
7.00	-92.3	5.77	-7.047	0.455
8.00	-96.8	5.84	-6.900	0.558
9.00	-100.8	5.91	-6.769	0.660
10.00	-104.7	5.98	-6.643	0.759
11.00	-108.5	6.04	-6.520	0.855
12.00	-112.2	6.11	-6.402	0.947
13.00	-115.8	6.17	-6.287	1.036

14.00	-119.3	6.23	-6.176	1.121
15.00	-122.6	6.29	-6.073	1.205
16.00	-125.8	6.34	-5.973	1.285
17.00	-129.0	6.40	-5.875	1.361
18.00	-132.3	6.45	-5.774	1.430
19.00	-135.3	6.50	-5.683	1.500
21.00	-141.6	6.61	-5.495	1.619
23.00	-147.8	6.72	-5.315	1.721
25.00	-154.1	6.83	-5.137	1.801
27.00	-160.6	6.94	-4.959	1.859
29.00	-167.2	7.05	-4.785	1.900
31.00	-174.0	7.17	-4.613	1.927

Titration No. 5

$E^{\ominus}{}''$ = 234.82 mV, s = 57.731 mV,

$[H^+]_0 = 2.345 \times 10^{-2}$ mol dm^{-3}, $[Ni^{2+}]_0 = 1.739 \times 10^{-3}$ mol dm^{-3},

$[etolen]_0 = 1.066 \times 10^{-2}$ mol dm^{-3},

$[H^+]_T = 0$, $[Ni^{2+}]_T = 0$,

$[etolen]_T = 5.110 \times 10^{-2}$ mol dm^{-3},

V_0 = 115.00 cm^3.

3.00	-71.7	5.31	-7.919	0.061
4.00	-86.1	5.56	-7.429	0.243
5.00	-95.2	5.72	-7.122	0.427
6.00	-102.4	5.84	-6.881	0.607
7.00	-108.8	5.95	-6.669	0.776
8.00	-114.7	6.05	-6.475	0.933
9.00	-120.1	6.15	-6.299	1.079
10.00	-125.0	6.23	-6.141	1.217
11.00	-129.6	6.31	-5.994	1.344
12.00	-134.0	6.39	-5.856	1.460
13.00	-138.3	6.46	-5.722	1.561
14.00	-142.3	6.53	-5.600	1.656
15.00	-146.3	6.60	-5.479	1.734
16.00	-150.2	6.67	-5.363	1.801
17.00	-154.1	6.74	-5.249	1.852
18.00	-157.9	6.80	-5.140	1.895
19.00	-161.5	6.86	-5.038	1.937
20.00	-165.1	6.93	-4.939	1.968
21.00	-168.7	6.99	-4.842	1.991
22.00	-172.3	7.05	-4.747	2.008
23.00	-175.9	7.11	-4.654	2.020
24.00	-179.5	7.18	-4.564	2.029
26.00	-187.2	7.31	-4.377	2.019
28.00	-195.2	7.45	-4.193	2.012
30.00	-204.3	7.61	-3.995	1.986

Titration No. 6

$E^{\ominus\prime\prime}$ = 240.92 mV, s = 58.347 mV,

$[H^+]_0 = 2.248 \times 10^{-2}$ mol dm^{-3}, $[Ni^{2+}]_0 = 2.499 \times 10^{-3}$ mol dm^{-3},

$[etolen]_0 = 1.022 \times 10^{-2}$ mol dm^{-3},

$[H^+]_T = 0$, $[Ni^{2+}]_T = 0$,

$[etolen]_T = 5.110 \times 10^{-2}$ mol dm^{-3},

$V_0 = 120.00$ cm^3.

3.00	-62.9	5.21	-8.141	0.054
4.00	-79.0	5.48	-7.597	0.180
5.00	-88.0	5.64	-7.296	0.311
6.00	-94.6	5.75	-7.077	0.443
7.00	-100.2	5.85	-6.892	0.573
8.00	-105.2	5.93	-6.729	0.699
9.00	-110.0	6.01	-6.573	0.820
10.00	-114.4	6.09	-6.431	0.937
11.00	-118.8	6.17	-6.290	1.045
12.00	-123.0	6.24	-6.156	1.148
13.00	-127.0	6.31	-6.030	1.245
14.00	-130.7	6.37	-5.915	1.339
15.00	-134.4	6.43	-5.801	1.425
16.00	-138.0	6.49	-5.692	1.505
17.00	-141.6	6.56	-5.583	1.576
18.00	-145.1	6.62	-5.479	1.642
19.00	-148.5	6.67	-5.380	1.703
20.00	-152.0	6.73	-5.279	1.752
21.00	-155.3	6.79	-5.185	1.801
22.00	-158.8	6.85	-5.087	1.836
23.00	-162.2	6.91	-4.994	1.868
24.00	-165.5	6.97	-4.905	1.900
26.00	-172.5	7.09	-4.723	1.934
28.00	-179.5	7.21	-4.548	1.959
30.00	-186.9	7.33	-4.373	1.971

Titration No. 7

$E^{\ominus\prime\prime}$ = 239.57 mV, s = 57.893 mV,

$[H^+]_0 = 2.248 \times 10^{-2}$ mol dm^{-3}, $[Ni^{2+}]_0 = 3.334 \times 10^{-3}$ mol dm^{-3},

$[etolen]_0 = 1.022 \times 10^{-2}$ mol dm^{-3},

$[H^+]_T = 0$, $[Ni^{2+}]_T = 0$,

$[etolen]_T = 5.110 \times 10^{-2}$ mol dm^{-3},

$V_0 = 120.00$ cm^3.

3.00	-60.4	5.18	-8.192	0.043
4.00	-74.0	5.42	-7.729	0.145
5.00	-82.1	5.56	-7.455	0.250

6.00	-87.9	5.66	-7.261	0.356
7.00	-92.8	5.74	-7.098	0.462
8.00	-97.2	5.82	-6.953	0.567
9.00	-101.3	5.89	-6.818	0.670
10.00	-105.1	5.95	-6.694	0.771
11.00	-108.9	6.02	-6.570	0.868
12.00	-112.5	6.08	-6.453	0.962
13.00	-116.0	6.14	-6.341	1.054
14.00	-119.5	6.20	-6.229	1.141
15.00	-122.9	6.26	-6.121	1.225
16.00	-126.1	6.32	-6.020	1.307
17.00	-129.3	6.37	-5.920	1.385
18.00	-132.4	6.43	-5.824	1.460
19.00	-135.4	6.48	-5.733	1.531
21.00	-141.6	6.58	-5.545	1.657
23.00	-147.9	6.69	-5.359	1.760
25.00	-154.3	6.80	-5.176	1.840
27.00	-160.8	6.92	-4.995	1.899
29.00	-167.4	7.03	-4.818	1.941
31.00	-174.4	7.15	-4.639	1.960
33.00	-181.4	7.27	-4.467	1.978
35.00	-188.9	7.40	-4.292	1.987

4. System: $H^+ + Ni^{2+}$ + oden

Titration No. 1

(a) Forward Titration (increasing $p[H^+]$)

$E^{\ominus}{}''$ = 248.35 mV, s = 57.864 mV,

$[H^+]_0 = 5.708 \times 10^{-3}$ mol dm^{-3}, $[Ni^{2+}]_0 = 9.793 \times 10^{-4}$ mol dm^{-3},

$[oden]_0 = 2.175 \times 10^{-3}$ mol dm^{-3},

Titrant A: $[OH^-]_T = 4.297 \times 10^{-2}$ mol dm^{-3},

Titrant B: $[Ni^{2+}]_T = 1.985 \times 10^{-3}$ mol dm^{-3},

V_0 = 92.00 cm^3.

4.00	4.00	-196.2	7.68	-6.334	0.210
5.00	5.00	-210.2	7.92	-5.920	0.405
6.00	6.00	-221.3	8.12	-5.616	0.592
7.00	7.00	-232.5	8.31	-5.324	0.769
8.00	8.00	-245.6	8.54	-4.989	0.929
9.00	9.00	-261.1	8.80	-4.613	1.067
10.00	10.00	-277.0	9.08	-4.289	1.194
11.00	11.00	-292.6	9.35	-4.088	1.340
12.00	12.00	-309.7	9.64	-4.138	1.550
13.00	13.00	-323.1	9.88	-	-
14.00	14.00	-332.3	10.04	-	-

(b) Reverse Titration (decreasing $p[H^+]$)

$E^{\ominus\prime\prime}$ = 248.35 mV, s = 57.864 mV,

$[OH^-]_0 = 6.368 \times 10^{-4}$ mol dm^{-3}, $[Ni^{2+}]_0 = 9.824 \times 10^{-4}$ mol dm^{-3},

$[oden]_0 = 1.667 \times 10^{-3}$ mol dm^{-3},

$[H^+]_T = 4.000 \times 10^{-2}$ mol dm^{-3}, $[Ni^{2+}]_T = 1.000 \times 10^{-3}$ mol dm^{-3},

$[oden]_T = 0$,

V_0 = 120.00 cm^3.

2.00	-299.7	9.47	-4.679	1.584
4.00	-271.3	8.98	-4.562	1.176
6.00	-243.4	8.50	-5.173	0.881
8.00	-223.0	8.15	-5.689	0.575
10.00	-199.7	7.74	-6.366	0.275

Titration No. 2

$E^{\ominus\prime\prime}$ = 245.16 mV, s = 57.906 mV,

$[H^+]_0 = 1.005 \times 10^{-2}$ mol dm^{-3}, $[Ni^{2+}]_0 = 1.001 \times 10^{-3}$ mol dm^{-3},

$[oden]_0 = 4.485 \times 10^{-3}$ mol dm^{-3},

$[OH^-]_T = 4.049 \times 10^{-2}$ mol dm^{-3},

$[Ni^{2+}]_T = 0$, $[oden]_T = 0$,

V_0 = 90.00 cm^3.

3.00	-156.9	6.94	-7.430	0.121
4.00	-190.5	7.52	-6.301	0.312
5.00	-203.1	7.74	-5.898	0.510
6.00	-213.2	7.92	-5.583	0.705
7.00	-223.4	8.09	-5.269	0.887
8.00	-234.6	8.29	-4.925	1.045
9.00	-246.1	8.48	-4.579	1.169
11.00	-264.5	8.80	-4.063	1.377
13.00	-278.4	9.04	-3.728	1.583
15.00	-290.5	9.25	-3.488	1.804
17.00	-302.4	9.46	-3.306	2.055
19.00	-314.7	9.67	-3.192	2.409
21.00	-328.1	9.90	-3.205	3.035
23.00	-342.9	10.16	-4.289	4.385

Titration No. 3

$E^{\ominus}{}''$ = 250.66 mV, s = 57.934 mV,

$[H^+]_0 = 1.112 \times 10^{-2}$ mol dm^{-3},

$[Ni^{2+}]_0 = 5.007 \times 10^{-4}$ mol dm^{-3}, $[oden]_0 = 4.485 \times 10^{-3}$ mol dm^{-3},

$[OH^-]_T = 4.129 \times 10^{-2}$ mol dm^{-3}, $[Ni^{2+}]_T = 0$, $[oden]_T = 0$,

V_0 = 90.00 cm^3.

6.00	-191.7	7.64	-6.082	0.481
7.00	-209.3	7.94	-5.509	0.828
8.00	-225.2	8.21	-5.001	1.105
9.00	-239.8	8.47	-4.547	1.282
10.00	-251.1	8.66	-4.212	1.415
11.00	-259.9	8.81	-3.967	1.545
12.00	-267.2	8.94	-3.779	1.682
14.00	-280.1	9.16	-3.480	1.921
16.00	-291.5	9.36	-3.261	2.182
18.00	-302.3	9.54	-3.102	2.540
20.00	-313.2	9.73	-2.999	3.120
22.00	-324.6	9.93	-2.979	4.231
24.00	-337.1	10.15	-3.177	6.488
26.00	-351.2	10.39	-	-

Titration No. 4

$E^{\ominus}{}''$ = 254.85 mV, s = 59.117 mV,

$[H^+]_0 = 2.249 \times 10^{-2}$ mol dm^{-3},

$[Ni^{2+}]_0 = 5.000 \times 10^{-3}$ mol dm^{-3}, $[oden]_0 = 1.000 \times 10^{-2}$ mol dm^{-3},

$[H^+]_T = 0$, $[Ni^{2+}]_T = 0$, $[oden]_T = 5.001 \times 10^{-2}$ mol dm^{-3},

V_0 = 120.00 cm^3.

3.00	-150.8	6.86	-7.177	-0.004
4.00	-164.4	7.09	-6.721	0.076
5.00	-172.1	7.22	-6.465	0.156
6.00	-177.8	7.32	-6.276	0.236
7.00	-182.6	7.40	-6.118	0.316
8.00	-187.0	7.47	-5.973	0.396
9.00	-191.1	7.54	-5.838	0.475
10.00	-195.2	7.61	-5.704	0.554
11.00	-199.4	7.68	-5.566	0.632
12.00	-204.1	7.76	-5.412	0.708
13.00	-209.1	7.85	-5.248	0.782
14.00	-214.7	7.94	-5.064	0.852
15.00	-220.6	8.04	-4.871	0.918
16.00	-226.6	8.14	-4.675	0.979
17.00	-232.1	8.24	-4.497	1.037

18.00	-237.0	8.32	-4.339	1.093
19.00	-241.3	8.39	-4.202	1.147
20.00	-245.0	8.46	-4.085	1.201
21.00	-248.3	8.51	-3.982	1.255
22.00	-251.5	8.57	-3.882	1.305
24.00	-257.1	8.66	-3.710	1.403
26.00	-262.3	8.75	-3.553	1.492
28.00	-267.0	8.83	-3.414	1.572
30.00	-271.2	8.90	-3.292	1.648

Titration No. 5

$E^{\ominus\prime\prime}$ = 254.43 mV, s = 59.028 mV,

$[H^+]_0$ =2.249 x 10^{-2} mol dm^{-3}, $[Ni^{2+}]_0$ = 1.667 x 10^{-3} mol dm^{-3},

$[oden]_0$ = 1.000 x 10^{-2} mol dm^{-3},

$[H^+]_T$ = 0, $[Ni^{2+}]_T$ = 0, $[oden]_T$ = 5.001 x 10^{-2} mol dm^{-3},

V_0 = 120.00 cm^3.

3.00	-162.2	7.06	-6.785	-0.021
4.00	-180.3	7.36	-6.177	0.202
5.00	-191.9	7.56	-5.790	0.422
6.00	-202.8	7.75	-5.426	0.628
7.00	-215.0	7.95	-5.021	0.800
8.00	-226.6	8.15	-4.639	0.933
9.00	-235.7	8.30	-4.342	1.045
10.00	-242.8	8.42	-4.114	1.148
11.00	-248.5	8.52	-3.933	1.247
12.00	-253.4	8.60	-3.779	1.337
13.00	-257.5	8.67	-3.652	1.428
14.00	-261.3	8.74	-3.536	1.506
15.00	-264.8	8.80	-3.431	1.573
16.00	-267.9	8.85	-3.338	1.638
17.00	-270.8	8.90	-3.253	1.694
19.00	-276.0	8.99	-3.103	1.786
21.00	-280.6	9.06	-2.974	1.849
23.00	-284.5	9.13	-2.868	1.912
25.00	-288.1	9.19	-2.772	1.944
27.00	-291.3	9.25	-2.689	1.969
30.00	-295.5	9.32	-2.583	1.997

Titration No. 6

$E^{\ominus\prime\prime}$ = 254.92 mV, s = 59.091 mV,

$[H^+]_0$ = 1.499 x 10^{-2} mol dm^{-3}, $[Ni^{2+}]_0$ = 1.667 x 10^{-3} mol dm^{-3},

$[oden]_0$ = 6.668 x 10^{-3} mol dm^{-3},

$[H^+]_T$ = 0, $[Ni^{2+}]_T$ = 0, $[oden]_T$ = 5.001 x 10^{-2} mol dm^{-3},

V_0 = 120.00 cm^3.

2.00	-165.8	7.12	-6.835	-0.017
3.00	-184.8	7.44	-6.197	0.211
4.00	-196.8	7.64	-5.797	0.436
5.00	-208.5	7.84	-5.408	0.647
6.00	-221.4	8.06	-4.981	0.828
7.00	-233.9	8.27	-4.572	0.967
8.00	-243.5	8.43	-4.262	1.088
9.00	-250.8	8.56	-4.030	1.201
10.00	-256.7	8.66	-3.846	1.308
11.00	-261.9	8.75	-3.686	1.401
12.00	-266.3	8.82	-3.553	1.492
13.00	-270.2	8.89	-3.437	1.575
14.00	-273.9	8.95	-3.328	1.642
15.00	-277.2	9.01	-3.233	1.705
16.00	-280.3	9.06	-3.146	1.756
18.00	-285.8	9.15	-2.994	1.836
20.00	-290.5	9.23	-2.868	1.899
23.00	-296.5	9.33	-2.714	1.960

Titration No. 7

$E^{\ominus}{}''$ = 255.58 mV, s = 59.220 mV,

$[H^+]_0 = 2.184 \times 10^{-2}$ mol dm^{-3}, $[Ni^{2+}]_0 = 5.042 \times 10^{-3}$ mol dm^{-3},

$[oden]_0 = 1.009 \times 10^{-2}$ mol dm^{-3},

$[H^+]_T = 0$, $[Ni^{2+}]_T = 0$, $[oden]_T = 5.001 \times 10^{-2}$ mol dm^{-3},

V_0 = 119.00 cm^3.

3.00	-163.8	7.08	-6.751	0.076
4.00	-171.6	7.21	-6.492	0.156
5.00	-177.7	7.32	-6.290	0.237
6.00	-182.4	7.40	-6.135	0.317
7.00	-187.0	7.47	-5.984	0.397
8.00	-191.2	7.54	-5.846	0.476
9.00	-195.2	7.61	-5.715	0.555
10.00	-199.5	7.68	-5.575	0.633
11.00	-204.2	7.76	-5.421	0.709
12.00	-209.1	7.85	-5.260	0.784
13.00	-214.6	7.94	-5.080	0.855
14.00	-220.6	8.04	-4.884	0.921
15.00	-226.5	8.14	-4.692	0.984
16.00	-232.1	8.24	-4.511	1.042
17.00	-237.2	8.32	-4.347	1.098
18.00	-241.5	8.39	-4.210	1.153
19.00	-245.2	8.46	-4.094	1.209
20.00	-248.6	8.51	-3.987	1.262
21.00	-251.6	8.56	-3.894	1.316
23.00	-257.6	8.67	-3.710	1.412

5. System: $H^+ + Co^{2+}$ + etolen

Titration No. 1

$E^{\ominus}$" = 245.00 mV; s = 58.541 mV,

$[H^+]_0 = 3.716 \times 10^{-3}$ mol dm^{-3},

$[Co^{2+}]_0 = 5.005 \times 10^{-4}$ mol dm^{-3}, $[etolen]_0 = 1.488 \times 10^{-3}$ mol dm^{-3},

$[OH^-]_T = 2.284 \times 10^{-2}$ mol dm^{-3},

$[Co^{2+}]_T = 0$, $[etolen]_T = 0$,

$V_0 = 100.00$ cm^3.

1.00	51.6	3.30	-12.813	-0.011
3.00	- 6.0	4.29	-10.855	-0.007
4.00	-101.7	5.92	-7.641	0.018
5.00	-127.6	6.36	-6.838	0.039
6.00	-143.5	6.64	-6.389	0.080
7.00	-156.4	6.86	-6.059	0.143
8.00	-168.4	7.06	-5.783	0.235
9.00	-180.9	7.28	-5.525	0.359
10.00	-194.8	7.51	-5.269	0.532
11.00	-210.3	7.78	-5.019	0.774
12.00	-224.8	8.03	-4.828	1.101
13.00	-238.4	8.26	-4.693	1.482
14.00	-251.0	8.47	-4.624	1.894
17.00	-308.3	9.45	-	-

Titration No. 2

$E^{\ominus}$" = 249.29 mV, s = 58.499 mV,

$[H^+]_0 = 6.208 \times 10^{-3}$ mol dm^{-3},

$[Co^{2+}]_0 = 5.005 \times 10^{-4}$ mol dm^{-3}, $[etolen]_0 = 2.976 \times 10^{-3}$ mol dm^{-3},

$[OH^-]_T = 2.294 \times 10^{-2}$ mol dm^{-3},

$[Co^{2+}]_T = 0$, $[etolen]_T = 0$,

$V_0 = 100.00$ cm^3.

1.00	-12.1	4.47	-10.186	-0.005
2.00	-81.7	5.66	-7.838	0.025
3.00	-104.0	6.04	-7.116	0.036
4.00	-117.2	6.26	-6.708	0.052
5.00	-127.0	6.43	-6.419	0.078
6.00	-135.0	6.57	-6.195	0.116
7.00	-142.1	6.69	-6.006	0.163
8.00	-148.7	6.80	-5.838	0.220
10.00	-161.6	7.02	-5.534	0.358
12.00	-174.9	7.25	-5.253	0.557
14.00	-190.4	7.52	-4.960	0.835

16.00	-208.0	7.82	-4.668	1.273
19.00	-244.3	8.44	-4.132	2.155
24.00	-304.3	9.46	-3.487	3.609

Titration No. 3

$E^{\ominus}$" = 252.92 mV, s = 58.610 mV,

$[H^+]_0 = 1.009 \times 10^{-1}$ mol dm^{-3}, $[Co^{2+}]_0 = 1.389 \times 10^{-2}$ mol dm^{-3},

$[etolen]_0 = 4.947 \times 10^{-2}$ mol dm^{-3},

$[H^+]_T = 0$, $[Co^{2+}]_T = 0$,

$[etolen]_T = 1.977 \times 10^{-1}$ mol dm^{-3},

$V_0 = 120.00$ cm^3.

1.00	-42.1	5.03	-7.827	0.020
2.00	-77.3	5.63	-6.639	0.059
3.00	-90.0	5.85	-6.217	0.111
4.00	-98.2	5.99	-5.949	0.168
5.00	-104.0	6.09	-5.761	0.231
6.00	-108.6	6.17	-5.615	0.298
7.00	-112.8	6.24	-5.482	0.362
8.00	-116.2	6.30	-5.376	0.431
9.00	-119.3	6.35	-5.281	0.499
10.00	-122.5	6.41	-5.183	0.561
12.00	-128.0	6.50	-5.017	0.689
14.00	-133.1	6.59	-4.867	0.810
16.00	-137.9	6.67	-4.729	0.926
18.00	-142.7	6.75	-4.593	1.029
20.00	-147.0	6.82	-4.474	1.136
22.00	-151.3	6.90	-4.359	1.235
24.00	-155.7	6.97	-4.243	1.323
26.00	-159.8	7.04	-4.138	1.417

Titration No. 4

$E^{\ominus}$" = 248.26 mV, s = 58.295 mV,

$[H^+]_0 = 1.134 \times 10^{-1}$ mol dm^{-3}, $[Co^{2+}]_0 = 1.389 \times 10^{-2}$ mol dm^{-3},

$[etolen]_0 = 5.376 \times 10^{-2}$ mol dm^{-3},

$[H^+]_T = 0$, $[Co^{2+}]_T = 0$,

$[etolen]_T = 2.932 \times 10^{-1}$ mol dm^{-3},

$V_0 = 120.00$ cm^3.

1.00	50.5	3.39	-11.057	-0.022
2.00	-77.4	5.59	-6.682	0.032
3.00	-94.8	5.88	-6.100	0.106
4.00	-104.3	6.05	-5.788	0.193
5.00	-110.9	6.16	-5.574	0.289
7.00	-121.0	6.33	-5.254	0.479
8.00	-125.2	6.41	-5.124	0.572
9.00	-128.9	6.47	-5.010	0.667
10.00	-132.5	6.53	-4.902	0.756
11.00	-135.9	6.59	-4.800	0.842
12.00	-139.2	6.65	-4.703	0.925
13.00	-142.4	6.70	-4.610	1.003
14.00	-145.6	6.76	-4.519	1.076
15.00	-148.6	6.81	-4.435	1.150
16.00	-151.4	6.86	-4.357	1.227
18.00	-157.3	6.96	-4.198	1.357
20.00	-163.3	7.06	-4.041	1.471
22.00	-169.3	7.16	-3.891	1.579
25.00	-178.9	7.33	-3.662	1.717

Titration No. 5

$E^{\ominus\prime\prime}$ = 248.60 mV, s = 58.547 mV,

$[H^+]_0 = 1.134 \times 10^{-1}$ mol dm^{-3}, $[Co^{2+}]_0 = 7.499 \times 10^{-3}$ mol dm^{-3},

$[etolen]_0 = 5.376 \times 10^{-2}$ mol dm^{-3},

$[H^+]_T = 0$, $[Co^{2+}]_T = 0$, $[etolen]_T = 2.932 \times 10^{-1}$ mol dm^{-3},

V_0 = 120.00 cm^3.

1.00	62.6	3.18	-11.489	-0.023
2.00	-80.0	5.61	-6.631	0.047
3.00	-99.9	5.95	-5.969	0.135
4.00	-110.3	6.13	-5.630	0.253
5.00	-117.9	6.26	-5.387	0.375
7.00	-129.5	6.46	-5.025	0.612
8.00	-134.4	6.54	-4.876	0.720
9.00	-138.7	6.62	-4.748	0.832
10.00	-142.8	6.69	-4.628	0.935
11.00	-146.6	6.75	-4.519	1.037
12.00	-150.3	6.81	-4.415	1.131
13.00	-153.8	6.87	-4.319	1.226
14.00	-157.3	6.93	-4.224	1.310
15.00	-160.7	6.99	-4.134	1.392
16.00	-164.0	7.05	-4.048	1.476
18.00	-171.0	7.17	-3.872	1.602
20.00	-178.1	7.29	-3.702	1.721
22.00	-185.9	7.42	-3.524	1.808
25.00	-198.9	7.64	-3.245	1.941

Titration No. 6

$E^{\ominus}$" = 247.31 mV, s = 58.754 mV,

$[H^+]_0 = 5.282 \times 10^{-2}$ mol dm^{-3}, $[Co^{2+}]_0 = 1.389 \times 10^{-2}$ mol dm^{-3},

$[etolen]_0 = 2.445 \times 10^{-2}$ mol dm^{-3},

$[H^+]_T = 0$, $[Co^{2+}]_T = 0$,

$[etolen]_T = 1.223 \times 10^{-1}$ mol dm^{-3},

$V_0 = 120.00$ cm^3.

1.00	84.8	2.77	-12.654	-0.005
3.00	-83.4	5.63	-6.934	0.024
4.00	-97.2	5.86	-6.477	0.059
5.00	-105.4	6.00	-6.209	0.100
6.00	-111.2	6.10	-6.023	0.143
7.00	-115.8	6.18	-5.877	0.189
8.00	-119.7	6.25	-5.754	0.235
9.00	-123.1	6.30	-5.648	0.282
10.00	-126.1	6.36	-5.556	0.330
12.00	-131.5	6.45	-5.393	0.425
14.00	-136.3	6.53	-5.251	0.519
16.00	-140.7	6.60	-5.123	0.612
18.00	-144.8	6.67	-5.006	0.703
20.00	-148.8	6.74	-4.894	0.792
22.00	-152.7	6.81	-4.787	0.878
24.00	-156.6	6.87	-4.683	0.960
26.00	-160.3	6.94	-4.585	1.042
28.00	-164.1	7.00	-4.488	1.121
30.00	-167.8	7.07	-4.395	1.199
32.00	-171.6	7.13	-4.302	1.274

Titration No. 7

$E^{\ominus}$" = 246.77 mV, s = 58.589 mV,

$[H^+]_0 = 5.282 \times 10^{-2}$ mol dm^{-3}, $[Co^{2+}]_0 = 7.499 \times 10^{-3}$ mol dm^{-3},

$[etolen]_0 = 2.445 \times 10^{-2}$ mol dm^{-3},

$[H^+]_T = 0$, $[Co^{2+}]_T = 0$, $[etolen]_T = 1.223 \times 10^{-1}$ mol dm^{-3},

$V_0 = 120.00$ cm^3.

1.00	85.2	2.76	-12.671	-0.008
3.00	-85.7	5.67	-6.844	0.033
4.00	-101.4	5.94	-6.323	0.077
5.00	-110.6	6.10	-6.024	0.131
6.00	-117.1	6.21	-5.815	0.192
7.00	-122.0	6.29	-5.661	0.260
8.00	-126.3	6.37	-5.527	0.328
9.00	-130.1	6.43	-5.411	0.396

10.00	-133.4	6.49	-5.311	0.468
11.00	-136.4	6.54	-5.221	0.540
13.00	-142.1	6.64	-5.054	0.678
15.00	-147.4	6.73	-4.903	0.810
17.00	-152.4	6.81	-4.764	0.938
19.00	-157.2	6.89	-4.634	1.061
21.00	-161.8	6.97	-4.513	1.182
23.00	-166.5	7.05	-4.392	1.293
25.00	-171.0	7.13	-4.280	1.408
27.00	-175.9	7.21	-4.162	1.508
29.00	-180.7	7.30	-4.050	1.612
31.00	-185.6	7.38	-3.939	1.718

Titration No. 8

$E^{\ominus}{}''$ = 244.84 mV, s = 58.461 mV,

$[H^+]_0 = 5.282 \times 10^{-2}$ mol dm^{-3}, $[Co^{2+}]_0 = 4.166 \times 10^{-3}$ mol dm^{-3},

$[etolen]_0 = 2.445 \times 10^{-2}$ mol dm^{-3},

$[H^+]_T = 0$, $[Co^{2+}]_T = 0$,

$[etolen]_T = 1.223 \times 10^{-1}$ mol dm^{-3},

V_0 = 120.00 cm^3.

1.00	81.6	2.79	-12.601	-0.030
3.00	-91.6	5.75	-6.686	0.019
4.00	-107.0	6.02	-6.177	0.074
5.00	-116.5	6.18	-5.869	0.140
6.00	-123.2	6.30	-5.655	0.221
7.00	-128.9	6.39	-5.477	0.300
8.00	-133.7	6.47	-5.329	0.382
9.00	-137.9	6.55	-5.202	0.467
10.00	-141.6	6.61	-5.093	0.557
11.00	-145.4	6.68	-4.981	0.630
12.00	-148.7	6.73	-4.887	0.714
13.00	-152.0	6.79	-4.793	0.788
14.00	-155.2	6.84	-4.704	0.859
15.00	-158.4	6.90	-4.617	0.922
17.00	-164.4	7.00	-4.458	1.054
19.00	-170.3	7.10	-4.307	1.176
21.00	-176.2	7.20	-4.162	1.291
23.00	-182.3	7.31	-4.017	1.397
25.00	-188.7	7.42	-3.872	1.499
27.00	-195.4	7.53	-3.726	1.606
29.00	-203.1	7.66	-3.566	1.696
31.00	-211.9	7.81	-3.390	1.784

Titration No. 9

$E^{\ominus}$" = 242.47 mV, s= 58.397 mV,

$[H^+]_0 = 5.285 \times 10^{-2}$ mol dm^{-3}, $[Co^{2+}]_0 = 1.389 \times 10^{-2}$ mol dm^{-3},

$[etolen]_0 = 2.421 \times 10^{-2}$ mol dm^{-3},

$[H^+]_T = 0$, $[Co^{2+}]_T = 0$,

$[etolen]_T = 1.211 \times 10^{-1}$ mol dm^{-3},

$V_0 = 120.00$ cm^3.

3.00	-78.7	5.50	-7.189	0.017
4.00	-97.8	5.83	-6.549	0.045
5.00	-107.3	5.99	-6.236	0.081
6.00	-113.5	6.10	-6.034	0.122
7.00	-118.4	6.18	-5.877	0.165
8.00	-122.4	6.25	-5.751	0.210
9.00	-125.9	6.31	-5.642	0.255
10.00	-129.0	6.36	-5.546	0.301
11.00	-131.8	6.41	-5.460	0.347
13.00	-136.8	6.49	-5.310	0.440
15.00	-141.2	6.57	-5.180	0.534
17.00	-145.4	6.64	-5.059	0.625
19.00	-149.3	6.71	-4.948	0.715
21.00	-153.1	6.77	-4.843	0.802
23.00	-156.9	6.84	-4.739	0.886
25.00	-160.5	6.90	-4.643	0.970
27.00	-164.1	6.96	-4.549	1.051
29.00	-167.7	7.02	-4.456	1.131
31.00	-171.4	7.09	-4.364	1.206
33.00	-175.0	7.15	-4.276	1.283
35.00	-178.8	7.21	-4.185	1.356

6. System: $H^+ + Co^{2+}$ + oden

Titration No. 1

$E^{\ominus}$" = 247.17 mV, s = 57.971 mV,

$[H^+]_0 = 6.672 \times 10^{-3}$ mol dm^{-3},

$[Co^{2+}]_0 = 9.992 \times 10^{-4}$ mol dm^{-3}, $[oden]_0 = 2.243 \times 10^{-3}$ mol dm^{-3},

$[OH^-]_T = 4.057 \times 10^{-2}$ mol dm^{-3},

$[Co^{2+}]_T = 0$, $[oden]_T = 0$,

$V_0 = 90.00$ cm^3.

5.00	-66.9	5.42	-10.784	0.035
6.00	-232.2	8.27	- 5.158	0.132
7.00	-247.5	8.53	- 4.708	0.278
8.00	-257.7	8.71	- 4.441	0.439

Titration No. 2

$E^{\ominus}$" = 248.92 mV, s = 57.668 mV

$[H^+]_0 = 1.006 \times 10^{-2}$ mol dm^{-3},

$[Co^{2+}]_0 = 9.992 \times 10^{-4}$ mol dm^{-3}, $[oden]_0 = 4.485 \times 10^{-3}$ mol dm^{-3},

$[OH^-]_T = 4.041 \times 10^{-2}$ mol dm^{-3},

$[Co^{2+}]_T = 0$, $[oden]_T = 0$,

$V_0 = 90.00$ cm^3.

3.00	-188.6	7.59	-6.147	0.074
5.00	-233.9	8.37	-4.660	0.266
7.00	-249.1	8.64	-4.221	0.519
9.00	-260.8	8.84	-3.915	0.768

Titration No. 3

$E^{\ominus}$" = 248.42 mV, s = 58.757 mV,

$[H^+]_0 = 5.570 \times 10^{-3}$ mol dm^{-3},

$[Co^{2+}]_0 = 4.996 \times 10^{-4}$ mol dm^{-3}, $[oden]_0 = 2.243 \times 10^{-3}$ mol dm^{-3},

$[OH^-]_T = 1.024 \times 10^{-2}$ mol dm^{-3},

$[Co^{2+}]_T = 0$, $[oden]_T = 0$,

$V_0 = 90.00$ cm^3.

11.00	-208.1	7.77	-6.125	0.080
11.50	-217.2	7.92	-5.827	0.101
12.00	-223.5	8.03	-5.624	0.126
12.50	-228.6	8.12	-5.461	0.151
13.00	-232.6	8.19	-5.336	0.179
13.50	-236.1	8.25	-5.228	0.207
14.00	-239.1	8.30	-5.138	0.238
15.00	-244.5	8.39	-4.977	0.297
16.00	-248.9	8.46	-4.850	0.360
17.00	-252.7	8.53	-4.744	0.427
18.00	-256.2	8.59	-4.649	0.493
19.00	-259.4	8.64	-4.565	0.560
20.00	-262.4	8.69	-4.489	0.628

Titration No. 4

$E^{\ominus\prime\prime}$ = 252.67 mV, s = 58.399 mV,

$[H^+]_0 = 9.499 \times 10^{-3}$ mol dm^{-3},

$[Co^{2+}]_0 = 4.996 \times 10^{-4}$ mol dm^{-3}, $[oden]_0 = 4.485 \times 10^{-3}$ mol dm^{-3},

$[OH^-]_T = 1.024 \times 10^{-2}$ mol dm^{-3},

$[Co^{2+}]_T = 0$, $[oden]_T = 0$,

$V_0 = 90.00$ cm^3.

6.00	-167.5	7.19	-6.936	0.107
6.50	-185.9	7.51	-6.314	0.114
7.00	-195.8	7.68	-5.982	0.126
7.50	-202.7	7.80	-5.753	0.140
8.00	-207.8	7.88	-5.585	0.157
8.50	-212.1	7.96	-5.445	0.174
9.00	-215.5	8.02	-5.336	0.195
11.00	-226.1	8.20	-5.001	0.279
13.00	-233.6	8.33	-4.772	0.370
15.00	-239.4	8.43	-4.601	0.469
18.00	-246.7	8.55	-4.395	0.614
21.00	-252.8	8.66	-4.230	0.761
24.00	-258.4	8.75	-4.085	0.895

Titration No. 5

$E^{\ominus\prime\prime}$ = 252.62 mV, s = 58.966 mV,

$[H^+]_0 = 2.249 \times 10^{-2}$ mol dm^{-3}, $[Co^{2+}]_0 = 4.998 \times 10^{-3}$ mol dm^{-3},

$[oden]_0 = 1.000 \times 10^{-2}$ mol dm^{-3},

$[H^+]_T = 0$, $[Co^{2+}]_T = 0$, $[oden]_T = 5.001 \times 10^{-2}$ mol dm^{-3},

$V_0 = 120.00$ cm^3.

3.00	-191.7	7.54	-5.834	-0.024
4.00	-208.7	7.82	-5.266	0.034
5.00	-216.8	7.96	-4.998	0.099
6.00	-222.6	8.06	-4.808	0.164
7.00	-227.1	8.14	-4.662	0.231
8.00	-230.8	8.20	-4.543	0.298
9.00	-234.1	8.25	-4.438	0.365
10.00	-237.0	8.30	-4.345	0.432
12.00	-242.7	8.40	-4.166	0.560
14.00	-247.7	8.48	-4.010	0.686
16.00	-252.5	8.57	-3.862	0.805
18.00	-256.9	8.64	-3.728	0.919
20.00	-261.2	8.71	-3.598	1.024
22.00	-265.2	8.78	-3.479	1.124
24.00	-268.9	8.84	-3.371	1.219

26.00	-272.6	8.91	-3.264	1.302
28.00	-275.9	8.96	-3.171	1.384
30.00	-279.2	9.02	-3.079	1.454

Titration No. 6

$E^{\ominus\prime\prime}$ = 256.60 mV, s = 59.315 mV,

$[H^+]_0 = 2.249 \times 10^{-2}$ mol dm^{-3}, $[Co^{2+}]_0 = 1.666 \times 10^{-3}$ mol dm^{-3},

$[oden]_0 = 1.000 \times 10^{-2}$ mol dm^{-3},

$[H^+]_T = 0$, $[Co^{2+}]_T = 0$, $[oden]_T = 5.001 \times 10^{-2}$ mol dm^{-3},

V_0 = 120.00 cm^3.

3.00	-195.8	7.63	-5.652	-0.092
4.00	-215.8	7.96	-4.988	0.045
5.00	-226.0	8.14	-4.654	0.192
6.00	-233.2	8.26	-4.421	0.342
7.00	-239.1	8.36	-4.232	0.485
8.00	-244.4	8.45	-4.063	0.616
9.00	-249.0	8.52	-3.919	0.741
10.00	-253.1	8.59	-3.792	0.859
11.00	-257.0	8.66	-3.672	0.963
12.00	-260.6	8.72	-3.562	1.056
13.00	-263.8	8.77	-3.466	1.147
14.00	-266.8	8.82	-3.377	1.229
16.00	-272.2	8.92	-3.220	1.372
18.00	-277.1	9.00	-3.080	1.477
20.00	-281.2	9.07	-2.966	1.583
22.00	-285.0	9.13	-2.863	1.657
24.00	-288.3	9.19	-2.776	1.732
26.00	-291.4	9.24	-2.696	1.780
28.00	-294.2	9.29	-2.626	1.822
30.00	-296.8	9.33	-2.562	1.849

Titration No. 7

$E^{\ominus\prime\prime}$ = 252.96 mV, s = 58.878 mV,

$[H^+]_0 = 1.499 \times 10^{-2}$ mol dm^{-3}, $[Co^{2+}]_0 = 1.666 \times 10^{-3}$ mol dm^{-3},

$[oden]_0 = 6.668 \times 10^{-3}$ mol dm^{-3},

$[H^+]_T = 0$, $[Co^{2+}]_T = 0$, $[oden]_T = 5.001 \times 10^{-2}$ mol dm^{-3},

V_0 = 120.00 cm^3.

2.00	-201.6	7.72	-5.639	-0.077
3.00	-223.4	8.09	-4.912	0.065
4.00	-233.6	8.26	-4.578	0.223
5.00	-241.0	8.39	-4.338	0.379
6.00	-247.2	8.49	-4.140	0.526
7.00	-252.6	8.59	-3.970	0.664
8.00	-257.3	8.67	-3.824	0.795
9.00	-261.8	8.74	-3.685	0.909
10.00	-265.8	8.81	-3.564	1.015
11.00	-269.5	8.87	-3.454	1.111
12.00	-273.0	8.93	-3.351	1.193
13.00	-276.1	8.99	-3.261	1.274
15.00	-281.7	9.08	-3.103	1.410
17.00	-286.7	9.17	-2.965	1.511
19.00	-291.0	9.24	-2.851	1.598
21.00	-294.8	9.30	-2.753	1.671

Titration No. 8

$E^{\ominus}{}''$ = 252.50 mV, s = 58.787 mV,

$[H^+]_0 = 2.249 \times 10^{-2}$ mol dm^{-3}, $[Co^{2+}]_0 = 4.998 \times 10^{-3}$ mol dm^{-3},

$[oden]_0 = 1.000 \times 10^{-2}$ mol dm^{-3},

$[H^+]_T = 0$, $[Co^{2+}]_T = 0$, $[oden]_T = 5.001 \times 10^{-2}$ mol dm^{-3},

$V_0 = 120.00$ cm^3.

6.00	-220.5	8.05	-4.834	0.167
7.00	-225.2	8.13	-4.681	0.233
8.00	-228.9	8.19	-4.561	0.301
9.00	-232.2	8.25	-4.455	0.368
10.00	-235.3	8.30	-4.356	0.434
12.00	-241.0	8.39	-4.176	0.563
14.00	-246.1	8.48	-4.016	0.688
16.00	-250.9	8.56	-3.868	0.807
18.00	-255.4	8.64	-3.730	0.919
20.00	-259.7	8.71	-3.600	1.025
22.00	-263.7	8.78	-3.481	1.125
24.00	-267.5	8.85	-3.369	1.217
26.00	-271.2	8.91	-3.262	1.301
28.00	-274.6	8.97	-3.165	1.379
30.00	-277.8	9.02	-3.076	1.451

7. System: $H^+ + Zn^{2+}$ + etolen

Titration No. 1

$E^{\ominus}{}''$ = 244.83 mV, s = 58.447 mV,

$[H^+]_0 = 4.417 \times 10^{-2}$ mol dm^{-3}, $[Zn^{2+}]_0 = 1.000 \times 10^{-2}$ mol dm^{-3},

$[etolen]_0 = 1.997 \times 10^{-2}$ mol dm^{-3},

$[H^+]_T$ = 0, $[Zn^{2+}]_T$ = 0, $[etolen]_T$ = 9.987 x 10^{-2} mol dm^{-3},
V_0 = 120.00 cm^3.

3.00	- 81.5	5.58	-7.108	-0.02
4.00	- 94.8	5.81	-6.664	0.03
5.00	-102.7	5.95	-6.404	0.08
6.00	-108.2	6.04	-6.225	0.13
7.00	-112.5	6.11	-6.087	0.19
8.00	-115.9	6.17	-5.979	0.25
9.00	-119.0	6.23	-5.881	0.31
10.00	-121.7	6.27	-5.797	0.37
11.00	-124.0	6.31	-5.727	0.43
13.00	-128.4	6.39	-5.593	0.55
15.00	-132.4	6.45	-5.473	0.67
17.00	-136.0	6.52	-5.367	0.79
19.00	-139.5	6.58	-5.265	0.91
21.00	-142.7	6.63	-5.173	1.03
23.00	-146.1	6.69	-5.077	1.14
25.00	-149.4	6.75	-4.985	1.25
27.00	-152.9	6.81	-4.889	1.35
29.00	-156.5	6.87	-4.791	1.45
31.00	-160.3	6.93	-4.690	1.54
33.00	-164.3	7.00	-4.586	1.62
35.00	-168.7	7.08	-4.473	1.69
37.00	-173.4	7.16	-4.356	1.75
39.00	-178.5	7.24	-4.233	1.81

Titration No. 2

$E^{\ominus}$" = 246.94 mV, s = 58.697 mV,
$[H^+]_0$ = 4.610 x 10^{-2} mol dm^{-3}, $[Zn^{2+}]_0$ = 5.218 x 10^{-3} mol dm^{-3},
$[etolen]_0$ = 2.084 x 10^{-2} mol dm^{-3},
$[H^+]_T$ = 0, $[Zn^{2+}]_T$ = 0, $[etolen]_T$ = 9.987 x 10^{-2} mol dm^{-3},
V_0 = 115.00 cm^3.

2.00	- 30.9	4.73	-8.776	-0.10
3.00	- 83.4	5.63	-7.002	-0.05
4.00	- 98.4	5.88	-6.504	0.02
5.00	-107.3	6.04	-6.214	0.10
6.00	-113.5	6.14	-6.014	0.19
7.00	-118.4	6.22	-5.859	0.28
8.00	-122.6	6.30	-5.727	0.37
9.00	-126.1	6.36	-5.619	0.47
10.00	-129.4	6.41	-5.518	0.57
11.00	-132.4	6.46	-5.428	0.66
12.00	-135.1	6.51	-5.347	0.76
13.00	-137.9	6.56	-5.264	0.85
15.00	-143.0	6.64	-5.116	1.03
17.00	-148.2	6.73	-4.967	1.19
19.00	-153.2	6.82	-4.828	1.34
21.00	-158.4	6.91	-4.687	1.47

23.00	-163.7	7.00	-4.548	1.59
25.00	-169.5	7.10	-4.399	1.67
27.00	-175.5	7.20	-4.251	1.74
29.00	-182.2	7.31	-4.093	1.78
31.00	-189.4	7.43	-3.930	1.81
33.00	-197.8	7.58	-3.748	1.82
35.00	-207.4	7.74	-3.551	1.82
37.00	-218.7	7.93	-3.331	1.83
39.00	-231.3	8.15	-3.097	1.85

Titration No. 3

$E^{\ominus}$" = 246.79 mV, s = 58.639 mV,

$[H^+]_0 = 4.417 \times 10^{-2}$ mol dm^{-3}, $[Zn^{2+}]_0 = 3.332 \times 10^{-3}$ mol dm^{-3},

$[etolen]_0 = 1.997 \times 10^{-2}$ mol dm^{-3},

$[H^+]_T = 0$, $[Zn^{2+}]_T = 0$, $[etolen]_T = 9.987 \times 10^{-2}$ mol dm^{-3},

$V_0 = 120.00$ cm^3.

2.00	- 18.2	4.52	-9.223	-0.15
3.00	- 83.0	5.62	-7.027	-0.07
4.00	- 99.7	5.91	-6.473	0.01
5.00	-109.4	6.07	-6.156	0.11
6.00	-116.2	6.19	-5.937	0.22
7.00	-121.5	6.28	-5.770	0.33
8.00	-126.0	6.36	-5.629	0.45
9.00	-129.9	6.42	-5.509	0.57
10.00	-133.5	6.49	-5.400	0.69
11.00	-136.8	6.54	-5.301	0.81
12.00	-139.9	6.59	-5.209	0.93
13.00	-143.0	6.65	-5.118	1.04
14.00	-146.0	6.70	-5.032	1.14
15.00	-148.9	6.75	-4.949	1.24
16.00	-151.8	6.80	-4.868	1.33
17.00	-154.7	6.85	-4.788	1.42
18.00	-157.6	6.90	-4.709	1.49
19.00	-160.6	6.95	-4.629	1.56
20.00	-163.6	7.00	-4.550	1.62
21.00	-166.7	7.05	-4.469	1.67
22.00	-169.8	7.10	-4.391	1.72
23.00	-173.1	7.16	-4.309	1.75
24.00	-176.5	7.22	-4.226	1.77
25.00	-179.9	7.28	-4.145	1.80
26.00	-183.5	7.34	-4.061	1.82
27.00	-187.3	7.40	-3.975	1.83
28.00	-191.3	7.47	-3.886	1.83
29.00	-195.7	7.55	-3.791	1.83
30.00	-200.3	7.62	-3.694	1.82
31.00	-205.3	7.71	-3.591	1.82
32.00	-210.9	7.81	-3.480	1.81
33.00	-216.8	7.91	-3.365	1.81
34.00	-223.2	8.02	-3.244	1.81
35.00	-229.8	8.13	-3.122	1.82
36.00	-236.4	8.24	-3.003	1.84

Titration No. 4

$E^{\ominus\prime\prime}$ = 246.63 mV, s = 58.679 mV,

$[H^+]_0 = 2.349 \times 10^{-2}$ mol dm^{-3}, $[Zn^{2+}]_0 = 5.218 \times 10^{-3}$ mol dm^{-3},

$[etolen]_0 = 1.042 \times 10^{-2}$ mol dm^{-3},

$[H^+]_T = 0$, $[Zn^{2+}]_T = 0$, $[etolen]_T = 4.993 \times 10^{-2}$ mol dm^{-3},

V_0 = 115.00 cm^3.

2.00	37.6	3.56	-11.411	-0.06
3.00	- 70.9	5.41	-7.720	-0.04
4.00	-94.0	5.81	-6.947	-0.02
5.00	-104.6	5.99	-6.599	0.02
6.00	-111.5	6.10	-6.376	0.06
7.00	-116.6	6.19	-6.213	0.11
8.00	-120.6	6.26	-6.088	0.16
9.00	-124.1	6.32	-5.979	0.21
10.00	-127.0	6.37	-5.890	0.26
11.00	-129.6	6.41	-5.812	0.32
13.00	-134.4	6.49	-5.668	0.42
15.00	-138.5	6.56	-5.549	0.53
17.00	-142.1	6.63	-5.446	0.64
19.00	-145.7	6.69	-5.344	0.75
21.00	-149.0	6.74	-5.253	0.86
23.00	-152.2	6.80	-5.166	0.97
25.00	-155.4	6.85	-5.081	1.07
27.00	-158.7	6.91	-4.994	1.17
29.00	-162.1	6.97	-4.906	1.27
31.00	-165.6	7.03	-4.817	1.36
33.00	-169.2	7.09	-4.727	1.45
35.00	-173.1	7.15	-4.632	1.53
37.00	-177.3	7.23	-4.532	1.60
39.00	-181.8	7.30	-4.427	1.66

Titration No. 5

$E^{\ominus\prime\prime}$ = 248.08 mV, s = 58.861 mV,

$[H^+]_0 = 2.252 \times 10^{-2}$ mol dm^{-3}, $[Zn^{2+}]_0 = 1.666 \times 10^{-3}$ mol dm^{-3},

$[etolen]_0 = 9.987 \times 10^{-3}$ mol dm^{-3},

$[H^+]_T = 0$, $[Zn^{2+}]_T = 0$, $[etolen]_T = 4.993 \times 10^{-2}$ mol dm^{-3},

V_0 = 120.00 cm^3.

2.00	27.7	3.74	-11.064	-0.21
3.00	-74.6	5.48	- 7.597	-0.15
4.00	-97.3	5.87	-6.842	-0.10
5.00	-108.9	6.07	-6.464	-0.02

6.00	-116.8	6.20	-6.210	0.06
7.00	-122.9	6.30	-6.018	0.15
8.00	-127.9	6.39	-5.863	0.24
9.00	-132.1	6.46	-5.735	0.35
10.00	-135.9	6.52	-5.620	0.45
11.00	-139.3	6.58	-5.520	0.55
12.00	-142.6	6.64	-5.423	0.65
13.00	-145.6	6.69	-5.337	0.75
14.00	-148.5	6.74	-5.255	0.85
15.00	-151.3	6.79	-5.177	0.95
17.00	-156.8	6.88	-5.026	1.13
19.00	-162.3	6.97	-4.880	1.29
21.00	-168.0	7.07	-4.734	1.41
23.00	-173.9	7.17	-4.587	1.52
25.00	-180.2	7.28	-4.437	1.59
27.00	-187.0	7.39	-4.282	1.65
29.00	-194.6	7.52	-4.115	1.69
31.00	-203.5	7.67	-3.930	1.70
33.00	-213.9	7.85	-3.724	1.71
35.00	-226.2	8.06	-3.492	1.72
37.00	-239.1	8.28	-3.259	1.76
39.00	-250.5	8.47	-3.059	1.83

Titration No. 6

$E^{\ominus\prime\prime}$ = 246.84 mV, s = 58.758 mV,

$[H^+]_0 = 4.610 \times 10^{-2}$ mol dm^{-3}, $[Zn^{2+}]_0 = 5.218 \times 10^{-3}$ mol dm^{-3},

$[\text{etolen}]_0 = 2.084 \times 10^{-2}$ mol dm^{-3},

$[H^+]_T = 0$, $[Zn^{2+}]_T = 0$, $[\text{etolen}]_T = 9.987 \times 10^{-2}$ mol dm^{-3},

$V_0 = 115.00$ cm^3.

2.00	-22.4	4.58	-9.078	-0.10
3.00	-82.1	5.60	-7.061	-0.04
4.00	-97.7	5.86	-6.543	0.03
5.00	-106.7	6.02	-6.249	0.11
6.00	-113.1	6.13	-6.043	0.20
7.00	-118.1	6.21	-5.884	0.29
8.00	-122.2	6.28	-5.756	0.39
9.00	-125.9	6.34	-5.641	0.48
10.00	-129.1	6.40	-5.543	0.58
11.00	-132.2	6.45	-5.449	0.68
12.00	-135.0	6.50	-5.365	0.77
13.00	-137.7	6.54	-5.286	0.87
15.00	-142.9	6.63	-5.134	1.05
17.00	-148.0	6.72	-4.988	1.22
19.00	-153.1	6.81	-4.846	1.37
21.00	-158.3	6.90	-4.705	1.50
23.00	-163.7	6.99	-4.562	1.61
25.00	-169.5	7.09	-4.413	1.69

27.00	-175.6	7.19	-4.262	1.76
29.00	-182.2	7.30	-4.106	1.80
31.00	-189.5	7.43	-3.940	1.83
33.00	-197.8	7.57	-3.760	1.84
35.00	-207.4	7.73	-3.563	1.84
37.00	-218.7	7.92	-3.343	1.84
38.00	-224.8	8.03	-3.228	1.85

TABLE 7.2

Titration calorimetric data for the various systems.

1. System: H^+ + etolen

Titration No. 1

$[H^+]_0 = 0$, $[\text{etolen}]_0 = 9.958 \times 10^{-3}$ mol dm^{-3},
$[H^+]_T = 5.001 \times 10^{-1}$ mol dm^{-3}, $[\text{etolen}]_T = 0$,
$V_0 = 95.00$ cm^3.

0.1698	-4.341
0.3890	-5.285
0.6081	-5.332
0.8273	-5.052
1.0464	-5.205
1.2655	-5.141
1.4847	-5.130
1.7038	-5.283
1.9230	-5.108
2.1421	-4.654
2.3613	-4.637
2.5804	-4.619
2.7995	-4.656
3.0187	-4.526
3.2378	-4.562
3.4570	-4.430
3.6761	-4.520

Titration No. 2

$[H^+]_0 = 0$, $[\text{etolen}]_0 = 9.958 \times 10^{-3}$ mol dm^{-3},
$[H^+]_T = 5.001 \times 10^{-1}$ mol dm^{-3}, $[\text{etolen}]_T = 0$,
$V_0 = 95.00$ cm^3.

0.1644	-4.176
0.3837	-5.385
0.6029	-5.325
0.8222	-5.209
1.0414	-5.145
1.2607	-5.135
1.4799	-5.234
1.6992	-5.334
1.9184	-5.049
2.1377	-4.705

2.3569	-4.633
2.5762	-4.560
2.7954	-4.597
3.0147	-4.522
3.2339	-4.502
3.4532	-4.538
3.6724	-4.461

Titration No. 3

$[H^+]_0 = 0$, $[\text{etolen}]_0 = 9.958 \times 10^{-3}$ mol dm^{-3},
$[H^+]_T = 5.001 \times 10^{-1}$ mol dm^{-3}, $[\text{etolen}]_T = 0$,
$V_0 = 95.00$ cm^3.

0.1810	-4.456
0.4005	-5.413
0.6199	-5.135
0.8393	-5.070
1.0587	-5.223
1.2782	-5.158
1.4976	-5.257
1.7170	-5.081
1.9365	-4.848
2.1559	-4.888
2.3753	-4.596
2.5947	-4.633
2.8142	-4.503
3.0336	-4.594
3.2530	-4.686
3.4725	-4.443
3.6919	-4.421

2. System: H^+ + oden

Titration No. 1

$[H^+]_0 = 0$, $[\text{oden}]_0 = 8.303 \times 10^{-3}$ mol dm^{-3},
$[H^+]_T = 5.000 \times 10^{-1}$ mol dm^{-3}, $[\text{oden}]_T = 0$,
$V_0 = 95.00$ cm^3.

0.1076	-2.714
0.2799	-4.278
0.4521	-4.417
0.6243	-4.340
0.7966	-4.370
0.9688	-4.347
1.1410	-4.431

1.3133	-4.408
1.4855	-4.438
1.6577	-4.468
1.8300	-4.498
2.0022	-4.419
2.1744	-4.558
2.3467	-4.644
2.5189	-4.509
2.6911	-4.594
2.8634	-4.624
3.0356	-4.431

Titration No. 2

$[H^+]_0 = 0$, $[oden]_0 = 8.303 \times 10^{-3}$ mol dm^{-3},
$[H^+]_T = 5.000 \times 10^{-1}$ mol dm^{-3}, $[oden]_T = 0$,
$V_0 = 95.00$ cm^3.

0.0969	-2.355
0.2908	-5.018
0.4846	-5.057
0.6785	-5.041
0.8723	-5.080
1.0662	-5.009
1.2600	-5.101
1.4539	-5.139
1.6477	-5.067
1.8416	-5.104
2.0354	-5.141
2.2293	-5.234
2.4231	-4.995
2.6170	-5.196
2.8108	-5.178
3.0047	-4.936

3. System: $H^+ + Ni^{2+}$ + etolen

Titration No. 1

$[H^+]_0 = 1.091 \times 10^{-1}$ mol dm^{-3}, $[Ni^{2+}]_0 = 2.676 \times 10^{-2}$ mol dm^{-3},
$[etolen]_0 = 6.081 \times 10^{-2}$ mol dm^{-3},
$[H^+]_T = 0$, $[Ni^{2+}]_T = 0$, $[etolen]_T = 1.274$ mol dm^{-3},
$V_0 = 95.838$ cm^3.

0.2192	-8.157
0.4383	-8.227
0.6574	-8.242

0.8766	-8.202
1.0957	-8.326
1.3149	-8.450
1.5340	-8.353
1.7532	-9.034
1.9723	-8.382
2.1914	-8.282
2.4106	-8.684
2.6297	-8.753
2.8489	-8.596
3.0680	-8.325
3.2872	-8.163
3.5063	-7.886
3.7254	-7.604

Titration No. 2

$[H^+]_0 = 1.091 \times 10^{-1}$ mol dm^{-3}, $[Ni^{2+}]_0 = 2.676 \times 10^{-2}$ mol dm^{-3},
$[etolen]_0 = 6.078 \times 10^{-2}$ mol dm^{-3},
$[H^+]_T = 0$, $[Ni^{2+}]_T = 0$, $[etolen]_T = 1.274$ mol dm^{-3},
$V_0 = 95.836$ cm^3.

0.2190	-8.267
0.4381	-8.119
0.6572	-8.299
0.8763	-8.260
1.0954	-8.275
1.3145	-8.455
1.5335	-8.525
1.7526	-8.318
1.9717	-8.664
2.1908	-8.511
2.4099	-8.860
2.6290	-8.538
2.8480	-8.381
3.0671	-8.221
3.2862	-8.058
3.5053	-7.611
3.7244	-7.271
3.9435	-6.415
4.1625	-5.607
4.3816	-4.790

Titration No. 3

$[H^+]_0 = 1.091 \times 10^{-1}$ mol dm^{-3}, $[Ni^{2+}]_0 = 2.677 \times 10^{-2}$ mol dm^{-3},
$[etolen]_0 = 6.063 \times 10^{-2}$ mol dm^{-3},
$[H^+]_T = 0$, $[Ni^{2+}]_T = 0$, $[etolen]_T = 1.274$ mol dm^{-3},
$V_0 = 95.824$ cm^3.

0.2187	-7.950
0.4374	-8.237
0.6561	-8.308
0.8749	-8.267
1.0936	-8.281
1.3123	-8.461
1.5310	-8.530
1.7497	-8.322
1.9684	-8.668
2.1871	-8.681
2.4059	-8.526
2.6246	-8.594
2.8433	-8.436
3.0620	-8.388
3.2807	-8.001
3.4994	-7.609
3.7181	-7.212

4. System: $H^+ + Ni^{2+}$ + oden

Titration No. 1

$[H^+]_0 = 4.001 \times 10^{-2}$ mol dm^{-3}, $[Ni^{2+}]_0 = 0$,

$[oden]_0 = 2.900 \times 10^{-2}$ mol dm^{-3},

$[H^+]_T = 0$, $[Ni^{2+}]_T = 1.667 \times 10^{-1}$ mol dm^{-3}, $[oden]_T = 0$,

$V_0 = 95.00$ cm^3.

0.2464	-2.081
0.5624	-2.725
0.8783	-2.646
1.1943	-2.564
1.5103	-2.371
1.8262	-2.065
2.1422	-1.864
2.4581	-1.605
2.7741	-1.397
3.0900	-1.241
3.4060	-0.971
3.7219	-0.921
4.0379	-0.758
4.3538	-0.705
4.6698	-0.538
4.9857	-0.426
5.3017	-0.312
5.6176	-0.253
5.9336	-0.194
6.2495	-0.191

Titration No. 2

$[H^+]_0 = 4.001 \times 10^{-2}$ mol dm^{-3}, $[Ni^{2+}]_0 = 0$,
$[oden]_0 = 2.900 \times 10^{-2}$ mol dm^{-3},
$[H^+]_T = 0$, $[Ni^{2+}]_T = 1.667 \times 10^{-1}$ mol dm^{-3}, $[oden]_T = 0$,
$V_0 = 95.00$ cm^3.

0.2097	-1.803
0.4945	-2.493
0.7794	-2.356
1.0642	-2.380
1.3491	-2.185
1.6339	-2.042
1.9188	-1.731
2.2036	-1.692
2.4885	-1.375
2.7733	-1.164
3.0582	-1.118
3.3430	-0.903
3.6279	-0.853
3.9127	-0.746
4.1976	-0.694
4.4824	-0.584
4.7673	-0.416
5.0521	-0.360
5.3370	-0.246
5.6218	-0.244

Titration No. 3

$[H^+]_0 = 4.001 \times 10^{-2}$ mol dm^{-3}, $[Ni^{2+}]_0 = 0$,
$[oden]_0 = 2.900 \times 10^{-2}$ mol dm^{-3},
$[H^+]_T = 0$, $[Ni^{2+}]_T = 1.667 \times 10^{-1}$ mol dm^{-3}, $[oden]_T = 0$,
$V_0 = 95.00$ cm^3.

0.2017	-1.713
0.4864	-2.542
0.7712	-2.405
1.0559	-2.320
1.3407	-2.234
1.6254	-1.982
1.9102	-1.836
2.1949	-1.632
2.4797	-1.425
2.7644	-1.160
3.0492	-1.058
3.3339	-1.011
3.6187	-0.794
3.9034	-0.743

4.1882	-0.635
4.4729	-0.582
4.7577	-0.415
5.0424	-0.359
5.3272	-0.245
5.6119	-0.187

Titration No. 4

$[H^+]_0 = 4.001 \times 10^{-2}$ mol dm^{-3}, $[Ni^{2+}]_0 = 0$,
$[oden]_0 = 2.900 \times 10^{-2}$ mol dm^{-3},
$[H^+]_T = 0$, $[Ni^{2+}]_T = 1.667 \times 10^{-1}$ mol dm^{-3}, $[oden]_T = 0$,
$V_0 = 95.00$ cm^3.

0.2039	-1.733
0.4884	-2.531
0.7729	-2.447
1.0574	-2.363
1.3419	-2.222
1.6264	-2.024
1.9109	-1.878
2.1954	-1.620
2.4799	-1.413
2.7644	-1.203
3.0489	-1.101
3.3334	-0.998
3.6179	-0.838
3.9024	-0.731
4.1869	-0.566
4.4714	-0.569
4.7559	-0.459
5.0404	-0.290
5.3249	-0.290
5.6094	-0.175

5. System: $H^+ + Co^{2+}$ + etolen

Titration No. 1

$[H^+]_0 = 1.091 \times 10^{-1}$ mol dm^{-3}, $[Co^{2+}]_0 = 2.974 \times 10^{-2}$ mol dm^{-3},
$[etolen]_0 = 6.085 \times 10^{-2}$ mol dm^{-3},
$[H^+]_T = 0$, $[Co^{2+}]_T = 0$, $[etolen]_T = 1.274$ mol dm^{-3},
$V_0 = 95.842$ cm^3.

0.2192	-4.326
0.4383	-4.745
0.6574	-4.782
0.8766	-4.985
1.0957	-5.244
1.3149	-5.340
1.5340	-5.325
1.7532	-5.143
1.9723	-5.015
2.1914	-4.885
2.4106	-4.697
2.6297	-4.787
2.8489	-4.654
3.0680	-4.349
3.2872	-4.549
3.5063	-4.412
3.7254	-4.329

Titration No. 2

$[H^+]_0 = 1.091 \times 10^{-1}$ mol dm^{-3}, $[Co^{2+}]_0 = 2.973 \times 10^{-2}$ mol dm^{-3},
$[etolen]_0 = 6.102 \times 10^{-2}$ mol dm^{-3},
$[H^+]_T = 0$, $[Co^{2+}]_T = 0$, $[etolen]_T = 1.274$ mol dm^{-3},
$V_0 = 95.855$ cm^3.

0.2191	-4.550
0.4382	-4.530
0.6574	-5.004
0.8765	-4.767
1.0957	-5.520
1.3148	-4.953
1.5340	-5.156
1.7531	-5.194
1.9722	-4.842
2.1914	-4.821
2.4105	-4.799
2.6297	-4.553
2.8488	-4.585
3.0680	-4.561
3.2871	-4.367
3.5062	-4.454
3.7254	-4.144

Titration No. 3

$[H^+]_0 = 1.091 \times 10^{-1}$ mol dm^{-3}, $[Co^{2+}]_0 = 2.974 \times 10^{-2}$ mol dm^{-3},
$[etolen]_0 = 6.086 \times 10^{-2}$ mol dm^{-3},
$[H^+]_T = 0$, $[Co^{2+}]_T = 0$, $[etolen]_T = 1.274$ mol dm^{-3},
$V_0 = 95.843$ cm^3.

0.2189	-4.398
0.4378	-4.543
0.6567	-4.744
0.8756	-4.836
1.0945	-5.151
1.3134	-5.246
1.5323	-5.287
1.7512	-5.161
1.9701	-4.921
2.1890	-4.903
2.4079	-4.660
2.6268	-4.750
2.8457	-4.560
3.0646	-4.481
3.2836	-4.457
3.5025	-4.376
3.7214	-4.407

6. System: $H^+ + Co^{2+}$ + oden

Titration No. 1

$[H^+]_0 = 4.001 \times 10^{-2}$ mol dm^{-3}, $[Co^{2+}]_0 = 0$,

$[oden]_0 = 2.900 \times 10^{-2}$ mol dm^{-3},

$[H^+]_T = 0$, $[Co^{2+}]_T = 1.667 \times 10^{-1}$ mol dm^{-3}, $[oden]_T = 0$,

$V_0 = 95.00$ cm^3.

0.1913	-1.089
0.4760	-1.521
0.7606	-1.427
1.0453	-1.332
1.3299	-1.181
1.6146	-1.137
1.8992	-0.982
2.1839	-0.825
2.4685	-0.777
2.7532	-0.616
3.0378	-0.620
3.3225	-0.513
3.6071	-0.347
3.8918	-0.405
4.1764	-0.350
4.4611	-0.238
4.7457	-0.295
5.0304	-0.182
5.3150	-0.181
5.5997	-0.180

Titration No. 2

$[H^+]_0 = 4.001 \times 10^{-2}$ mol dm^{-3}, $[Co^{2+}]_0 = 0$,

$[oden]_0 = 2.900 \times 10^{-2}$ mol dm^{-3},

$[H^+]_T = 0$, $[Co^{2+}]_T = 1.667 \times 10^{-1}$ mol dm^{-3}, $[oden]_T = 0$,

$V_0 = 95.00$ cm^3.

0.1935	-1.083
0.4779	-1.577
0.7623	-1.374
1.0467	-1.387
1.3311	-1.290
1.6155	-1.082
1.8999	-0.981
2.1843	-0.824
2.4687	-0.720
2.7531	-0.670
3.0375	-0.563
3.3219	-0.511
3.6063	-0.402
3.8907	-0.348
4.1751	-0.293
4.4595	-0.238
4.7439	-0.238
5.0283	-0.239
5.3127	-0.182
5.5971	-0.125

Titration No. 3

$[H^+]_0 = 4.001 \times 10^{-2}$ mol dm^{-3}, $[Co^{2+}]_0 = 0$,

$[oden]_0 = 2.900 \times 10^{-2}$ mol dm^{-3},

$[H^+]_T = 0$, $[Co^{2+}]_T = 1.667 \times 10^{-1}$ mol dm^{-3}, $[oden]_T = 0$,

$V_0 = 95.00$ cm^3.

0.2057	-1.169
0.4906	-1.547
0.7754	-1.400
1.0603	-1.305
1.3451	-1.264
1.6300	-1.111
1.9148	-0.901
2.1997	-0.854
2.4845	-0.695
2.7694	-0.644
3.0542	-0.537
3.3391	-0.485
3.6239	-0.431
3.9088	-0.377
4.1936	-0.321

4.4785	-0.265
4.7633	-0.265
5.0482	-0.151
5.3330	-0.207
5.6179	-0.207

Titration No. 4

$[H^+]_0 = 4.001 \times 10^{-2}$ mol dm^{-3}, $[Co^{2+}]_0 = 0$,
$[oden]_0 = 2.900 \times 10^{-2}$ mol dm^{-3},
$[H^+]_T = 0$, $[Co^{2+}]_T = 1.667 \times 10^{-1}$ mol dm^{-3}, $[oden]_T = 0$,
$V_0 = 95.00$ cm^3.

0.1804	-1.000
0.4653	-1.591
0.7501	-1.389
1.0350	-1.403
1.3198	-1.197
1.6047	-1.099
1.8895	-0.943
2.1744	-0.841
2.4592	-0.793
2.7441	-0.577
3.0289	-0.581
3.3138	-0.473
3.5986	-0.420
3.8835	-0.310
4.1683	-0.311
4.4532	-0.255
4.7380	-0.256
5.0229	-0.200
5.3077	-0.200
5.5926	-0.200

7. System: $H^+ + Zn^{2+}$ + etolen

Titration No. 1

$[H^+]_0 = 1.089 \times 10^{-1}$ mol dm^{-3}, $[Zn^{2+}]_0 = 2.971 \times 10^{-2}$ mol dm^{-3},
$[etolen]_0 = 6.018 \times 10^{-2}$ mol dm^{-3},
$[H^+]_T = 0$, $[Zn^{2+}]_T = 0$, $[etolen]_T = 1.139$ mol dm^{-3},
$V_0 = 95.903$ cm^3.

0.3201	-6.293
0.6402	-6.693
0.9603	-6.820
1.2803	-7.060
1.6004	-7.302
1.9205	-7.435
2.2406	-7.624
2.5607	-7.591
2.8808	-7.668
3.2009	-7.803
3.5210	-7.824
3.8411	-7.845
4.1612	-7.579
4.4813	-7.423
4.8014	-7.148
5.1215	-6.811
5.4416	-6.410
5.7617	-5.829

Titration No. 2

$[H^+]_0 = 1.089 \times 10^{-1}$ mol dm^{-3}, $[Zn^{2+}]_0 = 2.972 \times 10^{-2}$ mol dm^{-3},
$[etolen]_0 = 5.981 \times 10^{-2}$ mol dm^{-3},
$[H^+]_T = 0$, $[Zn^{2+}]_T = 0$, $[etolen]_T = 1.139$ mol dm^{-3},
$V_0 = 95.870$ cm^3.

0.3221	-6.384
0.6441	-6.841
0.9662	-6.973
1.2883	-7.216
1.6104	-7.517
1.9325	-7.654
2.2546	-7.680
2.5767	-7.874
2.8988	-7.957
3.2209	-8.152
3.5430	-7.895
3.8651	-7.861
4.1872	-7.654
4.5093	-7.558
4.8314	-7.229
5.1535	-6.779
5.4756	-6.322
5.7977	-5.682

Titration No. 3

$[H^+]_0 = 1.089 \times 10^{-1}$ mol dm^{-3}, $[Zn^{2+}]_0 = 2.971 \times 10^{-2}$ mol dm^{-3},
$[etolen]_0 = 6.015 \times 10^{-2}$ mol dm^{-3},
$[H^+]_T = 0$, $[Zn^{2+}]_T = 0$, $[etolen]_T = 1.139$ mol dm^{-3},
$V_0 = 95.900$ cm^3.

0.3219	-6.294
0.6438	-6.751
0.9657	-6.827
1.2876	-7.235
1.6095	-7.425
1.9315	-7.506
2.2534	-7.530
2.5753	-7.835
2.8972	-7.804
3.2191	-7.942
3.5410	-7.910
3.8629	-7.819
4.1848	-7.555
4.5067	-7.515
4.8286	-7.128
5.1505	-6.850
5.4724	-6.278
5.7943	-5.755

Titration No. 4

$[H^+]_0 = 1.088 \times 10^{-1}$ mol dm^{-3}, $[Zn^{2+}]_0 = 2.971 \times 10^{-2}$ mol dm^{-3},
$[etolen]_0 = 6.034 \times 10^{-2}$ mol dm^{-3},
$[H^+]_T = 0$, $[Zn^{2+}]_T = 0$, $[etolen]_T = 1.139$ mol dm^{-3},
$V_0 = 95.916$ cm^3.

0.3221	-6.392
0.6441	-6.629
0.9662	-6.978
1.2882	-6.943
1.6103	-7.129
1.9323	-7.540
2.2544	-7.732
2.5764	-7.813
2.8985	-7.837
3.2205	-7.861
3.5425	-7.770
3.8646	-7.848
4.1866	-7.812
4.5087	-7.487
4.8307	-7.156
5.1528	-6.820
5.4748	-6.420
5.7969	-5.723

7.10. Preparation of various solid complexes

The assumption that the total strain energies developed in the ring systems for oden and etolen are rather similar, can be checked with the aid of conformational strain energy calculations. For such calculations to be possible the crystal structures of the complexes must be known. To this end attempts were made to prepare crystals, of crystallographic quality, of the various complexes studied.

7.10.1. Preparation of $[Ni(etolen)_2](NO_3)_2$

A quantity of $Ni(NO_3)_2.6H_2O$ was dissolved in the minimum amount of hot ethanol. This solution was then added dropwise to a sample of neat etolen. The mole ratio of the metal salt to the ligand was 1:2. To the ethanolic solution was added an equal volume of a mixture containing 90 % acetone and 10 % butanol. On cooling of the mixture in ice, crystals were obtained. This preparation sometimes yielded blue crystals and at other times purple crystals. In fact, when the above procedure was repeated with the use of a liquid diffusion method (170) and without cooling in ice, both types of crystals were obtained in the same tube.

The space group and approximate cell constants of each type of crystal were determined by standard oscillation and Weissenberg techniques using Co-K_α radiation with λ = 1.7902 Å. (Mrs P Sommerville is thanked for help given with these measurements.) Only the blue crystals were suitable for an X-ray structural study. These were sent to the Chemistry Department of the University of the Witwatersrand, where Mr P W Wade determined the crystal structure (171).

The results of all the above measurements are given in Section 8.8.

7.10.2. Attempted preparations of other solid complexes

Despite numerous attempts to grow crystals of Ni^{2+} and oden, no crystals of this complex were obtained.

Attempts were also made to grow crystals of Zn^{2+} and etolen. The following

procedure was used. A quantity of etolen (2 mmol) was added to $Zn(NO_3)_2.4H_2O$ (1 mmol) which had been previously dissolved in the minimum amount of hot ethanol. Acetone was then added as the precipitant. White crystals were obtained when the liquid diffusion method described by Jones (170) was used. However these crystals turned yellow on standing in air for a couple of hours, which indicated possible oxidation. No attempt was made to prepare these crystals under an inert atmosphere.

7.11. Electronic Spectra

The electronic spectra of the complexes of etolen and oden with Ni^{2+} were recorded. For these measurements solutions with a metal to ligand ratio of 1:2 were prepared. The spectra of these solutions were recorded on a Pye Unicam SP1800 UV-visible spectrophotometer. The spectra obtained are shown and discussed in Section 8.9.

CHAPTER EIGHT

RESULTS AND DISCUSSION

In this chapter the results derived from the potentiometric and calorimetric data are described and discussed in detail. In addition the results of the crystallographic and spectroscopic studies are discussed.

The analysis of the potentiometric data listed in Table 7.1 was started by plotting the appropriate formation curve. In the plots of these curves the symbols ⊙, △, +, ×, ◇, ⊕, ⊠, ⊿, and Y were used, in that order, to represent the successive titrations. (In those cases where forward and reverse titrations were performed, separate symbols were used for the forward run and the reverse run.) Once the choice of model had been made the final stability constants were calculated by using either MINIQUAD or ESTA. The program used is indicated in the tables together with the results obtained. These stability constants were then used to arrive at 'calculated' formation curves. These are depicted as solid lines on the various figures.

The program LETAGROP KALLE was used to calculate all the enthalpy changes from the corrected calorimetric data listed in Table 7.2. In those cases where four titrations were performed the data from three were input at a time. The resulting four sets of output were then averaged.

For all the results obtained in this work the standard deviation calculated by the program is shown in parentheses after the appropriate result. In the calculation of stability constants and enthalpy changes fixed values of certain constants were used, some of which were taken from the literature. Table 8.1 lists those values.

8.1. The hydrogen ion - etolen system

The formation curves for this system are shown in Figure 8.1 and can be seen to be superimposable. Hence the titrations were considered to be reproducible. Unfortunately the titrations were not carried out to $p[H^+]$ values high enough to achieve complete deprotonation of the ligand. As far as can be determined, however, the formation curves are symmetrical

TABLE 8.1

Constants used in the calculation of stability constants and enthalpy changes. All data are for 25°C and μ = 0.5 mol dm^{-3}, except where indicated.

Reaction	log β	$\Delta H^{\ominus}$/kJ mol^{-1}	Reference
$H_2O \rightleftharpoons H^+ + OH^-$	-13.74	56.69	160
$Ni^{2+} + H_2O \rightleftharpoons Ni(OH)^+ + H^+$	-10.15[a]	32.47[b]	168,172
$Co^{2+} + H_2O \rightleftharpoons Co(OH)^+ + H^+$	- 9.84		168
$Zn^{2+} + H_2O \rightleftharpoons Zn(OH)^+ + H^+$	- 9.28[c]		173

[a] Corrected from μ = 0.1 to μ = 0.5 with the Davies equation (174).

[b] Value for μ = 1.0 mol dm^{-3}.

[c] Corrected from μ = 0 to μ = 0.5 with the Davies equation (174).

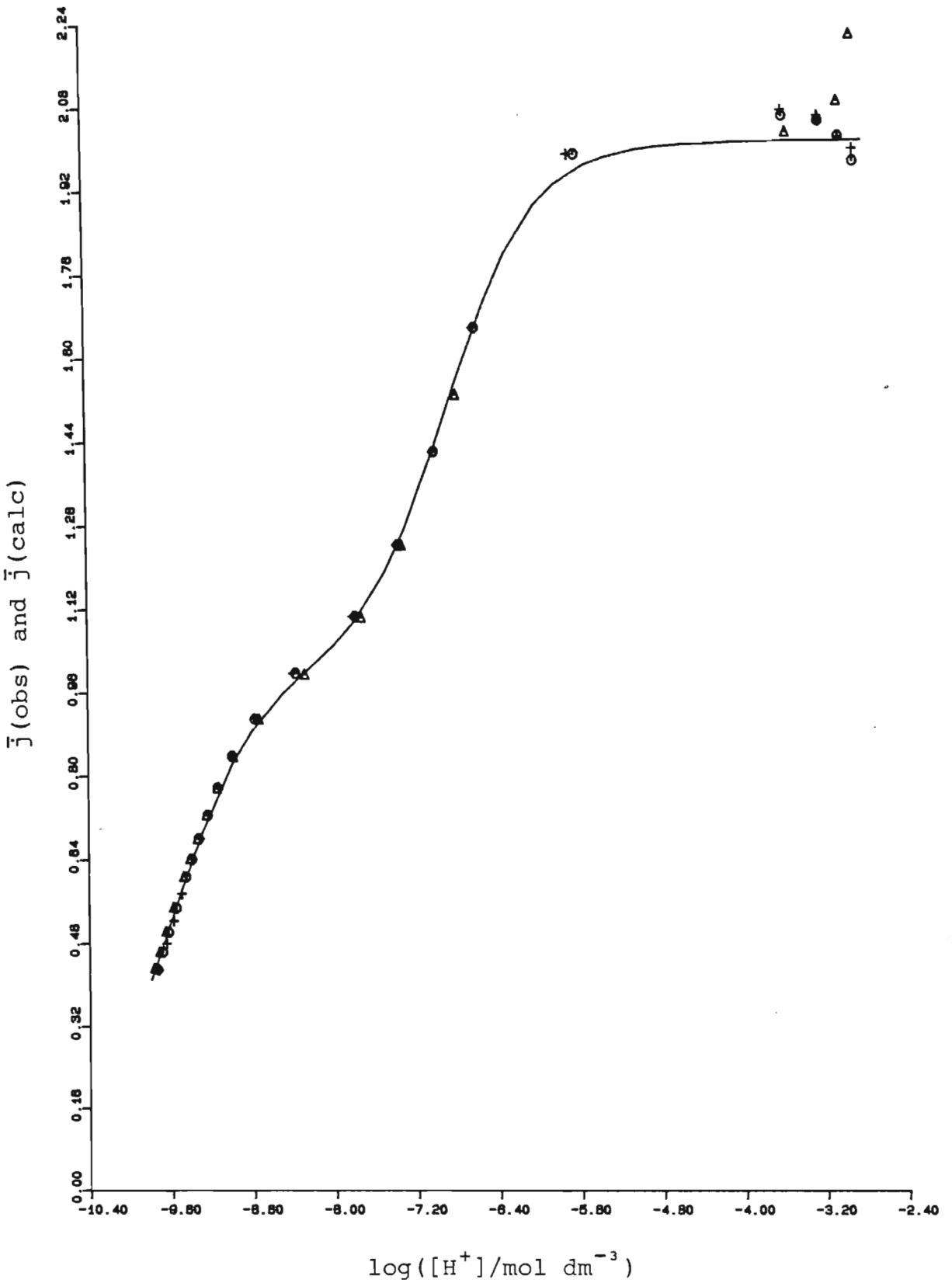

Figure 8.1 Formation curves for the protonation of etolen.

under rotation about their mid-point - a property of formation curves for dibasic acids. The fact that the $\bar{j}(\log[H^+])$ curves level off at $\bar{j} = 2$ is of course consistent with the diprotic nature of etolen.

A single value was used for the ionic product of water throughout the calculation of the protonation constants of etolen. The values obtained for these constants, together with the values available from the literature, are shown in Table 8.2.

In reference 182 the compilers give the following values (inter alia) for the protonation constants of etolen: $\log K_{101} = 10.12$ and $\log K_{201} = 7.21$. In the original paper (183), however, these values (stated as pK values) refer to the dissociation of a proton or protons from $Cu(etolen)^{2+}$, and not to the protonation of etolen. Similarly, the constant $\log K_{101} = 7.3$ quoted in reference 182 as being reported by Martell *et al.* (184) refers to the dissociation reaction depicted below, and not to the protonation of etolen.

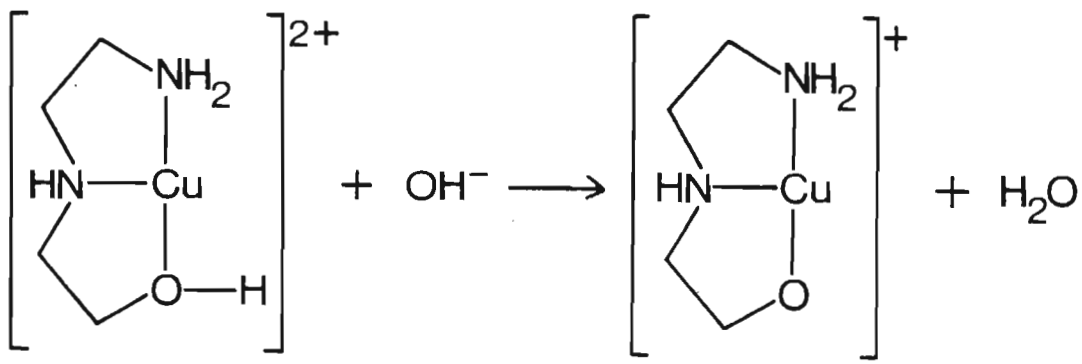

TABLE 8.2

Protonation constants obtained for the ligand etolen, together with values reported in the literature. (All values are for 25°C.)

$\log K_{101}$	$\log K_{201}$	Medium	Reference
9.641(3)	6.88(2)	0.5 mol dm^{-3} KNO_3	This work (MINIQUAD)
9.74 - 0.01	6.85 ± 0.1	0.5	167
9.74	6.84	0.5 mol dm^{-3} $NaClO_4$	175
9.73	6.93	0.5 mol dm^{-3} KNO_3	176
9.83	6.72	0.5 mol dm^{-3} KNO_3	177
9.59 ± 0.03	6.60 - 0.01	0.1	167
9.56 ± 0.01	6.60 ± 0.01	0.1 mol dm^{-3} KNO_3	178
9.52	6.49	0.1 mol dm^{-3} KNO_3	179
9.82	6.83	1 mol dm^{-3} KCl	180, 181
9.56	6.34	0	167, 175

The value of the first protonation constant of etolen (log K_{101}) obtained in this work is much lower than any of those reported in the literature and referring to the same conditions. This could be due to the fact that not many points were obtained at low values of $\bar{j}$ (i.e. below $\bar{j} = 0.42$), and so the value of log K_{101} is less precise than that of log K_{201}, for which points were obtained for the full range from $\bar{j} = 1$ to $\bar{j} = 2$. The value obtained for log K_{201} agrees fairly well with the reported values.

The protonation constants obtained were then used to calculate a formation curve for the protonation of etolen. This curve (see Figure 8.1) fits the experimental values fairly well, which indicates that the calculated protonation constants explain the experimental data adequately. Nevertheless it was found, when processing the calibration data for those potentiometric titrations in which the cell had been calibrated with strong acid and ligand, that the relation of cell e.m.f. to log $[H^+]$ was persistently non-linear if the protonation constants obtained in this work were used. When the values quoted in reference 167 (viz. log $K_{101} = 9.74$ and log $K_{201} = 6.85$) were used, linear plots resulted. In all subsequent calculations, therefore, these latter values were used.

The protonation constants for etolen reflect the fact that protonation in etolen can occur at both primary and secondary nitrogen atoms. These values are compared with those of several other amines in Table 8.3. One sees that substitution of a hydroxyethyl group on one nitrogen atom of en decreases the base strength of the ligand. This is to be expected because the electron-withdrawing effect of the oxygen atom means that protonation must occur at a more positive centre. The value of K_{101} for etolen is slightly larger than one might have expected, possibly because of the stabilizing effect of hydrogen bond formation. (See Figure 8.2.) Such bond formation causes steric hindrance, however, and thereby decreases the ability of the second nitrogen to attract a proton from solution, which is reflected in a lower value of K_{201}.

Delfini *et al.* (57) have shown, by means of n.m.r. techniques, that in triamines protonation occurs first at the primary nitrogen atoms and only thereafter at the secondary nitrogen atoms. We can therefore conclude that K_{101} for dien is associated with the protonation of a primary nitrogen atom. The similarity of this value to the corresponding value

TABLE 8.3

Protonation constants of various amines. (All values are for t = 25.00°C and μ = 0.5 mol dm^{-3}.)

Amine*	log K_{101}	log K_{201}	log K_{301}	Reference
en	9.980	7.280		185
eten	10.27	7.33		186
dien	9.79	8.98	4.25	57
etolen	9.74	6.85		167
2-hn	9.32	6.52		177

* en = ethylenediamine
eten = N-ethylethylenediamine
dien = diethylenetriamine
etolen = 2-(2-aminoethyl)aminoethanol
2-hn = N,N'-di(2-hydroxyethyl)ethylenediamine

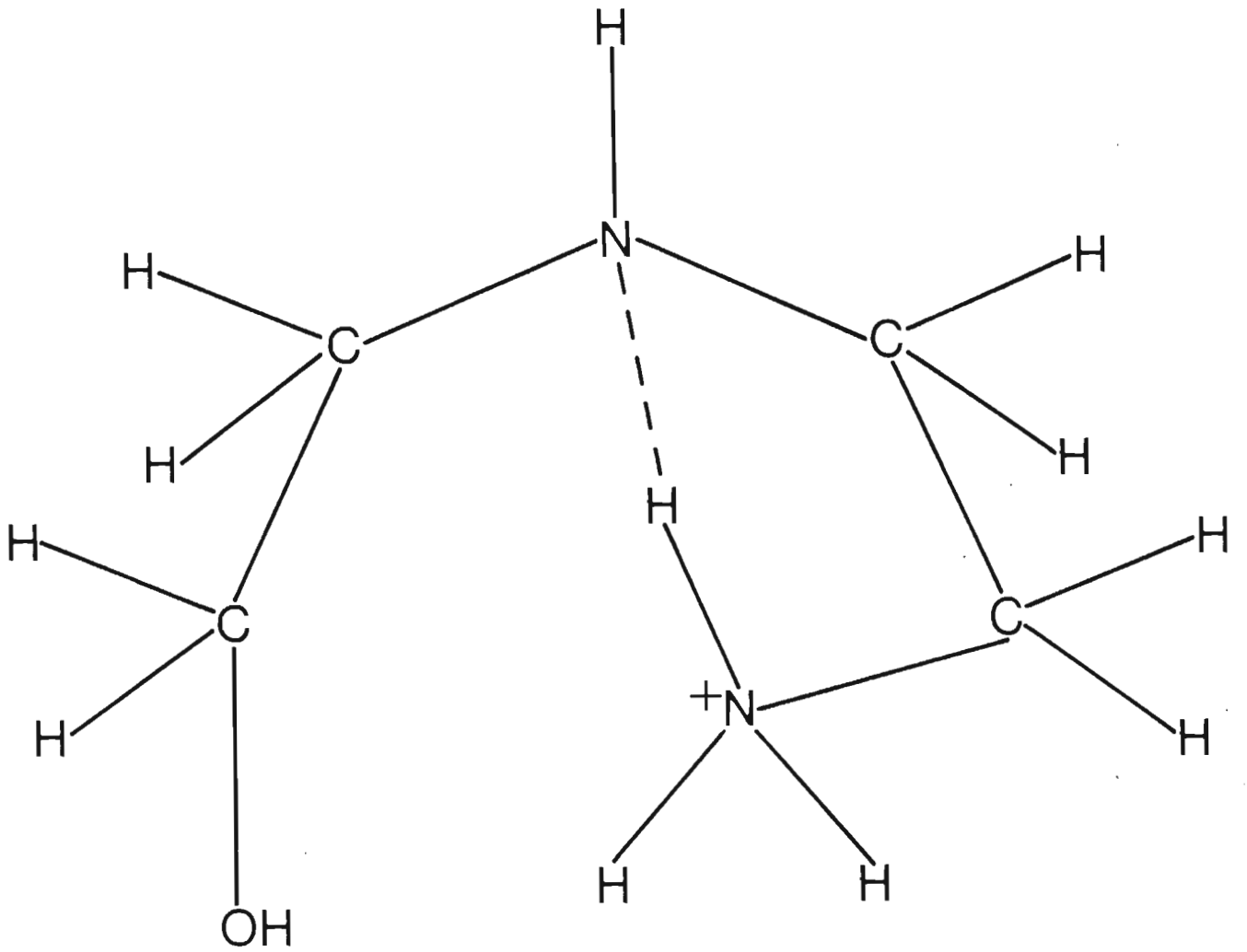

Figure 8.2 Possible hydrogen bonding in the (etolen)H^+ ion.

for etolen suggests that in etolen protonation must also occur first at the primary nitrogen atom. This implies that the secondary nitrogen atom in etolen is less basic than the primary one. This is in fact the tentative conclusion reached by Keller and Edwards (181).

The stability constant and enthalpy change associated with the dissociation of water, and the protonation constants of the ligand, were used as inputs in the calculation of the heats of protonation of etolen. In Table 8.4 the results obtained are compared with similar values reported in the literature. Relative to the standard deviations quoted, these results agree very well with the reported values.

The value of $|\Delta H^{\ominus}_{101}|$ for the protonation of etolen is greater than $|\Delta H^{\ominus}_{201}|$, as is also the case for other diamines (55). This trend has been explained by Barbucci and Barone (55) as follows. The presence of a positively charged group, in this case possibly the protonated primary nitrogen group, withdraws electron density from the second protonation site. (This effect may be increased by hydrogen bond formation.) This causes a decrease in the strength of the second N-H bond formed and an increase in the repulsion between the incoming hydrogen ion and the atoms of the amine. These effects result in a less exothermic $\Delta H^{\ominus}_{201}$.

The value of $\Delta S^{\ominus}_{201}$ is less than that of $\Delta S^{\ominus}_{101}$, in accordance with the results for other diamines. The positive entropy change for the first stage of protonation reflects the fact that the reaction proceeds with the liberation of several molecules of water. The entropy change for the second stage of protonation, however, is negative. This is caused by an increase in the rigidity of the molecule, which is in turn due to the repulsion between the two positively charged centres which in etolen are in close proximity. This chain-stiffening effect counteracts any entropy increase which might result from the release of water molecules in the second step of protonation.

8.2. The hydrogen ion - oden system

The first step in the analysis of the potentiometric data was the calculation of values of $\bar{j}(\log [H^+])$. It was found that, if the $\bar{j}$ values were calculated by taking into account the amount of carbonate present in the

TABLE 8.4

Thermodynamic parameters obtained for the protonation of the ligand etolen together with the values reported in the literature. All data are for 25°C and μ = 0.5 mol dm^{-3}.

Reaction	log K	$\Delta H^{\ominus}$/kJ mol^{-1}	$\Delta S^{\ominus}$/J $mol^{-1}K^{-1}$	Reference
$H^+ + L \rightleftharpoons HL^+$	9.74	-47.0(2)	28.8	This work
$H^+ + HL^+ \rightleftharpoons H_2L^{2+}$	6.85	-41.6(3)	-8.4	This work
$H^+ + L \rightleftharpoons HL^+$	9.74	-46.6(3)	30.1(8)	77
$H^+ + HL^+ \rightleftharpoons H_2L^{2+}$	6.84	-42.1(6)	-10.5(2.1)	77

sodium hydroxide titrant (see Section 4.1.1), the plots of $\bar{j}$ against $\log[H^+]$ were not superimposable. These plots are shown in Figure 8.3. However, when the $\bar{j}$ values were calculated by using the total base concentration obtained from the Gran plot, the formation curves were found to be superimposable for values of $\bar{j}$ greater than about 0.5. (See Figure 8.4.) Unfortunately, this procedure produced some negative $\bar{j}$ values, which are of course meaningless. This suggests that the carbonate present in the system need only be distinguished from hydroxide above a certain value of the solution $p[H^+]$. In order to select this cutoff value, $\bar{j}$ values were calculated for the protonation of oden, with -9.5, -10.0, and -10.5 as the cutoff value for $\log[H^+]$. Figure 8.5 illustrates the effect of varying the cutoff point for one of the titrations. From these calculations it was concluded that $\log[H^+] = -10.0$ was the best cutoff point, since for this value the formation curve was most symmetrical under rotation about the point with $\bar{j} = 1$ - a required property of the formation curve of a diprotic base such as oden.

Thus, in all the subsequent calculations for solutions in which carbonate was present, the following assumptions were made.

1. At values of $p[H^+] \leqslant 10$ the carbonate anion was assumed to behave like two moles of hydroxide because of the following equilibria:

$$CO_3^{=} + H_2O \rightleftharpoons 2OH^- + CO_2\uparrow$$

and

$$CO_3^{=} + 2H^+ \rightleftharpoons H_2O + CO_2\uparrow.$$

These equilibria were driven to the right because nitrogen was bubbled through the solution in the reaction vessel and this expelled carbon dioxide from the system (187). In this region the total base concentration (as obtained from the right-hand branch of the appropriate Gran plot) could be used as the 'base' concentration.

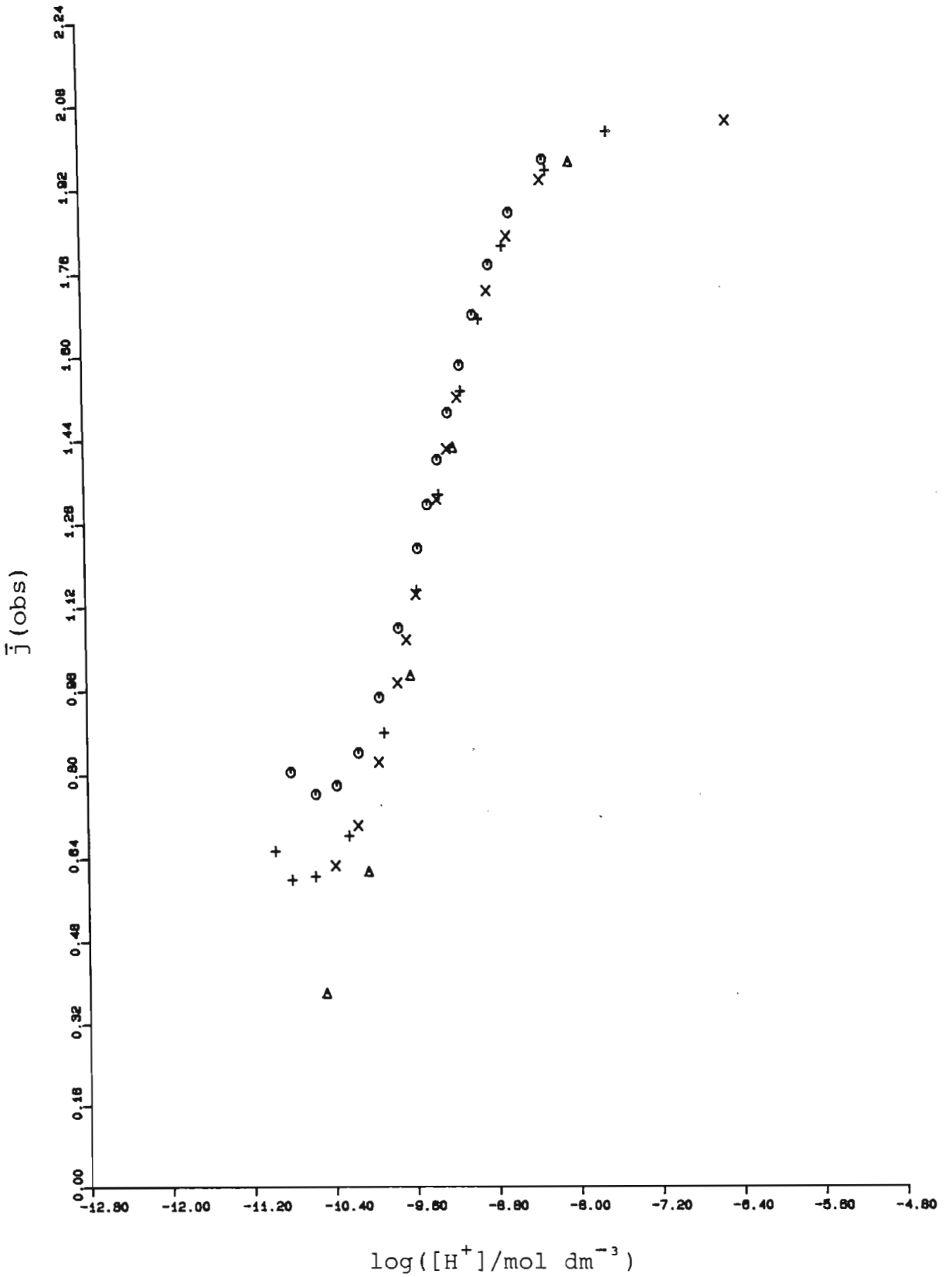

Figure 8.3 Formation curves for the protonation of oden. These curves were computed by taking into account the amount of carbonate present in the sodium hydroxide titrant.

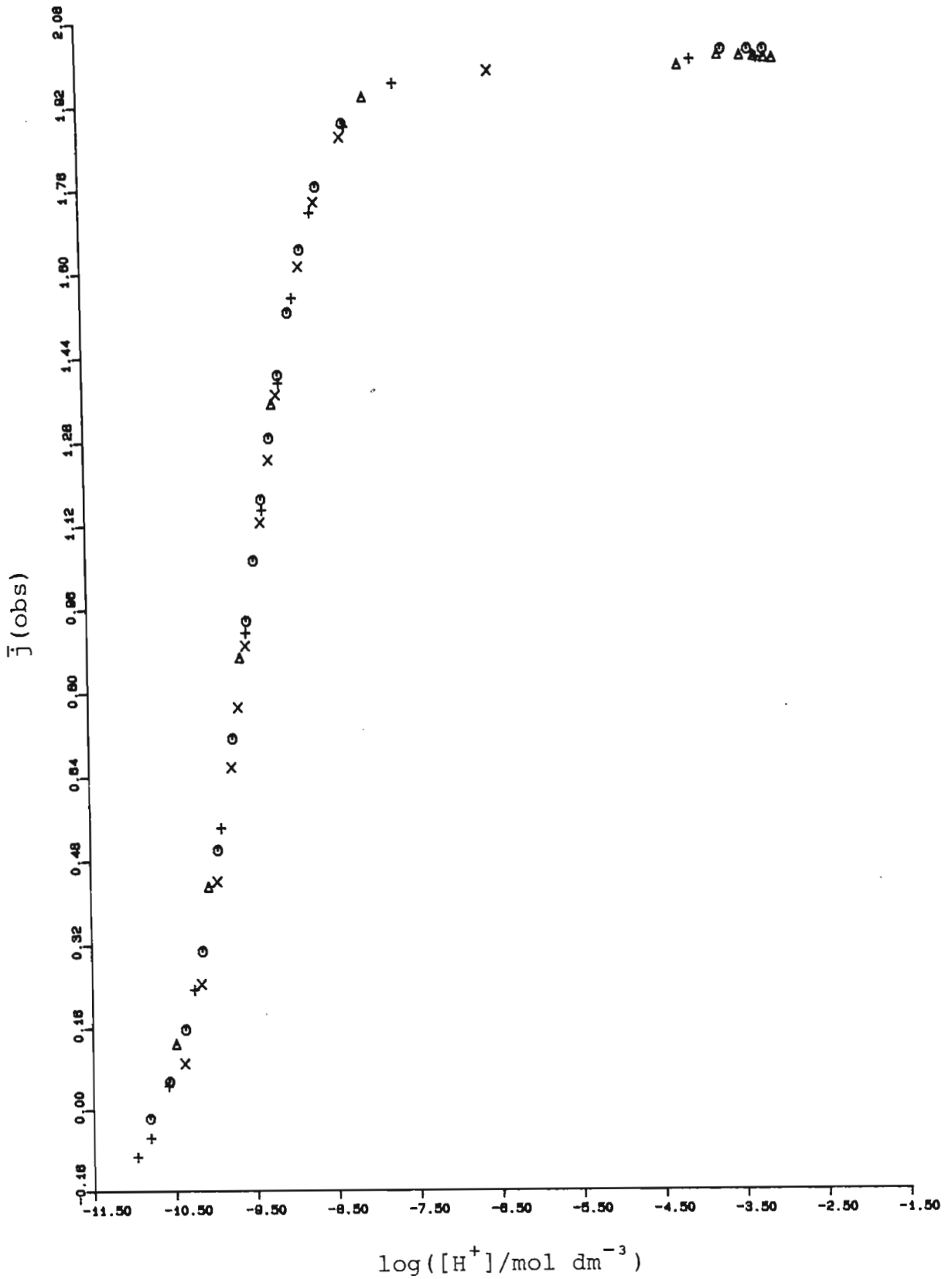

Figure 8.4 Formation curves for the protonation of oden, computed by using the total base concentration.

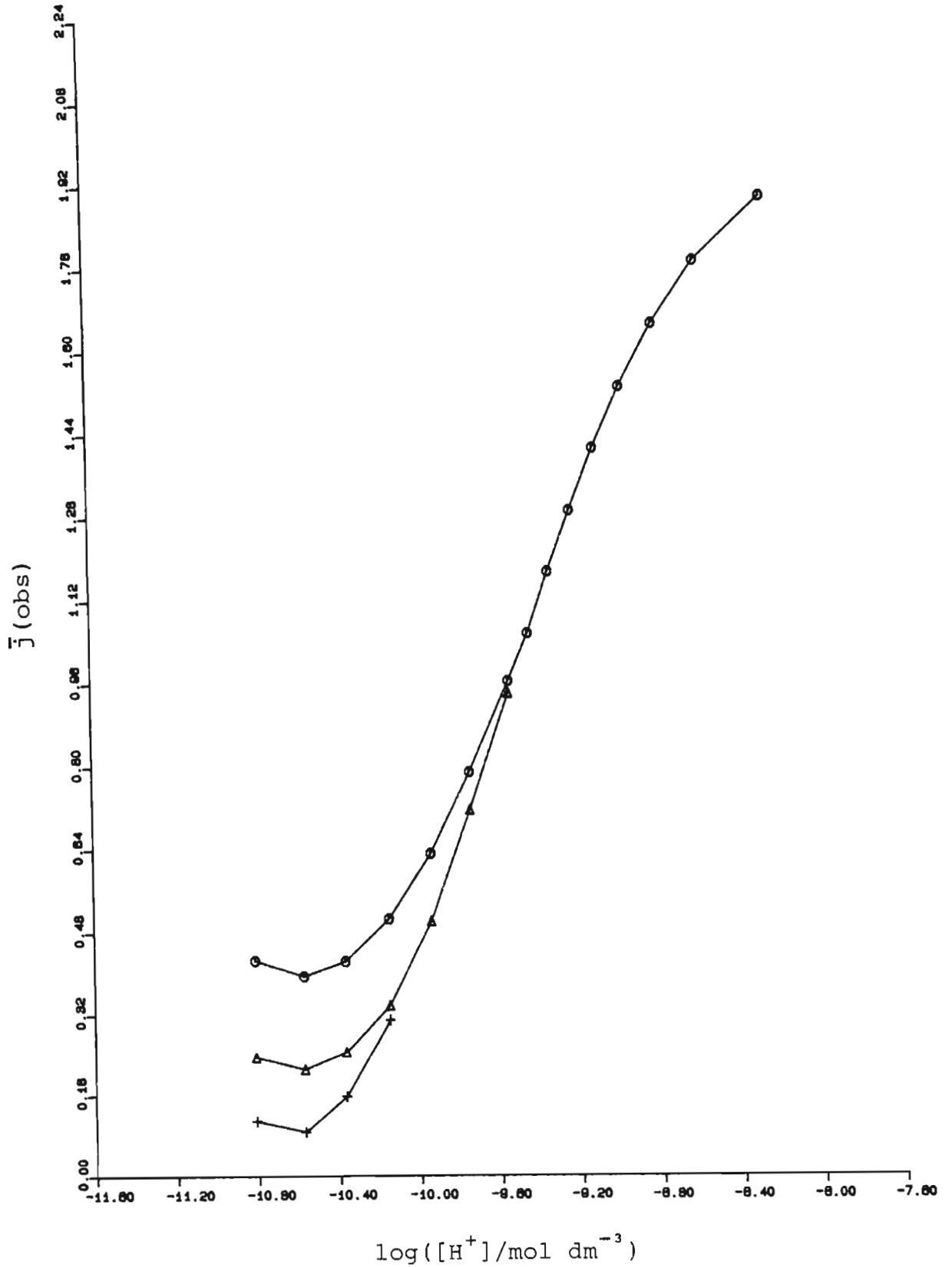

Figure 8.5 Formation curves computed for titration 1 for the protonation of oden, with different cutoff values of log $[H^+]$. The symbols ⊙, △ and + refer to cutoff values of -9.5, -10.0 and -10.5 respectively.

2. At $p[H^+]$ values above 10 the carbonate present will react as follows:

$$CO_3^{=} + H_2O \rightleftharpoons HCO_3^- + OH^-.$$

In these solutions the carbonate present had to be distinguished from hydroxide. The actual hydroxide concentration as obtained from the left-hand branch of the Gran plot was used, and the effects of the above equilibrium were accounted for from a knowledge of the appropriate equilibrium constant.

The formation curves for the protonation of oden, calculated in accordance with the above assumptions, are shown in Figure 8.6. The curves obtained for different titrations are superimposable - an indication that the titrations were reproducible. The curves level off at $\bar{j} = 2$, as one would expect for a diprotic base.

In the calculation of the protonation constants of oden the ionic product of water was held constant. The titration points having values of log $[H^+]$ below -10.6 were not included in the data set, because in this region the formation curves were irreproducible. The protonation constants obtained in this work, together with those reported in the literature, are shown in Table 8.5.

As can be seen from Figure 8.6, the fit of $\bar{j}$(calc) to $\bar{j}$(obs) is satisfactory. Hence the constants obtained were considered to give an adequate account of the available data.

The value of log K_{101} obtained for the protonation of oden is much lower than that reported by Barbucci and Vacca (78). Since the details of the experiments performed by Barbucci and Vacca are not available, it is difficult to explain this difference. Nevertheless the value obtained in this work agrees fairly well with the value given in reference 188. (The difference in ionic strength between the two measurements may not greatly affect the first protonation constant, since the ligand is uncharged.) If the value of log K_{201} reported in reference 188 is corrected from μ = 0 mol dm^{-3} to μ = 0.5 mol dm^{-3} by means of the Davies equation (174), the same value as reported in this work is obtained. This value is also very close to that of Barbucci and Vacca (78).

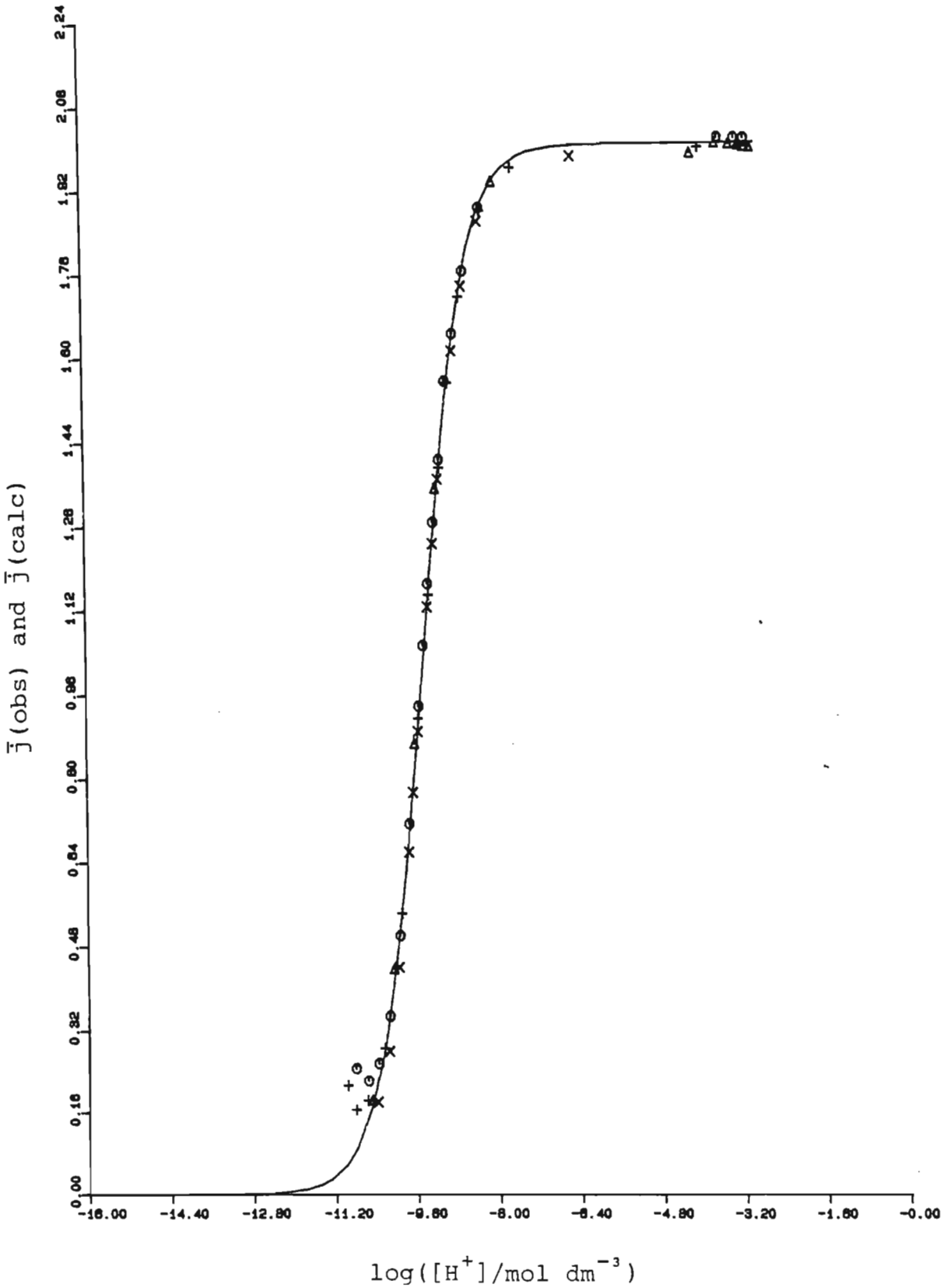

Figure 8.6 Formation curves for the protonation of oden, computed by using log[H$^+$] = -10.0 as the cutoff point.

TABLE 8.5

Protonation constants obtained for the ligand oden, together with the values reported in the literature.

log K_{101}	log K_{201}	Temperature/°C	Medium	Reference
9.77(1)	9.17(2)	25	0.5 mol dm^{-3} KNO_3	This work (MINIQUAD)
9.888	9.146	25	0.5 mol dm^{-3} KNO_3	78
9.75	8.90	25	0	188
10.20(1)	9.26(1)	10	0_{corr}	189*
9.88(1)	8.94(3)	20	0_{corr}	
9.59(2)	8.62(2)	30	0_{corr}	
9.33(1)	8.28(1)	40	0_{corr}	

*In this case the numbers in parentheses represent 95 % confidence limits.

The $\bar{j}$ ($\log[H^+]$) plots for both oden and etolen show no plateau at $\bar{j} = 1$ because the difference between the stepwise formation constants is insufficient to prevent overlap of the successive protonation steps. For oden this difference, i.e. between $\log K_{101}$ and $\log K_{201}$, is much smaller (0.6) than for etolen (2.89). This is to be expected, since oden has two primary nitrogen atoms (which one would expect to have very similar protonation constants) and etolen has one primary and one secondary nitrogen atom. In addition, the protonation sites in oden are much further apart than in etolen and thus exert less influence on each other. The protonation constant of the second nitrogen atom in oden has nevertheless a lower value than the first. This too is possibly due to hydrogen bonding of the type depicted in Figure 8.2 and the increased repulsion of the incoming hydrogen ion caused by the presence of a positively charged centre. These effects, though, are less marked than in etolen because of the greater distance between the amine groups. Oden is more basic than etolen because of the symmetric nature (175) of the former ligand and because there is less steric hindrance for the incoming hydrogen ions.

In the calculation of the heats of protonation of oden, the stability constant and enthalpy change associated with the dissociation of water, and the protonation constants of the ligand,were used as inputs. The results obtained in this work, together with the values reported in the literature, are shown in Table 8.6. The enthalpy changes of protonation obtained for oden are in good agreement with the reported values.

As can be observed, $|\Delta H^{\ominus}_{201}| > |\Delta H^{\ominus}_{101}|$ for oden, unlike the situation for most other diamines. This reversal of trend was explained by Barbucci and Barone (55) as follows.

Since oden is symmetric about the oxygen atom, when it is diprotonated it exists as two terminal centres of positive charge separated by a central negative charge. This configuration generates a new orientation of the solvent water molecules (as depicted in Figure 8.7) about the diprotonated amine. Barbucci and Barone have calculated that this produces a favourable energy contribution of 3.3 kJ mol^{-1}. This value is in close agreement with the difference $|\Delta H^{\ominus}_{201}| - |\Delta H^{\ominus}_{101}|$ obtained in this work (3.2 kJ mol^{-1}).

TABLE 8.6

Thermodynamic parameters obtained for the protonation of the ligand oden together with the values reported in the literature.

$\log K_{101}$	$\Delta H^{\ominus}_{101}$/ kJ mol^{-1}	$\Delta S^{\ominus}_{101}$/ J $mol^{-1}K^{-1}$	$\log K_{201}$	$\Delta H^{\ominus}_{201}$/ kJ mol^{-1}	$\Delta S^{\ominus}_{201}$/ J $mol^{-1}K^{-1}$	Temperature/°C	Medium	Reference
9.77	-50.2(5)	18.7	9.17	-53.4(7)	-3.6	25	0.5 mol dm^{-3} KNO_3	This work
9.888	-50.7	19.3	9.146	-54.2	-6.7	25	0.5	78
9.75	-50	17	8.90	-54	-13	25	0	188
10.20		21	9.26		-17	10		
9.88		21	8.94		-17	20		
	-49.0			-55.2			0_{corr}	189
9.59		21	8.62		-17	30		
9.33		21	8.28		-17	40		

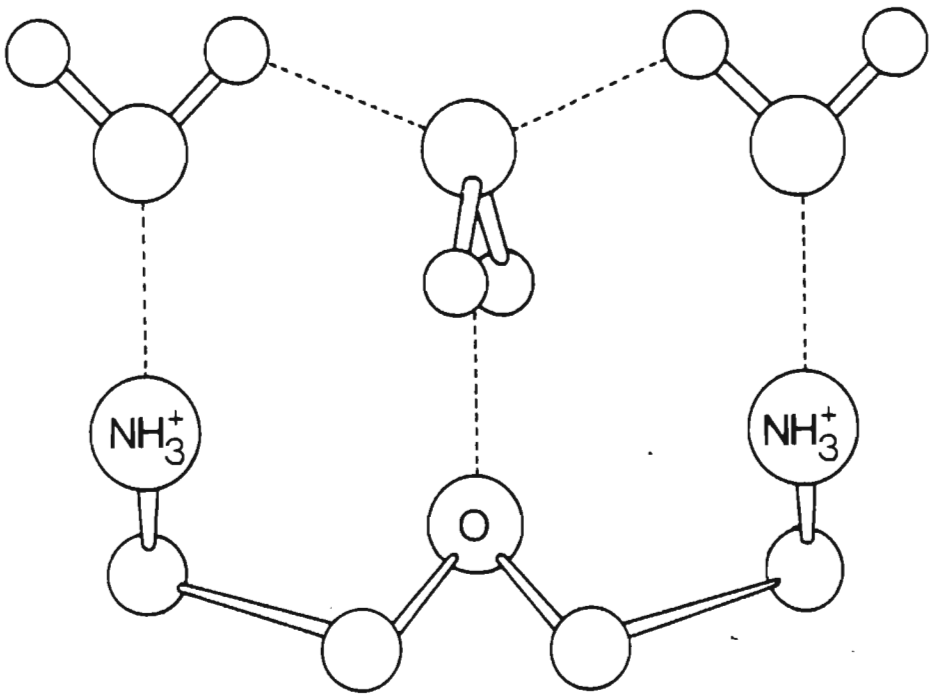

Figure 8.7 Arrangement of the solvent water molecules in the vicinity of diprotonated oden.

The decrease in ΔS° with successive protonations observed for etolen is also observed for oden. However, the decrease is smaller for oden than for etolen. This is possibly because the two centres of positive charge are further apart in oden and this leads to a smaller decrease in the ligand entropy, i.e. a smaller increase in rigidity of the ligand. The solvent orientation effects discussed above may tend to increase the rigidity of the ligand, but presumably this causes only a small decrease in entropy.

8.3. The nickel ion - etolen system

The observed formation curves for the Ni-etolen system are shown in Figure 8.8. A number of features of these curves will now be discussed.

One sees that the formation curves are fairly superimposable up to a value of $\bar{Z} = 1.5$. Above this value there is a 'fanning out' effect, as well as 'shoot-up' and 'curl-back'. The fanning out for $\bar{Z}$ values between 1.5 and 2.0 is most probably due to small errors in the solution concentrations. From an analysis of the formation curves obtained by varying the solution concentrations slightly, it was found that $\bar{Z}$ was more sensitive to errors in the concentrations of the components at high $p[H^+]$ values than at low values. These findings are in keeping with those of Cabani (190) and Avdeef *et al.* (191). The reason why $\bar{Z}$ is not very sensitive to concentration errors at low values of $p[H^+]$ is that in this region $[H]_t$ is always significantly larger than $[H]$. This results from the presence of substantial amounts of protonated ligand. All the data points with $\bar{Z} \geqslant 1.5$ were obtained at $p[H^+]$ values greater than about 6.5, where these errors become more significant.

The reverse runs of titrations 2 and 3 exhibit 'shoot-up' and 'curl-back' at $\bar{Z}$ values greater than 2. These data points were all obtained at basic $p[H^+]$values (above $p[H^+] = 7.5$), i.e. when $[H]_t$ in equation (4.98) becomes negative. In these cases the expression for $[L]$, given by equation (4.103), has a numerator which is the difference between two numbers of similar magnitude. It was found that a small uncertainty in the value of $[H]_t$ results in a large uncertainty in the value of $\bar{Z}$ for $\bar{Z} > 2$, i.e.

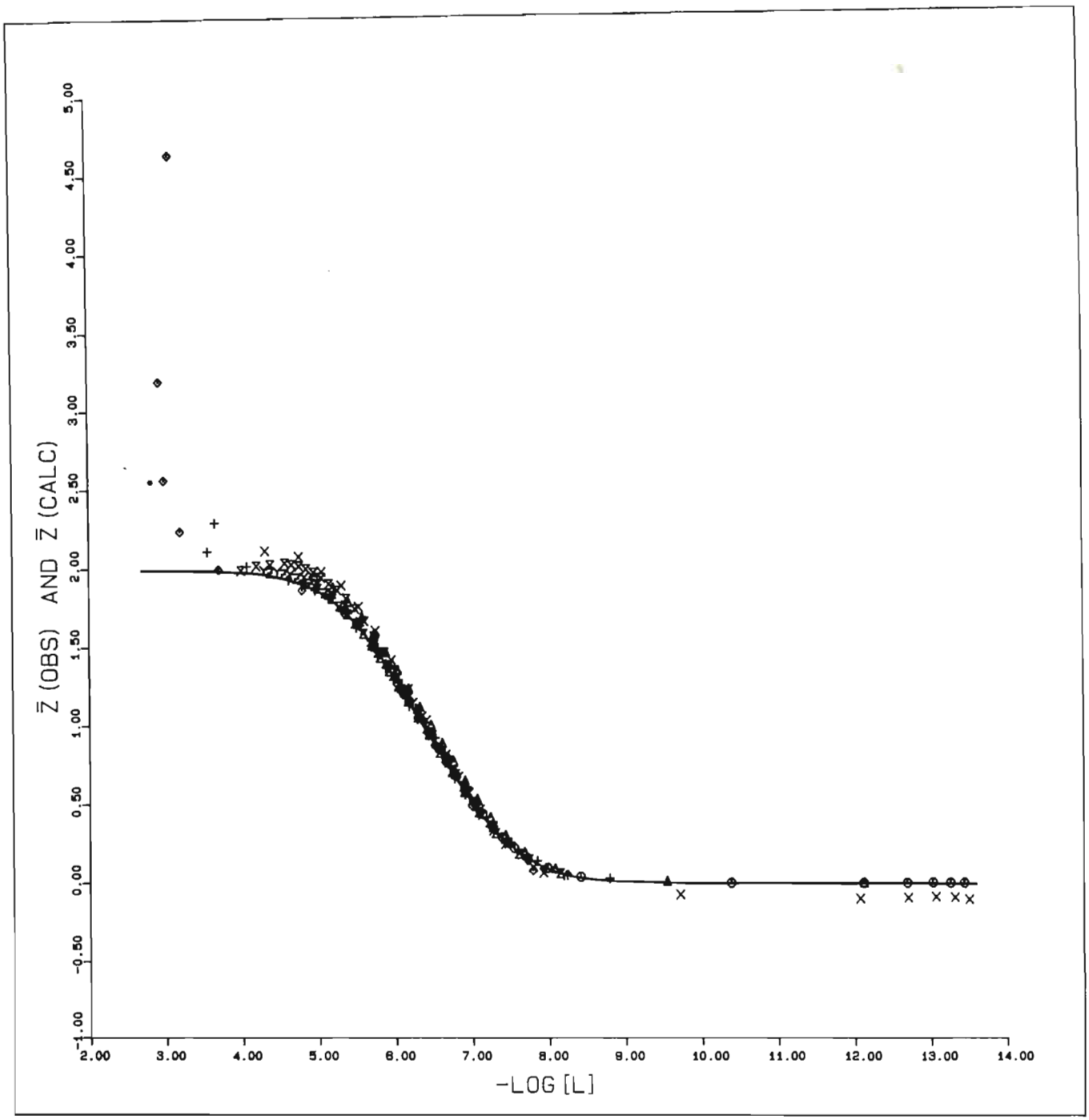

Figure 8.8 Formation curves for the nickel - etolen system.

when excess hydroxide is present. Hence this 'curl-back' and 'shoot-up' effect may well be a manifestation of experimental error. It is noted that these effects occur only in those titrations in which no excess protonated ligand is present. One cannot exclude the possibility, though, that these effects may arise from the formation of ternary hydroxo-complexes, or traces of ML_3, or the deprotonation of the alcoholic group of etolen.

Thus, within estimated experimental error, the formation curves obtained for $\bar{Z}$ values between 0 and 2 are superimposable. Since the metal ion concentration was varied, and repeat and reverse titrations were performed, one can conclude that no polynuclear species are present, the results are reproducible, and the equilibria are reversible.

Because the highest reliable value of $\bar{Z}$ reached was approximately 2, and there was evidence of a plateau at this value, the highest major mononuclear complex formed was taken to be ML_2. Also, the formation curves are fairly symmetrical under rotation about the point with $\bar{Z} = 1$, which suggests that only two major species, viz. ML and ML_2, are present. Attempts were made to introduce various minor species into the model, but with no success.

During the calculation of the stability constants for this system, fixed values of the stability constants for the species H_2O, HL^+, H_2L^{2+} and $Ni(OH)^+$, as given in Table 8.1 and Section 8.1, were used. The results obtained, together with pertinent values reported in the literature, are shown in Table 8.7.

The $\bar{Z}$ (calc) curve derived from these results, and shown in Figure 8.8, agrees fairly well with the experimental formation curves. Hence it was concluded that the complexes $Ni(etolen)^{2+}$ and $Ni(etolen)_2^{2+}$ adequately account for the potentiometric data.

The stability constants obtained for this system agree very well with those reported in references 167 and 175 and obtained under similar experimental conditions. However, they do not agree well with those obtained by Hall *et al.* (183), and even less with those reported by Edwards (180, 192).

TABLE 8.7

Stability constants obtained for Ni(II) with etolen, together with the values reported in the literature. (All data are for 25°C.)

$\log K_{011}$	$\log K_{012}$	Medium	Reference
6.955(9)	5.83(1)	0.5 mol dm^{-3} KNO_3	This work (ESTA)
6.96(1)	5.82(2)	0.5 mol dm^{-3} KNO_3	This work (MINIQUAD)
6.97 - 0.3	5.83	0.5 mol dm^{-3}	167
6.97	5.83	0.5 mol dm^{-3} $NaClO_4$	175
6.66	5.80	0.5 mol dm^{-3} KNO_3	183
6.82	5.62	0.1 mol dm^{-3}	167
7.78	6.08	1 mol dm^{-3} KCl	180, 192
6.76	5.52	0	167

The values reported by Edwards are very high relative to the others, even if one takes into account the differences in ionic strength used. However, if the results for other systems reported by Edwards in reference 192 are compared with other literature values, it will be noticed that his values are all considerably higher. When the formation curves obtained by Edwards are compared with those obtained in this work the former are seen to lie at lower free ligand concentrations, which implies greater stability of the complexes present. Thus there seems to be something inherent in the experimental method employed by Edwards that gives rise to higher values. His manner of calculating log K values by the 'half $\bar{n}$ method' may be the problem. The equilibria in this system are not sufficiently separated for this method to be reliable. As his 'raw' data were not available it was not possible to re-analyze his data to see if any improvement could be achieved.

Although the value reported by Hall *et al.* for log K_{012} is in fair agreement with the values reported later, the value of log K_{011} is substantially lower. The reason for this discrepancy is not apparent.

These studies, like those of other authors (175, 183, 192), do not provide evidence for the formation of a $Ni(etolen)_3^{2+}$ complex in solution. Breckenridge (67) and Karpeiskaya *et al.* (193) report the formation of such a complex in the solid state, however. It has been shown (65) by means of n.m.r. contact shifts that etolen behaves as a tridentate ligand in aqueous solution. This seems to indicate that the ML_3 complex, which requires etolen to bind as a bidentate ligand, does not form in solution.

To calculate the heats of formation of the Ni-etolen complexes, LETAGROP KALLE was provided with the stability constants and enthalpy changes for the species H_2O, HL^+, H_2L^{2+} and $Ni(OH)^+$, and the stability constants for ML^{2+} and ML_2^{2+}. The thermodynamic parameters obtained for the formation of $Ni(etolen)^{2+}$ and $Ni(etolen)_2^{2+}$ are shown in Table 8.8, together with pertinent values reported in the literature.

The enthalpy changes obtained for the formation of the Ni-etolen complexes do not agree well with the values reported by Barbucci (77). However, the calorimetric results obtained for the protonation experiments agree very well with those of Barbucci. This seems to indicate that the experi-

TABLE 8.8

Thermodynamic parameters of complex formation for Ni(II) with etolen. All data are for 25°C.

$\log K_{011}$	$\Delta H^{\ominus}_{011}$/ kJ mol^{-1}	$\Delta S^{\ominus}_{011}$/ J $mol^{-1}K^{-1}$	$\log K_{012}$	$\Delta H^{\ominus}_{012}$/ kJ mol^{-1}	$\Delta S^{\ominus}_{012}$/ J $mol^{-1}K^{-1}$	Medium	Reference
6.96	-29.7(2)	33.6	5.82	-37.8(4)	-15.4	0.5 mol dm^{-3} KNO_3	This work
6.97	-32.6(5)	24.3(1.7)	5.83	34.8(1.0)	-5.0(3.3)	0.5 mol dm^{-3} $NaC\ell O_4$	77

mental methods used here are not in question. The discrepancy could arise from the way Barbucci performed the complex formation titrations. He destroyed the Ni-etolen complexes by addition of excess nitric acid. This indirect method has the disadvantage that the heat liberated by the reactions of interest is overshadowed by the heat liberated by the protonation reactions. In this work the heat liberated was a direct measure of the extent of complex formation. The $p[H^+]$ in Barbucci's experiments would also have been higher than in these experiments where part of the background electrolyte was replaced by protonated ligand. This higher $p[H^+]$ may have led to hydrolysis reactions which were not corrected for. Apart from the reasons mentioned above, it is difficult to explain the discrepancy, especially as the same model of the species in solution and virtually the same stability constants were used in the calculations.

The exothermicity of the complex formation reactions is expected, because these are reactions between a fairly 'soft' ligand and a metal ion which is borderline (194) between 'hard' and 'soft'. Hence the energy released to form the metal-nitrogen bonds greatly exceeds that required to displace the coordinated water molecules. The greater exothermicity on reaction with a second ligand molecule is in keeping with the behaviour of many 3d metal ions when reacted with polyamines, and has been explained as follows (42). On the addition of a molecule of ligand the charge on the metal ion is partially neutralized and the soft character of the metal ion is enhanced. Thus the reaction with a second ligand molecule will involve a more covalent interaction, with a correspondingly greater (exothermic) heat of reaction.

The entropy change for the first step is positive and that for the second step is negative. This is in keeping with the model for metal-polyamine complex formation suggested by Paoletti *et al.* (42), and they explain the observation as follows. On complex formation solvent molecules attached to the metal ion and ligand are released, which makes a positive contribution to the entropy change. This positive contribution is partially offset by the loss of ligand entropy on formation of the chelate ring. However, for the first step of complex formation the former contribution is greater than the second and so the overall entropy change observed is positive. The addition of a ligand molecule to the metal ion causes a dielectric screening of the metal ion, which in turn results in a decrease

in the interaction with the solvent. Hence, on the addition of a second chelating ligand, fewer water molecules will be released and the loss in ligand entropy exceeds the positive contribution made by the release of solvent molecules. This results in decreasing entropy changes with successive steps of complexation.

In considering the entropy change for the reaction $Ni^{2+} + 2L \rightleftharpoons NiL_2^{2+}$, Barbucci (77) used the fact that the value for etolen (19.2 J mol^{-1} K^{-1}) is larger than that for dien (0) to suggest that one of the alcohol groups in $Ni(etolen)_2^{2+}$ is not coordinated to the metal ion. The value obtained here for this entropy change (18.2 J mol^{-1} K^{-1}) is only slightly smaller. One can however explain the entropy changes observed for the formation of the Ni-etolen complexes by making use of the results of Everhart *et al.* (65). They showed for $Ni(etolen)(H_2O)_3^{2+}$ that, although $\Delta H^{\ominus}$ for coordination of the alcoholic oxygen is 0, coordination is favoured by a gain in entropy of about 6.3 J mol^{-1} K^{-1}. When this result is used in conjunction with the entropy changes for the Ni-dien complexes in the equation

$$\Delta S^{\ominus}_{pqr}(etolen) = 2[\Delta S^{\ominus}_{pqr}(dien)/3] + 6.3,$$

one obtains $\Delta S^{\ominus}_{011}$ = 30.0 J $mol^{-1}K^{-1}$ and $\Delta S^{\ominus}_{012}$ = -17.4 J mol^{-1} K^{-1} for the stepwise formation of the Ni-etolen complexes. These estimates are fairly close to the experimentally observed values. It therefore seems reasonable to assume that etolen behaves as a tridentate ligand in these complexes.

8.4. The nickel ion - oden system

The formation curves obtained from the potentiometric data for this system are shown in Figure 8.9.

One notable feature is that, except for low values of -log[L], the curve for titration no. 3 (denoted by $\times$) lies slightly above the others. This titration was carried out at the lowest metal ion concentration used ($[Ni^{2+}]_0$ = 5.007 x 10^{-4} mol dm^{-3}). It is well known that titrations involving sub-millimolar concentration levels are more prone to experimental error, so it was concluded that this upward displacement was merely a reflection of slight inaccuracies in the solution concentrations.

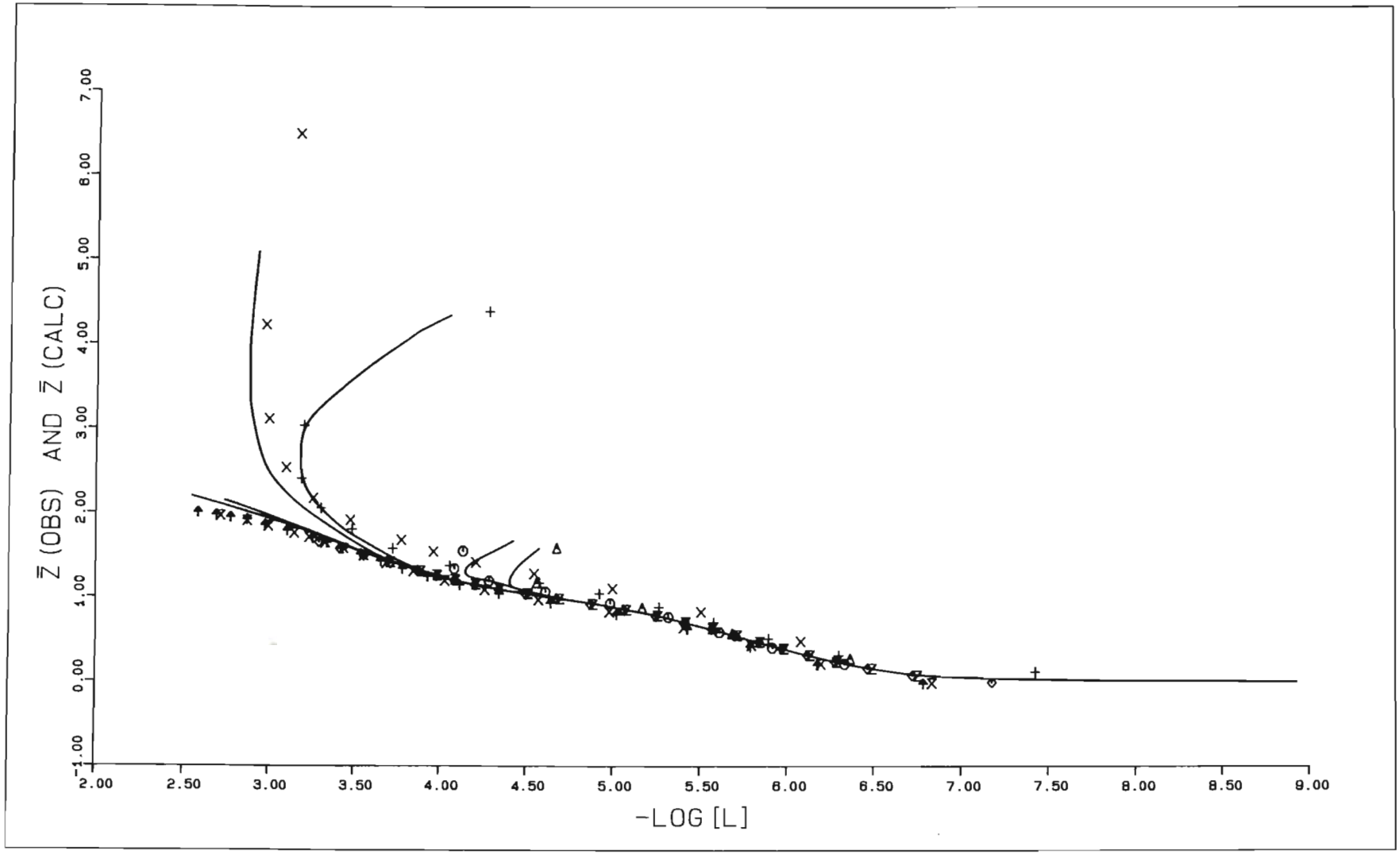

Figure 8.9 Formation curves for the nickel - oden system.

Those titrations (nos. 1 - 3) which were carried out at higher $p[H^+]$ values exhibit 'curl-back' and 'shoot-up'. These effects are observed even for $\bar{Z}$ values somewhat less than 2 (which was not the case for the Ni-etolen system). This suggests that these effects may not be due only to experimental error, and that the possible presence of hydrolysed or protonated species needs to be investigated. The 'curl-back' feature starts at lower $\bar{Z}$ values for titration no. 1 than for the other two. This is not surprising, because no. 1 was carried out at the highest metal to ligand ratio of the three. The operating $p[H^+]$ was therefore higher and hydrolysis more likely to occur at an early stage. It is interesting to note that those titrations (nos. 4 - 7) which were carried out with protonated ligand as part of the background electrolyte exhibit no hydrolysis and level off at $\bar{Z} = 2$.

The plots of the repeat titrations (nos. 4 and 7) were completely superimposable, which indicates that the results are reproducible. The forward and reverse runs of titration no. 1 are also superimposable, up to $\bar{Z} \sim 1$. Thus within experimental error the formation curves are superimposable (apart from the 'curl-back' and 'shoot-up'), and one can conclude that no polynuclear species are present.

For species selection purposes, ML and ML_2 were treated as the major complexes present. Attempts were then made to introduce various protonated and hydrolysed species into the model. Fixed values were used for the stability constants of the species H_2O, HL^+, H_2L^{2+} and $Ni(OH)^+$. Table 8.9 lists the results obtained for the 'successful' models tried, i.e. those models for which the program ESTA yielded successful refinements.

For models 1 and 2 the data were divided into two sets. One set (titrations 4 - 7) consisted of those titrations which were carried out with protonated ligand as part of the background electrolyte, and exhibited no 'shoot-up' or 'curl-back'. The titrations in the other set (nos. 1 - 3) did not use protonated ligand, and did exhibit 'shoot-up' and 'curl-back'. All attempts to include hydroxy species in the model failed when the two sets were treated separately. The 'curl-back' and 'shoot-up' effects could be reproduced only when the complete data set was used. On the basis of the value of the objective function U, model 4 was taken to be the best description of the species present in solution. It is

TABLE 8.9

Stability constants* for Ni(II)-oden complexes obtained from different models.

Model	1	2	3	4
ML^{2+}	5.86	5.75	5.75	5.78
ML_2^{2+}	9.91	9.30	9.20	9.25
$ML(OH)^{+}$			-3.60	-4.65
$ML_2(OH)^{+}$				-0.33
Titrations used	1 - 3	4 - 7	1 - 7	1 - 7
No. of points	44	83	127	127
U_{ESTA}	3124	81	635	369
R_{ESTA}	0.030	0.004	0.012	0.009

*For complexes containing the hydroxide ion, e.g. $ML_r(OH)_p$, the values given in the table represent log β_{-p1r} + p(log K_w).

pleasing to note that the stability constants in model 4 for the species ML and ML_2 are fairly close to those obtained in model 2. The formation curves obtained from the data used in model 2 exhibit all the features expected when only two mononuclear species are present in solution. The results obtained for model 4 are compared with literature values in Table 8.10.

The formation curves calculated by using the stability constants from model 4 are depicted in Figure 8.9. One can see that they reproduce the essential features of the observed formation curves. The agreement is very good except at $\bar{Z}$ values above 1.8. It is known, however, that the results are more sensitive to experimental error in the solution concentrations for high $\bar{Z}$ values than low.

As can be seen from Table 8.10, the results obtained for log K_{011} and log K_{012} do not agree closely with any of the values previously reported, but they do lie well between the extremes of those values. It is possible that the values reported by Barbucci and Vacca (78) are higher because they did not consider the possibility that any species other than ML and ML_2 were present in solution. In their potentiometric titrations the $p[H^+]$ values covered ranged from 3.0 to 11.2. This range is wider than that covered in this work (6.9 - 10.4). Thus the formation of hydroxy species in their experiments was most likely. On the basis of model 4, one would expect to find hydroxy complexes in the work of Lotz *et al.* (189).

There are no literature values available for comparison with the stability constants found for the mixed hydroxy complexes. The $ML(OH)^+$ complex is also formed in the systems involving oden and Cu^{2+} or Zn^{2+}. It is most likely that this complex is formed by the deprotonation of a coordinated water molecule (42). The $ML_2(OH)^+$ complex is possibly formed by substitution of a hydroxide ion for one of the coordinated ligand donor atoms. In this case the atom could be either a primary nitrogen atom or the ethereal oxygen atom. The fact that hydroxy species were formed here but not in the Ni-etolen system is in keeping with the higher basicity of oden, and the precipitation encountered in the preliminary calorimetric experiments.

TABLE 8.10

Stability constants obtained for Ni(II) with oden together with values reported in the literature.

log K_{011}	log K_{012}	log β_{-111}	log β_{-112}	Medium	Temperature/°C	Reference
5.78(1)	3.47(3)	9.1(3)	13.41(6)	0.5 mol dm^{-3} KNO_3	25	This work (ESTA)
5.895(5)	3.62(2)			0.5 mol dm^{-3} KNO_3	25	78
5.62	3.39			0	25	188
5.93(1)	3.69(7)			0_{corr}	10	189*
5.75(1)	3.50(6)			0_{corr}	20	
5.54 (1)	3.19(6)			0_{corr}	30	
5.41(1)	3.18(6)			0_{corr}	40	

*In this case the numbers in parentheses represent 95 % confidence limits.

In order to visualize the amounts of ternary complexes present at some typical concentrations and metal to ligand ratios, two species distribution diagrams were drawn. These are Figures 8.10 and 8.11. Figure 8.10 refers to a titration which used protonated ligand as part of the background electrolyte. At the highest $p[H^+]$ reached in this titration, viz. 8.90, less than 11 % of the total nickel is present as ternary species. Figure 8.11 refers to a titration which did not use protonated ligand in the background electrolyte and for which the metal to ligand ratio is much lower. At the highest $p[H^+]$ reached here, viz. 10.39, about 90 % of the total nickel is present as ternary species. From these examples it is clear that the substitution of part of the background electrolyte by protonated ligand leads to a marked decrease in the formation of hydrolysed species. The protonated ligand prevents the working $p[H^+]$ from rising to too high a value near the end of the titration.

In the calculation of the heats of formation of the Ni-oden complexes fixed values were used for the stability constants and enthalpy changes of the species H_2O, HL^+, H_2L^{2+} and $Ni(OH)^+$, and for the stability constants of ML^{2+}, ML_2^{2+}, $ML(OH)^+$ and $ML_2(OH)^+$. The results obtained are shown in Table 8.11, together with pertinent values reported in the literature.

The enthalpy changes obtained for the ML and ML_2 complexes agree fairly well with the reported values. No reliable value of $\Delta H^{\ominus}$ could be determined for the formation of the $ML(OH)^+$ complex. (A species distribution calculation confirmed that no significant amount of $ML(OH)^+$ was formed during the calorimetric titrations.)

The magnitude of $\Delta H^{\ominus}_{011}$ is greater than that of $\Delta H^{\ominus}_{012}$, which reverses the usual order for polyamines (cf. etolen). Barbucci and Vacca (78) suggested that the second ligand addition step is less exothermic for the following reason. The complex ML (where L is tridentate) may exist in solution as the meridional or the facial isomer. However, in the ML_2 complexes the ligands are usually equatorially placed and a certain amount of facial → meridional conversion therefore takes place during the second ligand addition step. It was found by Evilia *et al.* (66) that this conversion is endothermic in the case of Ni^{2+} and oden. Hence this conversion decreases the value of $\Delta H^{\ominus}_{012}$.

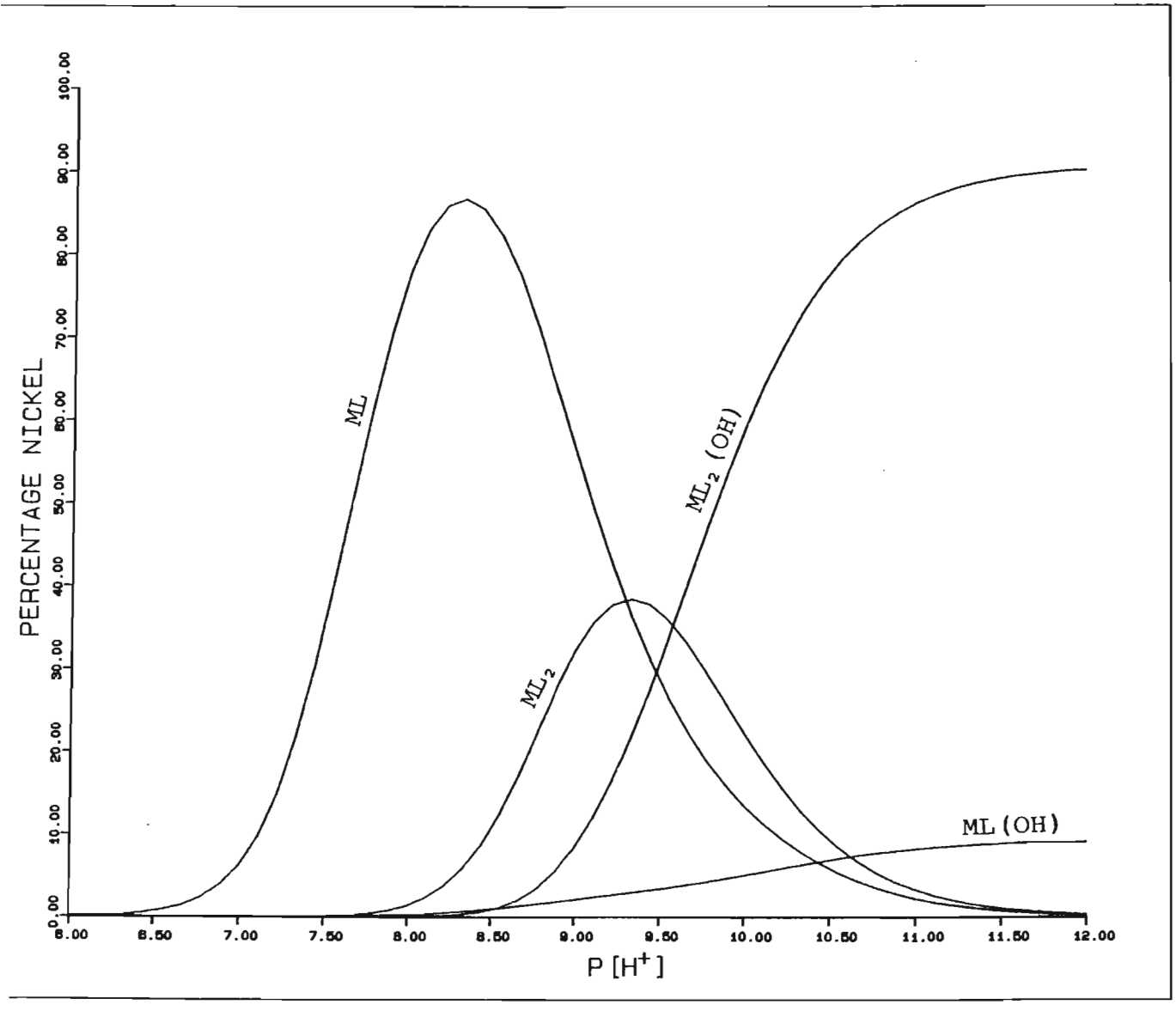

Figure 8.10 Species distribution diagram for the nickel-oden system, for the case $[Ni^{2+}]_t = 5.0 \times 10^{-3}$ mol dm^{-3} and $[oden]_t/[Ni^{2+}]_t = 2.0$.

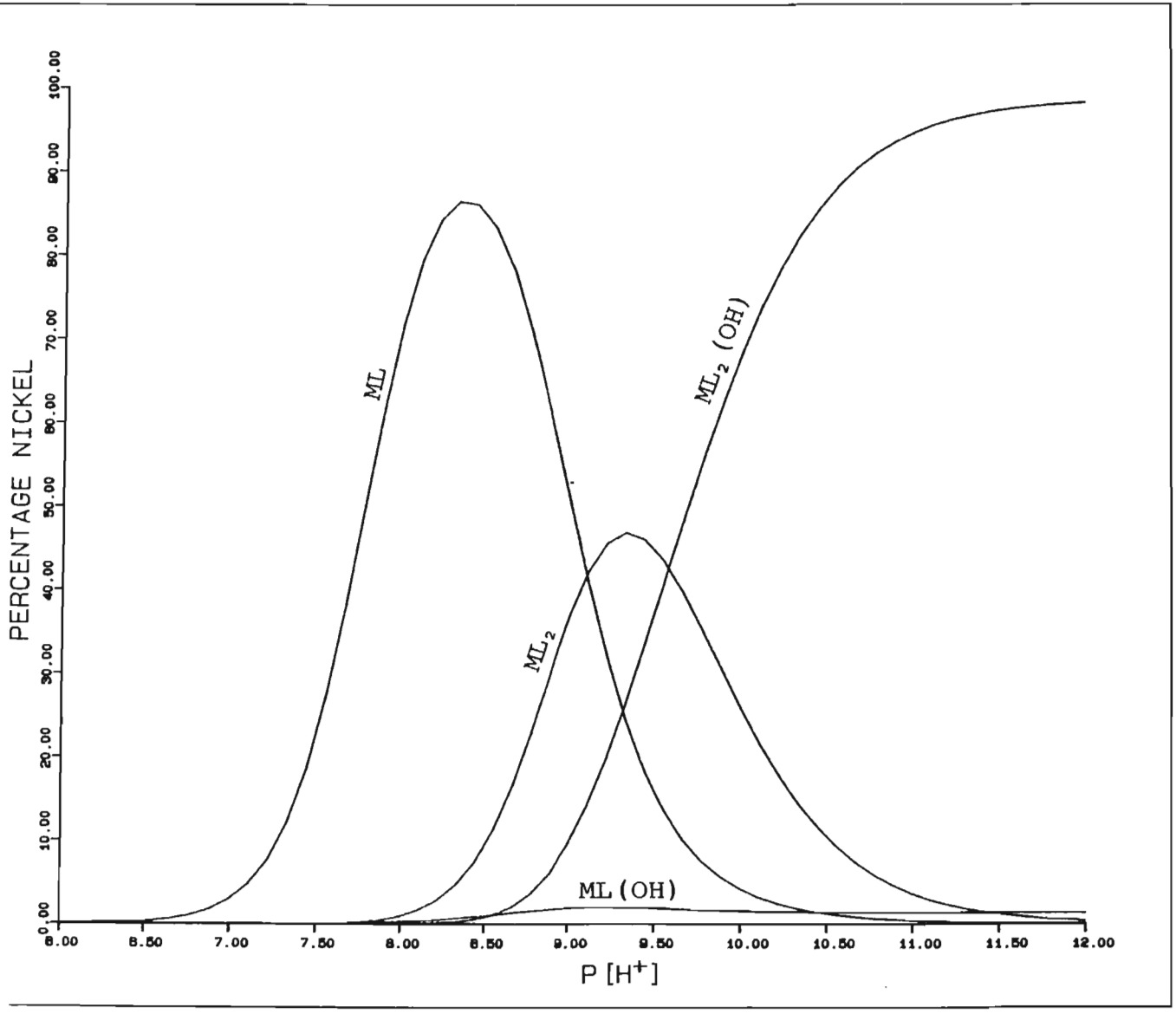

Figure 8.11 Species distribution diagram for the nickel-oden system, for the case $[Ni^{2+}]_t = 5.0 \times 10^{-4}$ mol dm^{-3} and $[oden]_t/[Ni^{2+}]_t = 9.0$.

TABLE 8.11

Thermodynamic parameters of complex formation for Ni(II) with oden.

Reaction	log K	$\Delta H^{\ominus}$/kJmol^{-1}	$\Delta S^{\ominus}$/Jmol^{-1} K^{-1}	Temperature/°C	Medium	Reference
$Ni^{2+} + L \rightleftharpoons NiL^{2+}$	5.78	-29.1(2)	13.1	25	0.5 mol dm^{-3} KNO_3	This work
$NiL^{2+} + L \rightleftharpoons NiL_2^{2+}$	3.47	-26.7(6)	-23.1	25		
$Ni^{2+} + 2L + OH^- \rightleftharpoons NiL_2(OH)^+$	13.41*	-36.69(4)	133.7	25		
$Ni^{2+} + L \rightleftharpoons NiL^{2+}$	5.895	-28.0(8)	19(3)	25	0.5 mol dm^{-3} KNO_3	78
$NiL^{2+} + L \rightleftharpoons NiL_2^{2+}$	3.62	-27(2)	-21(8)	25		
$Ni^{2+} + L \rightleftharpoons NiL^{2+}$	5.62	-29	8	25	0	188
$NiL^{2+} + L \rightleftharpoons NiL_2^{2+}$	3.39	-29	-33.5	25		
$Ni^{2+} + L \rightleftharpoons NiL^{2+}$	5.93	-29.7	8	10	0_{corr}	189
	5.75			20		
	5.54			30		
	5.41			40		
$NiL^{2+} + L \rightleftharpoons NiL_2^{2+}$	3.69	-31.4	-42	10		
	3.50		-42	20		
	3.19		-42	30		
	3.18		-38	40		

* log β_{-112}

The above explanation presupposes that the ML_2 complex is meridional. This assumption is justified by Barbucci and Vacca on the grounds that the rather similar $Ni(dien)_2^{2+}$ complex is meridional in the solid state. There is however no evidence to suggest that the stereochemistry observed in the solid state is maintained in solution. In fact there are suggestions to the contrary (42). The crystal structure of $Ni(oden)_2^{2+}$ has not yet been reported.

This decrease in the enthalpy change on addition of a second ligand molecule was also observed in studies of the ligand dpt with Ni^{2+}, where it was known that all the nitrogens are coordinated to the metal ion in solution (195). In that case steric repulsion between the two ligand molecules was used to account for the phenomenon. This may also be the explanation in the case of oden.

Another possible explanation for this phenomenon is that in the second step of complex formation more water molecules are lost. This endothermic effect lowers the heat liberated in spite of the fact that the second step is a softer interaction and should be more exothermic than the first. If this increased desolvation effect were operative it would manifest itself in abnormally large $\Delta S^{\ominus}$ values. As this does not obviously occur, the previous explanation is the more plausible of the two.

Again, the entropy changes observed follow the usual trend for polyamines.

A comparison of the stability constants obtained for the etolen and oden complexes of Ni(II) shows that the oden complexes are weaker than those of etolen. This is in keeping with the supposition that the stability of a nickel-polyamine complex increases as the number of secondary nitrogen donors increases at the expense of primary nitrogen donors. But Barbucci and Vacca (78) and Lotz *et al.* (189) ascribed this lower stability of the oden complexes to the destabilizing effect of the ether oxygen. This lower stability cannot be ascribed to non-coordination of the ether oxygen, because it has been shown that in aqueous solution oden behaves as a tridentate ligand towards Ni^{2+} (66). The lower stability of oden complexes is also due to a somewhat less favourable enthalpic contribution. The smaller positive entropy change observed for the formation of the ML^{2+} complex involving oden suggests differing degrees of solvation of the ML^{2+} complexes of the two ligands. The difference between the $\Delta S^{\ominus}_{011}$ values of etole

and oden (20.5 J mol^{-1} K^{-1}) suggests that in the reaction with oden at least one water molecule fewer is liberated. (The liberation of one water molecule corresponds to an increase in translational entropy of at least 21 J mol^{-1} K^{-1} (42).) If this is so, then it would be in keeping with the findings of Evilia *et al.* (66) that at 300 K $Ni(oden)^{2+}$ is found to exist primarily as the facially coordinated species, and that this geometry may be stabilized by coordinated water molecules. The presence of these coordinated water molecules may sterically hinder the attachment of the second ligand molecule and thus give rise to the unexpected lower value of $\Delta H^{\ominus}_{012}$.

8.5. The cobalt ion - etolen system

The observed formation curves for this system are shown in Figure 8.12. One noticeable feature is the fanning out of the curves at $\bar{Z}$ values greater than about 1.3. This is thought to be due to small inaccuracies in the solution concentrations, as in the case of the Ni-etolen system. The curves of the repeat titrations (nos. 6 and 9) are completely superimposable, which indicates that the results are reproducible. Titrations 1 and 2 (i.e. those in which protonated ligand was not substituted for background electrolyte) exhibit 'shoot-up' from about $\bar{Z}$ = 0.8 upwards. Apart from this 'shoot-up' the curves corresponding to different metal ion concentrations are superimposable within the limits of experimental error. This rules out the presence of polynuclear complexes.

Titrations 1 and 2 were carried out at higher operating $p[H^+]$ and lower solution concentrations than the others. Both were carried out at a metal ion concentration of 5.005×10^{-4} mol dm^{-3}. These conditions favour the formation of ternary complexes, although the 'shoot-up' may also merely reflect experimental error. The possible presence of ternary complexes was investigated by adding such species to the initial model, which consisted of ML and ML_2. As usual, fixed values of the stability constants of the relevant species (H_2O, HL^+, H_2L^{2+} and $Co(OH)^+$) were used in the calculations. The various 'successful' models obtained are listed in Table 8.12.

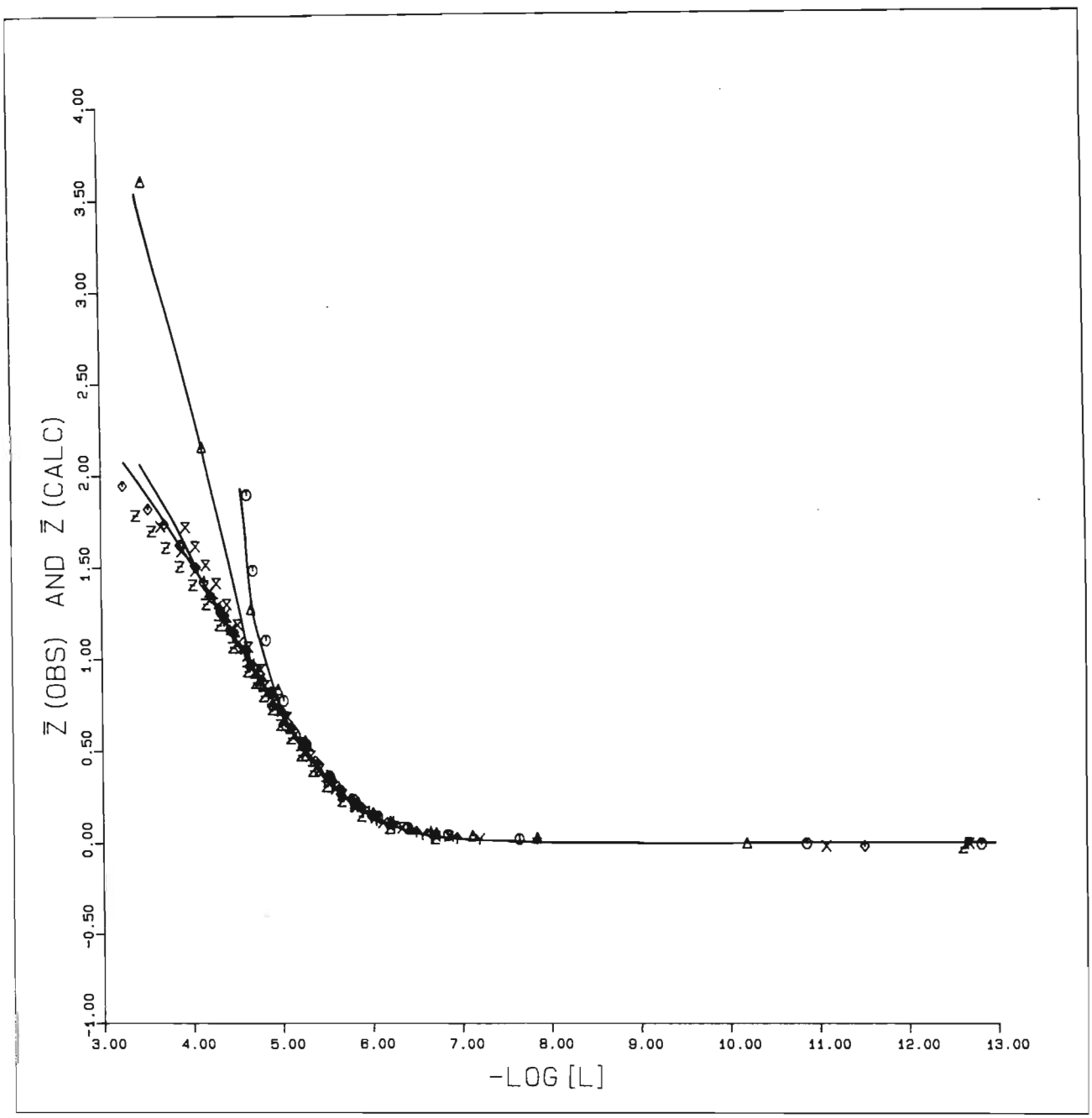

Figure 8.12 Formation curves for the cobalt - etolen system.

TABLE 8.12

Stability constants* for Co(II)-etolen complexes obtained from various models.

Model	1	2	3	4	5	6+
ML^{2+}	5.20	5.19	5.20	5.19	5.19	5.17
ML_2^{2+}	9.22	9.31	9.21	9.21	9.25	9.25
$ML(OH)^{+}$			-3.42		-3.42	
$ML_2(OH)^{+}$	1.10		1.01	1.11	1.00	
$ML_3(OH)^{+}$		4.56				
MLH^{3+}					10.63	
ML_2H^{3+}				15.21		
U	95	311	85	96	80	4×10^{-6}
R	0.008	0.014	0.007	0.008	0.007	0.002
Titrations used			1 - 9			3 - 9
No. of points			167			134

*For complexes containing the hydroxide ion, e.g. $ML_r(OH)_p$, the values given in the table represent log β_{-p1r} + p(log K_w).

+MINIQUAD was used to determine model 6, and ESTA for the others. The objective value (U) for model 6 is therefore not comparable with the others.

Obviously model 6 is not comparable with the others because it cannot reproduce the 'shoot-up' observed. On the basis of the values of U and the numbers of complexes included in the models, possibilities 2 and 4 were rejected. From inspection of the remaining three models it appears that inclusion of species other than ML^{2+}, ML_2^{2+} and $ML_2(OH)^+$ does not greatly improve the objective value. Model 1 was therefore preferred because of its simplicity and because it reproduces the essential features of the observed formation curves. It should be noted that the inclusion of various minor species does not greatly alter the values of the stability constants for the ML^{2+} and ML_2^{2+} complexes. The results obtained from model 1 are compared with various reported values in Table 8.13.

The $\bar{Z}$(calc) curves based on model 1 and depicted in Figure 8.12 are able to reproduce the 'shoot-up' and fanning out to a very satisfactory extent. Therefore it was decided that this model of the species present in solution adequately describes the data collected.

The value of log K_{011} obtained is higher than that of Hall *et al.* (183), and vice versa for the value of log K_{012}. However, as stated by Hall *et al.*, their value of log K_{012} is unreliable because further action with base was required in order to obtain complete formation of the ML_2 complex. It should be noted that Martell and Smith, in their stability constant compilation (167), quote as unreliable both values reported by Hall *et al.* The values obtained in this work are in keeping with those obtained for other, similar, systems in that log K_{011} > log K_{012}, whereas the results of Hall *et al.* reverse this relation.

The fact that the stability constants obtained by Edwards (180, 192) for this system are much higher than the other sets of values is perhaps to be expected, in view of the comments made in Section 8.3.

Species distribution diagrams for this system are shown in Figures 8.13 and 8.14. In 8.13, which relates to a typical titration with no protonated ligand in the background electrolyte and a high metal to ligand ratio, the ternary complex $ML_2(OH)^+$ accounts for over 90 % of the total cobalt at the end of the titration, i.e. at $p[H^+] = 9.45$. In 8.14,

TABLE 8.13

Stability constants obtained for Co(II) with etolen, together with values reported in the literature. (All data are for 25°C.)

$\log K_{011}$	$\log K_{012}$	$\log K^*$	$\log \beta_{-112}$	Medium	Reference
5.205(6)	4.02(1)		14.84(3)	0.5 mol dm^{-3} KNO_3	This work (ESTA)
4.87	5.0	9.07		0.5 mol dm^{-3} KNO_3	183
6.58	5.25			1 mol dm^{-3} KCℓ	180, 192

* $K = \dfrac{[ML]}{[ML(OH)][H^+]}$

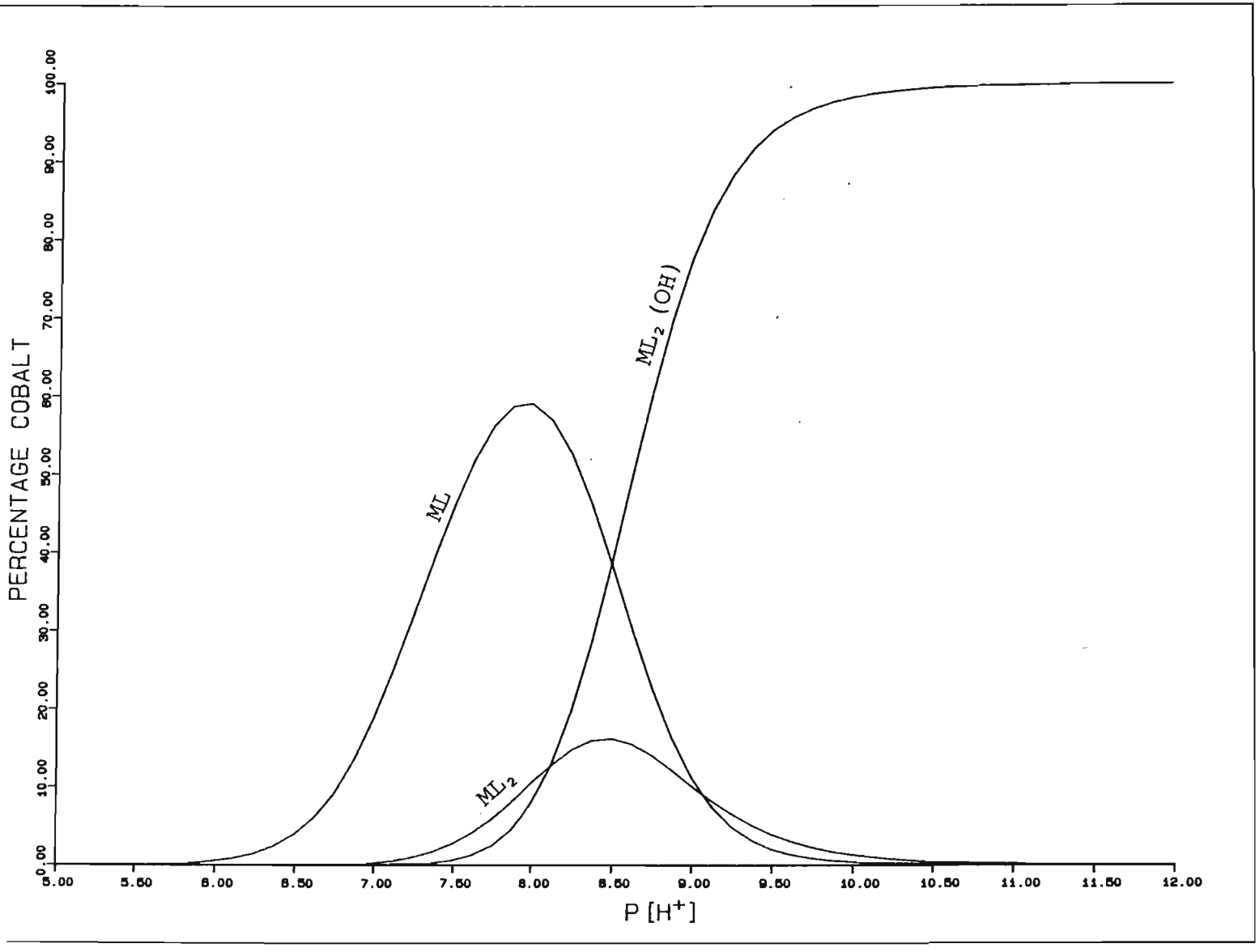

Figure 8.13 Species distribution diagram for the cobalt-etolen system, for the case $[Co^{2+}]_t$ = 5.0 x 10^{-4} mol dm^{-3} and $[etolen]_t/[Co^{2+}]_t$ = 3.0.

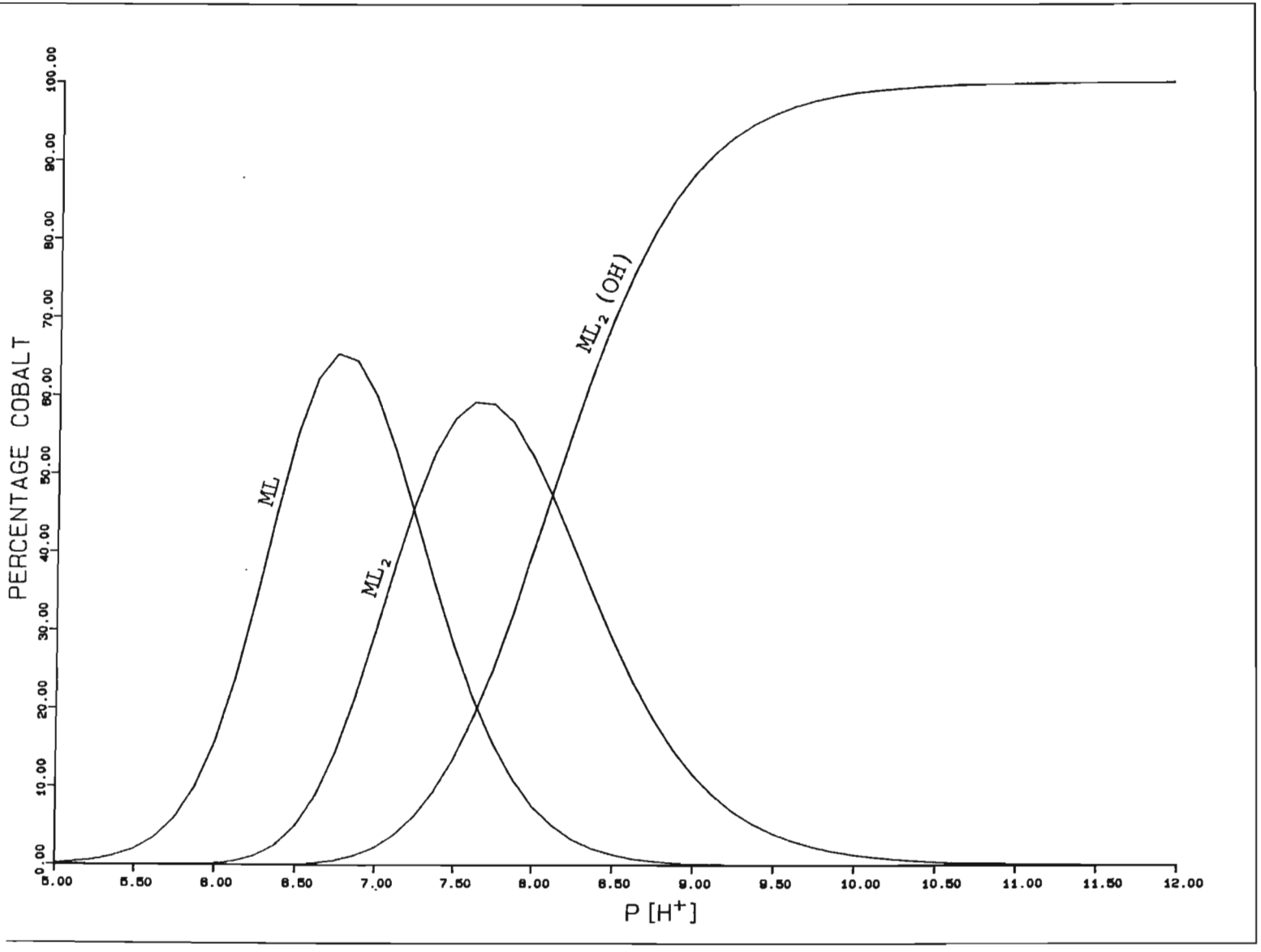

Figure 8.14 Species distribution diagram for the cobalt-etolen system, for the case $[Co^{2+}]_t$ = 7.5 x 10^{-3} mol dm^{-3} and $[etolen]_t/[Co^{2+}]_t$ = 7.2.

which is for a titration with protonated ligand in the background electrolyte, and a fairly low metal to ligand ratio, the ternary complex accounts for less than 20 % of the total cobalt at the end, i.e. at $p[H^+] = 7.64$. These results are in keeping with the presence or absence of 'shoot-up' in the $\bar{Z}$(obs) curves.

In the calculation of the heats of formation of the Co-etolen complexes fixed values of the stability constants and enthalpy changes for the species H_2O, HL^{2+} and H_2L^{2+}, and of the stability constants for ML^{2+}, ML_2^{2+} and $ML_2(OH)^+$, were used. The results obtained are shown in Table 8.14. The enthalpy changes obtained for this system are new and thus cannot be compared with literature values. No reliable value of the enthalpy change for the formation of the $ML_2(OH)^+$ complex could be determined.

Again, as for the Ni-etolen system, $|\Delta H^{\ominus}_{012}| > |\Delta H^{\ominus}_{011}|$ and the entropy changes show the expected decrease with each step of complexation. The stability constants and the enthalpy changes found are lower than those obtained for the corresponding Ni^{2+} complexes. This is in keeping with the Irving-Williams order and the results for other, similar, systems. If one takes the difference between log K_{011} and log K_{012}, and similar differences for the other thermodynamic quantities, one finds that within experimental error the values obtained for the Co-etolen complexes are virtually the same as those for the Ni-etolen complexes.

The entropy changes observed do not suggest non-coordination of one of the donor atoms of etolen. This is in keeping with the results of Everhart *et al.* (65). They found, from n.m.r. studies of the ML^{2+} complex in aqueous solution, that all three donor atoms of etolen were coordinated to Co^{2+}. Thus one must assume that in these complexes etolen behaves as a tridentate ligand.

8.6. The cobalt ion - oden system

The $\bar{Z}$(obs) curves for this system are shown in Figure 8.15. Apart from those of titrations 3 and 4, the curves are superimposable within the limits of experimental error. Titrations 3 and 4 were carried out at the lowest initial metal ion concentration, viz. 5.0×10^{-4} mol dm^{-3},

TABLE 8.14

Thermodynamic parameters of complex formation for Co(II) and etolen. (All values are for 25°C and μ = 0.5 mol dm^{-3}.)

Reaction	log K	$\Delta H^{\ominus}$/kJ mol^{-1}	$\Delta S^{\ominus}$/J $mol^{-1}K^{-1}$
$Co^{2+} + L \rightleftharpoons CoL^{2+}$	5.20	-21.4(3)	27.8
$CoL^{2+} + L \rightleftharpoons CoL_2^{2+}$	4.02	-32(2)	-30

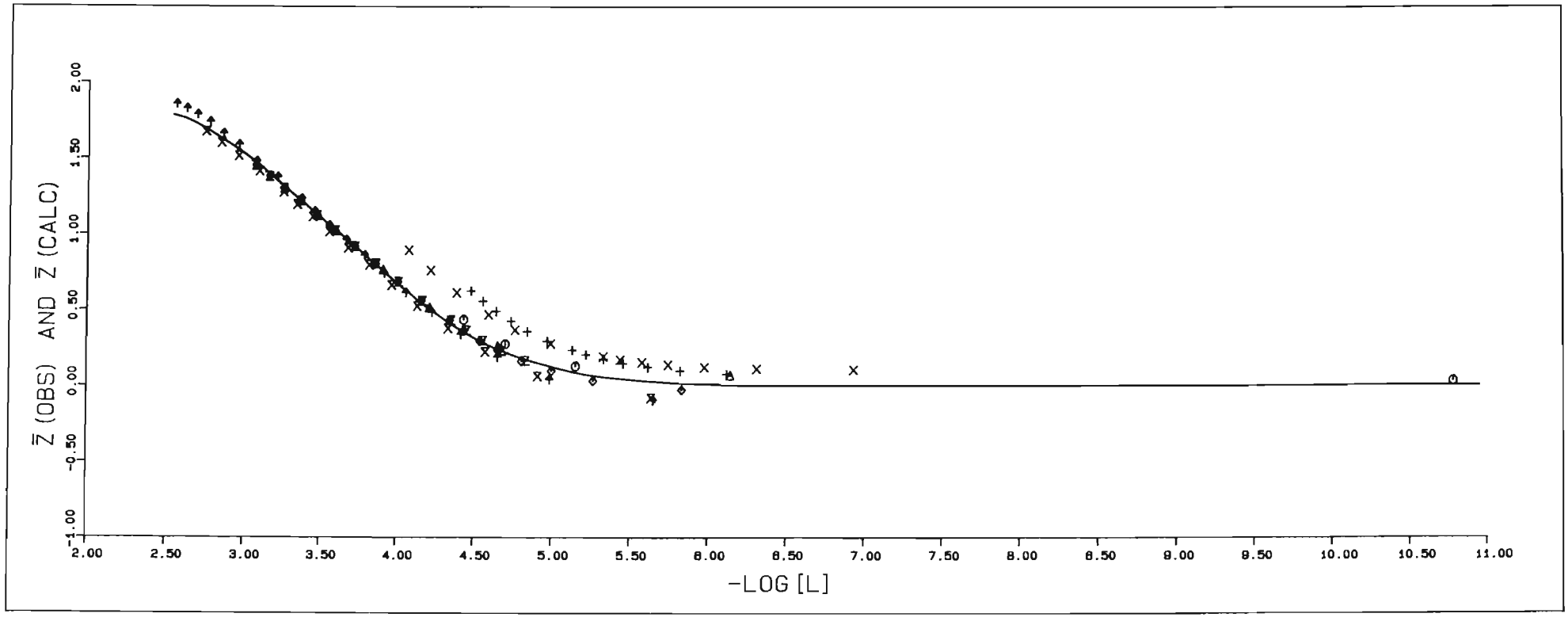

Figure 8.15 Formation curves for the cobalt - oden system.

so it is very likely that the upward shift in the $\bar{Z}$ curves reflects experimental error rather than the formation of polynuclear complexes. Nevertheless attempts were made to include various polynuclear complexes in the model to see whether the upward shift could be explained thus. The repeat titrations (nos. 5 and 8) are completely superimposable, and the results are therefore reproducible. Apart from nos. 3 and 4 the curves are straightforward and what one would expect if only two mononuclear complexes ML and ML_2 were present. During the calculation of stability constants, fixed values of the stability constants of the species H_2O, HL^+, H_2L^{2+} and $Co(OH)^+$ were used. The various 'successful' models tested are shown in Table 8.15.

The attempts to introduce polynuclear complexes into the model were unsuccessful. This meant that the upward bias of the $\bar{Z}$ curves for titrations 3 and 4 could not be reproduced. The data for these titrations were subsequently removed from the data set.

The U values of the models determined from the remaining six titrations can be seen to be very similar. The simplest of these models, viz. model 7, was therefore selected. The results are new and hence cannot be compared with any reported values. Figure 8.15 displays the calculated formation curve based on the model selected. Clearly the observed and calculated formation curves match very satisfactorily.

In the calculation of the heats of formation of these complexes fixed values were used for the stability constants and enthalpy changes of H_2O, HL^+ and H_2L^{2+}, and the stability constants of ML^{2+} and ML_2^{2+}. The thermodynamic parameters of complexation of Co(II) and oden are given in Table 8.16.

As in the Ni-oden case, $|\Delta H^{\ominus}_{011}|$ is greater than $|\Delta H^{\ominus}_{012}|$. However, the entropy values do not display the usual pattern. Both are positive, and in fact the value of $\Delta S^{\ominus}_{012}$ is surprisingly high. This is almost suggestive of non-coordination of one of the ligand donor atoms. However, if this is so it is not reflected in the enthalpy changes. So one must conclude tentatively that both ligands in the ML_2^{2+} complex are tridentate.

TABLE 8.15

Stability constants* for Co(II)-oden complexes obtained from different models.

Model	1	2	3	4	5	6+	7
ML^{2+}	4.16	3.76	4.12	4.09	4.07	4.13	4.12
ML_2^{2+}	6.88		7.26	7.24	7.09	7.25	7.26
$ML(OH)^{+}$	-4.97	-4.55			-5.32		
$ML(OH)_2$			-16.4				
MLH^{3+}		12.49					
ML_2H^{3+}				15.43			
U	1032	816	172	168	163	2.7×10^{-7}	169
R	0.014	0.013	0.006	0.006	0.005	0.003	0.006
Titrations used	1 - 8	1 - 8	1,2,5 - 8	1,2,5 - 8	1,2,5 - 8	5 - 8	1,2,5 - 8
No. of points	103	103	77	77	77	69	77

*For complexes containing the hydroxide ion, e.g. $ML_r(OH)_p$, the values given in the table represent $\log \beta_{-p1r} + p(\log K_w)$.

+MINIQUAD was used to determine model 6, and ESTA for the others. The objective value (U) for model 6 is therefore not comparable with the others.

TABLE 8.16

Thermodynamic parameters of complex formation for Co(II) and oden. (All values are for 25°C and μ = 0.5 mol dm^{-3}.)

Reaction	log K	$\Delta H^{\ominus}$/kJ mol^{-1}	$\Delta S^{\ominus}$/J mol^{-1} K^{-1}
$Co^{2+} + L \rightleftharpoons CoL^{2+}$	4.12(1)	-18.7(2)	16.2
$CoL^{2+} + L \rightleftharpoons CoL_2^{2+}$	3.14(2)	-15.2(4)	9.13

The complexes of oden with Co^{2+} are weaker than the analogous complexes of Ni^{2+}. This is a consequence of the less favourable enthalpy contribution, because the entropy term makes a larger contribution to the stabilization of the Co-oden complexes than to that of the Ni-oden complexes. The larger entropy stabilization is in keeping with the greater hardness of Co^{2+} (196).

The complexes of Co^{2+} with oden are also weaker than those with etolen, which is further evidence of the greater donor power of secondary nitrogen atoms. The difference between the $\Delta S^{\ominus}_{012}$ values for oden and etolen is rather large at 39.13 J mol^{-1} K^{-1}. A possible explanation is that in the second step of complexation two more molecules of water are liberated in the case of oden than for etolen. Such greater desolvation would imply a larger endothermic contribution to $\Delta H^{\ominus}_{012}$ for the oden complex. This could also account for the fact that $|\Delta H^{\ominus}_{012}|$ is less than $|\Delta H^{\ominus}_{011}|$. (This explanation can however be shown to be invalid in the case of Ni^{2+}.)

8.7. The zinc ion - etolen system

In Figure 8.16 are shown the formation curves for this system. It can be seen that the curve for one titration (no. 5) is displaced downwards from the rest. This titration was carried out at the lowest metal ion concentration (1.67×10^{-3} mol dm^{-3}) and the lowest initial metal to ligand ratio (1 : 6). These conditions may have increased the likelihood of experimental error but it is not clear that this is in fact so. The fact that the remaining curves, including those of the repeat titrations, are superimposable makes one suspect that the data from no. 5 may be unreliable. This titration was therefore excluded from the data set for calculation purposes. The rest of the curves show an interesting feature in that, instead of levelling off at $\bar{Z} \sim 2$ as might be expected, they consistently level off at $\bar{Z} \sim 1.8$. As has been shown by Avdeef *et al.* (191), such an effect is produced by small systematic errors in the solution concentrations. It was however thought safest not to alter these solution concentrations during the calculation of the stability constants.

During the calculation of the stability constants of the species present in solution fixed values of the stability constants for H_2O, HL^+, H_2L^{2+}

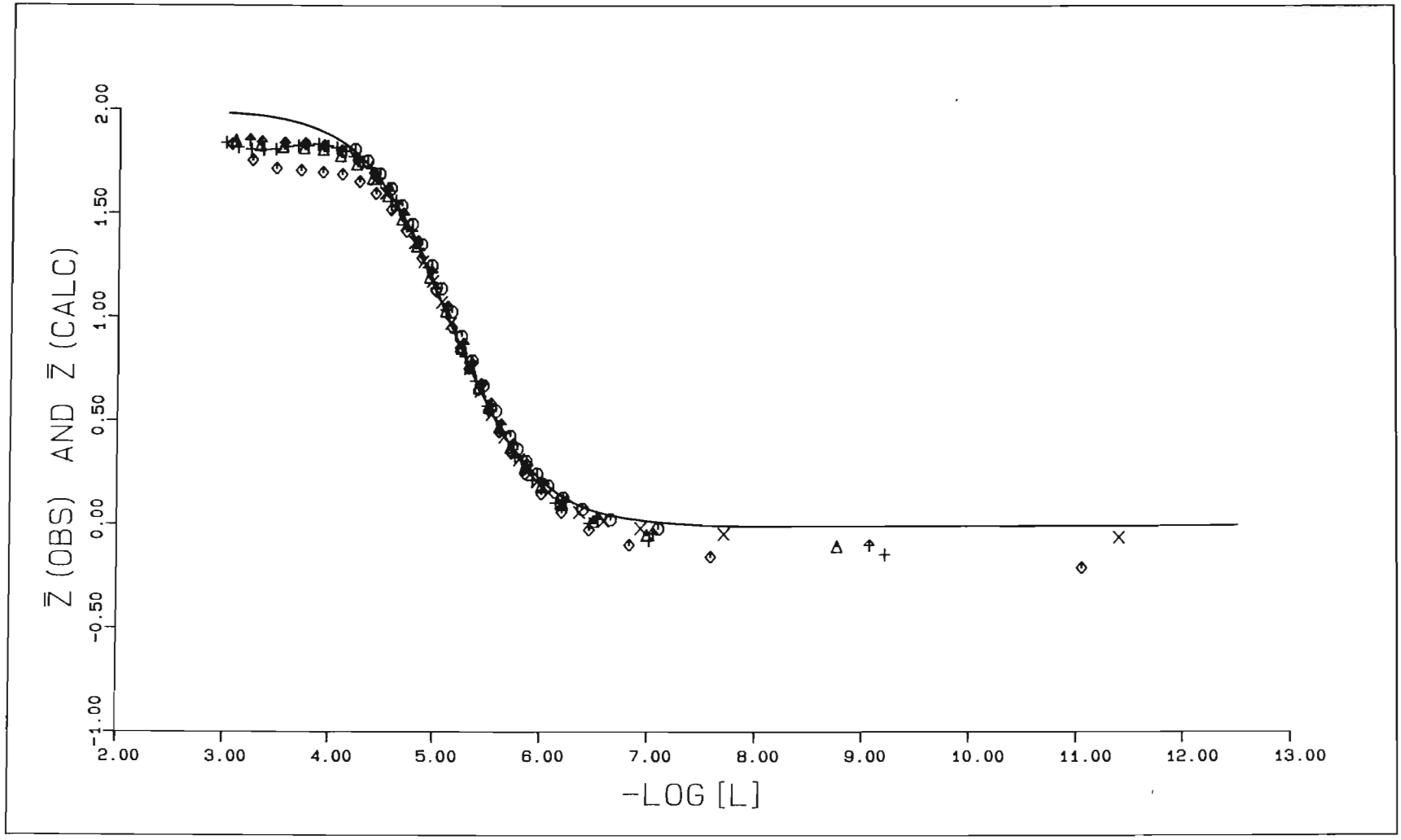

Figure 8.16 Formation curves for the zinc - etolen system.

and $Zn(OH)^+$ were used. The 'successful' models are shown in Table 8.17.

On the basis of its U value model 4 should be selected. However this model does not produce formation curves with the correct curvature at high values of $\bar{Z}$. Furthermore, log K_{012} > log K_{011}, which is not in keeping with other reported systems involving Zn^{2+} and various polyamines. Therefore model 4 was not chosen. Model 5 differs from model 1 by the inclusion of the $ML(OH)^+$ species. The addition of this species merely improves the U value by about 2 %. In addition, the $\bar{Z}$(obs) curves obtained are simple and do not feature any 'curl-back' - the usual sign of the formation of hydrolysed complexes. One would in any case not expect hydrolysis to occur, because all the potentiometric titrations were performed with protonated ligand in the background electrolyte. It was therefore felt that the simpler model 1 should be selected. The results obtained by using this model are listed in Table 8.18 and compared with various reported values.

The $\bar{Z}$(calc) curve obtained by using these results and depicted in Figure 8.16 reproduces the experimental curves apart from the plateau at $\bar{Z}$ ~ 1.8.

The results obtained agree best with those of Thöm *et al.* (197) despite the difference in ionic strength. The results of Hall *et al.* (183) again differ in the same way as did their Co - etolen results from the results given in Section 8.5. Their value of log K_{012} for $Zn(etolen)_2^{2+}$ is however only an approximate one, because further action with base was required. The value of log K_{011} obtained by Gaur *et al.* (198) is very much higher than any of the other values reported, yet their log K_{012} value is much lower. They also report a value of log K_{013} for the $Zn(etolen)_3^{2+}$ complex, in which etolen presumably behaves as a bidentate ligand. No evidence for such a complex was obtained in this work.

When the heats of formation of the Zn - etolen complexes were calculated, fixed values of the stability constants and enthalpy changes of the species H_2O, HL^{2+} and H_2L^{2+}, and of the stability constants of ML^{2+} and ML_2^{2+}, were used. The results obtained are shown in Table 8.19. The enthalpy changes obtained for this system are new and therefore cannot be compared with literature values.

The enthalpy and entropy changes obtained for the Zn - etolen complexes show the same variations as did the results for the other etolen complexes.

TABLE 8.17

Stability constants* for Zn(II)-etolen complexes obtained from different models.

Model	1	2	3	4	5
ML^{2+}	5.37	4.94		5.00	5.23
ML_2^{2+}	10.27			10.23	9.97
$ML(OH)^{+}$		-1.28	-1.29		-1.62
ML_2H^{3+}			16.66	17.01	
U(ESTA)	1202	1230	1281	1112	1179
R(ESTA)	0.025	0.025	0.025	0.023	0.024
Titrations Used		1 - 4, 6			
No. of points		132			

*For the complex containing the hydroxide ion, viz. $ML(OH)^{+}$, the values given in the table represent log β_{-111} + log K_W.

TABLE 8.18

Stability constants obtained for Zn(II) with etolen, together with values reported in the literature.

$\log K_{011}$	$\log K_{012}$	$\log K_{013}$	$\log K^*$	Medium	Temperature/°C	Reference
5.37(3)	4.90(5)			0.5 mol dm^{-3} KNO_3	25	This work (ESTA)
4.75	5.4		8.05	0.5 mol dm^{-3} KNO_3	25	183
5.28	4.79			0.1 mol dm^{-3} $NaNO_3$	25	197
8.00	3.30	3.31		KNO_3	30	198

* $K = \frac{[ML]}{[ML(OH)][H^+]}$

TABLE 8.19

Thermodynamic parameters of complex formation for Zn(II) and etolen. (All data were obtained at 25°C and μ = 0.5 mol dm^{-3}.)

Reaction	log K	$\Delta H^{\ominus}$/kJ mol^{-1}	$\Delta S^{\ominus}$/J $mol^{-1}K^{-1}$
$Zn^{2+} + L \rightleftharpoons ZnL^{2+}$	5.37	-19.6(1)	37.1
$ZnL^{2+} + L \rightleftharpoons ZnL_2^{2+}$	4.90	-30.8(1)	-9.50

The complexes of etolen with Zn^{2+} are less stable than the corresponding complexes with Ni^{2+}, but more stable than those with Co^{2+} in spite of the less favourable enthalpy contribution. The fact that the Zn^{2+} complexes are more stable than those of Co^{2+} can therefore be attributed to a more favourable entropy contribution, as can be expected for a d^{10} ion, which has no CFSE. Also, Co^{2+} and Zn^{2+} have similar ionic radii and heats of hydration. This means that in the aquo state the water molecules are held by these two ions with equal strength, while the two etolen molecules are bound less strongly to Zn^{2+} than to Co^{2+}. Consequently the $Zn(etolen)_2^{2+}$ complex is less rigid and this is reflected in the larger value of (cumulative) ΔS°_{1-2}.

For comparison purposes the results of Barbucci and Vacca (78) for the zinc ion - oden system are presented in Table 8.20.

The results of the zinc - oden system differ markedly from those of the other oden systems. The ML^{2+} complex is only slightly less stable than that of Ni^{2+}, but the ML_2^{2+} complex is more stable than that of either Ni^{2+} or Co^{2+}. For the zinc - oden system (unlike the other oden systems), $|\Delta H^{\circ}_{012}| > |\Delta H^{\circ}_{011}|$, which is more in keeping with the behaviour of etolen systems. In fact the ML_2^{2+} complex is stabilized in comparison with the other oden complexes by the large enthalpic contribution. In the first step of complexation the fairly large positive entropy change makes a significant contribution to the stabilization of ML^{2+}. This is often the case with Zn^{2+} complexes of polyamines (11). However the ΔS°_{011} value is not large enough to suggest tetrahedral coordination, which has been suggested for other polyamines.

The complexes of etolen and oden with Zn^{2+} have virtually the same enthalpy changes. The $Zn(oden)^{2+}$ complex is more stable than the analogous etolen complex because of a more favourable positive entropy change. On the other hand, the $Zn(etolen)_2^{2+}$ complex is more stable than $Zn(oden)_2^{2+}$ because of a less negative entropy contribution. Here we have the first instance of secondary nitrogen donors apparently not enhancing the stability of the complexes.

TABLE 8.20

Thermodynamic parameters of complex formation for Zn(II) with oden. (All data are from reference 78 and were obtained at 25°C and μ = 0.5 mol dm^{-3} KNO_3.)

Reaction	log K	$\Delta H^{\ominus}$/kJ mol^{-1}	$\Delta S^{\ominus}$/J mol^{-1} K^{-1}
$Zn^{2+} + L \rightleftharpoons ZnL^{2+}$	5.74(1)	-20.1(4)	43(2)
$ZnL^{2+} + L \rightleftharpoons ZnL_2^{2+}$	4.12(3)	-30.5(8)	-24(4)
$ZnL^{2+} + OH^- \rightleftharpoons ZnL(OH)^+$	5.11(3)	1.7(2.1)	103(8)
$ZnL^{2+} + 2OH^- \rightleftharpoons ZnL(OH)_2$	8.37(3)	-	-

8.8. Crystallographic Results

The blue crystals of nickel and etolen (see Section 7.10.1) proved to be $[Ni(etolen)_2](NO_3)_2$. Some of the crystal data obtained for this complex by Wade (171) are compared in Table 8.21 with those obtained by Näsänen *et al.* (76) from powder diffraction data. From these results we see that the same compound was prepared. The structure of the molecule is shown in Figure 8.17 and the bond distances and angles, with their estimated standard deviations, are given in Table 8.22.

Each of the ligand molecules in solid $[Ni(etolen)_2](NO_3)_2$ is tridentate, coordinating in a meridional configuration. The geometric arrangement of ligand donors about the central nickel atom is a distorted octahedron with the primary nitrogen atoms and the oxygen atoms cis to each other, and the secondary nitrogen donors trans to each other. The Ni - secondary nitrogen bond lengths of 2.049(7) and 2.064(8) Å are somewhat shorter than the Ni - primary nitrogen bond distances of 2.08(1) and 2.121(7) Å. Wade (171) found that the Ni - O bond length in the above molecule is longer than the Ni - O bond length in $[Ni(en)(H_2O)_4](NO_3)_2$ and $[Ni(en)_2(H_2O)_2](NO_3)_2$. This most probably arises from steric strain caused by the ethylene bridge which, through its reluctance to bend, pulls the oxygen away from the nickel. This strain is easily observed from an examination of a Dreiding model of the $Ni(etolen)_2^{2+}$ cation.

From the measurements made on the purple crystals of Ni - etolen it was possible to conclude that $[Ni(etolen)_3](NO_3)_2$ was present. The unit cell was orthorhombic with the following approximate dimensions: a = 8.912 Å, b = 15.12 Å and c = 15.80 Å.

It is therefore evident that, in the solid state, etolen can form both the bis and the tris complex with Ni^{2+}. In the former complex it acts as a tridentate ligand, coordinating through the nitrogen atoms and the hydroxyl group, whereas in the latter complex it is bidentate, coordinating only through the nitrogen atoms. Karpeiskaya *et al.* (193) attributed the absorption band at 1408 cm^{-1} in the infrared spectrum of $[Ni(etolen)_3]Cl_2$ to the presence of two close hydroxy groups capable of forming a hydrogen bond. It is therefore possible that this hydrogen bond formation gives the $Ni(etolen)_3^{2+}$ ion its stability.

TABLE 8.21

Crystal data for bis[2-(2-aminoethyl)aminoethanol]nickel(II) nitrate.

	Results obtained by Wade (171)	Results obtained by Näsänen *et al.* (76)
Formula	$(NiC_8H_{24}N_4O_2)(NO_3)_2$	$(NiC_8H_{24}N_4O_2)(NO_3)_2$
M_r/g mol^{-1}	391.024	391.02
Space Group	centrosymmetric triclinic ($P\bar{1}$)	triclinic
a/Å	13.098(3)	13.141(8)
b/Å	8.737(4)	8.744(11)
c/Å	7.746(3)	7.734(9)
α/deg	112.66	112.55(10)
β/deg	90.65	90.55(10)
γ/deg	85.03	85.18(10)
V_c/Å^3	814.69	817.6
Z	2	2
D_{obs}/g cm^{-3}	1.58	1.58
D_{calc}/g cm^{-3}	1.59	1.59
μ_{eff}/B.M.	-	3.11

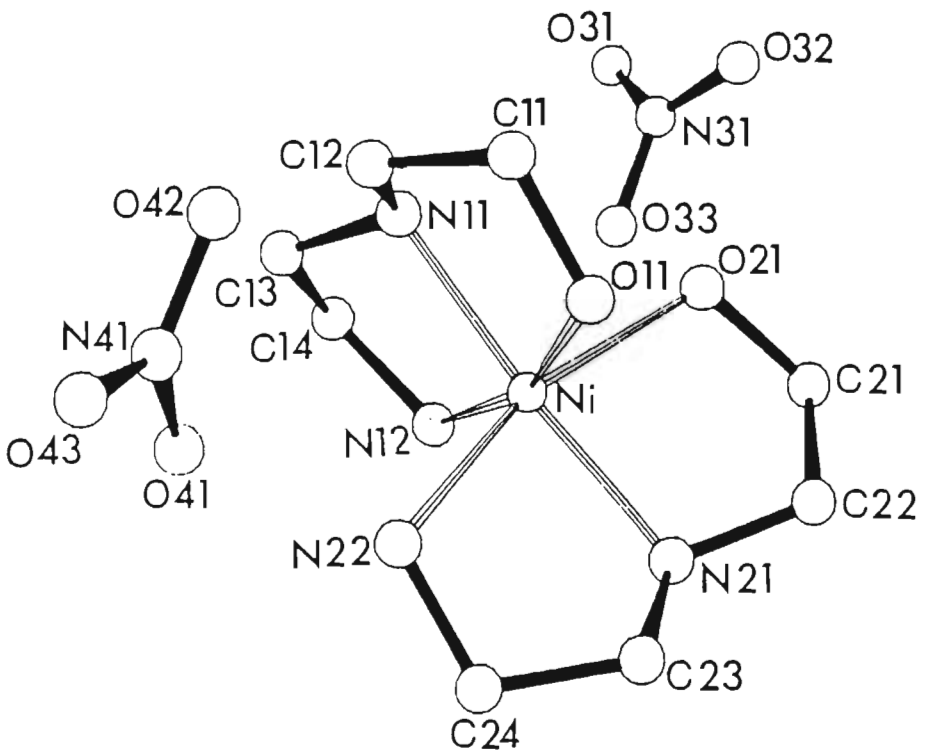

Figure 8.17 Structure of $[Ni(etolen)_2](NO_3)_2$. (Diagram reproduced from reference 171.)

TABLE 8.22

Bond lengths (Å) and bond angles (°) for $[Ni(etolen)_2](NO_3)_2$, with estimated standard deviations given in parentheses. (This table is reproduced from reference 171.)

$[Ni(etolen)_2]^{2+}$ cation

Ni-O11	2.162(5)	Ni-O21	2.136(5)
Ni-N11	2.049(7)	Ni-N21	2.064(8)
Ni-N12	2.08(1)	Ni-N22	2.121(7)
O11-C11	1.44(1)	O21-C21	1.42(1)
C11-C12	1.48(2)	C21-C22	1.54(2)
C12-N11	1.46(1)	C22-N21	1.45(1)
N11-C13	1.45(1)	N21-C23	1.49(1)
C13-C14	1.51(1)	C23-C24	1.49(1)
C14-N12	1.47(2)	C24-N22	1.48(1)
Ni-O11-C11	109.8(5)	Ni-O21-C21	111.2(5)
Ni-N11-C12	107.5(6)	Ni-N21-C22	109.2(5)
Ni-N11-C13	106.7(5)	Ni-N21-C23	106.4(5)
Ni-N12-C14	110.4(5)	Ni-N22-C24	108.0(5)
O11-Ni-N11	80.8(2)	O21-Ni-N21	80.4(2)
O11-Ni-N12	163.0(3)	O21-Ni-N22	161.5(3)
N11-Ni-N12	82.3(3)	N21-Ni-N22	83.0(3)
O11-Ni-O21	88.7(2)		
O11-Ni-N21	95.7(2)	O21-Ni-N11	96.0(2)
O11-Ni-N22	85.0(2)	O21-Ni-N12	94.6(3)
N11-Ni-N22	100.1(3)	N21-Ni-N12	101.3(3)
N12-Ni-N22	96.5(3)		
O11-C11-C12	108.9(7)	O21-C21-C22	107.7(7)
N11-C12-C11	110.8(7)	N21-C22-C21	108.4(8)
N11-C13-C14	109.6(8)	N21-C23-C24	107.9(9)
N12-C14-C13	109.5(9)	N22-C24-C23	110.6(7)

Nitrates

N31-O31	1.25(1)	N41-O41	1.231(8)
N31-O32	1.21(1)	N41-O42	1.22(1)
N31-O33	1.23(1)	N41-O43	1.23(1)
O31-N31-O32	121.1(8)	O41-N41-N42	122.1(7)
O31-N31-O33	117.3(9)	O41-N41-N43	120.8(8)
O32-N31-N33	121.6(9)	O42-N41-O43	117.0(7)

8.9. Electronic Spectra

The ultraviolet - visible spectra for the NiL_2^{2+} complexes, where L is either etolen or oden, are shown in Figure 8.18. Although the spectra are incomplete because of equipment limitations, one can see that the electronic transitions for the $Ni(oden)_2^{2+}$ complex occur at lower energies than for the $Ni(etolen)_2^{2+}$ complex. This is in agreement with the thermodynamic results, which showed that the complexes of Ni(II) with oden are less stable than those with etolen.

The wavenumbers corresponding to the electronic transitions of the various nickel - etolen complexes are displayed in Table 8.23. One notices that the tris complexes tend to have larger 10Dq values than do the bis complexes. Two causes of these larger values could be: the presence of an extra secondary nitrogen donor and the fact that the chelate rings are not linked. This of course assumes a priori that secondary nitrogens have greater donor power than primary. The nature of the counter ion in the various complexes also tends to cause a variation in the value of 10Dq.

8.10. The bonding capacity of primary nitrogen donors as compared to secondary nitrogen donors

The question of whether secondary nitrogen donors do indeed form stronger bonds with various metal ions than do primary will now be addressed. To aid the discussion the thermodynamic parameters of complex formation for metal ions for which both etolen and oden have been studied have been listed in Table 8.24. In this table only the values for the formation of the ML and ML_2 complexes have been included.

In Figure 8.19 the values of the thermodynamic parameters for the formation of the oden and etolen complexes of the first row transition metal ions considered are plotted against the atomic numbers of these metal ions. One immediately sees that the values of $\Delta G^{\ominus}$ present a simpler picture than do the values of either $\Delta H^{\ominus}$ or $\Delta S^{\ominus}$. For the ML complexes the usual trend is found in the variation of $\Delta G^{\ominus}$ and $\Delta H^{\ominus}$ with the atomic number of the metal ion. It will also be noted that:

1. Apart from the 1:1 complex with Zn^{2+}, the complexes of etolen are

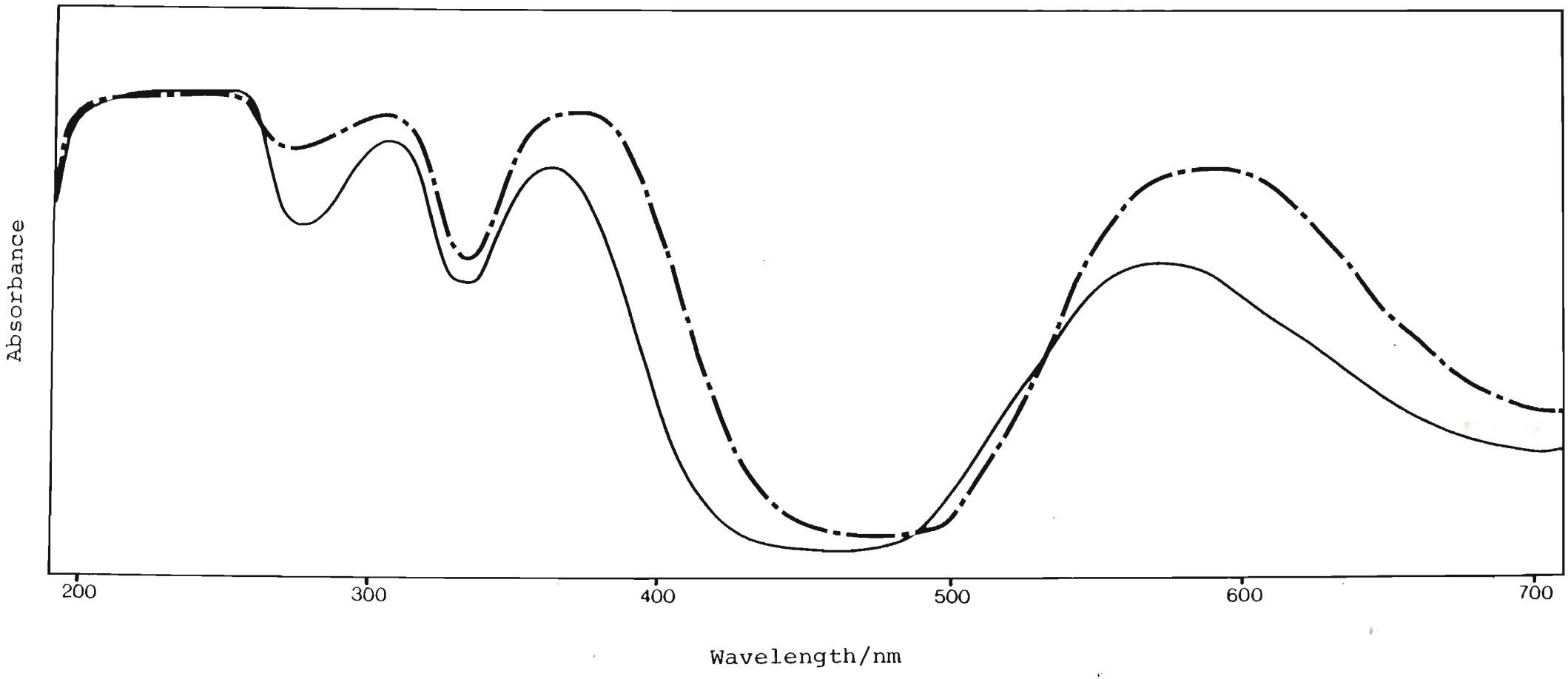

Figure 8.18 Ultraviolet-visible spectra of solutions of Ni^{2+} complexes in water: $Ni(etolen)_2^{2+}$ (——————) and $Ni(oden)_2^{2+}$ (—·—·—·—).

TABLE 8.23

Electronic spectra of various complexes of etolen involving Ni(II).

Complex	Wavenumbers corresponding to d-d electronic transitions/10^3 cm^{-1}				10Dq/cm^{-1}	B/cm^{-1}	Denticity of Ligand	Method	Reference
$NiL_2(NO_3)_2$	27.6	17.5	-		-	-	tridentate	Aqueous solution	This work
	27.9	17.9	11.2	8.4(sh)	11200	813	tridentate	Nujol mull of salt	76
					10950	870		Aqueous solution	199
					11100	850		Aqueous solution	200
					11250	860		Corrected for mixing	200
NiL_2SO_4	-	17.7	10.9		10900		tridentate	Aqueous solution	68
	27.8	18.2	10.6		10620	947	tridentate	Methanol	75
$NiL_3C\ell_2$	27.5	17.4	10.8		10800	833	bidentate	Aqueous solution	193
$NiL_2(NO_3)_2$	28.2	17.5	11.1	9.2(sh)	11100	827	tridentate	Reflectance spectrum	74
$NiL_2(C\ell O_4)_2$	27.8	17.3	10.8	9.3(sh)	10800	847	tridentate	Reflectance spectrum	74
NiL_2I_2	27.3	17.2	10.7	8.6(sh)	10700	784	tridentate	Reflectance spectrum	73
$NiL_2C\ell_2$	27.8	18.2	10.6		10600	947	tridentate	Reflectance spectrum	75
$NiL_3C\ell_2$	28.2	17.7	12.5 (sh)	10.9	10900	808	bidentate	Reflectance spectrum	73
NiL_3Br_2	28.2	17.5	12.1 (sh)	10.9	10880	824	bidentate	Reflectance spectrum	73
$NiL_2(NCS)_2$	28.2	17.6	12.0 (sh)	10.9	10900	814	bidentate	Reflectance spectrum	73
NiL_2SO_4	27.5	17.5	12.5	8.9			bidentate with sulphate covalently linked to Ni^{2+}	Reflectance spectrum	74
	27.8	17.5	10.5		10530	920	tridentate	Reflectance spectrum	75

TABLE 8.24

Thermodynamic parameters of complex formation for etolen and oden with various metal ions. (Unless otherwise indicated, all values are for 25°C and μ = 0.5 mol dm^{-3}.)

Parameters	etolen						oden					
	Co^{2+}	Ni^{2+}	Cu^{2+}	Zn^{2+}	Cd^{2+}	Pb^{2+}	Co^{2+}	Ni^{2+}	Cu^{2+}	Zn^{2+}	Cd^{2+}	Pb^{2+}
log K_{011}	5.20	6.96	10.33	5.37	5.02	5.58	4.12	5.78	8.970	5.74	5.27	6.10
log K_{012}	4.02	5.82	7.75	4.90	4.17		3.14	3.47	3.78	4.12	4.06	
$\Delta H^{\ominus}_{011}$/kJ mol^{-1}	-21.4	-29.7	-46.4	-19.6			-18.7	-29.1	-39.9	-20.1		
$\Delta H^{\ominus}_{012}$/kJ mol^{-1}	-32	-37.8	- 4.44	-30.8			-15.2	-26.7	-18.8	-30.5		
$\Delta S^{\ominus}_{011}$/J $mol^{-1}K^{-1}$	27.8	33.6	42.1	37.1			16.2	13.1	38.1	43		
$\Delta S^{\ominus}_{012}$/J $mol^{-1}K^{-1}$	-30	-15.4	133.5	-9.50			9.13	-23.1	8	-24		
Reference			77		197*	197*			78	78	197*	197*

* Values from this reference are for 25°C and μ = 0.1 mol dm^{-3}.

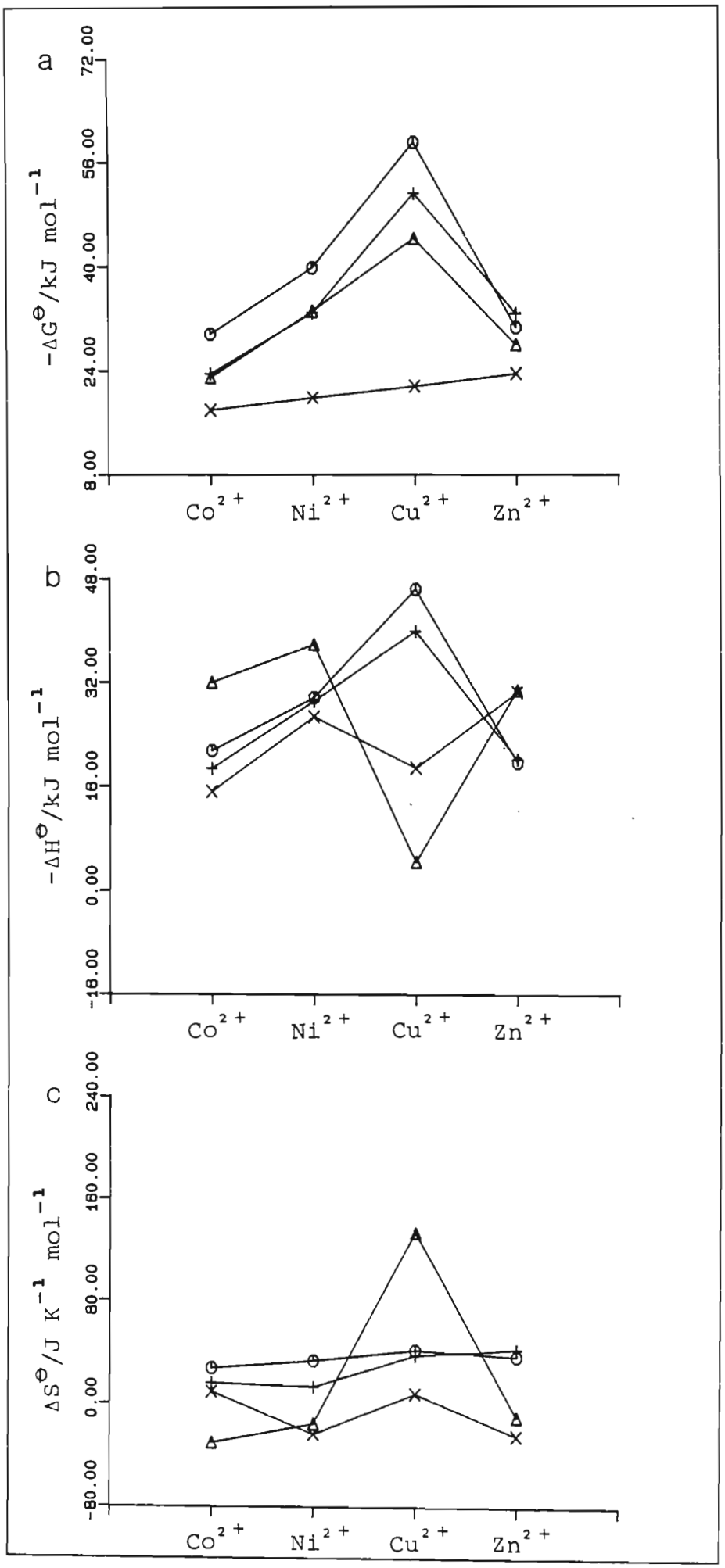

Figure 8.19 Thermodynamic parameters of stepwise formation for: $M(etolen)^{2+}$ (⏀), $M(oden)^{2+}$ (+), $M(etolen)_2^{2+}$ (△), and $M(oden)_2^{2+}$ (×)

more stable than the corresponding ones of oden.

2. Apart from the 1:1 complex with Zn^{2+} and the 1:2 complex with Cu^{2+}, the complex formation reactions of etolen are more exothermic than the corresponding ones of oden.

3. Apart from the 1:1 complex of Zn^{2+} and the 1:2 complex of Co^{2+}, the etolen complexes have greater entropy of formation than do the corresponding oden complexes.

From the above observations it is clear that the $Zn(oden)^{2+}$ complex does not follow the trend exhibited by the other oden complexes under consideration. However, a plot of log K_{011}(oden) against log K_{011}(etolen) (Figure 8.20) displays the interesting feature that those metal ions for which CFSE is expected (Co^{2+}, Ni^{2+} and Cu^{2+}) fall very close to a straight line, and those for which CFSE is not expected (Zn^{2+}, Cd^{2+} and Pb^{2+}) fall very close to a quite distinct straight line. For the first group the etolen complexes are the more stable, and for the second the oden complexes are. A similar split based on the presence or absence of CFSE was also observed by Hancock and Nakani (201) in their study of the oxygen donor ligands acetylacetonate and hydroxide.

It has been found (202) that if two very similar ligands A and B form complexes MA and MB with a series of metal ions such that the size, the number and the geometry of chelated rings is the same, a plot of log K_{MA} against log K_{MB} should be a straight line with a slope of one and an intercept of log K_{HA} - log K_{HB}. The line containing Co^{2+}, Ni^{2+} and Cu^{2+} does have a slope fairly close to one, viz. 0.95. However the other line has a much larger slope, 1.5. Thus it seems that the stereochemistry for the Zn^{2+}, Cd^{2+} and Pb^{2+} complexes may not be the same as for the remainder of the metal ions.

Let us now review what is known about the stereochemistry of the etolen and oden complexes with various metal ions. Information concerning the complexes in solution is summarized in Table 8.25, and Table 8.26 presents the information for the solid state. The complexes of the tridentate ligand dien are considered also, for comparison purposes. In addition the following points should be noted:

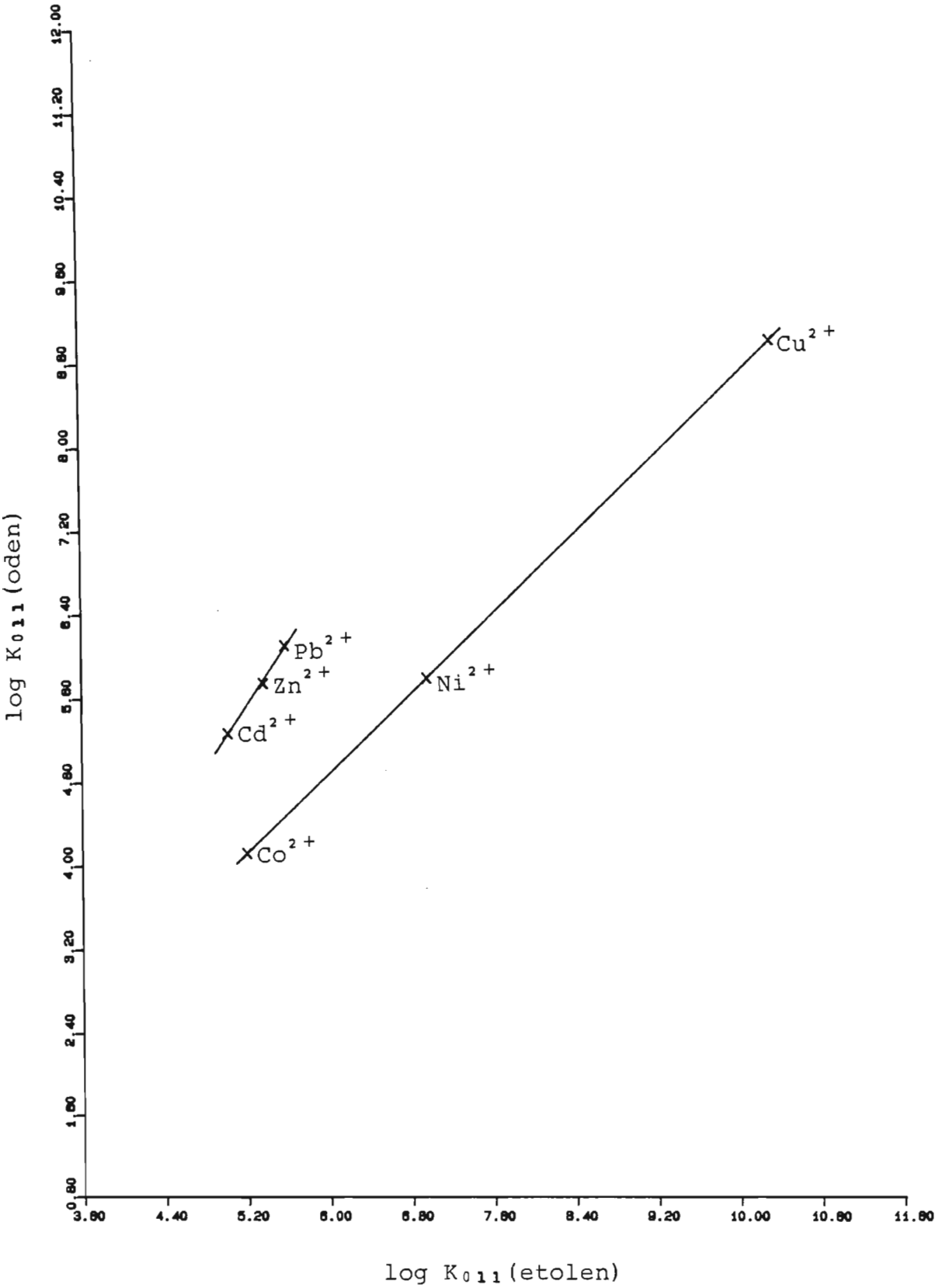

Figure 8.20 The linear free energy relationship of log K_{011}(oden) and log K_{011}(etolen).

TABLE 8.25

Structural details of etolen, oden and dien complexes in solution.

Complex	L = etolen[a]	L = oden[b]	L = dien[b]
$NiL(H_2O)_3^{2+}$	alcoholic oxygen coordinated 68% of the time ΔH for coordination of alcoholic oxygen is 0 and $\Delta S = 6.3$ J $K^{-1}mol^{-1}$	facial isomer at least 1.05 kJ mol^{-1} more stable in free energy terms than meridional isomer at 300 K ΔH for the isomerisation: facial $\rightleftharpoons$ meridional is positive ethereal oxygen coordinated to metal ion	facial isomer more stable than meridional isomer For the isomerisation: meridional $\rightleftharpoons$ facial $\Delta G = -4.90$ kJ mol^{-1} at 300 K and $\Delta H = 0$ dien is coordinated meridionally 7% of the time
$CoL(H_2O)_3^{2+}$	substantial amount of oxygen coordination		

[a]Reference 65.

[b]Reference 66.

TABLE 8.26

Structural details of etolen and dien complexes in the solid state.

Complex	Information	Reference
$Ni(dien)_2Cl_2.H_2O$	meridional Ni-1°N > Ni-2°N	46, 203
$Cu(dien)_2(NO_3)_2$	meridional Cu-1°N > Cu-2°N	204
$Cu(dien)_2Br_2.H_2O$	meridional	205
$MoO_3(dien)$	facial	206
$Mo(CO)_3(dien)$	facial	207
$Zn(dien)_2(NO_3)_2$	meridional Zn-1°N > Zn-2°N	208
$Zn(dien)_2Br_2.H_2O$	meridional Zn-1°N > Zn-2°N	209
$Cu(etolen)_2Cl_2$	etolen bidentate, hydroxyethyl arms of ligands free and trans to each other, four nitrogens lie at corners of a distorted square, Cu-1°N < Cu-2°N as in other asymmetrically substituted ethylene-diamine complexes, hydrogen bond between O and N on adjacent molecules	210
$Cu(etolen)_2(ClO_4)_2$	facial, distorted octahedron (tetragonal elongation), Cu-1°N < Cu-2°N, four nitrogens not co-planar to accommodate axial elongation, each 2°N displaced in direction of hydroxyethyl group to which it is attached, strain in two ligands at 2°N atoms,	211

	N-Cu-O ring angles are small because of strain in axial attachment of OH, O trans to O	
$Cu(etolen)_2(NO_3)_2$	distorted octahedron, one axial position occupied by NO_3^-, the other occupied by OH group	212
$Ni(etolen)_2(NO_3)_2$	meridional O trans to N Ni-1°N > Ni-2°N	171

1. From repulsion - energy calculations it has been shown (213) that in the solid state the meridional isomers of bis(tridentate ligand)-metal complexes are generally more stable than the facial isomers.

2. It is possible that the greater stability of the facial isomers of the ML complexes in solution is due to the presence of coordinated water molecules (66).

3. A study of the isomers of $[Co(NH_3)_3(dien)]^{3+}$ and $[Co(NH_3)(en)(dien)]^{3+}$ (214) revealed that facial isomers tend to have slightly lower strain energies than meridional.

We have seen from the UV-visible spectra of the Ni^{2+} complexes of oden and etolen that the ligand field is essentially octahedral. Hence we can reasonably assume that this is also the case for the metal ions Co^{2+} and Cu^{2+}.

On balance of the information available it seems likely that the facial isomers of the NiL^{2+} complexes are probably present in solution. One would also expect Co^{2+} to behave in this fashion.

Because of the tetragonally distorted octahedral coordination favoured by copper, one would expect the meridional isomers of the ML complexes to be stabilized relative to other stereochemistries. This meridional stereochemistry would enhance the CFSE for the ML complexes. This is in keeping with the trends observed in Figure 8.19(b). This planar structure would have a lower dipole moment and would therefore be able to orientate fewer water molecules, hence the somewhat higher value of $\Delta S^{\ominus}_{011}$ than those of Ni^{2+} and Co^{2+}. In the ML_2 complex the tetragonal distortion would be smaller, with a concomitant smaller CFSE resulting in a lower heat of formation for the ML_2 complex. This is especially marked in the case of the $Cu(etolen)_2^{2+}$ complex. For this complex, $\Delta H^{\ominus}_{012}$ is extremely low and out of line with the behaviour of the other etolen complexes, which suggests incomplete coordination of the second ligand molecule. The fact that $\Delta G^{\ominus}_{012}$ is not particularly low suggests that perhaps only the hydroxyethyl arm of the ligand is uncoordinated. If this is so, it would help to explain the extremely high value of $\Delta S^{\ominus}_{012}$. This latter value is consistent with a flexible structure for the complex.

Incomplete coordination of the ligand in the $Cu(oden)_2^{2+}$ complex is less likely. For this system, the value of $\Delta H^{\ominus}_{012}$ is less than that of $\Delta H^{\ominus}_{011}$, which is in keeping with the behaviour of Ni^{2+} and Co^{2+}, although the decrease is more pronounced. This could be because of the decreased CFSE. It is unlikely that the oxygen atom is not coordinated, as this would lead to the formation of an unstable eight-membered chelate ring with much steric hindrance between the atoms of the two ligands. If the second ligand were coordinated only through oxygen and one nitrogen, one would expect a somewhat lower $\Delta H^{\ominus}_{012}$ and higher $\Delta S^{\ominus}_{012}$, as is the case for the comparable etolen complex. Thus one must assume that the two ligand molecules in this complex are fully coordinated, but that the strain introduced by coordinating the ligand in the axial positions of the tetragonally distorted octahedron is reflected in the lower value of $\Delta H^{\ominus}_{012}$.

A comparison of the thermodynamic data for Zn^{2+} with those of other complexes of oden and etolen gives no reason to suppose that the complexes of zinc with these two ligands are anything but octahedral. We shall therefore assume that the ML complexes of zinc with etolen and oden are octahedral, probably with facial coordination.

Thus, if we exclude the ML_2^{2+} complexes of copper, we are able to compare directly the various thermodynamic quantities obtained for the complexes of etolen and oden. If we subtract the values obtained for the oden complexes from the corresponding ones for the etolen complexes, we should get a measure of the relative bonding capacities of primary and secondary nitrogen donors. These differences are listed in Table 8.27. In drawing conclusions from the differences, we assume that the conformational strains in the pairs of etolen and oden complexes are similar, and that there is no difference between the bonding capacities of alcoholic and ethereal oxygen atoms.

Examination of Figures 8.21 and 8.22 shows that the difference in complex stability, $\Delta(\log K_{011})$, between oden and etolen varies linearly with both the hardness and the ionic radius of the metal ion. We notice that, as the metal ion becomes harder or larger, the preference for coordination with etolen decreases. The same split of the metal ions into two groups as was observed previously is evident.

TABLE 8.27

Changes in thermodynamic parameters produced on changing from a primary to a secondary nitrogen donor.

Parameter	Co^{2+}	Ni^{2+}	Cu^{2+}	Zn^{2+}	Cd^{2+}	Pb^{2+}
$\Delta(\log K_{011})$	1.08(0.01)	1.18(0.01)	1.36(0.03)	-0.37(0.03)	-0.25(0.01)	-0.52(0.01)
$\Delta(\log K_{012})$	0.88(0.02)	2.35(0,03)	3.97(0.55)	0.78(0.06)	0.11(0.01)	
$\Delta(\Delta H^{\ominus}_{011})$/kJ mol^{-1}	-2.70(0.4)	-0.60(0.3)	-6.50(0.3)	0.50(0.4)		
$\Delta(\Delta H^{\ominus}_{012})$/kJ mol^{-1}	-17(2)	-11.1(0.7)	14.4(2.4)	-0.30(0.8)		
$\Delta(\Delta S^{\ominus}_{011})$/J mol^{-1}K^{-1}	11.6	20.5	4.0	-6		
$\Delta(\Delta S^{\ominus}_{012})$/J mol^{-1}K^{-1}	-39	7.7	126	14		
H_A*	4.34	3.37	2.68	4.26	3.31	6.69
r^{2+}/Å	0.74	0.72	0.69	0.74	0.97	1.20

* Reference 30.

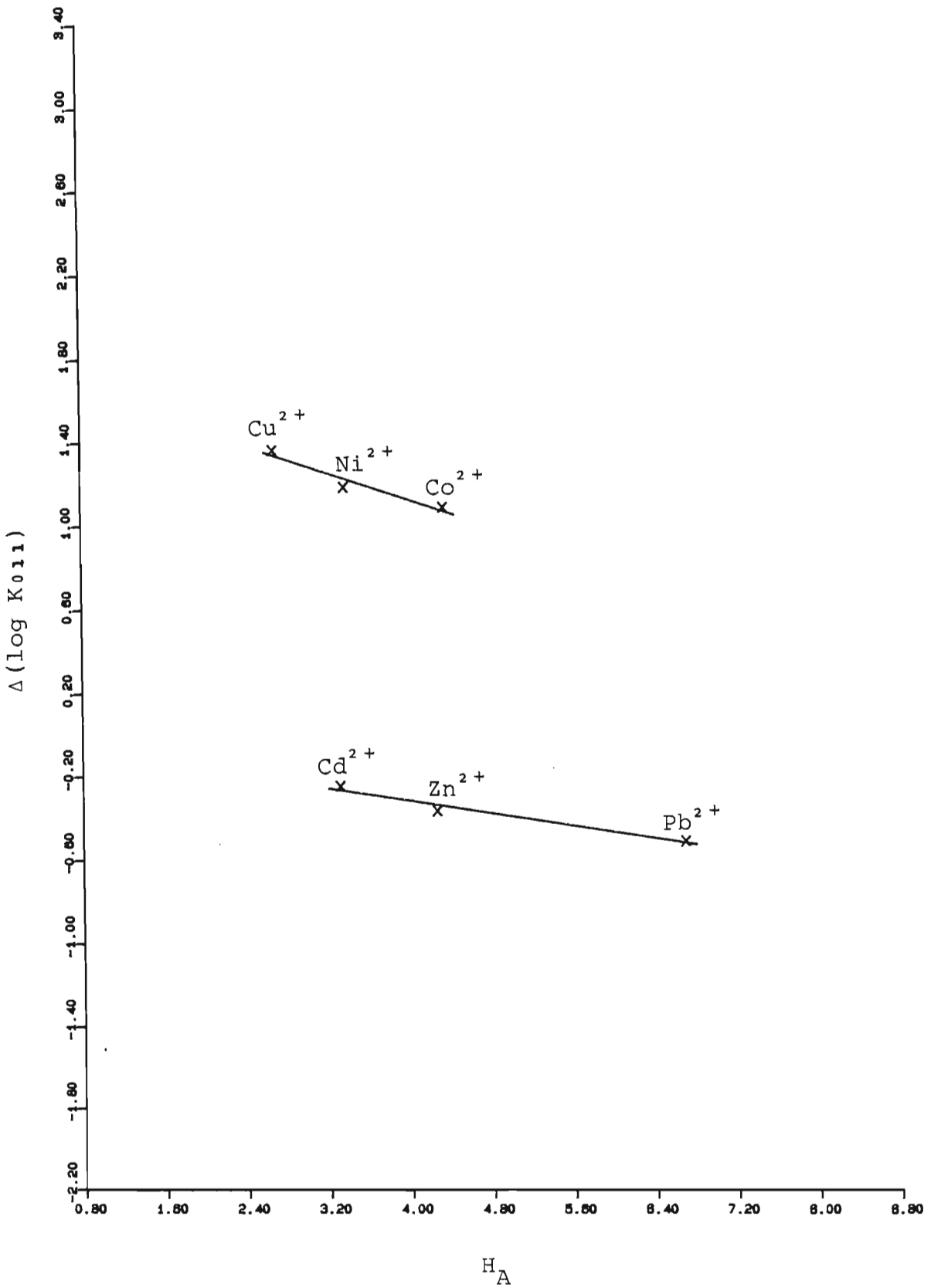

Figure 8.21 $\Delta(\log K_{011})$, the stability constant of the etolen complex minus that of oden, as a function of the hardness of the metal ion.

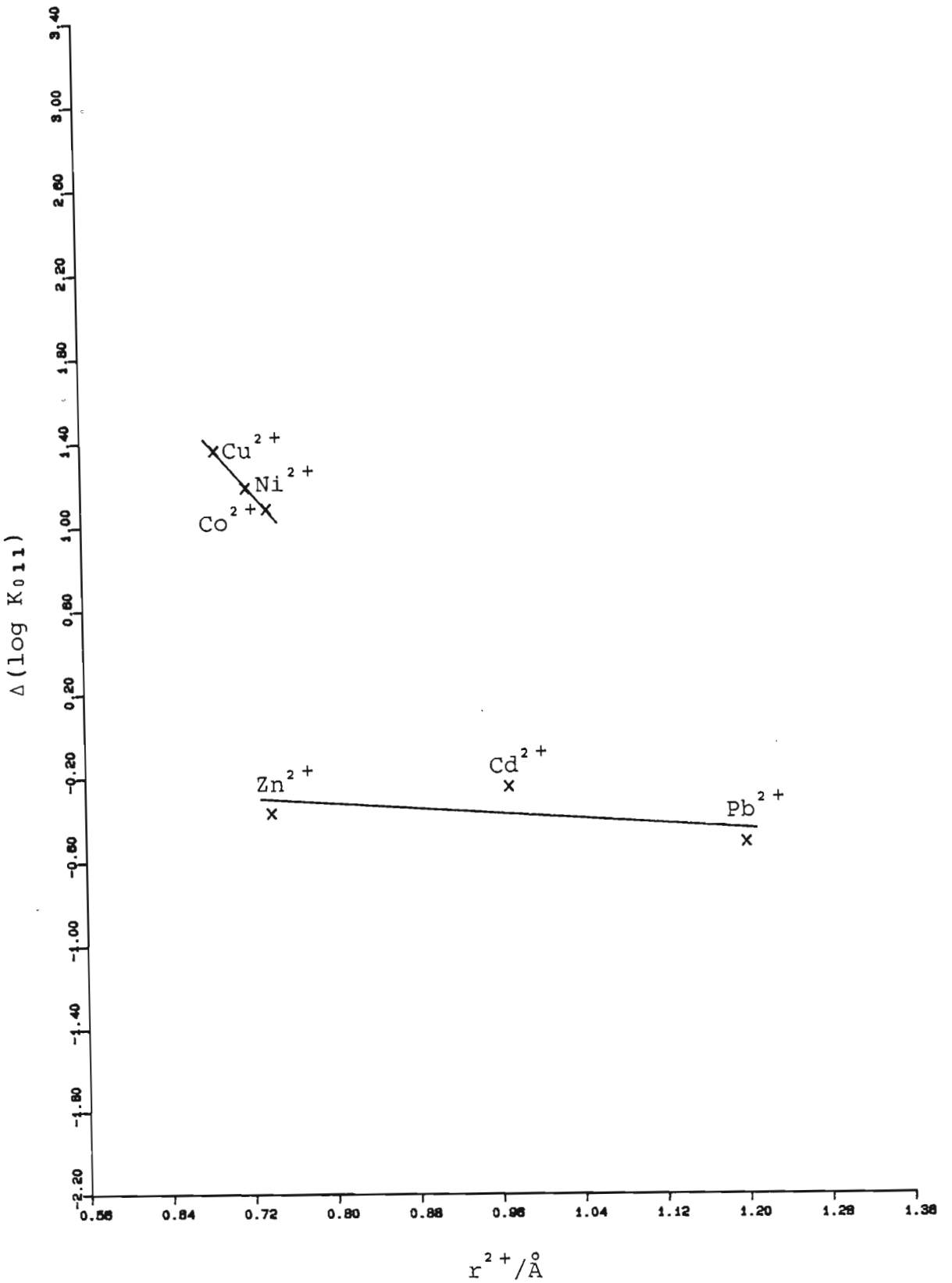

Figure 8.22 $\Delta(\log K_{011})$, the stability constant of the etolen complex minus that of oden, as a function of the radius of the metal ion.

If we consider the difference between the $\Delta H^{\ominus}_{011}$ values for etolen and those of oden, we see (Table 8.27) that this difference varies with the metal ion considered. However, there does not seem to be any obvious trend in $\Delta(\Delta H^{\ominus}_{011})$ with hardness or ionic radius.

It is noticeable that the value for nickel is -0.60 kJ mol^{-1}, which is very different from -7.1 kJ mol^{-1}, the value predicted by Hancock *et al.* (29). One possible explanation of this discrepancy is that the wrong stereochemistry has been assumed here for the $Ni(etolen)^{2+}$ complex, i.e. we have assumed it to be the facial isomer when it is in fact the meridional.

The $Ni(oden)^{2+}$ complex is known to be predominantly facial in solution (66). The above explanation therefore implies that we must correct the value of -29.7 kJ mol^{-1} obtained for $\Delta H^{\ominus}_{011}$ for $Ni(etolen)^{2+}$ in order that it should refer to the facial isomer and thus be directly comparable to the figure for $Ni(oden)^{2+}$. This can be accomplished as follows.

Yoshikawa *et al.* (214) have shown that the difference in strain energy between the meridional and facial isomers of $[Co(NH_3)_3(dien)]^{3+}$ is 3.7 kJ mol^{-1}, the facial isomer being the less strained. If we assume that the isomers of nickel and etolen behave similarly, we can correct the $\Delta H^{\ominus}_{011}$ value for nickel and etolen by means of the equation (1.33) of Hancock *et al.* (29):

$$\Delta H = n_p \Delta H_p + n_s \Delta H_s + \Delta U.$$

Assuming that ΔH_p and ΔH_s are the same for the two isomers, we then conclude that, for the facial isomer of $Ni(etolen)^{2+}$, $\Delta H^{\ominus}_{011}$ is approximately -33.4 kJ mol^{-1}. Hence the difference between the $\Delta H^{\ominus}_{011}$ values for the facial isomers of the $Ni(etolen)^{2+}$ and $Ni(oden)^{2+}$ complexes is -4.3 kJ mol^{-1}. When we use this value in plotting $\Delta(\Delta H^{\ominus}_{011})$ against hardness or ionic radius, it falls on a straight line with the values for Co^{2+} and Cu^{2+}. (See Figures 8.23 and 8.24.)

It therefore seems likely that the $Ni(etolen)^{2+}$ complex was predominantly meridional in solution, and that we have corrected adequately for this

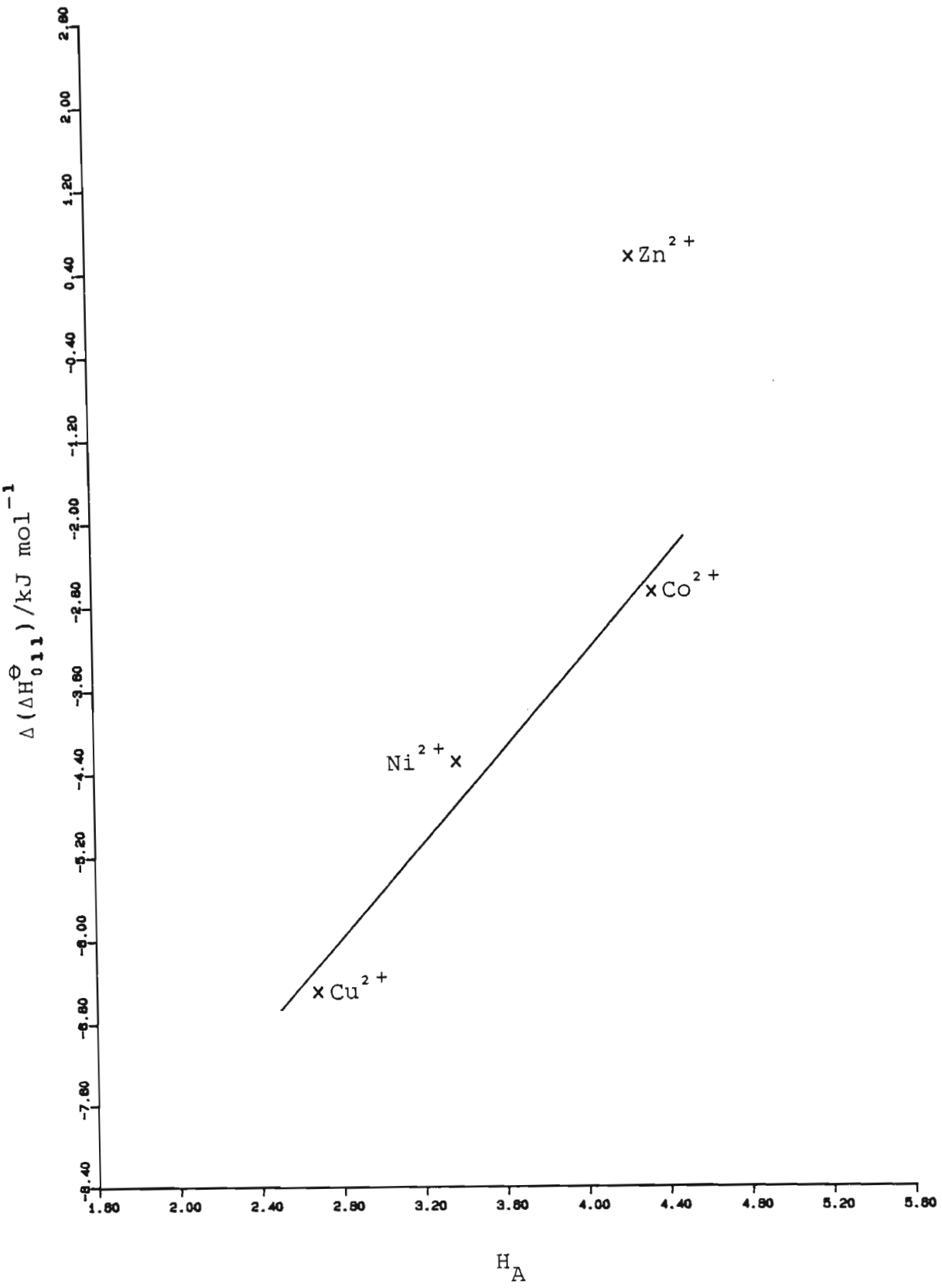

Figure 8.23 $\Delta(\Delta H^{\ominus}_{011})$, the enthalpy change for the etolen complex minus that of oden, as a function of the hardness of the metal ion.

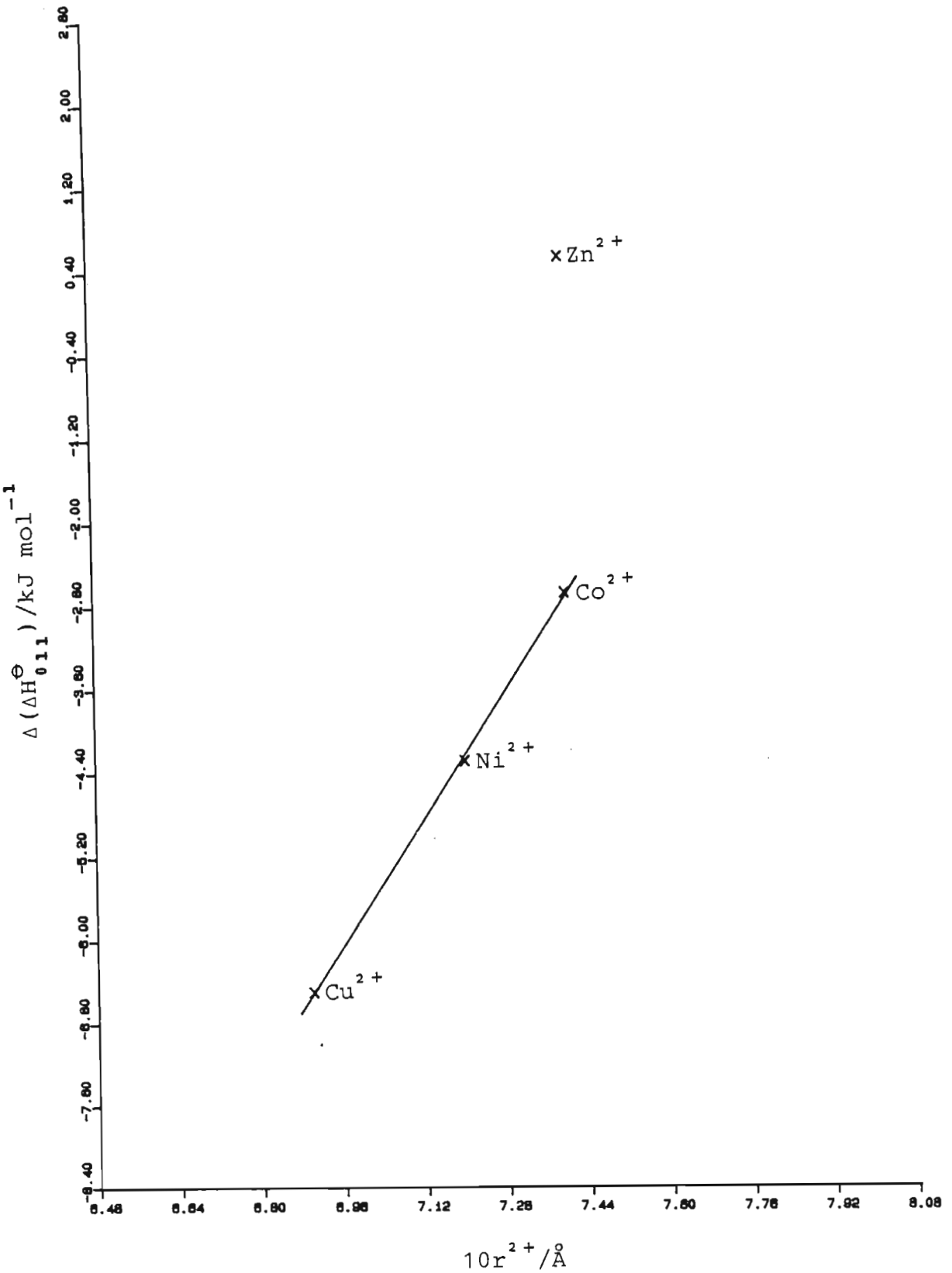

Figure 8.24. $\Delta(\Delta H^{\ominus}_{011})$, the enthalpy change for the etolen complex minus that of oden, as a function of the radius of the metal ion.

phenomenon.

Although the unavailability of enthalpy data for the cadmium and lead complexes makes it impossible to determine whether the six metal ions again split neatly into two groups, it can be seen at least that the behaviour of zinc is not consistent with that of cobalt, nickel and copper.

An interesting feature of the $\Delta(\Delta H^{\ominus}_{012})$ values for nickel and cobalt is that they are significantly greater in modulus than the corresponding $\Delta(\Delta H^{\ominus}_{011})$ values. This phenomenon could be due to the increased softness of the metal ion which results from the first addition of a ligand molecule. It could also occur because the strain induced by the addition of a second ligand molecule is less than that induced by the first. The strain energy calculations reported for the similar ligand dien (215) support this latter explanation in that the strain for the ML_2^{2+} complex is less than twice that for the ML^{2+} complex. It must be noted, however, that, in the case of the complexes of cobalt and nickel with oden, $|\Delta H^{\ominus}_{012}| < |\Delta H^{\ominus}_{011}|$, whereas for etolen (and many other polyamines) the opposite is true. This makes it difficult to draw any firm conclusions from the $\Delta(\Delta H^{\ominus}_{012})$ values. It might be possible to discover by means of strain energy calculations whether the above reversal of the usual trend is due to strain in the oden complexes.

No useful general conclusion can be drawn about the cumulative thermodynamic parameters for the ML_2^{2+} complexes, because the copper ion has to be excluded for the reasons previously mentioned, and lead has no ML_2^{2+} complex. This leaves two sets of only two points each.

The three metal ions considered which have no CFSE, Zn^{2+}, Cd^{2+} and Pb^{2+}, seem to fall into a different category as regards the behaviour of primary and secondary nitrogen donors. For these metal ions the $M(oden)^{2+}$ complexes are more stable than the $M(etolen)^{2+}$ complexes. However, the opposite is true for the stepwise formation of the ML_2^{2+} complexes from the ML^{2+} complexes. Thus, as in the case of cobalt and nickel, the second addition of a ligand molecule involves a softer interaction than does the first and so the enhancement of secondary over primary nitrogen bonding is observed. This is in accordance with what has been observed

of the crystal structures of the $Zn(dien)_2^{2+}$ complexes, that is, that the zinc - primary nitrogen bonds are longer than the zinc - secondary nitrogen bonds (208, 209). (The secondary nitrogen donor is thus seen to have an inductive effect when one ligand molecule has already been attached to the zinc ion. This effect may provide an alternative explanation of the observations of Ciampolini *et al.* (8) in the case of the complexes of dien with zinc: they observed that $\Delta H^{\ominus}_{011}$ is much less exothermic than $\Delta H^{\ominus}_{012}$.)

The zinc ion does seem to be the crossover point for the difference in behaviour between the etolen and the oden complexes. It has also been noticed by Thöm and Hancock (216) that zinc does not seem to discriminate between oxygen and nitrogen donors in macrocycles.

This difference in behaviour between metal ions which have CFSE and those which do not, and the intermediate nature of zinc, can be observed in a number of other respects:

1. The variation in complex stability with changes in the number of atoms in the macrocyclic ring of tetraazamacrocycles (217 - 219).

2. The variation in complex stability when rings or pendent groups bearing neutral oxygen donors are added (220).

(In the above references, however, the variations are explained in terms of the sizes of the metal ions rather than the presence or absence of CFSE.)

There is evidence that in the gas phase all metal ions respond more favourably to secondary amines than to primary (215). There is also evidence of a similar preference for ethereal over alcoholic oxygens (215).

From this work we can conclude that only metal ions which have CFSE and are fairly small seem to show a preference for secondary over primary nitrogen donors. The size of this apparent effect increases linearly with increasing softness and decreasing size of the metal ion. Such metal ions do not seem to distinguish between alcoholic and ethereal oxygen donors. (This conclusion is consistent with those of Everhart *et al.*

(65) and Thöm *et al.* (215).) In fact it seems that, in complexes of these metal ions, the complexation of any neutral oxygen donor is destabilized by steric strain (221). On the other hand, metal ions which have no CFSE and are larger do not distinguish between types of nitrogen donor, but in fact do prefer the (harder) oxygen donors (197).

However, for all the metal ions investigated, the addition of a second ligand molecule to the ML complex leads to enhancement of secondary over primary nitrogen bonding. It seems that the addition of one ligand molecule softens the metallic centre sufficiently for the inductive effect of the secondary nitrogen donor to overcome all other effects.

We therefore conclude that the bonds between metal ions and secondary nitrogen donors are not in general stronger than those involving primary nitrogen. (This conclusion may need to be modified if evidence emerges that the larger metal ions distinguish between ethereal and alcoholic oxygen donors.) These bonds do, however, appear to be stronger in those cases where crystal field stabilization energy is present and the metal ion is small. This enhanced stability appears to decrease as the size or the hardness of the metal ion increases.

APPENDIX I

DERIVATION OF EQUATION (1.16)

The empirical equation of Hancock and Marsicano (28) states that

$$\log K_1(\text{polyamine}) = 1.152 \log \beta_n(NH_3) + (n-1) \log 55.5, \qquad (1.16)$$

where n is the denticity of the polyamine. The form of this equation can be shown to arise as a result of the conventional asymmetric choice of standard states of solute and solvent species for reactions taking place in aqueous solution.

Consider the following ligand replacement reaction:

$$MA_n(aq) + L(aq) \rightleftharpoons ML(aq) + nA(aq) + xH_2O,$$

where M is the metal ion, A is a monodentate ligand, L is an n-dentate ligand and x is the number (usually unknown) of water molecules released in the process.

The chemical potential μ_i of any species i can be written in terms of its chemical potential $\mu_i^{\ominus}$ in some defined standard state and a thermodynamic activity a_i, as follows:

$$\mu_i = \mu_i^{\ominus} + RT \ln a_i.$$

If the standard state of species i is defined as a hypothetical solution of unit molar concentration in which the environment of every molecule is the same as at infinite dilution, then, neglecting nonideal effects in the real solutions, we may replace a_i by c_i, the molarity of species i, since by assumption the activity coefficient γ_i is 1. Hence:

$$\mu_i = \mu_i^{\ominus c} + RT \ln c_i,$$

where the superscript $\ominus c$ serves to indicate that the standard state is taken to be unit molar concentration.

For the unit mole fraction standard state (denoted by the superscript $^{\ominus x}$) we obtain the following relation if once again we neglect nonideal solution effects:

$$\mu_i = \mu_i^{\ominus x} + RT \ln x_i,$$

where x_i is the mole fraction of species i. Now, for a solution of fixed volume, the mole fraction of any component i is given by

$$x_i = \frac{n_i}{\sum_i n_i} = \frac{c_i}{\sum_i c_i}.$$

In dilute solution $\sum_i c_i \sim 55.5$ mol dm^{-3}, i.e. the molarity of pure water.

Thus it follows that for any solution component i

$$\mu_i^{\ominus x} = \mu_i^{\ominus c} + RT \ln 55.5.$$

For the ligand replacement reaction considered above we can write

$$\Delta G^{\ominus x} = \mu_{ML}^{\ominus x} + n\mu_A^{\ominus x} + x\mu_{H_2O}^{\ominus x} - \mu_{MA_n}^{\ominus x} - \mu_L^{\ominus x}$$

$$= \mu_{ML}^{\ominus c} + n\mu_A^{\ominus c} + x\mu_{H_2O}^{\ominus x} - \mu_{MA_n}^{\ominus c} - \mu_L^{\ominus c} + (n-1)\, RT \ln 55.5$$

$$= \Delta G^{\ominus} + (n-1)\, RT \ln 55.5,$$

as shown by Jones and Harrop (17). In the above equation the superscript $^{\ominus}$ on ΔG indicates the conventional asymmetric choice of standard states.

If we then use the facts that

$$\Delta G^{\ominus} = -RT \ln K^{\ominus}$$

and $$\Delta G^{\ominus x} = -RT \ln K^{\ominus x},$$

the following expression is obtained:

$$\ln K^{\ominus}_{chelate} = \ln K^{\ominus x}_{chelate} + (n-1) \ln 55.5.$$

Now

$$K^{\ominus}_{chelate} = \frac{a_{ML}\, a_A^n}{a_{MA_n}\, a_L} ,$$

where it has been assumed that the activity of water is 1 (since in dilute aqueous solution $\gamma_{H_2O} \to 1$ as $x_{H_2O} \to 1$). The last expression can be rewritten as

$$K^{\ominus}_{chelate} = \frac{K^{\ominus}(ML)}{\beta^{\ominus}(MA_n)} ,$$

where the constants $K^{\ominus}$ and $\beta_n^{\ominus}$ refer to the equilibria:

$$M + L \rightleftharpoons ML \qquad K^{\ominus} = \frac{a_{ML}}{a_M\, a_L}$$

and

$$M + nA \rightleftharpoons MA_n \qquad \beta_n^{\ominus} = \frac{a_{MA_n}}{a_M\, a_A^n} .$$

Similar expressions can be written for $K^{\ominus x}_{chelate}$.

Thus

$$\ell n \frac{K^{\ominus}(ML)}{\beta_n^{\ominus}(MA_n)} = \ell n \frac{K^{\ominus x}(ML)}{\beta_n^{\ominus x}(MA_n)} + (n-1)\ \ell n\ 55.5.$$

Therefore, if we can assume that $\ell n \{K^{\ominus x}(ML)/\beta_n^{\ominus x}(MA_n)\} \sim 0$ (and Jones and Harrop (17) discuss an example which suggests that this may be so) we have:

$$\ell n\ K^{\ominus}(ML) \sim \ell n\ \beta_n^{\ominus}(MA_n) + (n-1)\ \ell n\ 55.5.$$

After conversion to logarithms to the base ten, this is equation (1.16) without the factor which takes into account the inductive effect of the chelate bridges.

APPENDIX II

THE PROGRAM CALCAL

```
C       THIS PROGRAM CALCULATES THE HEAT CAPACITY OF CALORIMETER AND
C        CONTENTS
C       P=POWER DISSIPATED BY HEATER
C       INPUT
C       ALL OTHER INPUT VARIABLES DEFINED IN PROGRAM CALCOR
        DIMENSION EP(150),RT(150),CRT(150)
        DIMENSION BB(20)
        READ(2,500)(BB(II),II=1,20)
  500   FORMAT(20A4)
        READ (2,1) B,P,THETOT,DTH,SI,SF
        READ (2,4) EX,EY,DTHETX,DTHETY
        READ(2,2) N
        READ (2,3) (EP(I),I=1,N)
        DELTAT=(EY-EX)/B
        DO 100 I=1,N
        RTX=SI
        RTY=SF
        RT(I)=SI+(SF-SI)*((EP(I)-EX)/(EY-EX))
  100   CONTINUE
        DO 9 I=1,N
        IF (I-1) 15,15,16
   15   CRT(I)=((DTH-DTHETX)/2.)*(RTX+RT(I))
        GO TO 9
   16   CRT(I)=CRT(I-1)+(DTH/2.)*(RT(I-1)+RT(I))
    9   CONTINUE
        CRTY = CRT(N)+DTHETY * ((RT(N)+RTY)/2.)
        TCORR =DELTAT - CRTY/8
        WRITE(3,500)(BB(II),II=1,20)
        WRITE(3,10)
        WRITE(3,11) DELTAT,TCORR
        HT = P/1000.*THETOT
        CP = HT/TCORR
         WRITE(3,12) CP
    1   FORMAT (F8.2,3X,F8.3,3X,F5.0,3X,F4.0,3X,2(F7.4,3X))
    4   FORMAT (2(F7.1,3X),2(F5.1,3X))
    2   FORMAT(I3)
    3   FORMAT(F6.0)
   10   FORMAT(5X,41HRESULTS OF DETERMINATION OF HEAT CAPACITY,/)
   11   FORMAT(7X,22HUNCORRECTED TEMP RISE=,F7.4,/,9X,
       120HCORRECTED TEMP RISE=,F7.4,//)
   12   FORMAT(14X,15HHEAT CAPACITY =,F9.4,1X,8HJOULES/K,/)
        STOP
        END
```

APPENDIX III

THE PROGRAM CALCOR

```
C       THIS PROGRAM CORRECTS TITRATION CALORIMETER READINGS FOR
C             1 ) NON-CHEMICAL ENERGY TERMS
C             2 ) TEMPERATURE DIFFERENCE BETWEEN TITRANT AND TITRATE
C             3 ) DILUTION OF TITRANT
C
C
C       IT DOES NOT CORRECT FOR HEAT CONTRIBUTIONS FROM SIDE REACTIONS
C
C       INPUT
C
C       B = THERMISTOR CALIBRATION CONSTANT
C       CPR=HEAT CAPACITY OF EMPTY CALORIMETER
C       DCPDV= RATE OF CHANGE OF CALORIMETER HEAT CAPACITY WITH
C       VOLUME OF LIQUID IN EXCESS OF 95 CC
C       CPT= VOLUMETRIC SPECIFIC HEAT OF TITRANT
C       CPS = VOLUMETRIC SPECIFIC HEAT OF TITRATE
C       VOS = INITIAL VOLUME OF TITRATE
C       DTH = PRINTOUT INTERVAL IN SECS
C       DTHETX = TIME FROM START OF BURETTE TO POINT X
C       VTOT = TOTAL VOLUME DELIVERED( METTLER )
C       THETOT = TOTAL DELIVERY TIME
C       SI = INITIAL THERMOGRAM SLOPE
C       SF = FINAL THERMOGRAM SLOPE
C       EX = OFF-BALANCE POTENTIAL AT START OF REACTION
C       EY = OFF-BALANCE POTENTIAL AT END OF REACTION
C       EP = OFF-BALANCE POTENTIAL AT ANY POINT P
        DIMENSION TIME(150),EP(150),EQ(150),DELTAT(150),CQP(150),QHL
       1(150),CQHL(150),CQTC(150),CQDP(150),CQCP(150)
        DIMENSION VTP(150),CPP(150),QTC(150),AVTP(150)
        DIMENSION BB(20)
        READ(2,500)(BB(II),II=1,20)
  500   FORMAT(20A4)
        READ (2,23) A,B,CPR,DCPDV
        READ (2,24) CPS,CPT,DTH
        READ (2,2) HDIL
    4   READ (2,5) VOS,VTOT,THETOT,DTHETX,TBATH
        READ (2,502) CT
        READ (2,1) SI,SF,EX,EY
        READ (2,501) N
        READ (2,2) (EP(I),I = 1,N)
C
C       CALCULATION OF TITRANT DELIVERY RATE
        UBURET = VTOT/THETOT
C       CALCULATION OF VOLUME OF TITRANT APPARENTLY ADDED AT EACH POINT
        DO 100 I = 1,N
        TIME (I) = DTH* FLOAT(I) - DTHETX
  100   AVTP(I) = TIME(I)*UBURET
C       CALCULATION OF VOLUME OF TITRANT ACTUALLY ADDED AT EACH POINT
        DO 2002 I = 1,N
 2002   VTP (I) = DTH*FLOAT(I) * UBURET
C       CALCULATION OF ACTUAL HEAT CAPACITY AND TOTAL VOLUME TITRATED
C       AT EACH POINT
        DO 1007 I =1,N
 1007   CPP(I) = CPR + VOS*CPS+VTP(I)*CPT+DCPDV*VTP(I)
        CPPX=CPR+VOS*CPS+VTP(1)*CPT+DCPDV*VTP(1)
C       CALCULATION OF GROSS HEAT CHANGE IN GOING FROM THE(N-1)TH
C       TO THE NTH POINT
        DO 7 I=1,N
        IF (I -1) 1008,1008,1009
```

```
 1008 DELTAT(I) = (EP(I)-EX)/B
      CP = (CPPX+CPP(I))/2.
      GO TO 7
 1009 DELTAT(I) = (EP(I)-EP(I-1))/B
      CP = (CPP(I-1)+CPP(I))/2.
    7 CQP(I)= (-1.)*CP*DELTAT(I)
C     CALCULATION OF HEAT EXCHANGE CORRECTIONS
      DO 8 I = 1,N
      QHLX = (-1.)*SI*CPPX/B
      VTY = UBURET*THETOT
      QHLY=(-1.)*SF*(CPR+VOS*CPS+VTY*CPT+DCPDV*VTY)/B
    8 QHL(I) = QHLX+(QHLY-QHLX)*((EP(I)-EX)/(EY-EX))
      DO 9 I = 1,N
      IF (I-1) 1010,1010,1011
 1010 CQHL(I) = (QHL(I)+QHLX)*(DTH-DTHETX)/2.
      GO TO 9
 1011 CQHL(I) = (QHL(I)+QHL(I-1))*DTH/2.
    9 CONTINUE
C     CALCULATION OF ENERGY TERM DUE TO TEMP DIFFERENCE BETWEEN
C     TITRATE AND TITRANT
      DO 10 I=1,N
      IF (I-1) 1012,1012,1013
 1012 QTC(I)=UBURET*(DTH-DTHETX)*(TBATH-(EP(I)-A)/B)
      GO TO 10
 1013 QTC(I)= UBURET*DTH*(TBATH-(EP(I)-A)/B)
   10 CQTC(I) = (-1.)*CPT*QTC(I)
C     CALCULATION OF THE ENTHALPY OF DILUTION OF THE TITRANT
C     FROM EXPERIMENTALLY MEASURED HDIL
 2501 DO 15 I = 1,N
      IF (I-1) 32,32,33
   32 DVTP = UBURET * (DTH-DTHETX)
      GO TO 34
   33 DVTP = UBURET*DTH
   34 CONTINUE
      DNT = CT*(DVTP/1000.)
   15 CQDP(I) = DNT*HDIL
C     CALCULATION OF CORRECTED HEAT
      DO 16 I = 1,N
   16 CQCP(I)=CQP(I)-CQHL(I)-CQTC(I)-CQDP(I)
C     OUTPUT
      WRITE(3,500)(BB(II),II=1,20)
      WRITE(3,17)
      WRITE (3,18) UBURET
      WRITE (3,19)
      DO 20 I = 1,N
   20 WRITE (3,21)AVTP(I),CQP(I),CQHL(I),CQTC(I),CQDP(I),CQCP(I)
      WRITE (3,22)
C     FORMAT STATEMENTS
    1 FORMAT (2(F7.4,3X),2(F7.1,3X))
    2 FORMAT (F6.0)
    5 FORMAT (F4.0,3X,F6.3,3X,F5.0,3X,F5.1,3X,F7.3)
  501 FORMAT (I3)
  502 FORMAT (F7.4)
   17 FORMAT (/,44X,30HCORRECTED CALORIMETRIC RESULTS,//)
   18 FORMAT (1X,22HTITRANT DELIVERY RATE=,F10.7,1X,6HCC/SEC,/)
   19 FORMAT (4X,11HAPP. VOL/ML,14X,4HQP/J,15X,5HQHL/J,
     115X,5HQTC/J,15X,4HQD/J,16X,4HQC/J,/)
   21 FORMAT (5X,F8.4,14X,F7.3,12X,F7.3,13X,F7.3,13X,F7.3,13X,F7.3)
   22 FORMAT(///)
   23 FORMAT (F8.0,3X,F8.2,3X,F7.3,3X,F8.5)
   24 FORMAT (2(F7.4,3X),F4.0)
      STOP
      END
```

REFERENCES

1. (a) SILLÉN, L.G. and MARTELL, A.E., 'Stability Constants of Metal-ion Complexes', 2nd edition, London, The Chemical Society, Special Publication No. 17, 1964.

   (b) SILLÉN, L.G. and MARTELL, A.E., 'Stability Constants of Metal-ion Complexes', London, The Chemical Society, Special Publication No. 25, 1971.

   (c) HÖGFELDT, E., 'Stability Constants of Metal-ion Complexes. Part A. Inorganic Ligands', IUPAC Chemical Data Series No. 21, Pergamon Press, 1982.

   (d) PERRIN, D.D., 'Stability Constants of Metal-ion Complexes. Part B. Organic Ligands', IUPAC Chemical Data Series No. 22, Pergamon Press, 1979.

   (e) SERJEANT, E.P. and DEMPSEY, B., 'Ionization Constants of Organic Acids in Aqueous Solution', IUPAC Chemical Data Series No. 23, Pergamon Press, 1979.

2. SMITH, R.M. and MARTELL, A.E., 'Critical Stability Constants', Vols 1 - 4, New York, Plenum Press, 1974, 1975, 1977, 1976.

3. CHRISTENSEN, J.J., HANSEN, L.D. and IZATT, R.M., 'Handbook of Proton Ionization Heats', New York, John Wiley and Sons, 1976.

4. CHRISTENSEN, J.J., EATOUGH, D.J. and IZATT, R.M., 'Handbook of Metal Ligand Heats and Related Thermodynamic Quantities', 2nd edition, New York, Marcel Dekker, 1975.

5. HANCOCK, R.D. and MARSICANO, F., J. Chem. Soc. (Dalton), 1832 (1976).

6. MARSICANO, F. and HANCOCK, R.D., J. Chem. Soc. (Dalton), 228 (1978).

7. SCHWARZENBACH, G., Helv. Chim. Acta, 35, 2344 (1952).

8. CIAMPOLINI, M., PAOLETTI, P. and SACCONI, L., J. Chem. Soc., 2994 (1961).

9. SACCONI, L., PAOLETTI, P. and CIAMPOLINI, M., J. Chem. Soc., 5115 (1961).

10. PAOLETTI, P. and VACCA, A., J. Chem. Soc., 5051 (1964).

11. SACCONI, L., PAOLETTI, P. and CIAMPOLINI, M., J. Chem. Soc., 5046 (1964).

12. NANCOLLAS, G.H., Coord. Chem. Revs, 5, 379 (1970).

13. CALVIN, M. and BAILES, R.H., J. Amer. Chem. Soc., 68, 949 (1946).

14. SCHWARZENBACH, G., Advan. Inorg. Chem. and Radiochem., 3, 257 (1961).

15. (a) COTTON, F.A. and HARRIS, F.E., J. Phys. Chem., 59, 1203 (1955).

(b) ibid., 60, 1451 (1956).

16. ADAMSON, A.W., J. Amer. Chem. Soc., 76, 1578 (1954).

17. JONES, G.R.H. and HARROP, R., J. Inorg. Nucl. Chem., 35, 173 (1973).

18. BEECH, G., Q. Rev. Chem. Soc., 23, 410 (1969).

19. MARTELL, A.E., Advances in Chemistry Series, Vol. 62, Washington, DC, The American Chemical Society, 1967, p. 272.

20. MUNRO, D., Chem. Brit., 13,100 (1977).

21. AGTERDENBOS, J., J. Chem. Ed., 45, 230 (1968).

22. SIMMONS, E.L., J. Chem. Ed., 56, 578 (1979).

23. PRUE, J.E., J. Chem. Ed., 46, 12 (1969).

24. BJERRUM, N., Kgl. Danske Videnskab. Selskab, Mat.-Fys. Medd., 7, 9 (1926).

25. FUOSS, R.M., J. Amer. Chem. Soc., 80, 5059 (1958).

26. EIGEN, M., Z. Phys. Chem.(Frankfurt), 1, 176 (1954).

27. ROSSEINSKY, D.R., J. Chem. Soc. (Dalton), 731 (1979).

28. HANCOCK, R.D. and MARSICANO, F., J. Chem. Soc. (Dalton), 1096 (1976).

29. HANCOCK, R.D., McDOUGALL, G.J. and MARSICANO, F., Inorg. Chem., 18, 2847 (1979).

30. HANCOCK, R.D. and MARSICANO, F., Inorg. Chem., 17, 560 (1978).

31. FRAÚSTO DA SILVA, J.J.R., J. Chem. Ed., 60, 390 (1983).

32. MYERS, R.T., Inorg. Chem., 17, 952 (1978).

33. ATKINSON, G. and BAUMAN Jr., J.E., Inorg. Chem., 2, 64 (1963).

34. (a) SPIKE, C.G. and PARRY, R.W., J. Amer. Chem. Soc., 75, 2726 (1953).

(b) ibid., 75, 3770 (1953).

35. RASMUSSEN, S.E., Acta Chem. Scand., 10, 1279 (1956).

36. ANDEREGG, G., Chem. Brit., 13, 437 (1977).

37. SANGER, A., Chem. Brit., 13, 242 (1977).

38. POWELL, H.K.J., Chem. Brit., 14, 220 (1978).

39. RODE, B.M., Chem. Phys. Lett., 26, 350 (1974).

40. IRVING, H., WILLIAMS, R.J.P., FERRETT, D.J. and WILLIAMS, A.E., J. Chem. Soc., 3494 (1954).

41. WILLIAMS, R.J.P., J. Phys. Chem., 58, 121 (1954).

42. PAOLETTI, P., FABBRIZZI, L. and BARBUCCI, R., Inorg. Chim. Acta Revs, 7, 43 (1973).

43. CIAMPOLINI, M., PAOLETTI,P. and SACCONI, L., J. Chem. Soc., 4553 (1960).

44. ANDEREGG, G., Adv. Mol. Relaxation Interact. Processes, 18, 79 (1980).

45. BARBUCCI, R., FABBRIZZI, L. and PAOLETTI, P., Coord. Chem. Revs, 8, 31 (1972).

46. PAOLETTI, P., BIAGINI, S. and CANNAS, M., Chem. Comm., 513 (1969).

47. McDOUGALL, G.J., HANCOCK, R.D. and BOEYENS, J.C.A., J. Chem. Soc. (Dalton), 1438 (1978).

48. BOEYENS, J.C.A., HANCOCK, R.D. and McDOUGALL, G.J., S. Afr. J. Chem., 32, 23 (1979).

49. POWELL, K., Chem. N.Z., 40, 9 (1976).

50. PAOLETTI, P., 'Coordination Compounds. Structural Information from Calorimetry', in 'International Symposium on Calorimetry in Chemical and Biological Sciences', Guildford, September 1969, p. 87.

51. FABBRIZZI, L., PAOLETTI, P. and CLAY, R.M., Inorg. Chem., 17, 1042 (1978).

52. HINZ, F.P. and MARGERUM, D.W., Inorg. Chem., 13, 2941 (1974).

53. HANCOCK, R.D. and McDOUGALL, G.J., J. Amer. Chem. Soc., 102, 6551 (1980).

54. HANCOCK, R.D. and McDOUGALL, G.J., Adv. Mol. Relaxation Interact. Processes, 18, 99 (1980).

55. BARBUCCI, R. and BARONE, V., J. Soln. Chem., 8, 427 (1979).

56. PAOLETTI, P., BARBUCCI, R. and VACCA, A., J. Chem. Soc. (Dalton), 2010 (1972).

57. DELFINI, M., SEGRE, A.L., CONTI, F., BARBUCCI, R., BARONE, V. and FERRUTI, P., J. Chem. Soc. (Perkin II), 900 (1980).

58. CHRISTENSEN, J.J., IZATT, R.M., WRATHALL, D.P. and HANSEN, L.D., J. Chem. Soc. (A), 1212 (1969).

59. DEGISCHER, G. and NANCOLLAS, G.H., J. Chem. Soc. (A), 1125 (1970).

60. GURNEY, R.W., 'Ionic Processes in Solution', New York, McGraw-Hill, 1953.

61. MUNSON, M.S.B., J. Amer. Chem. Soc., 87, 2332 (1965).

62. JONES III, F.M. and ARNETT, E.M., Prog. Phys. Org. Chem., 11, 263 (1974).

63. DRAGO, R.S., VOGEL, G.C. and NEEDHAM, T.E., J. Amer. Chem. Soc., 93, 6014 (1971).

64. McMILLIN, D.R., DRAGO, R.S. and NUSZ, J.A., J. Amer. Chem. Soc., 98, 3120 (1976).

65. EVERHART, D.S., McKOWN, M.M. and EVILIA, R.F., J. Coord. Chem., 9, 185 (1979).

66. EVILIA, R.F., YOUNG, D.C. and REILLEY, C.N., J. Coord. Chem., 3, 17 (1973).

67. BRECKENRIDGE, J.G., Can. J. Research, 26B, 11 (1948).

68. HARVEY, J.L., TEWKSBURY, C.I. and HAENDLER, H.M., J. Amer. Chem. Soc., 71, 3641 (1949).

69. KELLER, R.N. and EDWARDS, L.J., J. Amer. Chem. Soc. 74, 215 (1952).

70. DRINKARD, W.C., BAUER, H.F. and BAILAR, Jr., J.C., J. Amer. Chem. Soc., 82, 2992 (1960).

71. DAS SARMA, B., TENNENHOUSE, G.J. and BAILAR, Jr., J.C., J. Amer. Chem. Soc., 90, 1362 (1968).

72. DAS SARMA, B. and BAILAR, Jr., J.C., J. Amer. Chem. Soc., 91, 5958 (1969).

73. BASSETT, J., GRZESKOWIAK, R. and O'LEARY, B.L., J. Inorg. Nucl. Chem., 32, 3861 (1970).

74. BASSETT, J., GRZESKOWIAK, R. and O'LEARY, B.L., J. Inorg. Nucl. Chem., 32, 3867 (1970).

75. RUSTAGI, S.C. and RAO, G.N., Current Science, 42, 351 (1973).

76. NÄSÄNEN, R., LEMMETTI, L. and ULMANEN, S., Suom. Kemistilehti, 42B, 266 (1969).

77. BARBUCCI, R., Inorg. Chim. Acta, 12, 113 (1975).

78. BARBUCCI, R. and VACCA, A., J. Chem. Soc. (Dalton), 2363 (1974).

79. BECK, M.T., 'Chemistry of Complex Equilibria', London, Van Nostrand Reinhold, 1970, p. 27.

80. ROSSOTTI, F.J.C. and ROSSOTTI, H.S., 'The Determination of Stability Constants', New York, McGraw-Hill, 1961.

81. ROSSOTTI, H., 'The Study of Ionic Equilibria, An Introduction', London, Longman, 1978.

82. ROSSOTTI, H.S., Talanta, 21, 809 (1974).

83. BECK, M.T., 'Determination of Stability Constants of Metal Complexes', in 'Essays on Analytical Chemistry in Memory of Professor Anders Ringbom', Wänninen, E. (ed.), Oxford, Pergamon Press, 1977, p. 59.

84. ALBERT, A. and SERJEANT, E.P., 'The Determination of Ionization Constants', New York, Chapman and Hall, 1984.

85. CHRISTENSEN, J.J., IZATT, R.M., HANSEN, L.D. and PARTRIDGE, J.A., J. Phys. Chem., 70, 2003 (1966).

86. GRENTHE, I. and LEDEN, I., 'Calorimetric Titrations for the Study of Stepwise Equilibria in Solutions', in 'Proc. 8th Int. Conf. Coord. Chem.', Gutmann, V. (ed.), New York, Springer, 1964, p. 332.

87. ARNEK, R., Acta Chem. Scand., 23, 1986 (1969).

88. BARTHEL, J., 'Thermometric Titrations', New York, John Wiley and Sons, 1975, p. 148.

89. CHRISTENSEN, J.J., RUCKMAN, J., EATOUGH, D.J. and IZATT, R.M., Thermochimica Acta, 3, 203 (1972).

90. EATOUGH, D.J., CHRISTENSEN, J.J. and IZATT, R.M., Thermochimica Acta, 3, 219 (1972).

91. EATOUGH, D.J., IZATT, R.M. and CHRISTENSEN, J.J., Thermochimica Acta, 3, 233 (1972).

92. EATOUGH, D.J., IZATT, R.M. and CHRISTENSEN, J.J., Comprehensive Analytical Chemistry, 12B, 3 (1982).

93. HANSEN, L.D., IZATT, R.M. and CHRISTENSEN, J.J., 'Applications of Thermometric Titrimetry to Analytical Chemistry', in 'New Developments in Titrimetry', Jordan, J. (ed.), New York, Marcel Dekker, 1974, p.1.

94. VOGEL, A.I., 'A text-book of quantitative inorganic analysis including elementary instrumental analysis', 3rd edition, London, Longman , 1961, p. 238.

95. ibid., p. 241 (Procedure B).

96. ibid., p. 435.

97. MERCK, E., 'Complexometric Assay Methods with Titriplex', 3rd edition, Darmstadt, p. 32.

98. VOGEL, A.I., 'A text-book of quantitative inorganic analysis including elementary instrumental analysis', 3rd edition, London, Longman , 1961, p. 433.

99. 'CRC Handbook of Chemistry and Physics', 65th edition, Boca Raton, CRC Press Inc., 1984, p. C-294.

100. POUCHERT, C.J., 'The Aldrich Library of Infrared Spectra', 3rd edition, Milwaukee, Aldrich Chemical Company, 1981, p. 204A.

101. SEGAL, L. and EGGERTON, F.V., Applied Spectroscopy, 15, 148 (1961).

102. 'Dictionary of Organic Compounds', Volume 2, 4th edition, London, Eyre and Spottiswoode, 1965, p. 865.

103. POUCHERT, C.J., 'The Aldrich Library of Infrared Spectra', 3rd edition, Milwaukee, Aldrich Chemical Company, 1981, p. 200H.

104. KIPRIYANOV, A.I. and KIPRIYANOV, G.I., Journal of General Chemistry of the U.S.S.R., 2, 585 (1932).

105. I.G. FARBENIND. A.-G., Nitriles and Derivatives, French Patent 730 760, Appl. 30 January 1932.

106. STEWART, F.H.C., Journal of Organic Chemistry, 27, 687 (1962).

107. BENEDIKOVIČ, I., RIEČANSKÁ, E. and MAJER, J., Acta Fac. Pharm. Univ. Comenianae, 26, 59 (1974).

108. TAYLOR, D.A.H., Personal communication.

109. VOGEL, A.I., 'A Text-book of Macro and Semimicro Qualitative Inorganic Analysis', 4th edition, London, Longman , 1976, p. 340.

110. POUCHERT, C.J., 'The Aldrich Library of Infrared Spectra', 3rd edition, Milwaukee, Aldrich Chemical Company, 1981, p. 339D.

111. JANKOWSKI, K. and BERSE, C., Canadian Journal of Chemistry, 46, 1939 (1968).

112. TAKAGI, N., HSU, H.Y. and TAKEMOTO, T., Yakugaku Zasshi, 90, 899 (1970) cited in Chemical Abstracts, 73: 127782u (1970) as well as 'Dictionary of Organic Compounds', Tenth and cumulative supplement, 4th edition, London, Eyre and Spottiswoode, 1974, p. 779.

113. TIMAKOVA, L.M., YAROSHENKO, G.F., LASTOVSKII, R.P., SIDORENKO, V.V., RYKOV, S.V. and SIZOV, V.V., N-(2-Hydroxyethyl)aminoacetic acid, U.S.S.R. Patent 681050, Appl. 17 March 1978, Acc. 25 August 1979, cited in Chemical Abstracts, 92: 22058b (1980).

114. LEIMU, R.and JANSSON, J.I., Suomen Kemistilehti, 18B, 40 (1945).

115. VIÈLES, P. and SÉGUIN, J., Comptes Rendus, 234, 1980 (1952).

116. VIÈLES, P. and SÉGUIN, J., Societe Chimique de France Bulletin, 287 (1953).

117. HOPE, D.B. and HORNCASTLE, K.C., Biochemical Journal, 102, 910 (1967).

118. LOWE, K., FORBES, A.W. and MARSICANO, F., 'The construction and testing of a precision calorimeter', Johannesburg, National Institute for Metallurgy, Report No. 1582, October 1973, 19 pp.

119. GRAN, G., Acta Chem. Scand., 4, 559 (1950).

120. GRAN, G., Analyst, 77, 661 (1952).

121. ROSSOTTI, F.J.C. and ROSSOTTI, H., J. Chem. Ed., 42, 375 (1965).

122. INGMAN, F. and STILL, E., Talanta, 13, 1431 (1966).

123. MASCINI, M., Ion-Selective Electrode Rev., 2, 17 (1980).

124. ROSSOTTI, F.J.C. and ROSSOTTI, H., J. Phys. Chem., 68, 3773 (1964).

125. BARTHEL, J., 'Thermometric Titrations', New York, John Wiley and Sons, 1975, p.24.

126. WILLIAMS, D.R., J. Chem. Ed., 48, 480 (1971).

127. WILLIAMS, D.R., J. Chem. Soc. (Dalton), 1064 (1973).

128. CORRIE, A.M. and WILLIAMS, D.R., Annali di Chimica, 68, 821 (1978).

129. INGRI, N., KAKOŁOWICZ, W., SILLÉN, L.G. and WARNQVIST, B., Talanta, 14, 1261 (1967).

130. MAY, P.M., WILLIAMS, D.R., LINDER, P.W. and TORRINGTON, R.G., Talanta, 29,249 (1982).

131. SABATINI, A., VACCA, A. and GANS, P., Talanta, 21, 53 (1974).

132. LEGGETT, D.J., Talanta, 24, 535 (1977).

133. GANS, P., SABATINI, A. and VACCA, A., Inorg. Chim. Acta, 18, 237 (1976).

134. SABATINI, A. and VACCA, A., J. Chem. Soc. (Dalton), 1693 (1972).

135. MAY, P.M., MURRAY, K. and WILLIAMS, D.R., Talanta, 32, 483 (1985).

136. MURRAY, K. and MAY, P.M., 'Metal-Ligand Formation Constants by Potentiometric Titration/Computing Techniques', Lecture presented at Chelsea College, London on 5 April 1984.

137. KIELLAND, J., J. Amer. Chem. Soc., 59, 1675 (1937).

138. LINDER, P.W. and MURRAY, K., Talanta, 29, 377 (1982).

139. MURRAY, K. and MAY, P.M., 'ESTA Users Manual', 1984.

140. ARNEK, R., Arkiv Kemi, 32, 81 (1970).

141. SILLÉN, L.G., Acta Chem. Scand., 18, 1085 (1964).

142. SILLÉN, L.G., and WARNQVIST, B., Arkiv Kemi, 31, 341 (1969).

143. MARKLUND, E., SJÖBERG, S. and ÖHMAN, L., Acta Chem. Scand., A40, 367 (1986).

144. VADASDI, K., J. Phys. Chem., 78, 816 (1974).

145. AVDEEF, A., Inorg. Chem., 19, 3081 (1980).

146. VACCA, A., SABATINI, A. and GRISTINA, M.A., Coord. Chem. Rev., 8, 45 (1972).

147. HAVEL, J. and MELOUN, M., Talanta, 32, 171 (1985).

148. GANS, P., Adv. Mol. Relaxation Interact. Processes, 18, 139 (1980).

149. JOHANSEN, E.S. and JØNS, O., Talanta, 31, 743 (1984).

150. ROSSOTTI, H., 'The Study of Ionic Equilibria, An Introduction', London, Longman, 1978, p. 83.

151. ibid., p. 91.

152. ibid., p. 92.

153. ROSSOTTI, F.J.C. and ROSSOTTI, H.S., 'The Determination of Stability Constants', New York, McGraw-Hill, 1961, p. 145.

154. MULLA, F., M.Sc. Thesis, University of Natal, Durban, 1981, p. 65.

155. BIEDERMANN, G. and SILLÉN, L.G., Arkiv Kemi, 5, 425 (1953).

156. ROSSOTTI, H.S., 'The Study of Ionic Equilibria, An Introduction', London, Longman, 1978, p. 85.

157. MOLINA, M., MELIOS, C., TOGNOLLI, J.O., LUCHIARI, L.C. and JAFELICCI Jr., M., J. Electroanal. Chem., 105, 237 (1979).

158. LINDER, P.W. and TORRINGTON, R.G., Research Progress Report, University of Cape Town, July 1979 - June 1980, p. 23.

159. BOTTARI, E., *et al.*, Annali di Chimica, 68, 813 (1978).

160. SMITH, R.M. and MARTELL, A.E., 'Critical Stability Constants, Vol. 4: Inorganic Complexes', New York, Plenum Press, 1976, p. 1.

161. LINDER, P.W. and TORRINGTON, R.G., Research Progress Report, University of Cape Town, July 1979 - June 1980, p. 24.

162. MARTELL, A.E. and SMITH, R.M., 'Critical Stability Constants, Vol. 3: Other Organic Ligands', New York, Plenum Press, 1977, p. 3.

163. LOWE, K., FORBES, A.W. and MARSICANO, F., 'The construction and testing of a precision calorimeter', Johannesburg, National Institute for Metallurgy, Report No. 1582, October 1973, pp. 9, 10.

164. ibid., p. 9.

165. ibid., p. 8.

166. 'Handbook of Chemistry and Physics', 53rd edition, Cleveland, The Chemical Rubber Company, 1972, pp. D-128, F-11.

167. SMITH, R.M. and MARTELL, A.E., 'Critical Stability Constants, Vol. 2: Amines', New York, Plenum Press, 1975, p. 95.

168. SMITH, R.M. and MARTELL, A.E., 'Critical Stability Constants, Vol. 4: Inorganic Complexes', New York, Plenum Press, 1976, p. 6.

169. LOWE, K., FORBES, A.W. and MARSICANO, F., 'The construction and testing of a precision calorimeter', Johannesburg, National Institute for Metallurgy, Report No. 1582, October 1973, p. 6.

170. JONES, P.G., Chem. Brit., 17, 222 (1981).

171. WADE, P.W., M.Sc. Thesis, University of the Witwatersrand, Johannesburg, 1985 .

172. SILLÉN, L.G. and MARTELL, A.E., 'Stability Constants of Metal-ion Complexes', London, The Chemical Society, Special Publication No. 25, 1971, p. 24.

173. SMITH, R.M. and MARTELL, A.E., 'Critical Stability Constants , Vol. 4: Inorganic Complexes',New York, Plenum Press, 1976, p. 9.

174. DAVIES, C.W., 'Ion Association', London, Butterworth, 1962, pp. 39 - 43.

175. NÄSÄNEN, R., TILUS, P. and RINNE, A.-M., Suomen Kemistilehti, B39, 45 (1966).

176. HALL, J.L., JOSEPH, E., and GUM, M.B., J. Electroanal. Chem., 34, 529 (1972).

177. HALL, J.L., Proc. W. Va. Acad. Sci., 35, 104 (1963).

178. CONDIKE, G.F. and MARTELL, A.E., J. Inorg. Nucl. Chem., 31, 2455 (1969).

179. GUSTAFSON, R.L. and MARTELL, A.E., J. Amer. Chem. Soc., 81, 525 (1959).

180. EDWARDS, L.J., Diss., Univ. of Michigan, Ann Arbor, 1950 .

181. KELLER, R.N. and EDWARDS, L.J., J. Amer. Chem. Soc., 74, 2931 (1952).

182. SILLÉN, L.G. and MARTELL, A.E., 'Stability Constants of Metal-ion Complexes', 2nd edition, London, The Chemical Society, Special Publication No. 17, 1964, p. 437.

183. HALL, J.L., DEAN, W.E. and PACOFSKY, E.A., J. Amer. Chem. Soc., 82, 3303 (1960).

184. MARTELL, A.E., CHABEREK Jr., S., COURTNEY, R.C., WESTERBACK, S. and HYYTIAINEN, H., J. Amer. Chem. Soc., 79, 3036 (1957).

185. PAOLETTI, P., BARBUCCI, R., VACCA, A. and DEI, A., J. Chem. Soc. (A), 310 (1971).

186. SMITH, R.M. and MARTELL, A.E., 'Critical Stability Constants , Vol. 2: Amines',New York, Plenum Press, 1975, p. 83.

187. COVINGTON, A.K., Chem. Soc. Rev., 14, 265 (1985).

188. SMITH, R.M. and MARTELL, A.E., 'Critical Stability Constants , Vol.2: Amines',New York, Plenum Press, 1975, p. 58.

189. LOTZ, J.R., BLOCK, B.P. and FERNELIUS, W.C., J. Phys. Chem., 63, 541 (1959).

190. CABANI, S., J. Chem. Soc., 5271 (1962).

191. AVDEEF, A., KEARNEY, D.L., BROWN, J.A. and CHEMOTTI Jr., A.R., Anal. Chem., 54, 2322 (1982).

192. KELLER, R.N. and EDWARDS, L.J., Univ. Col. Studies, Ser. Chem. Pharm. 3, 1 (1961).

193. KARPEISKAYA, E.I., KUKUSHKIN, Yu. N., TROFIMOV, V.A., YAKOVLEV, I.P. and VLASOVA, R.A., Russ. J. Inorg. Chem., 17 , 1411 (1972).

194. (a) AHRLAND, S., CHATT, J. and DAVIES, N.R., Quart. Revs Chem. Soc., 11, 265 (1958).

(b) KLOPMAN, G., J. Amer. Chem. Soc., 90,223 (1968).

195. PAOLETTI, P., NUZZI, F. and VACCA, A., J. Chem. Soc. (A), 1385 (1966).

196. HANCOCK, R.D. and MARSICANO, F., Inorg. Chem., 17, 560 (1978).

197. THÖM, V.J., SHAIKJEE, M.S. and HANCOCK, R.D., Inorg. Chem., 25, 2992 (1986).

198. GAUR, J.N., GUPTA, O.D. and GUPTA, K.D., Journal of Electrochemical Society of India, 27, 58 (1978).

199. HANCOCK, R.D. and THÖM, V.J., J. Amer. Chem. Soc., 104, 291 (1982).

200. HART, S.M., BOEYENS, J.C.A. and HANCOCK, R.D., Inorg. Chem., 22, 982 (1983).

201. HANCOCK, R.D. and NAKANI, B.S., S. Afr. J. Chem., 35, 153 (1982).

202. IRVING, H. and ROSSOTTI, H., Acta Chem. Scand., 10, 72 (1956).

203. BIAGINI, S. and CANNAS, M., J. Chem. Soc. (A), 2398 (1970).

204. STEPHENS, F.S., J. Chem. Soc. (A), 883 (1969).

205. STEPHENS, F.S., J. Chem. Soc. (A), 2233 (1969).

206. COTTON, F.A. and ELDER, R.C., Inorg. Chem., 3, 397 (1964).

207. COTTON, F.A. and WING, R.M., Inorg. Chem., 4,314 (1965).

208. MURPHY, A., MULLANE, J. and HATHAWAY, B., Inorg. Nucl. Chem. Letters, 16, 129 (1980).

209. HODGSON, P.G. and PENFOLD, B.R., J. Chem. Soc. (Dalton), 1870 (1974).

210. PAJUNEN, A. and NÄSÄKKÄLÄ, M., Suomen Kemistilehti, B45, 47 (1972).

211. CHASTAIN Jr., R.V. and DOMINICK, T.L., Inorg. Chem., 12, 2621 (1973).

212. ZIMMERMAN, D.N. and HALL, J.L., Inorg. Chem., 12,2616 (1973).

213. FAVAS, M.C. and KEPERT, D.L., J. Chem. Soc. (Dalton), 793 (1978).

214. YOSHIKAWA, Y., KATO, N., KIMURA, Y., UTSUNO, S. and NATU, G.N., Bull. Chem. Soc. Jpn , 59, 2123 (1986).

215. THÖM, V.J., BOEYENS, J.C.A., McDOUGALL, G.J. and HANCOCK, R.D., J. Amer. Chem. Soc., 106, 3198 (1984).

216. THÖM, V.J. and HANCOCK, R.D., Inorg. Chim. Acta, 77, L231 (1983).

217. THÖM, V.J. and HANCOCK, R.D., J. Chem. Soc. (Dalton), 1877 (1985).

218. THÖM, V.J., HOSKEN, G.D. and HANCOCK, R.D., Inorg. Chem., 24, 3378 (1985).

219. HANCOCK, R.D., BHAVAN, R., WAGNER, C.A. and HOSKEN, G.D., S. Afr. J. Chem., 39, 238 (1986).

220. HANCOCK, R.D., BHAVAN, R., SHAIKJEE, M.S., WADE, P.W. and HEARN, A., Inorg. Chim. Acta, 112, L23 (1986).

221. WADE, P.W. and HANCOCK, R.D., Inorg. Chim. Acta, 130, 251 (1987).